DURBAN UNIVERSITY OF TECHNOLOGY

PREDICTING MASS TRANSFER IN PILOT SCALE EXTERNAL LOOP AIRLIFT REACTORS USING NEURAL NETWORKS

NIRVANA NAIDOO

2018

PREDICTING MASS TRANSFER IN PILOT SCALE EXTERNAL LOOP AIRLIFT REACTORS USING NEURAL NETWORKS

Submitted in fulfillment of the requirements of the degree of Doctor of Engineering in the Faculty of Engineering and the Built Environment at the Durban University of Technology

Nirvana Naidoo (AMIChemE) (BSc. Eng. (Chemical); MSc. Eng. (Chemical))

March 2018

Supervisor: Dr W. J. Pauck

Co-supervisor: Prof. M. Carsky

2nd co-supervisor: Dr M. Chetty

DECLARATION

I, Nirvana Naidoo, declare that:

The experimental work described in this thesis was carried out in the Chemical Engineering laboratories of the Durban University of Technology and the University of KwaZulu Natal from January 2016 to July 2017.

i. The research reported in this thesis, except where otherwise indicated, is my original work.
ii. This thesis has not been submitted for any degree or examination at any other university.
iii. This thesis does not contain other persons' writing, unless specifically acknowledged as being sourced from other researchers. Where other written sources have been quoted, then:
    a. Their words have been re-written but the general information attributed to then has been referenced;
    b. Where their exact words have been used, their writing has been placed inside quotation marks and referenced.
iv. This thesis does not contain other persons' data, pictures, graphs or other information, unless specifically acknowledged as being sourced from other persons.
v. This thesis does not contain text; graphics or tables copied and pasted from the internet unless specifically acknowledged and the source detailed in the thesis Reference section.

Signed: 

Nirvana Naidoo

Supervisor: _____

Dr W. J. Pauck

Co-supervisor: 

Prof. M. Carsky

2nd Co-supervisor: _____

Dr M. Chetty

ACKNOWLEDGEMENTS

My sincere appreciation and thanks to Dr W.J. Pauck and Professor M. Carsky for their invaluable guidance, support and supervision, whom without, this project would never have been completed.

I am indebted to the highly knowledgeable and efficient Technicians in the Department of Chemical Engineering, Mr R.T. Christy, Mr M.J. Bux and Mr V.K. Moodley for their unwavering support in ensuring the smooth running of this project.

My sincere thanks to Mr M.O. Saib (Subject Librarian) for your prompt and efficient assistance for every article and book request. Your kindness will always be remembered.

A special thanks to:

- Mr S.R. Chetty (Senior Technician – Department of Chemistry) and Dr T. Singh (Technician – Department of Chemistry) for coming to my aid and performing the required fluid analysis at no cost.
- Marcieth Pinto and Anne-Marie Billet (Chemical Engineering - Toulouse)
- Dr S.L. Kiambi (Senior Lecturer – Department of Chemical Engineering) and Dr Y. Isa (Senior Lecturer – Department of Chemical Engineering) for your guidance and input in the initial stages of this project.
- Mr P.P. Chamane (Technician – Facilities) and Mr V.S. Nyawo (Technician – Mechanical Engineering) for always providing assistance whenever called upon.
- Mr K. Ponusamy for expediting all my purchase requests.
- The students at the University of KwaZulu Natal: Aveshni Reddy, Suraksha Ramsumar, Atlang Mojalemotho, Marcelle Pillay, Mouline Phumuse and Santhya Naidoo for your assistance with experimentation.
- Mr E. Obwaka (Lecturer – University of KwaZulu Natal – Department of Chemical Engineering) for arranging use of the reactors at the University of KwaZulu Natal.
- The staff in the Department of Chemical Engineering, Prof P. Musonge, Mr S. Ramsuroop, Mrs P. Dube, Dr. S. Rathilal, Mr G.K. Reddy and Miss K.N. Ntuli for your support.

Finally, I am most grateful to my husband, Naveshan Naidoo, my daughter's, Thejal Naidoo and Eshta Naidoo for their quiet encouragement, tolerance, patience and constant support throughout this journey.

ABSTRACT

Airlift reactors are a viable means for conducting large scale mass transfer operations. However, due to the difficulty experienced in understanding the complex behavioural characteristics of these reactors, the design of airlift reactors becomes very complicated and largely empirical. Existing correlations and traditional computational fluid dynamic modelling has proven to be mostly reactor dependent and not widely applicable thereby limiting their application. There is therefore a need to develop a model that does not require prior knowledge of relationships between parameters of these reactors but instead uses an alternate method to assist with the design of airlift reactors. An artificial neural network represents this method.

The aim of this investigation was to build an artificial neural network using selected input data of Newtonian fluids in pilot scale external loop airlift reactors of varying designs in order to predict the mass transfer coefficient in other external loop airlift reactors with more general geometry.

To achieve this, a large base of experimental data (663) was generated using glycerine-air and water-air systems in 5 configurations of external loop airlift reactors with 3 categories of sparger design. The data was modelled using the artificial neural network software, Predict (Version 3.30) by Neuralware. The Coefficient of Correlation for the neural network model was 0.98.

The neural network model was tested with unseen external data from various sources of which the R values ranged from 0.91 to 0.99. Additional external data was evaluated with the superficial gas velocity out of the range of the experimental data from this investigation and with a very different design of sparger. The R values for this additional data were 0.85 and 0.67-0.85 respectively.

To achieve good correlations it was found necessary to take into account the sparger design and pore size; the actual geometric dimensions of the reactors namely the riser and downcomer diameters and heights; the visual observations of the approximate bubble size and bubble flow patterns and static liquid height in addition to the more usual data of the area and aspect ratios; the fluid properties namely, surface tension, density and viscosity; the superficial gas velocity; the downcomer superficial liquid velocity; the riser gas holdup and the downcomer gas holdup. However, some parameters like the static liquid height although considered important appeared not to be.

By considering these as important input variables into the network, the artificial neural network was able to give excellent approximations for both seen and unseen data for some of the reactor configurations. However, the network also had the ability to pick up differences in the reactor configurations were it did not predict well, especially with respect to sparger design. An important conclusion arrived at in this investigation was the significant influence of the sparger and its design on the mass transfer. The sensitivity of the network to the sparger design means that a greater quantification of the influence of the sparger design is required.

DEDICATION

To my family, Naveshan, Thejal and Eshta.

Mum and Dad.

With all of you by my side, everything is possible.

Difficulties in your life do not come to destroy you, but to help you realise your hidden potential and power. Let difficulties know that you too are difficult.

Dr. A.P.J. Abdul Kalam

CONTENTS

Declaration...……..ii

Acknowledgements..……iii

Abstract……...…….....iv

Dedication……...……...v

Nomenclature……...xiv

List of Figures…….xvii

List of Tables…….xxiv

Chapter One

Introduction……1

Chapter Two

Airlift Reactors

2.1. Introduction…….8

2.2. Gas-liquid mass transfer……10

2.2.1. The mass transfer model…….12

2.3. Airlift reactors: general concepts and classification……..16

2.3.1. Flow regimes……..19

2.3.2. Flow visualization studies……..23

2.4. Gas-liquid hydrodynamics in airlift reactors…….24

2.4.1. Superficial gas velocity……..24

2.4.2. Superficial liquid velocity……..24

2.4.3. Gas holdup…….26

2.4.4. Mass transfer coefficient……28

2.5. Effects of superficial gas velocity on gas holdup, liquid circulation velocity and mass transfer……29

2.5.1. Conclusion……..41

2.6. Effects of reactor geometry on gas holdup and mass transfer……...41

2.6.1. Gas spargers……....41

2.6.1.1. Sparger location……...43

2.6.1.2. Effects on gas holdup and mass transfer…….45

2.6.2. Effects of an enlarged gas disengagement zone…….52

2.6.3. Effects of aspect ratio…….56

2.6.4. Effects of area ratio……57

2.7. Conclusion…….58

Chapter Three

Neural Networks

3.1. Introduction……...61

3.2. The structure of biological networks…….62

3.3. Structure of an artificial neural network……62

3.4. Feasibility and application of artificial neural networks……...65

3.4.1. Feasibility of artificial neural networks……..65

3.4.2. Application of artificial neural networks……66

3.4.2.1. Software……..68

3.4.2.2. Data requirements……68

3.5. Mathematical representation of an artificial neural network…….69

3.5.1. Background……69

3.5.2. Basic single layer artificial perceptron……...69

3.5.2.1. Types of activation functions……..70

3.5.2.2. Error minimization……..72

3.5.3. Multilayer Perceptron…….73

3.5.3.1. Back propagation algorithm……73

3.5.3.2. Network architecture……...75

3.5.3.3. Cascade correlation learning architecture……...76

3.5.3.3.1. Unit creation algorithm……77

3.6. Review of artificial neural network applications in airlift reactors……...78

3.6.1. Introduction……78

3.6.2. Neural networks and airlift reactors……...80

3.6.2.1. Predicting gas holdup and liquid velocity with neural networks……80

3.6.2.2. Flow regime prediction using artificial neural networks…….90

3.6.2.3. Predicting mass transfer using artificial neural network…….....90

3.6.3. Conclusion……..91

Chapter Four

Methodology

4.1. Introduction……...92

4.2. Preliminary investigations and procedures……93

4.2.1. Fluid selection and reactor configuration……...93

4.2.1.1. Viscosity, density and surface tension testing…….97

4.2.2. Sparger selection…….97

4.2.2.1. Sparger positioning……....100

4.2.3. Dissolved oxygen probe positioning and readings……...102

4.2.3.1 Dynamic de-aeration……...102

4.2.4. Liquid height in the disengagement tank……..102

4.2.5. Gas holdup measurements……103

4.2.6. Visualization studies…….105

4.2.7. Airlift reactor software and hardware……..106

4.3. Superficial liquid velocity measurements……....106

4.4. Superficial gas velocity measurements……107

4.5. Operational procedure…….107

4.6. The neural network……..109

Chapter Five

Results and Discussion

5.1. Introduction……..111

5.2. Flow visualization studies……111

5.2.1. Effect of sparger design, area ratio and fluid properties on bubble flow behaviour……112

5.2.1.1. Reactor configurations 1 and 2 with a perforated plate sparger design……...112

5.2.1.2. Reactor configurations 1 and 2 with a perforated disk sparger design……116

5.2.1.3. Reactor configurations 1 and 2 with a perforated pipe sparger design…..118

5.2.1.4. Reactor configuration 3…….120

5.2.1.5. Reactor configurations 4 and 5……..121

5.2.1.6. Observations of effects of sparger design and fluid properties……123

5.2.2. Conclusion……125

5.3. Effects of reactor geometry and sparger design on gas holdup, superficial liquid velocity and mass transfer……...126

5.3.1. Effects of sparger design, area ratio and aspect ratio on riser gas holdup, superficial liquid velocity and mass transfer……127

5.3.1.1. Reactor configurations 1 and 2 for the water-gas system……127

5.3.1.1.1. Conclusion……..131

5.3.1.2. A comparison between reactor configurations 1, 2 and 3 for water-gas systems……..132

5.3.1.2.1. Conclusion……...135

5.3.1.3. A comparison between reactor configurations 4 and 5 for a water-gas system……..136

5.3.1.4. Effects of sparger design, area ratio and aspect ratio on riser gas holdup, superficial liquid velocity and mass transfer glycerin-gas systems……139

5.3.1.4.1. Effects of glycerin concentrations……..140

5.3.2. Conclusion……150

5.4. Neural network modeling……151

5.4.1. Data classification and partitioning……..152

5.4.2. Building the neural network model……..153

5.4.3. Validation of the neural network…….164

5.4.3.1. Conclusion……164

5.4.3.2. Predictions outside the range of training data……..166

5.4.3.3. Application of the neural network to the data set of an internal loop airlift reactor…….....171

5.4.4. Conclusion……172

Chapter Six

General Conclusions and Recommendations

6.1. General Conclusions……174

6.2. Recommendations for further work ……176

References……..177

Appendices

Appendix A1: Neural network model inputs and predictions……193

Appendix A2: Statistical data for the neural network model…….216

Appendix A3: Applied weights (ω_{xi})……217

Appendix B1: Validation data (sparger type A for Fakhari et al. (2014))……..221

Appendix B2: Validation data (sparger type B for Fakhari et al. (2014))……..224

Appendix B3: Validation data (sparger type C for Fakhari et al. (2014))……..227

NOMENCLATURE

C^*	Steady state (or saturation) dissolved oxygen concentration	(kgm^{-3})
C_G	Oxygen concentration in the gas phase	(kgm^{-3})
C_{Gi}	Interfacial oxygen concentration on the gas side	(kgm^{-3})
C_L	Instantaneous concentration of oxygen in liquid	(kgm^{-3})
C_{Li}	Interfacial concentration on the liquid side	(kgm^{-3})
J	Mass flux	($kgm^{-2}s^{-1}$)
k_G	Gas-film mass transfer coefficient	(s^{-1})
k_La	Mass transfer coefficient	(s^{-1})
K_L	Overall mass transfer coefficient based on the liquid film	(s^{-1})
ΔC	Concentration gradient	(kgm^{-3})
$\bar{H}$	Henry's law constant	(-)
a_L	Gas-Liquid interfacial area per unit liquid volume	(m^{-1})
C_o	Distribution parameter	(-)
U_{SGR}	Superficial gas velocity in the riser	(ms^{-1})
U_{SLD}	Superficial Liquid velocity in the downcomer	(ms^{-1})
Q_{gas}	Gas flowrate	(kgm^{-3})
$\bar{U}_{LC}$	Mean liquid circulation velocity	(ms^{-1})
D	Molecular diffusivity	(m^2s^{-1})
x_c	Circulation path	(m)
t_c	Average time for complete circulation	(s)
$\dot{V}_{SLR}$	Linear liquid velocity	(ms^{-1})
V_G	Expanded liquid volume	(m^{-3})
V_L	Static liquid volume	(m^{-3})
h_D	Expanded liquid height	(m)
h_L	Static liquid height	(m)
dh_m	difference on liquid level	(m)

$d\hat{z}$	Distance between manometer tappings	(m)
D_R	Riser diameter	(m)
D_D	Downcomer diameter	(m)
H_R	Riser height	(m)
H_D	Downcomer height	(m)
A_R	Cross sectional area of the riser	(m^2)
A_D	Cross sectional area of the downcomer	(m^2)
a	Slope parameter	(-)
Ar	Archimedes number	(-)
a_s	Specific interfacial area	(m^{-1})
Bo	Bodenstein number	(-)
C_{fM}	Nassos and Bankoff (1967) coefficient	(-)
C_{fL}	Blasius coefficient	(-)
$C_{alcohol}$	Concentration of alcohol	(kgm^{-3})
D	Diameter/ sieve pore diameter	(m)
E	Error	(-)
G	Acceleration due to gravity	(ms^{-2})
H_e	Equivalent height of column	(m)
H	Height of column	(m)
Eo	Eötvös number	(m)
f_n	Threshold/activation function	(-)
Fr	Froude number	(-)
Ga	Galilei number	(-)
n	Number of sieve plates	(-)
Re	Reynolds number	(-)
Sc	Schmidt number	(-)
Sh	Sherwood number	(-)

T_{VR}	Volume ratio	(-)
t_m	Mixing time	(s)
t_c	Circulation time	(s)
U	Velocity	(ms^{-1})
x	Input data	(-)
y	Binary output data	(-)
V	Volume	(m^{-3})
p_1, p_2, p_3	Error coefficients	(-)
K_B	Frictional loss coefficient for bottom of reactor	(-)
U_{Gr}	Superficial gas velocity in the riser	(ms^{-1})
U_{Lr}	Superficial liquid velocity in the downcomer	(ms^{-1})

GREEK LETTERS

ε_R	Gas holdup in the riser	(-)
ε_D	Gas holdup in the downcomer	(-)
ε	Overall gas holdup	(-)
ω	Weight	(-)
η	Step size parameter	(-)
δ	Error	(-)
ρ	Density	(kgm^{-3})
ρ_p	Density of solid particles	(kgm^{-3})
μ	Viscosity	(Pa s)
σ	Surface tension	(kgs^{-2})
φ	Solids loading	(-)
β	Free area ratio of sieve plate	(-)

LIST OF FIGURES

1.1 Chaotic circulation cells in bubble columns 2

1.2 Operating range for bubble columns and airlift reactors depicted as a function of superficial gas velocity (U_{Gr}) vs superficial liquid velocity (U_{Lr}) 3

2.1 Oxygen/gas transfer path with resistances from the gas bubble to the micro-organism 11

2.2 The gas-liquid interface. The stagnant films and steady state oxygen concentration profiles 13

2.3 Internal and external loop airlift reactor configurations 17

2.4 Airlift reactor schematics with operational zones 17

2.5 Types of gas disengagement tanks 18

2.6 (a) and (b) closed channel (c) open channel 19

2.7 Flow regimes 21

2.8 Flow regimes for bubble columns 22

2.9 Gas Spargers 42

2.10 Location of sparger influence on gas distribution 44

2.11 Poor Dispersion on the central horizontal axis of the base 44

2.12 Volume ratio in gas disengagement tank 55

2.13 Reactor height 56

2.14 Effects of area ratio as a function of liquid superficial and gas superficial velocity 58

3.1 Schematic of a Biological Neuron 62

3.2 Schematic of an Artificial Neural Network 63

3.3 Fully connected artificial neural network with one hidden layer of neurons 64

3.4 Artificial neural network with three hidden layers of neurons 64

3.5 Single Layer Perceptron with Bias Weight, ω_o 70

3.6 Threshold Function 71

3.7 'S'-shape Sigmoid Function 71

3.8 Multi-layer Perceptron, 5-3-3 73

3.9 Over fitting of data. (a) Good fit to noisy data (b) Over-fitting 75

3.10 Schematic of the Cascade Correlation Architecture 77

3.11a Parity plot of estimated vs experimental gas holdup, training step 82

3.11b Parity plot of estimated vs experimental gas holdup, testing step 82

3.12 Parity plot of downcomer gas holdup. A comparison between predicted and experimental results by Al-Masry (2004) and Al-Masry (2006) 87

3.13 Parity plot of gas holdup in the riser using ANN 88

3.14 Experimental and predicted for ε_{GR} using correlation 89

4.1 Schematic of reactor configuration 1 and configuration 2 94

4.2 Schematic of reactor configuration 3 95

4.3 Schematic of reactor configuration 4 and configuration 5 96

4.4 Perforated Plate (A) (used in reactor configuration 1 and configuration 2) 98

4.5 Perforated Disk (B) (used in reactor configuration 1 and configuration 2) 99

4.6 Perforated Pipe (C) (used in reactor configuration 1 and configuration 2) 99

4.7 Perforated Plate (A) (used in reactor configuration 3) 100

4.8 Perforated Disk (B) (used in reactor configuration 4 and configuration 5) 100

4.9 Deflection of entering bubbles with sparger on the central horizontal axis of the base 101

4.10 Sparger positioned at the entrance to the riser 101

4.11 Inverted U-tube manometer 105

5.1 Fairly uniform flows at low (a) and high velocities (b) for a perforated plate sparger 113

5.2 Weeping at initial gas velocity (a) no weeping at higher velocity (b) 114

5.3 Schematic of initial bubble flow pattern ($A_D/A_R < 1$; perforated plate sparger; configurations 1, 2, 4 and 5) 115

5.4 Schematic of congregation and dispersion of bubbles 116

5.5 Bubble paths slightly wavy for perforated disk spargers. Bubbles flow toward central vertical axis of riser 117

5.6 Schematic of helical effect 118

5.7 Schematic of gas bubbles deflected to wall of riser 119

5.8 Deflection of bubbles at low velocity for reactor configuration 3 121

5.9 Bubbles congregating to the central axis of the riser when area ratio is less than 1 for reactor configuration 5 with a perforated disk sparger. Similar behaviour was noted for reactor configurations 1 and 2 with the perforated disk sparger 122

5.10 Weeping in a perforated pipe sparger 124

5.11 Comparison of riser to downcomer gas holdup in reactor configuration 1 for a water-gas system 126

5.12 Sparger effects on riser gas holdup in reactor configurations 1 and 2 using a gas-water system 127

5.13 Sparger effects on the mass transfer coefficient in reactor

configurations 1 and 2 using a gas-water system 129

5.14 Sparger effects on the downcomer superficial liquid velocity in reactor configurations 1 and 2 using a gas-water system 130

5.15 Area ratio effects on riser gas holdup in reactor configurations 1, 2 and 3 using a gas-water system 133

5.16 Area ratio effects on mass transfer in reactor configurations 1, 2 and 3 using a gas-water system 133

5.17 Area ratio effects on the downcomer superficial liquid velocity in reactor configurations 1, 2 and 3 using a gas-water system 134

5.18 Aspect ratio effects on the downcomer gas holdup in reactor configurations 1, 2 and 3 using a gas-water system 135

5.19 Aspect ratio effects on gas holdup in reactor configurations 1 and 4 using a gas-water system 136

5.20 Aspect ratio effects on mass transfer in reactor configurations 1 and 4 using a gas-water system 137

5.21 Aspect ratio effects on gas holdup in reactor configurations 2 and 5 using a gas-water system 137

5.22 Aspect ratio effects on mass transfer in reactor configurations 2 and 5 using a gas-water system 138

5.23 Area ratio effects on the riser gas holdup in reactor configurations 4 and 5 using a gas-water system 138

5.24 Area ratio effects on the mass transfer in reactor configurations 4 and 5 using a gas-water system 139

5.25 Effects of glycerin concentrations on the riser gas holdup for reactor configuration 1 using a perforated plate sparger 140

5.26 Effects of glycerin concentrations on the riser gas holdup for reactor configuration 2 using a perforated plate sparger 140
5.27 Effects of glycerin concentrations on the riser gas holdup for reactor configuration 2 using a perforated disk sparger 141
5.28 Effects of glycerin concentrations on the riser gas holdup for reactor configuration 2 using a perforated disk sparger 141
5.29 Effects of glycerin concentrations on the riser gas holdup for reactor configuration 2 using a perforated pipe sparger 142
5.30 Effects of glycerin concentrations on the riser gas holdup for reactor configuration 2 using a perforated pipe sparger 142
5.31 Effects of glycerin concentrations on the mass transfer coefficient for reactor configuration 1 using a perforated plate sparger 143
5.32 Effects of glycerin concentrations on the mass transfer coefficient for reactor configuration 2 using a perforated plate sparger 143
5.33 Effects of glycerin concentrations on the mass transfer coefficient for reactor configuration 1 using a perforated disk sparger 144
5.34 Effects of glycerin concentrations on the mass transfer coefficient for reactor configuration 2 using a perforated disk sparger 144
5.35 Effects of glycerin concentrations on the mass transfer coefficient for reactor configuration 1 using a perforated pipe sparger 145
5.36 Effects of glycerin concentrations on the mass transfer coefficient for reactor configuration 2 using a perforated pipe sparger 145
5.37 Comparison of area ratio effects on the riser gas holdup using different sparger types for a 15% glycerin solution in reactor configurations 1 and 2 146

5.38 Comparison of area ratio effects on the mass transfer coefficient using different sparger types for a 15% glycerin solution in reactor configurations 1 and 2 147
5.39 Comparison of area ratio effects on the riser gas holdup using different sparger types for a 22% glycerin solution in reactor configurations 1 and 2 147
5.40 Comparison of area ratio effects on the mass transfer coefficient using different sparger types for a 22% glycerin solution in reactor configurations 1 and 2 148
5.41 Comparison of area ratio effects on the riser gas holdup using different sparger types for a 28% glycerin solution in reactor configurations 1 and 2 148
5.42 Comparison of area ratio effects on the mass transfer coefficient using different sparger types for a 28% glycerin solution in reactor configurations 1 and 2 149
5.43 Comparison of area ratio effects on the riser gas holdup using different sparger types for a 31.25% glycerin solution in reactor configurations 1 and 2 149
5.44 Comparison of area ratio effects on the mass transfer coefficient using different sparger types for a 31.25% glycerin solution in reactor configurations 1 and 2 150
5.45 Parity plot of all predicted and experimental mass transfer data for neural network model 1 155
5.46 Parity plot of all predicted and experimental mass transfer data for neural network model 2 156
5.47 Parity plot of all predicted and experimental mass transfer data for neural network model 3 157
5.48 Parity plot of all predicted and experimental mass transfer data for neural network model 4 158

5.49 Parity plot of all predicted and experimental mass transfer data for neural network model 5 159
5.50 Parity plot of all predicted and experimental mass transfer data for neural network model 6 160
5.51 Parity plot of all predicted and experimental mass transfer data for neural network model 7 160
5.52 Parity plot of all predicted and experimental mass transfer data for neural network model 8 161
5.53 Prediction of mass transfer data, Nayager and Govender (2016) 165
5.54 Prediction of the 32 unseen mass transfer coefficient data points from the author's own investigation 165
5.55 Prediction of mass transfer coefficient data, Guo et al. (1997) 166
5.56 Prediction of mass transfer coefficient data, Al-Masry and Dukkan (1997) 168
5.57 Prediction of mass transfer coefficient data, Fakhari et al. (2014) using a perforated plate sparger (A) 169
5.58 Prediction of mass transfer coefficient data, Fakhari et al. (2014) using a perforated disk sparger (B) 170
5.59 Prediction of mass transfer coefficient data, Fakhari et al. (2014) using a perforated pipe sparger (C) 170
5.60 Prediction of mass transfer coefficient data, Shariati et al. (2007) 172

LIST OF TABLES

2.1 Summary of mass transfer correlations 35

2.2 Summary of correlations for gas holdup 39

2.3 Summary of correlations for gas holdup with differing spargers 48

3.1 Properties of liquids used 81

3.2 NMSE comparison 83

3.3 Correlation Parameters for riser gas holdup and fit statistics 89

4.1 Reactor dimensions 93

4.2 Fluid properties 97

4.3 Sparger classification 98

4.4 Dissolved oxygen probe position for each reactor configuration 102

4.5 Liquid heights in disengagement tanks 103

4.6 Distance between manometer tappings 105

5.1 Reclassification of sparger type for the neural network model 152

5.2 Classification of bubble size for the neural network 152

5.3 Classification of bubble flow patterns for the neural network 153

5.4 Variable weights 163

CHAPTER ONE

INTRODUCTION

The global shift toward environmental sustainability and stability has resulted in the need for a more improved and efficient processing of waste streams in the chemical, petrochemical, pharmaceutical, bioprocessing, pulp and paper and wastewater treatment industries. Even trace amounts of pollutants present in waste streams from these industries may have short and long term effects on environmental, as well as on human health. The implementation of strict environmental laws means that there is a demand for the development of equipment and processes that reduce or remove pollutants from process wastewaters and effluents (Mohanty et al, 2008). To this end, continuous stirred tank reactors, bubble columns and airlift reactors can be used for the treatment of wastewaters and effluents in these industries as well as increasing the overall efficiency of a process.

Continuous stirred tank reactors (CSTR's) have been the traditional method used for heat and mass transfer in fermentation and wastewater treatment. However, their design tends towards making them a non-ideal system for efficient heat and mass transfer characteristics. The mixing or agitation occurs at a central point in the reactor with a mechanical stirrer. This leads to centralized agitation resulting in dead zones away from the stirrer and toward the wall.

Continuous stirred tank reactors also require high power inputs to operate the mechanical stirrers for agitation. This reduces the efficiency of the overall process. In high shear systems, mechanical stirrers will compromise micro-organism cell integrity near the stirrer. It stands to reason that on an industrial scale, continuous stirred tank reactors will be highly

inefficient to accomplish good mixing and mass transfer due to these effects (Shariati et al., 2007; Bentifrauoine et al., 1999).

Bubble columns however, when compared to CSTR's provide better operating conditions for mass transfer as they are pneumatically agitated across the cross section of the column and there are no moving parts (Vial et al., 2002). Much like continuous stirred tank reactors, bubble columns also operate in batch mode and therefore have prolonged residence times. Air or gas (referred to as gas from here on) is sparged into the bottom of the column to create agitation and mixing. However, the flow patterns in bubble columns are not uniform (Chisti, 1989; Viswanathan, 1986) and mixing occurs in small chaotic circulation cells with backflow as in Figure 1.1.

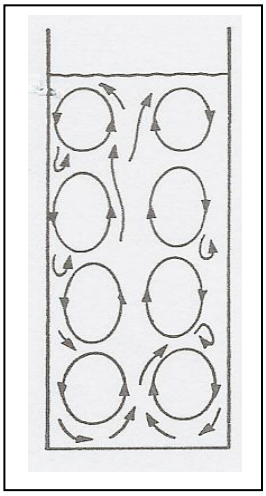

Figure 1.1 Chaotic circulation cells in bubble columns (Chisti, 1989).

This results in no net flow of liquids in the bubble columns (Viswanathan, 1986). The superficial gas velocity range in bubble columns is also limited between 0.03 – 1m/s with the common application in the lower velocities of the range (a superficial velocity is a hypothetical velocity of a selected phase flowing in a given cross sectional area without considering any other phase that is present). Only industrial scale bubble columns operate at 1m/s which tend to be very tall vessels with large aspect ratios i.e., ratio of riser height to riser diameter (H_R/D_R) (Kadic and Heindel, 2014). This limits their operating range as illustrated in Figure 1.2.

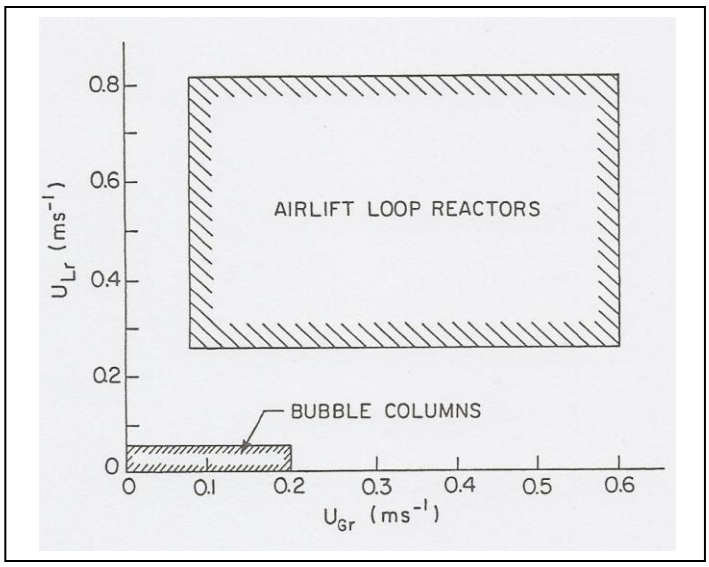

Figure 1.2 Operating range for bubble columns and airlift reactors depicted as a function of superficial gas velocity (U_{Gr}) and superficial liquid velocity (U_{Lr}) (Chisti, 1989).

Kadic and Heindel (2014) reported that the major disadvantage of bubble columns is the complex hydrodynamics which cannot be controlled, the undefined flow patterns, backmixing and large pressure drops. Although bubble columns may be better than the continuous stirred tank reactors when it comes to efficient mixing and high shear systems, they are not as efficient when compared to airlift reactors (Merchuk and Stein, 1981).

Airlift reactors are also simply designed pneumatically agitated devices with no moving parts, low power input and easy operation for gas-liquid and gas-liquid-solid phase systems. They differ from bubble columns and CSTR's in that they have clearly defined flow paths that enable good mixing and mass transfer and are highly suitable for high shear systems due to the absence of any moving parts (Gajbhiye et al., 2012; Merchuk and Gluz, 2002; Chisti, 1989).

Thus when compared to CSTR's and bubble columns, airlift reactors have an important role to play in the further treatment of the waste waters (Hinks et al., 1996) and effluents (Chisti and Moo-Young, 1987) as well as in the production of pharmaceuticals and micro-organisms (Khondee et al., 2012; Rengel et al., 2012; Wang et al., 2005; Sánchez Mirónet et al., 2004;

Kilonzo and Margaritis, 2004; Sánchez Mirónet et al., 2003; Jin et al., 1999) thus improving existing processes.

In fact, their popularity has been steadily increasing as more industries move towards the use of micro-organisms in their processes (Chisti and Moo-Young, 1993). Their versatility and wide operation range as in shown in Figure 1.2 means they can be applied in diverse applications which is briefly summarized here and includes:

- Studies on the removal of biologicial ammonium from synthetic metal refinery waste water using an airlift suspension reactor was done by Manipura et al., 2007. Granular activated carbon was used to remove the biological ammonium compounds from the metal refinery waste water. A removal efficiency of greater than 90% was achieved with the airlift suspension reactor.
- Activated carbon was also used in the treatment of phenolic waste water in a novel waste water specifically designed multistage airlift reactor by adsorption (Mohanty et al., 2008). Phenol is a highly toxic pollutant to the environment and humans, even in trace amounts. A 95% removal of phenol was achieved at a low superficial gas velocity up to a maximum of 0.0285m/s.
- The airlift reactor is ideally suited to shear sensitive micro-organisms due to there being no moving parts. Baker's yeast growth was increased in a specially designed external loop airlift bioreactor (Ghosh et al., 2010) with a yield of 0.51 which is close to the maximum achievable value.
- In recycling in the pulp and paper industry, Behin (2012) found that introducing an airlift reactor at the flotation step improved the deinking efficiency of recycled fibres. An increase of 1 - 4% in brightness and a decrease in 3 - 14% of inkspot was achieved. This yielded a good quality product while reducing capital investment, operation cost and preserving the environment.
- The de-flouridation of drinking water was achieved in an external loop airlift reactor adapted as an electrocoagulation cell with aluminum electrodes. No external gas was introduced into the system. The hydrogen gas produced by the optimally placed electrodes was sufficient to create a density difference and thus help circulate the

liquid and reduce the fluoride concentration to below 1.5mg/L from 10 to 20mg/L (Bennajah et al., 2009).

- Oil refinery waste water was treated using a three phase flow pilot scale airlift reactor (Xianling et al., 2005). The Peoples Republic of China has set discharge limits for chemical oxygen demand (COD) to 100 – 150mg/L and for ammonium-nitrogen reduction at 15 – 50mg/L to prevent this highly toxic waste water from entering the ocean. The airlift reactor produced better results than the traditional waste water treatment processes with COD and NH_4-H levels lower than 100 and 15mg/L.
- Raceway ponds have been the traditional method used for algae production outdoors (Ketheesan and Nirmalakhandan, 2011). However, they have low biomass productivity compared to engineered photobioreactors. Ketheesan and Nirmalakhandan (2011) developed a new airlift driven raceway reactor for more efficient algal production. The airlift reactor provided both the circulation and mass transfer in a closed system. Traditional raceway ponds use the paddle wheel method to drive the process which is energy intensive. By incorporating the airlift reactor, there was lower power input (a reduction of 80%) but the yield in algae increased (0.16dry g/L.day) even though this was a laboratory scale investigation with no sunlight.

There is no doubt that airlift reactors are a viable means for the treatment of waste water and the production of micro-organisms and that a significant amount of research has been done. The information that is available however, is very reactor specific and cannot be confidently applied to different systems (Kadic and Heindel, 2014; Amiri et al., 2011). There is a strong motivation from literature sources for further extensive investigations to be carried out to understand more about the influences of geometry on the hydrodynamic and mass transfer behaviour in these reactors so as to develop a single generalized correlation (Cozma et al., 2015; Roy et al., 2006; Garcia-Ochoa and Gomez, 2004; Camarasa et al., 2001) to enable easier design of industrial scale airlift reactors.

And, although extensive modeling of airlift reactors has been done using computational fluid dynamics, the information available is very reactor specific and requires an in-depth prior knowledge of the hydrodynamic behaviour of the reactors (Cozma et al., 2015; Kiambi and Luo, 2011; Roy et al., 2006; Garcia-Ochoa and Gomez, 2004; Camarasa et al., 2001). It is

important to develop a mathematical model that can predict the behaviour in any large scale external loop airlift reactor to enable easier design of industrial scale external loop airlift reactors. To do this, an in-depth analysis and understanding of geometry, hydrodynamics and physical properties of the system and their interdependence is needed.

For computational fluid dynamics, this may have been true, however in recent studies, predicting behaviour and mass transfer characteristics in airlift reactors has moved away from computational fluid dynamics towards artificial neural networks. A review of current literature on neural networks in airlift reactors has shown that an artificial neural network model is capable of performing this complex task without prior knowledge of the system under investigation. Neural networks have the ability to perform computations through a large parallel structure and it has the capability to learn and generalize (Cozma et al., 2015; Haykin, 2009; Al-Masry, 2006; Laberge et al., 2000).

Although some simple modeling has been done on airlift reactors using artificial neural networks, the problem arises in that the majority is based on laboratory scale systems and that they are not extensive where all parameters and conditions are taken into account especially on large pilot scale plant. What is required is a thorough investigation into the hydrodynamics of pilot scale external loop airlift reactors with varying geometry and the development of a generalized artificial neural network model using this information to assist in the design of industrial scale external loop airlift reactors irrespective of their geometry.

The aim of this research is to develop an artificial neural network model using selected hydrodynamic behavioral data of Newtonian fluids in pilot scale external loop airlift reactors in order to predict the mass transfer characteristics in other external loop airlift reactors irrespective of their geometry or configuration.

To fulfill the aim, a large amount of data input will be required to train the artificial neural network. This would require an investigation of some parameters and combinations of parameters that directly and indirectly influence the mass transfer characteristics of the external loop airlift reactor. To achieve this, the following objectives will be experimentally investigated on five pilot scale open channel external loop airlift reactors to determine their effects on the mass transfer coefficient:

- The gas flowrate;
- Liquid flowrate;
- Type of sparger;
- Area ratio, i.e. ratio of downcomer to riser cross sectional area;
- Aspect ratio i.e. ratio of riser height to riser diameter and
- Properties of the fluid i.e. viscosity, surface tension and density
- Bubble size and distribution

Once the data is analysed, the neural network software (Predict by Neuralware), will be used to build a model that will be able to predict the mass transfer characteristics of other external loop airlift reactors.

CHAPTER TWO

AIRLIFT REACTORS

2.1. INTRODUCTION

Reactor selection is not solely based on chemistry and kinetics of the system alone, but it also has to take into account the mixing and mass and heat transfer characteristics of the reactor as well (Freitas and Teixeira, 1998; Chisti, 1989). Reactors that offer mixing as well as heat and mass transfer characteristics are the conventional stirred tank reactors, bubble columns and airlift reactors. Conventional continuous stirred tank reactors are mechanically agitated whereas bubble columns and airlift reactors are agitated with gas to effect mixing or separation. All three types of reactors can either be used for gas-liquid mixing or for gas-liquid-solid mixing in which case the solid phase is increasingly being represented by micro-organisms. However, it must be noted that bubble columns and airlift reactors have a limited operating capacity when faced with increasingly viscous fluids as opposed to CSTR's which are able to deal with these highly viscous fluids.

In conventional stirred tank reactors, the mixing or agitation point is a mechanical stirrer and introduced at a point. This results in very high mixing and energy dissipation in the immediate vicinity of the stirrer and decreases away towards the walls. Possible dead zones are created at the wall as the size of the stirred tank reactor increases. The shear rate is also greatest at the stirrer as the energy is transferred to the fluid in the immediate surroundings. A fluid to fluid transfer of energy then occurs. This results in widely varying shear forces throughout the system. This non-uniform environment results in micro-organisms being exposed to undesirable temperature and concentration gradients. Although good heat and mass transfer occurs in the immediate vicinity of the stirrer, the integrity of the micro-

organism is lost due to the contact with the mechanical stirrer, which has the potential to damage the micro-organism reaction interface instead of enabling oxygen transfer to occur.

Bubble columns (BC) however, provide a slightly better environment than a conventional stirred tank reactor for the micro-organisms with their simple column design and no moving parts. Mixing and mass and heat transfer is achieved through pneumatic agitation. The compressed gas is introduced locally at the base of the column via a sparger which creates the circulation and movement of the fluid. The hydrodynamic behaviour in the bubble column, which has a direct influence on the mass transfer characteristics, is however very complex and cannot be regulated. The flow patterns are not well defined and very random with a significant amount of backmixing and chaotic circulation cells which result in large pressure fluctuations throughout the column (Kadic and Heindel, 2014; Martínez and Silva, 2013; Merchuk and Gluz, 1999; Chisti, 1989). The design and scale up of the bubble column becomes difficult as the reactor performance and behaviour is largely unknown and requires significant amounts of trial and error procedures (Kadic and Heindel, 2014).

Airlift reactors however, are considered to be far more suitable than the continuous stirred tank reactor or the bubble column (Merchuk and Gluz, 1999). The airlift reactor, like the bubble column, is also simply designed and with no mechanical moving parts and it still provides efficient mixing and mass and heat transfer. Pneumatically agitated like the bubble column, the difference lies in the well defined flow patterns that are present in the airlift reactor which provides more control (Kadic and Heindel, 2014; Martínez and Silva, 2013). The airlift reactor has two distinct channels for the circulating fluid and gas flows: an ascending flow channel called the riser and a descending flow channel called the downcomer. The driving force for circulation of the liquid in an airlift reactor is provided by the evenly distributed compressed gas entering the bottom of the riser. The entering gas creates a difference in the bulk densities of the liquid in the ascending and descending columns of the reactor, resulting in liquid circulation. Some of the advantages of airlift reactors, especially for biochemical processes are that there are no points of high energy dissipation rates (Schürgerl and Lübbert, 1995); significant residence times; a liquid-gas interface for the supply of oxygen and removal of waste gases; efficient agitation for nutrient distribution to the micro-organisms; reduced damage by the addition of acids and bases for pH control; good

temperature control and a contamination free environment as well as the advantage of being on a much larger scale than bubble columns (Kadic and Heindel, 2014; Vial et al., 2002; Merchuk and Gluz, 1999; Chisti, 1989).

However, although significant amounts of research has been done and reported on with respect to airlift reactors (Kadic and Heindel, 2014; Martínez and Silva, 2013), there is no single generalized correlation that can be used to describe or predict the general phenomena of airlift reactors especially with regards to the mass transfer. Kadic and Heindel (2014) also report that more focus needs to be concentrated on variable testing as most times multiple variables are adjusted with analysis focused on a single variable. Changes in the other variables are ignored. Comparative scale studies are also incorrect as comparisons are made between geometrically different airlift reactors. It therefore becomes very difficult to determine which variable has the most significant influence on the performance of airlift reactors.

2.2. GAS-LIQUID MASS TRANSFER

In biochemical and some chemical systems, reactions occur based on interactions between the gas phase and some soluble or insoluble materials suspended in the liquid phase. The gas would be required to be dissolved into the liquid for the reaction to proceed. This type of process occurs naturally in nature. Water bodies like rivers and lakes are cleaned by micro-organisms living within them. However for the micro-organisms to function, they require oxygen to survive with the oxygen source being provided by the ambient air. The oxygen very slowly diffuses into the water via a gas-liquid interface caused by the difference in oxygen concentration between the ambient air and the bulk water body (Whitman, 1923). This transfer of oxygen/gas from the gas phase to the suspended micro-organism occurs along a specific pathway.

Whitman (1923), Chisti (1989), Gaddis (1999) and Kadic and Heindel (2014) provide a detailed explanation of this process. Chisti (1989), Gaddis (1999) and Kadic and Heindel (2014) reported that while this pathway provides a means for transfer, it also offered various resistances to the transfer of the gas from the bulk liquid to the reaction site within the micro-

organism. The resistances encountered are the gas film within the gas bubble; the gas-liquid interface; the liquid film at the gas-liquid interface; the bulk liquid; the liquid film at the micro-organism – liquid interface; the micro-organism – liquid interface; the internal micro-organism interface and the biochemical reaction site. Figure 2.1 below is a schematic of the transfer pathway.

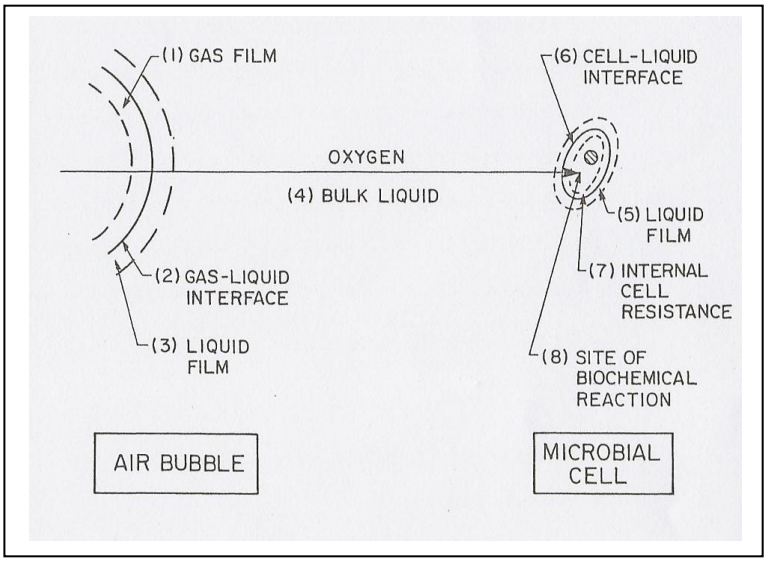

Figure 2.1 Oxygen/gas transfer path with resistances from the gas bubble to the micro-organism (Chisti, 1989).

Chisti (1989) as well as Whitman (1923) reported that not all the resistances play a significant role in the mass transfer. According to Chisti (1989), the resistance experienced in the bulk transfer zone (4) in Figure 2.1 can be neglected as airlift reactors and bubble columns operate at high levels of turbulence such that convective transport is dominant in this bulk phase. For single cell micro-organism or dispersed mycelia, the resistance due to the liquid film on the surface of the micro-organism (5) (Figure 2.1) may also be neglected due to the minute cellular size and its large surface area. Chisti (1989) was able to show that the results for the concentration differences are so small that the oxygen concentration in the liquid adjacent to the microbe (5) (Figure 2.1) was practically the same as that of the bulk liquid (4) (Figure 2.1). The resistances at the micro-organism-liquid interface (7) in Figure 2.1 and the site of the biochemical reaction (8) (Figure 2.1) could also be neglected. This, he reported was due to active oxygen transport through the micro-organism membrane and rapid rates of biochemical reactions. The intracellular resistance could also be disregarded as the enzymes

for terminal respiration occur in the micro-organism membranes rather than in the protoplasm according to Finn (Finn, 1967 cited in Chisti, 1989).

Thus the most important resistances to consider are those around the gas-liquid interface (2) (Figure 2.1) i.e., the mass transfer rate around the bubble (Whitman, 1923; Kadic and Heindel, 2014; Gaddis, 1999 and Chisti, 1989). Although the mass transfer rate in nature is very slow, it requires to be enhanced in industrial applications. To achieve this, mechanical or pneumatic mixing is done to increase turbulence thereby increasing mass transfer rates (Gaddis, 1999).

2.2.1. THE MASS TRANSFER MODEL

There are a number of mass transfer theories that exist which could be used to describe the convective mass transfer across an interfacial boundary (Kadic and Heindel, 2014; Geankoplis, 2009; Fogler, 1995; Chisti, 1989; Merchuk and Gluz, 2002; Manjo, 2014; Gaddis, 1999), with the simplest one presented by Nernst in 1904 (Kadic and Heindel, 2014).

For laminar flow, it is fairly easy to develop a mathematical equation describing the mass transfer. However, for the turbulent flows experienced in the airlift reactor and bubble column it becomes more complex. Increasing gas flow results in increased turbulence and random movement of the gas and liquid in the airlift reactor and bubble column. Although this results in higher mass transfer, the behaviour cannot be mathematically described.

By using the two-film theory proposed by Whitman (1923), it is possible to describe how the diffusion process occurs. The gas-liquid interface is described as adjacent, stagnant gas liquid films that have some finite thickness (Figure 2.2). The interface itself offers no resistance to mass transfer but the thin films close to the interface do. The interfacial concentrations are then defined by equilibrium relationships.

In the stagnant films the assumption is that mass transfer occurs mainly via molecular diffusion. This results in linear concentration profiles at steady state. By applying Fick's Law to the system, the mass flux of the diffusing species (oxygen) (J_{O_2}), is related to the concentration gradient in the film (ΔC), to the thickness of the film (Δx) (Chisti, 1989 and Kadic and Heindel, 2014),

$$J_{O_2} = \frac{D}{\Delta x} \Delta C$$

2.1

Where D = molecular diffusivity of the gas

Δx = film thickness

$\frac{D}{\Delta x}$ = mass transfer coefficient, k and

ΔC = concentration gradient.

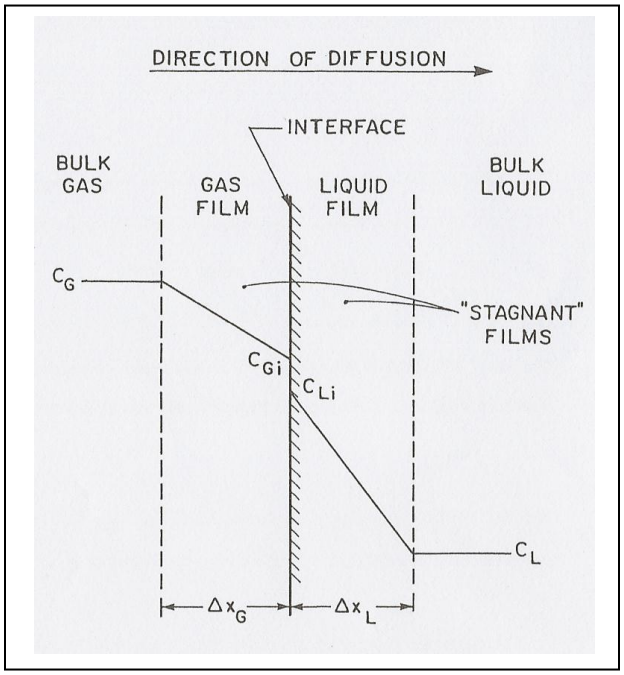

Figure 2.2 The gas-liquid interface. The stagnant films and steady state oxygen concentration profiles (Chisti, 1989).

At steady state equation 2.1 changes to (Chisti, 1989) for each of the two films:

$$J_{O_2} = k_G (C_G - C_{Gi}) = k_L (C_{Li} - C_L)$$

2.2

Where k_G = gas-film mass transfer coefficient

k_L = liquid-film mass transfer coefficient

C_G = gas concentration in the bulk gas phase

C_{Gi} = initial gas concentration at the gas film interface (on the gas side)

C_{Li} = interfacial concentration at the liquid film interface (on the liquid side)

C_L = instantaneous concentration of the gas in the bulk liquid

Due to the interfacial concentrations being in equilibrium, the flux can be written in terms of the overall concentration driving force:

$$J_{O_2} = K_L (C^* - C_L) \tag{2.3}$$

Where K_L = overall mass transfer coefficient based on the liquid film and

C^* = steady state (or saturation) dissolved gas (oxygen) concentration.

For a sparingly soluble gas like oxygen, C^* is related to C_G according to Henry's law:

$$C_G = \bar{H} C^* \tag{2.4}$$

Where $\bar{H}$ = Henry's law constant.

From equation 2.2 and 2.4 knowing that at the interface,

$$C_{L_i} = \bar{H} C_{G_i} \tag{2.5}$$

it can be shown that:

$$\frac{1}{K_L} = \frac{1}{k_L} + \frac{1}{\bar{H} k_G}$$

2.6

The Henry's law constant is much larger than one for sparingly soluble gases such as oxygen. Also the gas side mass transfer coefficient, k_G, is much larger than the liquid side mass transfer coefficient, k_L. This is due to the gas phase diffusivities being significantly larger than those in liquids. The gas phase film thicknesses are also smaller than that of the liquid films. Under these conditions, the second term in equation 2.6 becomes negligible and the equation reduces to:

$$\frac{1}{K_L} = \frac{1}{k_L}$$

2.7

This means that the resistance for sparingly soluble gas lies in the liquid film interface which makes the mass transfer liquid film controlled.

According to Chisti (1989) as well as Kadic and Heindel (2014) and Whitman (1923), the complexities of physically determining the actual values of the liquid film mass transfer coefficient, k_L, is almost impossible as the film thickness, exposure time and surface renewal rates cannot be quantified in any realistic bioreactor configuration. This means that the mass transfer rate is directly proportional to the concentration difference driving force in the absence of bulk flow which means that the gas mass transfer can be written as (Chisti, 1989):

$$J_{O_2} = k_L \, (C^* - C_L)$$

2.8

The relationship between the flux and the transfer rate is:

$$a_L J_{O_2} = \frac{dC_L}{dt}$$

2.9

This means that equation 2.8 can be written in terms of the gas mass transfer as

$$\frac{dC_L}{dt} = k_L a_L (C^* - C_L) \qquad 2.10$$

Where a_L = interfacial area per unit liquid volume

C^* = steady state (or saturation) dissolved gas (oxygen) concentration

C_L = instantaneous gas (oxygen) concentration in the liquid at any time, t.

Chisti (1989) stated that the evaluation of $k_L a_L$ is important as it is essential when designing an airlift bioreactor to predict the mass transfer rate as this is the value that requires to be optimized with minimal power input.

2.3. AIRLIFT REACTORS: GENERAL CONCEPTS AND CLASSIFICATION

Airlift reactors can be classified into two broad categories, viz., internal loop/baffled airlift reactors (ILALR) or external loop airlift reactors (ELALR). Both reactors have essentially the same operating zones but differ significantly in geometry (Figure 2.3).

Although both categories have separate pathways for the flow of liquids, the external loop airlift reactor differs in that it has distinct and separate channels while in the internal loop airlift reactor, the 'channels' are created by either a baffle of a strategically placed concentric /draft tube, Figure 2.3, for liquid flow.

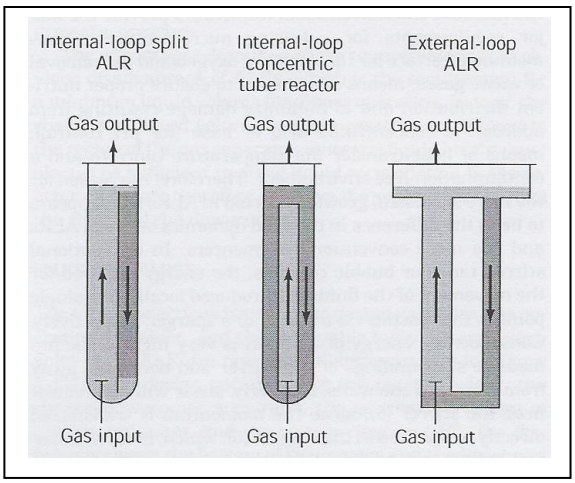

Figure 2.3 Internal and external loop airlift reactor configurations (Merchuk and Gluz, 2002).

These basic designs in Figure 2.3 above can be modified further by introducing gas at the top of the downcomer (Kadic and Heindel, 2014; Chisti and Moo-Young, 1987); at the sides (Mohanty et al., 2008), creating gas internally (Bennajah, 2009), sectioning the draft tube (Kadic and Heindel, 2014) or modifying the shape of the riser or downcomer (Gajbhiye, et al., 2012; Ghosh et al., 2010). However, regardless of the design of the airlift reactor, all of them have four distinct zones that have different flow characteristics. These zones are the riser, downcomer, gas disengagement zone and the base (Figure 2.4).

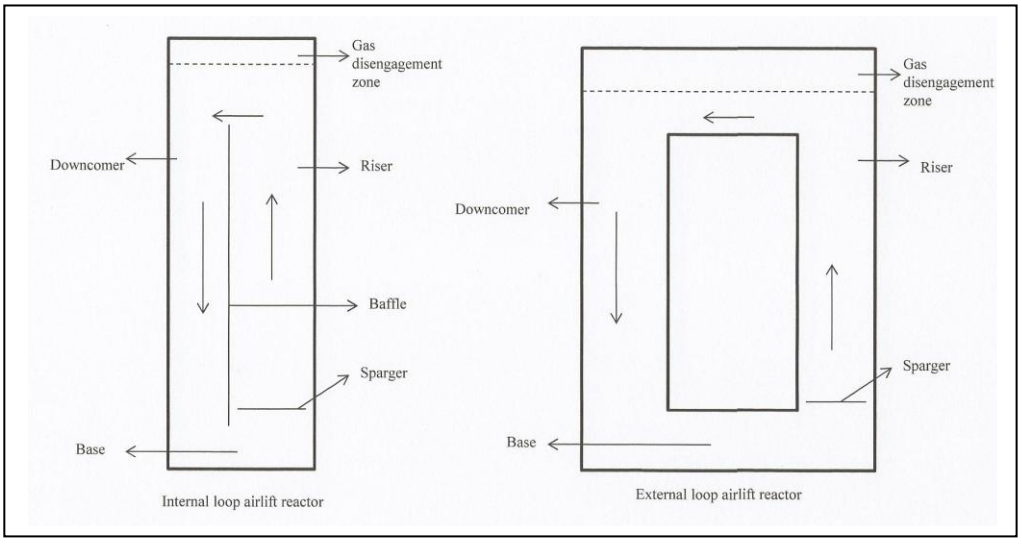

Figure 2.4 Airlift reactor schematics with operational zones.

Gas is generally injected at the entrance to the riser creating an upward flow of gas and liquid. At the top of the riser is the gas disengagement zone. This is often a tank or modified riser. This zone facilitates the removal of gas from the rising liquid as well as connecting the riser to the downcomer. This size or volume of the disengagement tank directly affects the amount of disengagement of gas bubbles from the liquid. The larger the zone, the greater the chance of having all bubbles disengage, which results in a minimum to no recirculation of gas via the downcomer. Larger gas disengagement zones could facilitate better gas disengagement. This is true when comparing closed channel and open channel disengagement zones. The gas disengagement zone can also have many different designs (Figure 2.5).

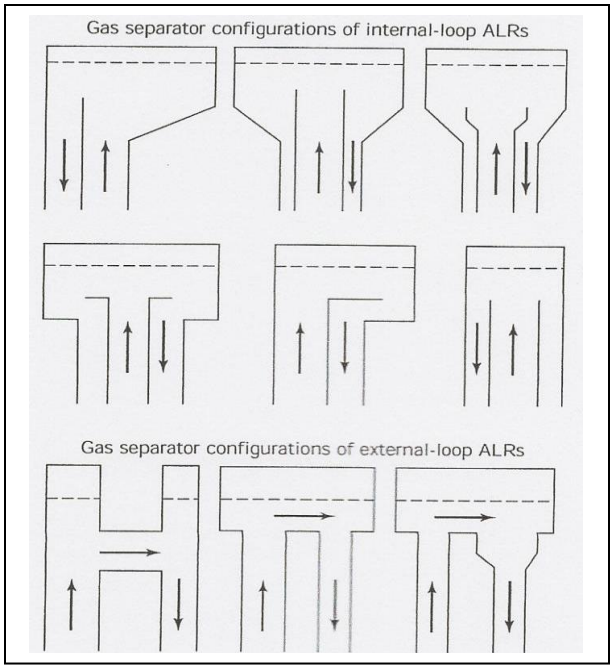

Figure 2.5 Types of gas disengagement tanks (Merchuk and Gluz, 2002).

Depending on how the gas disengagement zone connects the riser to the downcomer, the external loop airlift reactor can either be called a closed channel external loop airlift reactor or an open channel external loop reactor (Figure 2.6).

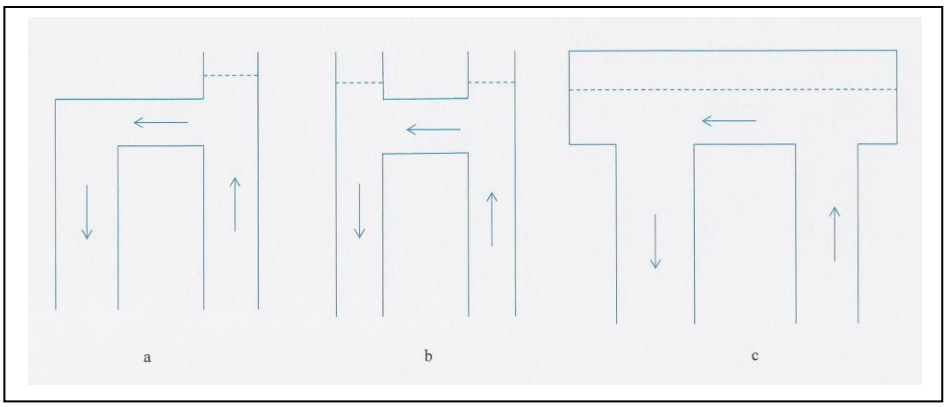

Figure 2.6 (a) and (b) closed channel (c) open channel. (a) – also referred to as a tube separator.

The base connects the riser and downcomer at the bottom and facilitates the recirculation of the liquid from the riser to the downcomer. The design of the base is especially significant in a rectangular airlift reactor. Should the base also have a rectangular shape, a dead-zone would develop at the bottom corners (Chisti, 1989). This can be overcome by changing the shape to a circular bend or positioning a prism into the corner to simulate a curved bend. Chisti (1989) also states that the length of the base affects the liquid circulation which is also noted by Merchuk et al. (1994) and Kodic et al. (1983) cited in Merchuk and Gluz (2002).

Although each zone in the airlift reactor has different flow behaviour and patterns which affect heat and mass transfer, all of them influence characteristics and performance in other zones as they are all interconnected (Merchuk and Gluz, 2002).

2.3.1. FLOW REGIMES

As stated in section 2.1 of this chapter, the hydrodynamics in airlift reactors have a significant effect on the heat and mass transfer characteristics of the reactor. This arises from the complex interdependence of the liquid and entering gas in the reactor. Circulation in the reactor is achieved by the change in density of the liquid in the riser created by the entering gas. This density change creates a pressure differential between the riser and downcomer which initiates liquid flow in the reactor. As the gas flowrate increases, different flow regimes and flow patterns can be observed.

At low flowrates of entering gas, small uniformly distributed bubbles will rise in straight lines up the reactor riser from the sparger. According to Kadic and Heindel (2014), the bubble diameter is controlled by the sparger design and the liquid properties. There is little to no interaction between the bubbles at this stage. This is called the homogeneous/bubbly (Figure 2.7a) flow regime (Kadic and Heindel, 2014; Martínez and Silva, 2013; Chisti and Moo-Young, 1987). This regime is ideally suited to some biochemical processes (Kadic and Heindel, 2014). In this regime the gas phase in most cases disengages completely from the liquid phase in the gas disengagement zone.

As the gas flowrate is increased, the amount of bubbles or gas holdup increases linearly in the riser. This in turn results in an increased liquid circulation velocity due to a greater density difference between the riser and downcomer. The bubbles in the riser do not flow in a straight path up the riser. Instead they tend to begin to follow a random path resulting in interaction between bubbles. This collision between bubbles results in coalescence which creates a slightly greater turbulence in the liquid. These coalesced bubbles also tend to break and reform randomly. This regime is known as the transition regime (Figure 2.7b) and precedes the fully developed churn turbulent regime (Kadic and Heindel, 2014; Merchuk and Gluz, 2002; Schürgerl and Lübbert, 1995; Chisti and Moo-Young, 1987). León-Becerril et al. (2002) cited in Kadic and Heindel (2014) reported that a more defined and shorter transition regime occurs at higher superficial gas velocities if the homogeneous regime was stable.

In the churn turbulent regime (Figure 2.7c), bubble sizes vary from a few millimeters to a few centimeters. Due to the turbulence in this regime the larger bubbles do not have a distinctive shape. The coalesced bubbles constantly vary in shape and sometimes rapidly break up into smaller bubbles and reform. The churn turbulent regime is considered the ideal regime for industrial applications as it has greater mixing and better gas holdup (Ruzicka et al., (2001a) cited in Kadic and Heindel, 2014) to give higher mass transfer.

At even higher gas flowrates, there are small bubbles but there is an increase in the number of large bubbles. The large bubbles are either spherical caps or bullet nose in shape (Chisti and Moo-Young, 1987). These types of bubbles are more pronounced in smaller diameter columns and lead to slugging in viscous fluids. This is called the slug flow regime (Figure

2.7d). Figure 2.7a-d, clearly shows the changing bubble flow behaviour as the gas flowrate increases in the riser that characterizes the different flow regimes in airlift reactors.

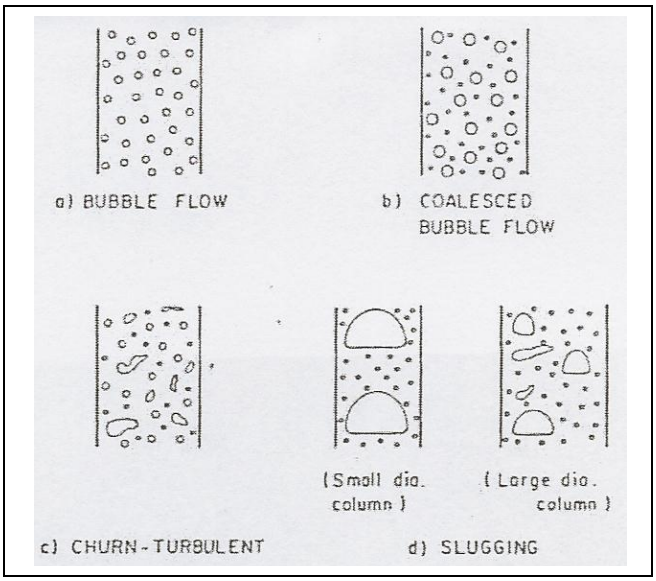

Figure 2.7 Flow regimes (Chisti and Moo-Young, 1987).

The occurrence of these regimes is not exactly known in each application as they are dependent on the superficial gas flowrate (see Section 2.4.1 for definition), the properties of the fluid and the reactor geometry (Kadic and Heindel, 2014; Chisti and Moo-Young, 1987). However, flow regime maps exist for bubble columns, Figure 2.8 (Viswanathan, 1986; Chisti and Moo-Young 1987).

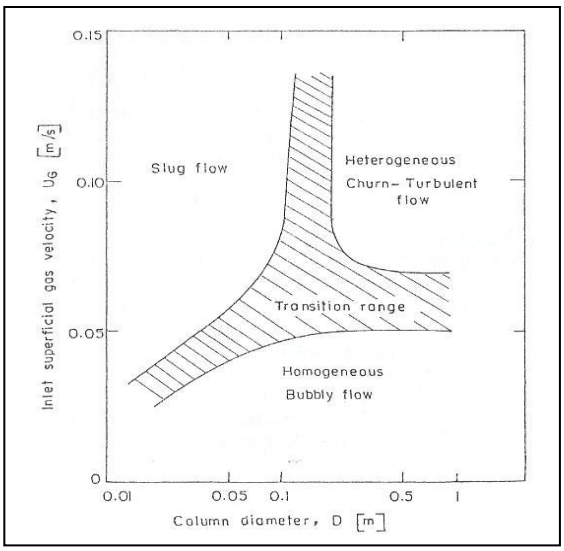

Figure 2.8 Flow regimes for bubble columns (Viswanathan, 1986).

The method that can be used to determine the change from homogeneous regime (Figure 2.7a and b) to transition regime is the drift-flux model of Zuber and Findley (1965). This method is more efficient for airlift reactors than bubble columns (Vial, et al., 2001). The method of Zuber and Findley (1965) consists of plotting the ratio of the superficial gas velocity, U_{SGR}, to the gas holdup, ε_{GR}, against the sum of the superficial liquid, U_{SLD}, and gas velocities, U_{SGR}. The change in the slope of the curve is indicative of the change in regime. These parameters have the following relation:

$$\frac{U_{SGR}}{\varepsilon_R} = C_o(U_{SGR} + U_{SLD}) + C_1 \qquad 2.11$$

The distribution parameter, C_o, is approximately equal to 1 indicating uniform radial flow when in the homogenous regime. In the transition regime the values for the distribution parameter increase to above 1 indicating a significant non-uniform radial flow. This is due to a macro-circulation pattern which disappears when the heterogeneous regime (Figure 2.7c) is established (Al-Masry, 2004; Vial et al., 2000; Guo and Rathor, 1997). In the heterogeneous regime the value of C_o decreases to values close to 0.8, indicating non-uniform flow but not as severe as the transition regime. Vial et al. (2002) also reported that the geometry or liquid

velocity has no effect on the regimes transitions when there is complete de-aeration of the riser fluid.

Due to the dependence of regimes on the superficial gas flowrate, a plot of superficial gas velocity against the superficial liquid velocity will be indicative of the regime change by the change of the slope of the graph. Visual observations with regards to dispersion will also give a better understanding of different regimes and therefore assist with better design and modeling of the reactor (Vial, et al., 2001).

2.3.2. FLOW VISUALIZATION STUDIES

Identifying flow regimes plays an important role in helping to obtain optimal mixing and heat and mass transfer characteristics. However, in airlift reactors flow regimes alone cannot explain the complex flow patterns that occur. Observational studies therefore also play a very important role in understanding the behavioral characteristics of the fluids within a reactor (Martinez, 2013; Chisti, 1989; Chisti and Moo-Young, 1987; Viswanathan, 1986). Physically observing flow patterns in an airlift reactor can provide insight into solid and gas dispersion patterns, dead-zones, areas of extreme turbulence, sparger location, effects of height of liquids in the disengagement zone and bubble velocity. These studies also give insight to the effects of reactor geometry and sparger design on the liquid and bubble flow patterns. Chisti (1989) and Chisti and Moo-Young (1987) state that very little information is available on flow visualization studies in airlift reactors. Chisti and Moo-Young (1987) reported on flow visualization studies on their internal loop airlift reactors. They found that the base plays a significant role in the recirculation of the bubbles from the downcomer to the riser. They were able to propose that the base cross section in internal loop airlift reactors should not exceed 1.65 times the downcomer cross section although this is not critical for external loop airlift reactors. They reported that detailed examinations need to be done to gain a better understanding of airlift reactors.

2.4. GAS-LIQUID HYDRODYNAMICS IN AIRLIFT REACTORS

The hydrodynamic parameters in airlift reactors that are of interest in this study are the riser and downcomer gas holdups, superficial liquid velocity and mass transfer coefficient. Calculations of these parameters are done from first principles. All three parameters are dependent on the incoming superficial gas flowrate and reactor geometry (Jones and Heindel, 2010; Ghosh et al., 2010; Yazdian et al., 2009; Gavrilescu and Tudose, 1997; Rajarajan et al., 1996; Wenge and Moo-Young, 1994; Kemblowski et al., 1993; Chisti, 1989; Merchuk, 1986).

2.4.1. SUPERFICIAL GAS VELOCITY

The gas enters the airlift reactor via a sparger at the entrance to the riser at a volumetric flowrate. To convert to superficial gas velocity (as defined in Chapter 1), the entering air flowrate is divided by the cross sectional area of the riser:

$$U_{SGR} = \frac{Q_{gas}}{A_R} \qquad 2.12$$

Where Q_{gas} is the volumetric gas flowrate.

The superficial gas velocity is sometimes referred to as the gas velocity in airlift reactors.

2.4.2. SUPERFICIAL LIQUID VELOCITY (CHISTI, 1989)

Liquid circulation is achieved by the difference in the bulk densities of the fluid between the riser and downcomer created by the entering gas. The liquid circulates along a clearly defined path i.e. upward flow in the riser and downward flow in the downcomer. To determine this mean liquid circulation velocity in an airlift reactor requires that the entrained bubbles be ignored. This is not possible in the riser resulting in various techniques being developed to detect mean liquid circulation velocity in the downcomer. Methods such as the tracer response technique, flow-followers, magnetic and ultrasonic flow measuring devices and the paddle wheel meters can be used.

The most common technique employed to determine the liquid superficial velocity is the tracer response technique (Chisti, 1989; Gavrilescu and Tudose, 1998; Merchuk and Gluz, 1999). This method involves the measurement of conductivity by the injection of a salt solution of known concentration over a measured distance.

The resulting mean circulation velocity, $\overline{U}_{Lc}$, and can be written as

$$\overline{U}_{Lc} = \frac{x_c}{t_c}$$

2.13

Where x_c = circulation path

t_c = average time for one complete circulation

Although it is useful to have an overall liquid velocity, it is more meaningful to have the liquid superficial velocities for the riser, U_{SLR}, and downcomer, U_{SLD} expressed as

$$U_{SLR}\, A_R = U_{SLD}\, A_D$$

2.14

Where A_R = cross sectional area of the riser and

A_D = cross sectional area of the downcomer.

The true linear liquid velocity (interstitial velocity), $\dot{V}_{LR}$, is related to the superficial velocity in the riser:

$$\dot{V}_{SLR} = \frac{U_{SLR}}{1 - \varepsilon_R}$$

2.15

Where ε_R = the riser gas holdup (see section 2.4.3).

And for the downcomer

$$\dot{V}_{SLD} = \frac{U_{SLD}}{1 - \varepsilon_D}$$

2.16

Where ε_D = downcomer gas holdup (see section 2.4.3).

By combining equations 2.14, 2.15 and 2.16, the relation between the liquid circulation velocity on the riser gas holdup is noted (Contreras, et al., 1998):

$$\varepsilon_D = \frac{\dot{V}_{SLR} A_R}{\dot{V}_{SLD} A_D} \varepsilon_R - \left(\frac{\dot{V}_{SLR} A_R}{\dot{V}_{SLD} A_D} + 1 \right)$$

2.17

Or

$$\varepsilon_D = \alpha \varepsilon_R - \beta$$

2.18

Where $\alpha = \frac{\dot{V}_{SLR} A_R}{\dot{V}_{SLD} A_D}$ and $\beta = \alpha + 1$

Contreras et al. (1998) notes that in literature, the above equation is sometimes written as

$$\varepsilon_D = \alpha \varepsilon_R$$

2.19

This they report is not valid as it indicates that when α is 1 the gas holdup in the riser is equivalent to the gas holdup in the downcomer which means that there is no liquid circulation.

2.4.3. GAS HOLDUP (CHISTI, 1989)

The gas holdup is defined as the volume fraction of the gas phase in the gas-liquid or gas-liquid-solid system in airlift reactors. It is the key variable in the design of airlift reactors as

the total design volume of the reactor is dependent on the maximum gas holdup. The gas holdup also influences residence time, bubble size and gas-liquid interfacial area. Asides from the geometric design of the reactor, the mass transfer coefficient is also affected by the gas holdup.

The overall gas holdup, ε, is the total fraction of gas that is present in the entire reactor volume. The total gas holdup in the reactor is calculated as:

$$\varepsilon = \frac{V_G}{V_G + V_L}$$

2.20

Or

$$\varepsilon = \frac{h_D - h_L}{h_D}$$

2.21

Where V_G = volume of gas

V_L = volume of liquid

h_D = expanded liquid height (aerated liquid)

h_L = static liquid height (non-aerated liquid).

Although the gas holdup is significant in the bubble column, in airlift reactors the riser and downcomer gas holdups are more important. The riser and downcomer gas holdups are average values integrated along the entire length of the riser or downcomer. To determine the riser and downcomer gas holdup, the pressure difference across the riser and downcomer is measured using the manometric method. The gas holdup for the entire riser or downcomer is calculated from first principles in Chisti (1989):

$$\varepsilon = \frac{\rho_L}{\rho_L - \rho_G} \frac{dh_m}{d\hat{z}}$$

2.22

Where ρ_L = density of the liquid

ρ_G = density of the gas

dh_m = difference in manometer liquid height

$d\hat{z}$ = distance between manometer tappings

The riser and downcomer gas holdups are related to the overall gas holdup by the total volume in the reactor. A balance equation for the amount of gas in the reactor is taken. If the riser and downcomer have uniform cross sections then the overall gas holdup is related to the riser and downcomer gas holdups by

$$\varepsilon = \frac{A_R\,\varepsilon_R + A_D\varepsilon_D}{A_R + A_D} \qquad 2.23$$

Where A_R and A_D are the cross sectional areas of the riser and downcomer respectively. Although this method is exact for internal loop airlift reactors, it can also be used for external loop airlift reactors if the dispersion heights in the riser and downcomer are equal.

2.4.4. MASS TRANSFER COEFFICIENT (MOUTAFCHIEVA et al., 2013; CHISTI, 1989)

Equation 2.10 illustrated the relationship between the mass transfer coefficient, $k_L a_L$, and the oxygen transfer:

$$\frac{dC_L}{dt} = k_L a_L\,(C^* - C_L) \qquad 2.10$$

The mass transfer coefficient is time invariant. The above equation can be integrated from time $t = 0$ to $t = t$. Therefore equation 2.10 becomes:

$$ln\frac{C^* - C_{LO}}{C^* - C_L} = k_L a_L t$$

2.24

Where C^* = steady state (or saturation) dissolved oxygen concentration

C_{LO} = dissolved oxygen concentration at time $t = 0$

C_L = changing dissolved oxygen concentration with t.

By using the fractional approach to equilibrium defined as the ratio of the instantaneous mass transfer to the maximum possible transfer (E), i.e. the ratio of the mass transfer ($C_L - C_{LO}$) to the maximum possible transfer ($C^* - C_{LO}$):

$$E = \frac{C_L - C_{LO}}{C^* - C_{LO}}$$

2.25

Equation 2.24 then becomes:

$$-\ln(1 - E) = k_L a_L t$$

2.26

At initial conditions the oxygen is zero, i.e. $E = 0$ and at saturation, $E = 1$. The mass transfer coefficient can then be determined as the slope of the semilog plot of ln $1/(1 - E)$ versus time.

2.5. EFFECTS OF SUPERFICIAL GAS VELOCITY ON GAS HOLDUP, LIQUID CIRCULATION VELOCITY AND MASS TRANSFER

The superficial gas velocity is the driving force in an airlift reactor. It influences the gas holdup and liquid circulation velocity which in turn affect the mass transfer characteristics in the reactor. Many studies have been done to investigate the hydrodynamics of internal and external loop airlift reactors, with the majority of studies done on laboratory scale devices. There are a number of correlations (Table 2.1 and 2.2) that have been developed with respect

to mass transfer and gas holdup, based on riser behaviour and conditions or based on global behaviour patterns in the airlift reactors. There is some agreement on the dependence of the superficial liquid velocity, gas holdup and mass transfer on the superficial gas velocity. These will be briefly summarized here with correlations noted in Table 2.1 and Table 2.2.

In the investigation by Wang et al. (2003), a mini-scale external loop airlift reactor was used to characterize the gas holdup, liquid circulation velocity and mass transfer. They found that at low superficial gas flowrates there is an increase in gas holdup due to the wall effects created by the size of the device which resulted in lower bubble rise velocities. A comparison of the riser and downcomer liquid velocities were done at varying gas flowrates using a correlation by Nakao et al. (1988) (cited in Wang et al. (2003)). They found good agreement between the correlated value and the observed values even though the type of reactor and conditions of Nakao et al. (1988) (cited in Wang et al. (2003)) were different to their investigations. With regards to the mass transfer coefficient they found that as the gas holdup increased the mass transfer coefficient also increased due to the viscosity.

In the study by Fakhari et al. (2014) a laboratory scale external loop airlift reactor was used to investigate the mass transfer with oily micro-emulsions. They found that there was an increase in the gas holdup for increasing superficial gas velocity however the rates were higher for the oily micro-emulsions than for pure water systems. This phenomenon was explained by considering the surface tension and coalescence of the micro-emulsions compared to only water. They reported that the viscosity increased the gas holdup and was due to the increased drag and resistance to the rising velocity of the bubble. Due to the bubble rise resistance caused by the viscosity of the solution, the liquid circulation velocity also decreased as liquid circulation is dependent on gas flow. They also found that the mixing time decreased for the increasing gas flowrate for the micro-emulsions when compared to water. The water system had longer mixing times and an increased liquid velocity. With regards to the mass transfer, the coefficient was higher for the emulsion than for water as the surface tension is lower in the micro-emulsion than water. This resulted in reduced bubble size and an increased surface area for the micro-emulsion which resulted in improved mass transfer. The increasing concentration of the emulsions however reduced the mass transfer coefficient as the viscosity of the solution increased. Wilke and Chang (1955) (cited in Fakhari et al. (2014))

reported that the viscosity plays a significant role in the overall mass transfer in the system. As the viscosity increased the coalescence of bubbles also increased which results in a decrease in the mass transfer area. The increased viscosity also influences the thickness liquid boundary layer and reduces the solute diffusivity. This results in a decrease in the mass transfer coefficient. Fakhari et al. (2014) developed correlations for the gas holdup and mass transfer coefficient based on their study (Table 2.1.).

Yazdian et al. (2009) investigated the effect of geometry, gas properties and operation parameters on hydrodynamics and mass transfer in a laboratory scale external loop airlift reactor for the production of natural gas from biomass. They found two zones for the mixing time that is dependent on the gas velocity. At low velocities there is less mixing time but at higher velocities the mixing time is constant. For the gas holdup they found that an increase in viscosity meant a decrease in gas holdup but at increased gas velocity it also increased. However at higher flowrates this did not matter. With regards to the mass transfer, they found that an increase in viscosity resulted in a decreased mass transfer and that the diffusion coefficient of the gas in water affects mass transfer significantly which is in agreement with Fakhari et al. (2014). They concluded that the separator, area ratio, diffusion coefficient and the liquid viscosity has a significant effect on gas holdup, mass transfer and mixing time.

Nikakhtari and Hill (2005) used a laboratory scale external loop airlift reactor with a packed mesh bed to investigate the hydrodynamics and mass transfer. The mesh packing was situated in the riser. They found that the packing improved the mass transfer by increasing the gas holdup as it reduced the bubble size and decreased liquid circulation as compared to the reactor without the packing. They developed a correlation for oxygen transfer for the reactor with and without the packing.

In the investigation by Guo et al. (1997) the effects of the solids holding, aspect ratio, perforated mesh and particle density on the gas holdup, mixing time, superficial liquid velocity and fluidized bed expansion was studied at varying superficial gas velocities. They used a laboratory scale external loop airlift reactor with a tube vent separator and a fluidized bed. The sparger was located in the upper region of the riser and fluidized bed was positioned below the sparger. With their design the gas holdup increased for increasing superficial gas velocities even with an increase in solids loading which was not the case in Freitas and

Teixeira (1998) (Table 2.2) and Sivasubramanian et al. (2008) who used traditionally designed external loop airlift designs. Guo et al. (1997) also found that there was an increase in gas holdup with the implementation of the fluidized bed as compared to conventionally designed airlift reactors. When the airlift reactor was configured as a bubble column, they found that the gas holdup achieved was same as the minimum gas holdup as a traditionally designed airlift reactor.

The liquid circulation velocity increased as the superficial gas velocity increased but decreased as the solids loading increased. This they concluded was due to the increased drag which reduced the liquid circulation velocity. For a particular solids loading, the liquid circulation velocity decreased and the pressure drop increased. However in the solids free section of the reactor, they found that the following relation existed between the superficial gas and liquid velocities:

$$U_{SLD} = U_{SGR}^{0.24} \qquad 2.27$$

They found this relation to be in agreement with other authors cited by them. By reducing the aspect ratio, the superficial liquid velocity remained unchanged but in the gas-liquid-solid phase there was a reduction of the liquid velocity. This they reported was due to a shorter aerated height which drastically affected the driving force for liquid circulation.

For a given solids loading, the mass transfer coefficient increased with increasing superficial gas velocity. As the solids loading increased the mass transfer increased and as the terminal particle velocity increases so does the mass transfer coefficient. This was due to the resistance to flow by the solid particles. A decrease in superficial liquid velocity means a higher gas holdup which results in an increase in mass transfer coefficient because of the retention time.

Sivasubramanian et al. (2008) also investigated the effects of the superficial gas velocity on the solids loading, gas holdup and mass transfer of a laboratory scale external loop airlift reactor. In their study they found that the although the mass transfer increased with increasing gas velocity, it decreased with increasing solids loading which is in conflict with Guo et al. (1997). This may be due to the reactor design but is in agreement with Freitas and Teixeira

(1998). They also concluded for the water system that as the dissolved oxygen probe was moved along the riser with varying gas velocity, the mass transfer decreased away from the sparger. This was attributed to larger bubble sizes. With respect to the superficial gas velocity and mass transfer coefficient they noted the same effect as Rahman-Al Ezzi and Najmuldeen (2013) in that the mass transfer increased for increasing gas velocity for all three systems but that mass transfer decreased for increasing concentration of solutions due to high coalescence of highly viscous solutions which reduce mass transfer area. In their later study, Sivasubramanian and Naveen Prasad (2009) found that the gas holdup increases with increasing gas velocity due to the increasing alcohol concentration which reduced bubble rise velocity which was due to surface tension.

In the investigation by Luo et al. (2013), an annulus sparged laboratory scale reactor was used to determine the effects of a sieve plate in the riser on the gas holdup and mass transfer. This study was similar to the study by Guo et al. (1997) in that modifications were made to enhance the gas holdup and mass transfer. They found that the sieve plate decreased the bubble size thereby increasing gas holdup which resulted in an increase in the mass transfer. This was however only possible if an optimum pore size was found for the sieve plate. Too small pore size and the bubbles tend to not pass through and form an air pocket below the plate resulting in a resistance to flow which resulted in a decrease in gas holdup and mass transfer.

Shariati et al. (2007) and Gharib et al. (2013) (Table 2.2) also found that surface tension played a significant role in the laboratory scale draft tube and external loop airlift reactor respectively. An increasing concentration of alcohols (Gharib et al., 2013) and micro-emulsions (Shariati et al., 2007) resulted in an increase in gas holdup and mass transfer due to the increased bubble concentration of both solutions as the surface tension decreased. However, Rahman-Al Ezzi and Najmuldeen (2013) found in their electrolyte solutions that the surface tension did not affect the gas holdup and mass transfer but rather the ionic forces in the bulk liquid which reduced the bubble rise velocity and coalescence thereby increasing the gas holdup.

It can be concluded that the increase in surface tension and viscosity increases the gas holdup but decreases the mass transfer of the system (Fakhari et al., 2014; Rahman-Al Ezzi and Najmuldeen, 2013; Gharib et al., 2013; Sivasubramanian et al., 2008; Shariati et al., 2007).

However, in the studies by Bentifraouine et al. (1999) and Rajarajan et al. (1996) on laboratory scale external loop airlift reactors, they found that there is an increase in gas holdup and liquid circulation velocity with an increasing superficial gas flowrate and that Rajarajan et al. (1996) notes that although the gas holdup increased with an increase in viscosity, it will decrease after reaching a critical viscosity value. Ghosh et al. (2010) (Table 2.2) also had the same findings for gas holdup and superficial gas velocity in their laboratory scale external loop airlift reactor.

Table 2.1 Summary of mass transfer correlations

Author	Reactor type	Parameters	Correlations
Wang et al. (2003)	ELALR		$k_L a_D = k_L a \left({}^{V_L}/_{V_{D,R}} \right)$
Fakhari et al. (2014)	ELALR	D_R: 0.1m D_D: 0.07m H_R: 1.7m H_D: 0.995m h_L: 1.215m A_D/A_R: 0.49	$\frac{\varepsilon}{(1-\varepsilon)^4} = 0.361 Bo^{0.125} Ga^{0.0218} Fr^{0.961}$ 2.027<Bo<2.173; 179.091<Ga<77548.257; 0.013<Fr<0.067 Mass transfer coefficient expressed using dimensionless numbers: $Sh = 0.00123 Re^{0.938} Sc^{0.881} Bo^{0.426}$ 14.742<Re<339.913; 3853.593<Sc<55942.303; 2.027<Bo<2.172
Yazdian et al. (2009)	ELALR	$H_{Reactor}$: 2.4m D_R: 0.01 &-0.09m H_R & H_D: 2.20m D_D : 0.03m $D_{gas\ separator}$: 0.11-0.18m Inlet gas – oxygen & CH_4	$\varepsilon_R = 13.19 U_{SGR}^{1.43} \left(1 + \frac{A_R}{A_D}\right)^{-0.62} (1+S)^{-0.58} \left(\frac{\mu_{gas}}{\mu_{N_2}}\right)^{-0.52}$ $k_L a = 0.097 U_{SGR}^{0.46} \left(1 + \frac{A_R}{A_D}\right)^{-0.63} (1+S)^{-0.61} \left(\frac{\mu_{gas}}{\mu_{N_2}}\right)^{-0.91} \left(\frac{D_{gas}}{D_{N_2}}\right)$

Nikakhtari and Hill (2005)	ELALR	Laboratory scale	$k_L a = 0.531 U_{SGR}^{0.762}$ For ELAB with packed bed; At low superficial gas velocities: $k_L a = 2.530 U_{SGR} - 0.003$ With packing $k_L a = 0.7369 U_{SGR} - 0.00005$ Without packing
Guo et al. (1997)	ELALR	Fluidized bed height – 0.49m D_R: 0.06 m H_R: 0.867m D_D: 0.06m H_D: 1.375m A_D/A_R: 1	$\varepsilon = 101.96 U_{SGR}^{0.338} \varphi^{0.581} \left(1 - \rho_L/\rho_p\right)^{0.514}$ ε in % $U_{SLD} = 0.2041 U_{SGR}^{0.94} \varphi^{-1.393} \left(1 - \rho_L/\rho_p\right)^{-0.866}$ $t_m = 424.8 U_{SGR}^{-0.871} \varphi^{1.448} \left(1 - \rho_L/\rho_p\right)^{0.8}$ $\varepsilon = (0.493 \varepsilon_{LF} + 0.483) \varphi^{1.029} \left(1 - \rho_L/\rho_p\right)^{1.025}$ $k_L a = 4.49 U_{SGR}^{0.384} \varphi^{0.595} \left(1 - \rho_L/\rho_p\right)^{0.337}$
Sivasubramanian et al. (2008)	ELALR	$H_{Reactor}$: 2.6m D_R : 0.084m Perforated plate: 243 1mm diameter holes Water; glycerol; CMC	$\varepsilon_R = 18.528 U_{SGR}^{\left(1.068 + 6.16 \times 10^{-5} \varphi\right)}$ $U_{SLD} = U_{SLR} = 2.012 U_{SGR}^{\left(0.4569 - 1.52 \times 10^{-4} \varphi\right)}$ $k_L a = 0.204 U_{SGR}^{0.782} \mu^{-0.595}$ Correlations for air-water

Rahman-Al Ezzi and Najmuldeen (2013)	Laboratory scale ILALR	$D_{draft\ tube}$: 0.045m $D_{reactor}$: 0.9m $H_{draft\ tube}$: 0.9m A_D/A_R: 0.249	$\varepsilon_R = \frac{h_D - h_L}{h_D - \left(V_i/S_O\right)}$ $k_L a = \frac{-2.303(1-\varepsilon_R)}{t} Log \frac{C^* - C_L}{C^* - C_o}$
Sivasubramanian and Naveen Prasad (2009)	ELALR	$H_{Reactor}$: 2.6m D_R: 0.084m Perforated plate with 243 1mm diameter holes Fluids – alcohol solutions	$\varepsilon_R = 18.577 U_{SGR}^{\left(0.984+1.16\times10^{-4}\varphi\right)} \sigma^{0.05} \rho_L^{-0.038} \mu_L^{0.996}$ $U_{SLD} = U_{SLR} = 2.72 U_{SGR}^{\left(0.384+6.52\times10^{-5}\varphi\right)} \sigma^{-0.0096} \rho_L^{-0.0034} \mu_L^{0.997}$ For $0 \leq U_{SGR} \leq 0.033$
Luo et al. (2013)	ILALR	$H_{reactor}$: 1.3m $D_{reactor}$: 0.284m H_R : 0.82m D_R : 0.07m Sieve plates	$\varepsilon_o = 107.72 d^{-0.21} \beta^{-0.16} n^{0.21} U_{SGR}^{0.75}$ $k_L a = 0.35 d^{0.19} \beta^{0.13} n^{0.48} U_{SGR}^{0.86}$
Shariati et al. (2007)	Draft tube ALR	$H_{draft\ tube}$: 1.1m $D_{draft\ tube}$: 0.1m $D_{reactor}$: 0.14m A_D/A_R : 0.906 Perforated pipes (ladder type) 25 1mm holes	$\varepsilon = 4.92 (U_{SGR})^{1.066} \mu^{-0.355}$ $U_{SLD} = 6.903 U_{SGR}^{0.703} \mu^{-0.264}$ $t_c = 0.278 U_{SGR}^{-0.662} \mu^{0.34}$ $t_m = 1.239 U_{SGR}^{-0.458} \mu^{0.325}$ $k_L a = 1.552 U_{SGR}^{0.935} \mu^{-0.683}$

Bentifraouline et al. (1999)	laboratory scale ELALR	D_R: 0.194m D_D: 0.092 $H_{reactor}$: 1.6m	
Rajarajan et al. (1996)	laboratory scale ELALR	D_R: 0.095m H_R; H_D: 2.3m D_D: 0.06m	
Šijački, et al. (2009)	Bubble Column and Draft Tube ALR		$y = p_1 U_{SGR}^{p_2} (1 + C_N)^{p_3}$ $y = \varepsilon_G, t_c, U_{SLD}, k_L a$
Lu, et al. (2000)	Modified square ALR (MSALR) and round ALR (RALR)	MSALR: A_D/A_R: 0.695; 0.3; 0.11 H_R : 1.45 RALR: H_R : 1.08 & 1.45m Fluid: tap water	MSALR: $\varepsilon = 0.046 U_{SGR}^{0.58} \left(\frac{A_R}{A_D}\right)^{-0.072}$ $U_{SLD} = 0.114 U_{SGR}^{0.557} \left(\frac{A_R}{A_D}\right)^{-0.073}$ $t_m = 53.15 U_{SGR}^{-0.377} \left(\frac{A_R}{A_D}\right)^{-0.269}$ RALR: $\varepsilon = 0.035 U_{SGR}^{0.647} \left(\frac{A_R}{A_D}\right)^{-0.085}$ $U_{SLD} = 0.124 U_{SGR}^{0.537} \left(\frac{A_R}{A_D}\right)^{0.08}$ $t_m = 45.75 U_{SGR}^{-0.377} \left(\frac{A_R}{A_D}\right)^{-0.319}$

Table 2.2 Summary of gas holdup correlations.

Author	**Reactor type**	**Parameters**	**Correlations**
Freitas and Teixeira (1998)	Draft tube – enlarged degassing zone		$\varepsilon_R = av_R^2 + bv_R + c$
Gharib et al. (2013)	ELALR	H_R: 1.7m D_R: 0.1m H_D: 0.995m D_D: 0.07m h_L : 1.215m Ceramic ball sparger 2cm diameter	$\varepsilon = a_s\, U_{SGR}^{b}\, C_{alcohol}^{c}$
Ghosh et al. (2010)	ELALR & Modified ALR	ELALR: D_R: 0.37m $D_{D:}$:0.5m $H_{reactor}$: 0.74m Modified ALR:D_R: 0.25 & 0.5m D_D: 0.5m $H_{reactor}$: 0.74m	$\varepsilon_R \propto U_{SGR}{}^{0.45}$

Chisti (1989)	ELALR	A_D/A_R : 0.25; 0.44 Fluid: water; aqueous salt solutions	$\varepsilon_D = 0.460\varepsilon_R - 0.024$
Chisti et al. (1995)	Annulus sparged concentric tube ALR	Outer tube diameter- 0.152m A_D/A_R : 0.13; 0.35; 0.56 h_D : 1.8m Height draft tube: 1.55m Fluid: water	$\varepsilon_R = \frac{U_{SLD}^2 \; K_B \left(\frac{A_R}{A_D}\right)^2}{2gH_D}$
Somnath and Someshwar (2015)	ILALR	Fluids: tap water and varying concentrations of methanol; ethanol; n-propanol; n-butanol	$\varepsilon = k \; U_{SGR}^m \; C_{alcohol}^n$

2.5.1. CONCLUSION

It can be concluded that many studies have been done to determine the effects of superficial gas velocity on mass transfer and hydrodynamic behaviour in airlift reactors. A review of which is also available in Kadic and Heindel (2014). However, understanding these behavioral characteristics of all the parameters and their interdependence on each other in airlift reactors is very complex. Many authors have not consolidated the available literature and at times comparisons are done on geometrically different reactors. This resulted in many conflicting theories put forward by researchers based on the researcher's interpretation and assumptions made during their investigations and analysis of their work. However, there is a common thread in all of this existing research. The reactor geometry (reactor size, sparger type) as well as the liquid properties (surface tension; viscosity and density) cannot be ignored. They will have to be taken into consideration simultaneously if a reliable correlation is to be developed as transferring knowledge onto pilot or industrial scale machines becomes an issue as the hydrodynamic behaviour and thus mass transfer characteristics change significantly with scale. However, due to these relationships being so complex, developing a correlation with the traditional approach of first knowing relationships between these parameters beforehand becomes very difficult.

2.6. EFFECTS OF REACTOR GEOMETRY ON GAS HOLDUP AND MASS TRANSFER

2.6.1. GAS SPARGERS

Air injection into an airlift reactor occurs via a sparger. The gas spargers are classified into two broad categories, viz., static spargers and dynamic spargers (Figure 2.9). Static spargers are the most common and are easy to use and cost effective to manufacture. Perforated plates and pipes, porous plates and single-hole spargers make up static spargers (Kadic and Heindel, 2014; Jones, 2007; Chisti, 1989; Chisti and Moo-Young, 1987). Of these, perforated plates and pipes are recommended for industrial or large scale operations as porous plates tend to clog and have higher pressure drops (Kadic and Heindel, 2014; Chisti and Moo-Young, 1987) and are suitable for laboratory scale applications. The single orifice spargers, although providing uniform gas flow at a greater distance away from the injection point, is at most times unstable (Kadic and Heindel, 2014).

Dynamic spargers are characterized by injector nozzles and venturies that depend on the kinetic energy of the liquid jet to help disperse the gas bubbles (Chisti and Moo-Young, 1987; Jones 2007). These types of spargers are not suitable for shear sensitive systems and are complex to design and manufacture. They also require external liquid circulation in the form of a pump.

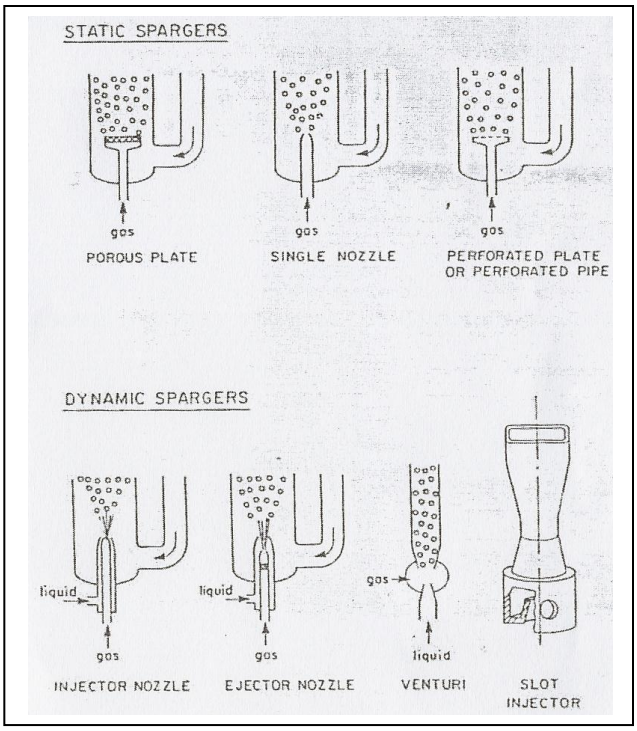

Figure 2.9 Gas Spargers (Chisti and Moo-Young, 1987).

Kulkarni et al. (2009) further classified static spargers into plate and pipe spargers. Perforated plate, sieve plates, sintered plate etc. fall under plate type spargers while straight pipe, ring spargers, ladder type and spider type spargers fall under pipe type spargers.

When selecting sparger category and design, it is important to take into consideration the process requirements, operational and fabrication considerations. The sparger design should be optimal to provide the best mass transfer characteristics for the process under investigation. Weeping, pore size, bubble size, pressure drop and gas exit velocities from the sparger are important parameters to consider. Weeping is when liquid enters the sparger pore after the bubble has left. In orifice spargers this occurs immediately when the bubble leaves. In pipe design spargers there is inconsistent flow through all pores at any one time. This

inconsistency occurs when the kinetic energy of the gas is not sufficient enough to support the liquid head above the sparger holes (Kulkarni et al., 2009). Weeping occurs through the pores from which bubbles do not exit. This would make pipe type spargers unsuitable for mass transfer operations. However, Kulkarni et al. (2009) reports that plate type spargers are mostly used for small diameter columns while pipe type spargers are used for large diameter columns. The pore size also plays a significant role in the available surface area for mass transfer as it influences to an extent, the size of bubbles emerging from the sparger (Kadic and Heindel, 2014). A generalized procedure for sparger design is unavailable, however Kulkarni and Joshi (2011), Kulkarni et al. (2009) and Kulkarni (2005) have done a fair amount of work to arrive at a possible design procedure, especially for pipe type spargers and Ruff et al. (1978) proposed a design procedure for perforated plate spargers to ensure flow through all pores.

2.6.1.1. SPARGER LOCATION

The location of the sparger in the riser in an airlift reactor is very significant. Locating the sparger at the base of the riser is not ideal as the returning fluid from the downcomer tends to result in the entering gas stream from the sparger being distributed towards the opposite wall of the riser as illustrated in Figure 2.10(a) and (b) below (Chisti and Moo-Young, 1987; Kadic and Heindel, 2014).

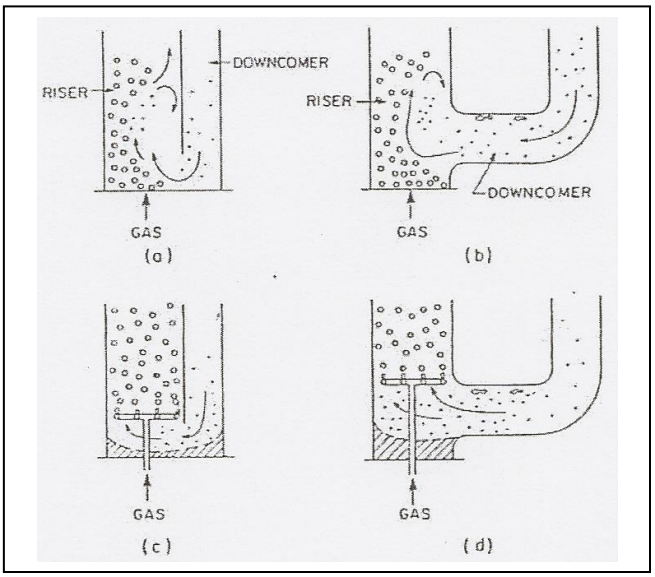

Figure 2.10 Location of sparger influence on gas distribution (Chisti and Moo-Young, 1987).

Positioning the sparger on the central horizontal axis of the base also results in poor distribution (Figure 2.11).

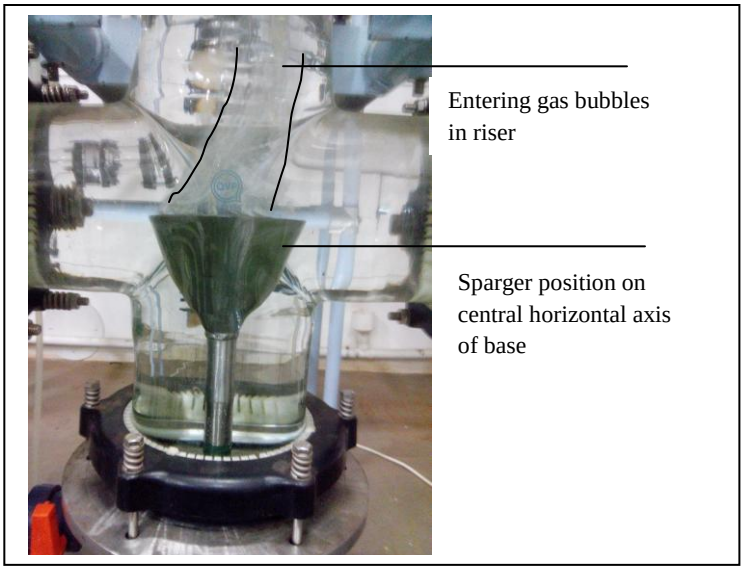

Figure 2.11 Poor Dispersion on the central horizontal axis of the base.

The bubbles only disperse across the cross section of the riser by turbulence further up the riser. The maximum height of these channels is not more than 1m (Chisti and Moo-Young,

1987). This was also observed in the initial studies in this investigation. The most suitable position of the sparger is at the entrance to the riser as illustrated in Figure 2.10 (c) and (d).

2.6.1.2. EFFECTS ON GAS HOLDUP AND MASS TRANSFER

There are many sparger designs that are available for the airlift reactors as reported by Chisti and Moo-Young (1987) and Kulkarni et al. (2009). Of the sparger designs that are available the perforated plate and sintered/porous plate spargers are recommended (Lin et al., 2004; Chisti, 1989) for their better distribution and bubble size characteristics (Luo et al., 2011) and reduced shear effects.

However, there exists many conflicting views on the effects of sparger design on gas holdup and mass transfer in either the bulk flow or local flow in airlift reactors (Kulkarni et al., 2009; Lin et al., 2004; Luo et al., 2011; Chisti, 1989; Contreras et al., 1999; Kojić et al., 2015; Salehi et al., 2014; Snape et al., 1995; Gavrilescu and Tudose, 1997; Kemblowski et al., 1993; Merchuk, 1986a and 1986b; Merchuk and Stein, 1981), a summary of correlations which appear in Table 2.3.

In the study by Snape et al. (1995) (Table 2.3) in an external loop airlift reactor using two perforated plate spargers with pore size diameters of 0.5mm and 1.6mm respectively, they reported that liquid height, liquid properties and sparger design affect gas holdup. Yet in their previous study, Snape et al (1992) cited in Snape et al. (1995), they reported that sparger design, free plate area and decreasing pore size, had no effects on the gas holdup. They concluded in Snape et al. (1995) that the liquid phase properties and design of the sparger are not independent properties and need to be considered together for reactor design. All three parameters, liquid height, sparger design and liquid properties need to be carefully selected when it comes to creating a balance between all parameters and sacrifices may have to be made in terms of one in place of the others.

In the study by Gavrilescu and Tudose (1998 Part 1) a comparative study was done on a bench scale and pilot scale airlift reactor using air-water as well as non-newtonian fluids. A porous plate sparger was used in the bench scale reactor and a multi-radial sparger was used in the pilot scale reactor. They found that the sparger design did not affect the gas holdup but that

the type of fluid, area ratio especially and the liquid height in the riser to the downcomer affected the gas holdup. This study raises a few questions. Both systems are geometrically different with respect to sparger design and reactor design. It brings into question the reliability and validity of the conclusions drawn from this research.

In the study by Salehi et al. (2011), they used variations of the perforated pipe on a bench scale bubble column and found that the sparger influences the bubble size distribution which affects the gas holdup and mass transfer. Kulkarni et al. (2009) also reported that the sparger design influences the performance of bubble columns for a low aspect ratio.

Luo et al. (2011) also reported that the sparger influences the gas holdup and mass transfer. In their study of a bench scale annulus sparged internal loop airlift reactor using three different variations of a perforated plate sparger i.e. 4 orifice nozzle, o-ring and 2 orifice nozzle, they reported that their 4 orifice nozzle sparger produced the best gas holdup due to the smaller diameter hole size and increased number of holes compared to a 2 orifice nozzle. Their o-ring sparger should have produced the best gas holdup actually produced the lower mass transfer even though it had smaller diameter pore size and the most amount of holes. They proposed that this was due to the decrease in gas velocity through each pore as the number of pores was the greatest. This effect they stated reduced the impact between the gas phase and liquid phase which creates a larger bubble in the sparger region and therefore a decrease in gas holdup.

Kojić et al. (2015b), Contreras et al. (1999) and Lin et al. (2004) reported that at low gas velocities i.e. in the homogenous or bubbly flow regime, the sparger hole size has an effect on the bubble dispersion and coalescence. For porous plate sparger, the bubble size can remain the same until the transition zone from homogenous to heterogeneous flow regimes after which bubbles increase in size due to coalescence and turbulence. However, if non-coalescing liquids are used, the bubbles have fewer tendencies to increase in bubble diameter. With an increase in pore size for the porous plate the bubble size increases and therefore the gas holdup decreases. The perforated plate showed no effects on the bubble diameter in either the homogenous or heterogeneous regions. These authors concluded that the reactor geometry and fluid medium play a more important role in the gas holdup and mass transfer that the sparger design which is in agreement with Chisti (1989).

Kemblowski et al. (1993) investigated the effects of sparger design on two laboratory scale and one pilot scale external loop airlift reactors. They concluded that the gas sparger geometry effects were insignificant and that their proposed correlation for gas holdup was independent of sparger geometry.

In the articles by Merchuk (1986b) and Merchuk and Stein (1981) it was found that the sparger has a significant effect on the gas holdup and the liquid circulation velocity but that this depended on the reactor design, scale and setup. In Merchuk and Stein (1981) and Merchuk (1986b) although the gas holdup increases with the increasing gas velocity, the sparger design affected the gas holdup when the reactor was pressurized and the area ratio, A_D/A_R decreased. As the resistance to flow increased the gas holdup increased and reduced liquid circulation velocity. But in the study by Merchuk (1986a) the sparger had no effect on the gas holdup in a laboratory scale external loop airlift reactor. Here he found that the gas holdup is low at high gas velocities and that there was complete disengagement when the liquid velocity increased with gas velocity.

All the authors are in agreement that from their observations the effects of the sparger and geometry are very complex and that no general correlation can be proposed for airlift reactors which would make the design of airlift reactors easier. This situation has arisen as there has been no consolidation of the available literature to determine gaps in the body of knowledge.

Table 2.3 Summary of correlations for gas holdup with differing sparger designs.

Author	**Reactor Type**	**Parameters**	**Correlations**
Snape et al. (1995)	ELALR	Bench scale: Perforated plate A 0.5mm pore Plate B 1.6mm pore; triangular pitch D_R : 0.158m D_D : 0.05m Fluids- water; sucrose solutions; NaCl; KCl; $CaCl_2$; Na_2SO_4; $MgSO_4$ solutions	$\varepsilon_R = \varepsilon \frac{V}{V_R}$ $U_{LR} = \frac{U_{SLR}}{1 - \varepsilon_R}$ $\varepsilon_R = \frac{U_{SGR}}{C_o(U_{SGR} - U_{SLR}) + U_{b,\infty}}$
Gavrilescu and Tudose (1998 Part 1)	ELALR	Fluids: tap water; power law starch solutions and fermentation liquids Pilot scale: Multi-radial sparger A_D/A_R : 0.1225 and 0.04 D_R : 0.2m D_D : 0.07 and 0.04 m Bench scale: Perforated plate sparger	$\varepsilon_R = \alpha U_{SGR}^{\beta}$

		A_D/A_R : 1; 0.36 and 0.11 D_R:1.88; 1.382 and 1.189m D_D : 0.03m	
Salehi et al. (2011)	ILALR	Bench scale: Perforated pipes : types 1 to 4 with 1mm pore diameter H_R : 4 and 5cm	
Kulkarni et al. (2009)	Bubble column reactor	$D_{reactor}$: 1.5m	
Luo et al. (2011)	Annulus sparged ILALR	Bench scale: 2 orifice nozzle- 2.6mm 4 orifice nozzle- 1.84mm O-ring- 63 1mm diameter pores	$\varepsilon_R = 1 - \frac{\Delta P_R}{\rho_L g \Delta h_R}$ $\varepsilon_D = 1 - \frac{\Delta P_D}{\rho_L g \Delta h_D}$ $\frac{C^* - C_L}{C^* - C_{LO}} = e^{-k_L a t}$
Kojić et al. (2015b)	ELALR	Bench scale: Single orifice 4mm id Perforated plate 1mm 7holes triangular pitch Sintered plate 100-160microns- pore size 115microns- porosity 8%	$\varepsilon_R = \frac{\Delta z}{\Delta H}$ $(y)_{calc} = A U_{SGR}^{8} \sigma^{C} d_o^{D} \left(\frac{A_D}{A_R}\right)^{E}$

		Fluids- tap water; alcohol solutions	
Contreras et al. (1999)	Concentric tube ALR	Bench scale: Porous plate: 120-160 microns Perforated pipe 38 1000 to 500 microns	$K_L a_L = \alpha(\gamma)^{\beta}$
Lin et al. (2004)	ELALR	Pilot scale: Perforated plate 1mm id pores Sintered plate 30 micron diameter H_R : 4.8m D_R : 0.23m D_D : 0.19m Fluid- tap water	$0.1k + C_{D.Eo}(Eo-1)\frac{d\varepsilon_g}{dr} + \left(C_T U_{slip}\frac{du_1}{dr} + C_w\frac{d_B}{2} \times \left(\frac{1}{(R-r)^2} - \frac{1}{(R+r)^2}\right)U_{slip}^2\right)\varepsilon_g = 0$
Kemblowski et al. (1993)	ELALR	Pilot scale: $H_{reactor}$: 7.18m D_R : 0.2m D_D : 0.2 and 0.15m Sparger: 3mm pore diameter Laboratory scale: $H_{reactor}$:1.95m D_R and D_D - 0.1m Porous plates of glass beads 100-160,	$\varepsilon_R = 0.203\frac{Fr^{0.31}}{Mo^{0.012}}\left(\frac{V_{SGR}A_R}{V_{SLR}A_D}\right)^{0.74}$

		160-250, 250-500μm Single nozzle spargers 1, 1.4, 2, 2.8, 3, 4mm diameter; Fluids: tap water with surfactants (glycol, sugar syrup); CMC solutions	
Merchuk (1986b)		Review paper	
Merchuk and Stein (1981)	ELALR	Sparger: o-ring; single orifice H_R: 4.05m D_R: 0.14m H_D: 4.05m D_D: 0.14m Reactor volume: $0.3m^3$	$\varepsilon = \frac{2U_{SLD}^2}{gD_R}\left[\left(1+\frac{U_{SGR}}{U_{SLD}}\right)C_{fM} + C_{fL}\left(1+\frac{H_e}{H}\right)\frac{A_R}{A_D}^{2.5}\right]$
Merchuk (1986a)	ELALR	Laboratory scale rectangular column Straight copper tubes with orifices Fluids- tap water	$\varepsilon = 0.047U_{SGR}^{0.59}$

2.6.2. EFFECTS OF AN ENLARGED GAS DISENGAGEMENT ZONE

There are two types of gas disengagement zones in external loop airlift reactors as described in Figure 2.6 Section 2.3 of this chapter. Although a large amount of research has been done on airlift reactors, the importance of the design of the disengagement zone/tank and its influence on the hydrodynamics and mass transfer have not been taken into account (Al-Masry, 2004; Bentifraouine et al., 1997). A lack of the description of the geometry as well as the liquid height is common (Al-Masry, 2004; Chisti, 1989).

The design and liquid height of the gas disengagement tank influences the return of bubble to the downcomer which in turn affects the driving force of the liquid circulation velocity, gas holdup and mass transfer characteristics of the external loop airlift reactor (Al-Masry, 2004; Freitas and Teixeira, 1998; Al-Masry and Dukkan, 1997; Bentifraouine et al., 1997). Returning bubbles to the downcomer are nutrient deficient (Al-Masry, 2004; Kadic and Heindel, 2014) as transfer would have already occurred in the riser. The nutrient deficient bubbles increase the gas holdup in the downcomer and riser but reduce the mass transfer coefficient in the reactor. A low liquid height in the disengagement tank also increases the chances of returning bubbles to the downcomer (Al-Masry, 2006; Al-Masry, 2004; Al-Masry and Dukkan, 1997; Bentifraouine et al., 1997; Chisti, 1989). Some work has been done to determine these effects on gas holdup and mass transfer in airlift reactors and will be summarized here.

Bentifraouine et al. (1997) investigated the effects of liquid height in a laboratory scale airlift reactor. They found that two regimes exist. The first is that the non-aerated liquid height in the disengagement tank does affect the liquid velocity and gas holdup. As the liquid height in the tank increased the liquid velocity increased due to the increase in the hydrostatic pressure between the riser and downcomer. This resulted in a decrease in the gas holdup. In the second regime, they also found that after increasing the liquid height further no effects were found on the liquid velocity and gas holdup as the pressure difference between the riser and downcomer does not change. A minimal and maximum non-aerated liquid height was found in their investigation that does not affect the liquid velocity and the gas holdup. However, the transition zone between these regimes is dependent on the gas flowrate. An increase in the gas flowrate decreases the maximum height of the non-aerated liquid. This is due to the

higher degree of expansion of the liquid due to an increase of entering gas. They concluded that the limit between the two regimes is controlled by the height of the dispersion of and not by the volume of the liquid.

Al-Masry and Dukkan (1997) investigated the effects of open channel and closed gas disengagement tanks on the hydrodynamics and mass transfer characteristics in external loop airlift reactors using an air-water system. They found that the open channel external loop airlift reactor is more efficient than a closed channel external loop airlift reactor as it allows for almost complete disengagement of all bubbles exiting the riser depending on the design. They also reported that the disengagement of the bubbles affects the liquid circulation velocity and other hydrodynamic and mass transfer characteristics. In their pilot scale external loop airlift reactor, they found a 30% reduction in gas holdup in the riser by using an open channel disengagement tank. This indicated that the entrained bubbles in the downcomer had decreased due to the size of the disengagement zone.

The open channel configuration also produced a higher mass transfer coefficient than the closed channel configuration. They concluded that a properly designed gas disengagement tank enables the external loop airlift reactor a more flexible and easily controlled environment.

In the investigation by Freitas and Teixeira (1998), the hydrodynamic studies were done on a lab scale internal loop airlift reactor with an enlarged degassing zone for a three phase system. Although they did not investigate the liquid height in the disengagement zone, they found that an increase in gas flowrate resulted in a decrease in liquid circulation time which was due to the returning bubbles in the downcomer. A decrease in solids loading and density increased the gas holdup in the riser and downcomer with increasing gas flowrate. At low flowrates there was an increase in the gas holdup which was explained by the change in flux regime. At high flowrates, there was an increase in coalescence. Coalesced bubbles travel faster up the column which results in a decrease in residence time of the gas phase and thus gas holdup. As air was increased to 13.6l/min, the gas holdup also increased after which there was no change in gas holdup. An enlarged disengagement zone in the internal loop airlift reactor allowed for complete gas disengagement at low flowrates up to 13.6l/min.

Al-Masry (2004) investigated the effect of liquid height in a large gas disengagement tank using an air-water system and air-glycerin system in a pilot scale external loop airlift reactor. The volume ratio, T_{VR}, which is expressed as

$$T_{VR} = \frac{V_{LGS}}{V_L} \times 100 \qquad 2.28$$

Where V_{LGS} – un-aerated volume in the gas separator

V_L – total liquid volume in the reactor.

The three levels of liquid height as defined by Al-Masry (2004) in the gas disengagement zone are illustrated in Figure 2.12.

At 0% volume ratio (T_{VR}), there is a high return of bubbles to the downcomer. At the transitional value of volume ratio, T_{VRS}, there is a small entrainment of bubbles into the downcomer but at a volume ratio greater than the transitional volume ratio, i.e. optimum volume ratio, T_{VRO}, there is very little to no entrainment of bubbles in the downcomer. Al-Masry (2004) reported that this design parameter needs to be taken into consideration when gas recirculation needs to be minimized. He concluded that there is an optimal liquid level in the gas disengagement tank which provides minimal gas entrainment into the downcomer. This was not taken into consideration in the work of Albijanic et al. (2007) cited in Kadic and Heindel (2014).

Although Al-Masry (2004) proposed a design procedure for the disengagement tank, he found that experimental and theoretical results were different in that the theory gave complete disengagement which was not true in reality. However, this does not nullify the importance of the gas separator design as it directly affects the driving force of the reactor. In his later study (Al-Masry, 2006), used the volume ratio as an input value into the neural network that he employed and obtained excellent results with the prediction. The optimal final liquid level in the disengagement tanks in this investigation was determined by observation.

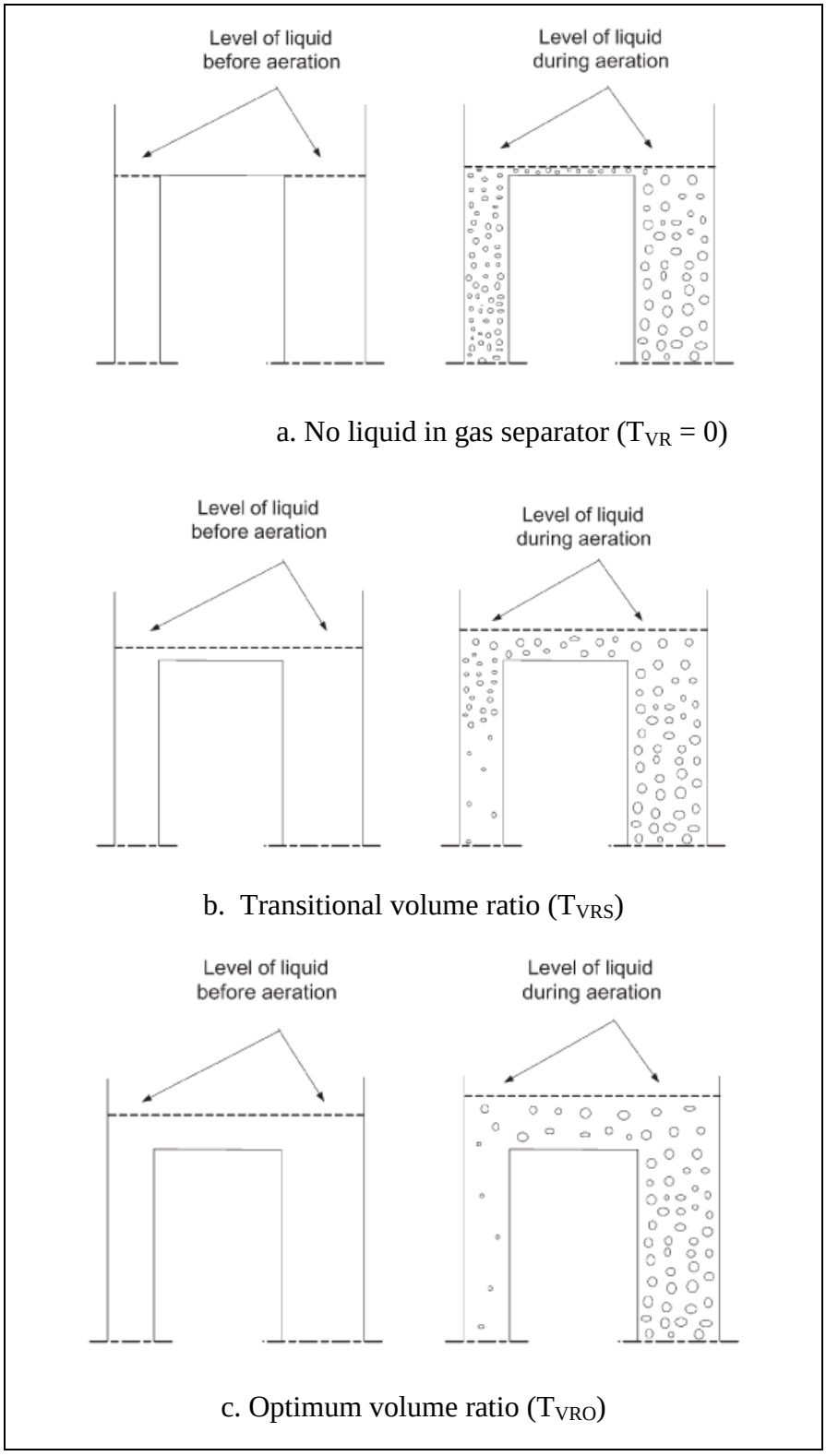

Figure 2.12 Volume ratio in gas disengagement tank (Al-Masry, 2004).

2.6.3. EFFECTS OF ASPECT RATIO

The height of the reactor is often expressed in terms of the aspect ratio (H_R/D_R), i.e. the ratio of the riser height to the riser diameter. This parameter is important as noted in the preceding discussion and needs further elaboration. The height of the reactor is defined to be the distance from the base of the reactor to the bottom of the disengagement tank or it can be the un-aerated liquid height which is the distance from the base to the un-aerated fluid surface as in Figure 2.13 below:

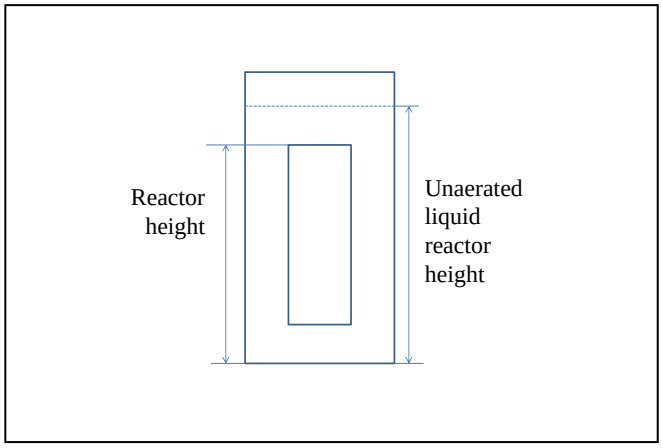

Figure 2.13 Reactor height.

As noted from Al-Masry (2004), Bentifraouine et al., (1997) and Kadic and Heindel (2014) the reactor height influences the liquid circulation path which affects the liquid circulation velocity, gas disengagement and the hydraulic pressure (Kadic and Heindel, 2014). A larger circulation path increases the liquid velocity which increases the gas disengagement but decreases gas holdup and therefore mass transfer. Large circulation paths also lead to increased residence times of the nutrient deficient bubbles which can result in the starvation of micro-organisms in bioreactors (Al-Masry, 2004; Kadic and Heindel, 2014).

An increase in aspect ratio does not change the liquid circulation velocity but allows the gas phase to achieve its equilibrium bubble diameter over the longer length (Kadic and Heindel, 2014). If the un-aerated liquid height is less than the reactor height then bubble column conditions exist. Any increase in liquid height would result in an increase in liquid circulation velocity and a decrease in gas holdup (Bentifraouine et al., 1997; Al-Masry, 2004). The investigation by Al-Masry (2004) and Luo et al. (2000) revealed that an optimal un-aerated

liquid height needs to be achieved for there to be no effect on the hydrodynamics of the reactor as discussed.

2.6.4. EFFECTS OF AREA RATIO

Investigations by Jones and Heindel (2010); Al-Masry (2004); Yazdian et al. (2009); Lu et al. (2000); Korpijarvi et al. (1999); Gavrilescu and Tudose (1998 and 1997a); Kawase and Hashiguchi (1995); Chisti et al. (1994); Merchuk (1986 and 1984); and Merchuk and Stein (1981) have been done on the effects of the area ratio (A_D/A_R) (scale up ratio in literature) on the hydrodynamics in airlift reactors with some comparisons between closed channel and open channel laboratory and pilot scale airlift reactors. All are in agreement that by decreasing the diameter of the downcomer, i.e. decreasing the area ratio, there is an increase in the resistance to flow for the liquid (Figure 2.14).

This means that the liquid circulation velocity decreases which results in increased gas holdup in the riser as there is a reduced flow path due to the resistance to flow. Although there would be increased gas holdup, the bubbles would be nutrient deficient due to the longer residence time. A decrease in area ratio also results in a decreased mixing time. However, Kawase and Hashiguchi (1995) found that an increasing area ratio resulted in a slight decrease in mass transfer.

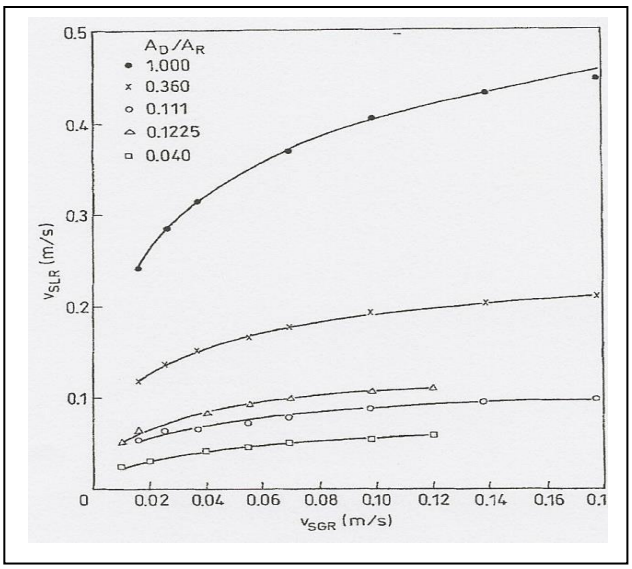

Figure 2.14 Effects of area ratio as a function of liquid superficial (V_{SLR}) and gas superficial (V_{SGR}) velocity Gavrilescu and Tudose (1997a).

Al-Masry (2004) also investigated effects of area ratio and volume ratio on hydrodynamics of external loop for air-water and air glycerol systems. The area ratio for the 135L and 170L external loop airlift reactors were 0.29 and 0.54 respectively. The gas disengagement tanks were of the same size for both reactors. He found than an increase in area ratio resulted in a decrease in the optimum volume ratio. For the reactor with an area ratio of 0.29, the optimum volume ratio was 30% while the reactor with an area ratio of 0.54 had an optimal volume ratio of 18% for both the air-water and air-glycerol systems. He concluded that this was possible as the larger column reached stability in operation much faster than the smaller column.

The area ratio plays a significant role in the mass transfer characteristics of an airlift reactor as it affects the flow path of the liquid. Ensuring less resistance to flow or less opposition to liquid flow and allows for reduced friction and for the reactor to reach stability sooner as well as improving mixing and mass transfer characteristics.

2.7. CONCLUSION

As stated previously significant amounts of research has been undertaken by many authors on airlift reactors. Many theories and models have been put forward for airlift reactors, as well as

theories from bubble columns which some authors have tried to superimpose onto airlift reactors. The correlations proposed have raised many questions. In some cases, theories proposed by some authors are in direct conflict with the research of other authors. This is due in part, to each researcher's assumptions and interpretation of their results. The proposed significant parameter according to literature referred to as scale up ratio (A_D/A_R) as well is a source of confusion. This parameter is widely used in literature for airlift reactors to describe the ratio of the cross sectional area of the downcomer to the cross sectional area of the riser. This parameter would be better described as the area ratio and this is in agreement with Kadic and Heindel (2014). The term scale up ratio is misleading and the change to area ratio is more appropriate and is a source for discussion later in this thesis.

The importance of each parameter varies per reactor and author. The ability to quantify some of these parameters on a large scale is difficult especially since the majority of investigations have been performed on laboratory scale reactors. Knowledge transference from laboratory scale to pilot or industrial scale airlift reactors is also a problem as the hydrodynamics change significantly with scale. Even an in-depth analysis into any comparisons that have been done in literature between laboratory and pilot or industrial scale reactors are difficult as the reactors differed in design and application (i.e., type of fluid). It must be noted that most investigations, correlations and models proposed are very reactor specific and no generalized theory currently exists. The design of the large scale reactors would have to depend on design from first principles and not the empirical or design specific correlations proposed in literature. It is known that the behavioral characteristics of all parameters (geometric or hydrodynamic) and their interdependence on each other are very complex therefore trying to develop correlations based on traditional practices is difficult as not all relationships are known.

Conclusions from literature cannot be reliably drawn on whether the results are affected by area ratio, aspect ratio, tank size, fluid or gas properties, bubble sizes, etc. What is required in the correlation or model is a more flexible approach to design where the knowledge of prior relationships are unnecessary and design from first principles are used initially to translate data into a more useful form. The model or correlation should be adaptive to each case based scenario. An approach to this is the use of artificial neural networks. It does not require prior

in-depth knowledge and is adaptive to changes in data. It provides the means to a more generalized approach to design of airlift reactors.

CHAPTER THREE

NEURAL NETWORKS

3.1. INTRODUCTION

The speed, complexity and efficiency at which the human brain works, provides the inspiration for artificial neural networks (Haykin, 2009; Hopfield, 1988). Designed to mimic the learn, recall and generalize (pattern recognition) functions of this biological network, the artificial neural network (ANN) has been developed to become a useful tool in science, engineering and finance assisting in pattern recognition and classification where input data can vary between numbers, symbols or pictures.

The advantages (Amiri, et al., 2011) of using artificial neural networks include:

1. Artificial neural networks are able to represent highly nonlinear processes with complex structures.
2. Artificial neural networks are flexible networks.
3. They are robust and are able to handle noisy data.
4. After an ANN is developed and its coefficients are determined, it can be used to provide rapid response to any new input.

Thus the learning ability of artificial neural networks has produced an entirely new set of algorithms capable of offering solutions were traditional algorithms and models fail (Amiri, et al., 2011).

3.2. THE STRUCTURE OF BIOLOGICAL NETWORKS

The human brain can take in vast amounts of information, identify important messages from the information provided and provide an appropriate response within milliseconds. It may not be able to operate as fast as a computer, but it can still distribute, retain and recall all information across millions of interlinked neurons and is able to provide the appropriate response to suit each situation unlike traditional computational applications which perform operations one at a time. The following figure is a schematic of a basic biological neuron or nerve cell that makes up the biological neural network.

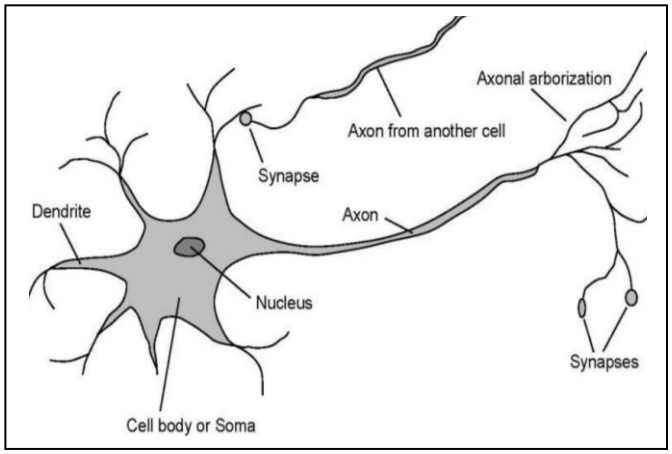

Figure 3.1 Schematic of a Biological Neuron (Anon, n.d.).

A single neuron is made up of dendrites (input/output channel), soma (cell body), axon (input/output channel) and synapses (space between dendrite and axon). The neuron receives inputs (electrical signals) from other neurons via the axon and dendrite through the synapse. Only if the electrochemical signal received is strong enough, does the neuron transmit an output to the other neurons. The brain is composed of millions of these interconnected neurons that effectively represent a massively parallel interconnected network (Haykin, 2009). Each neuron is connected to approximately 10 000 other neurons (Pauck, 2011).

3.3. STRUCTURE OF AN ARTIFICIAL NEURAL NETWORK

An artificial neural network is a mathematical representation of a biological neural network. Haykin (2009) defines the artificial neural network as a massively distributed parallel processor that is made up of simple processing units that have the natural ability for storing

experiential knowledge and making it available for use. According to Haykin (2009), it resembles the brain in two respects:

- Knowledge is acquired by the network from its environment through a learning process
- Interneuron connection strengths, known as synaptic weights, are used to store the acquired knowledge.

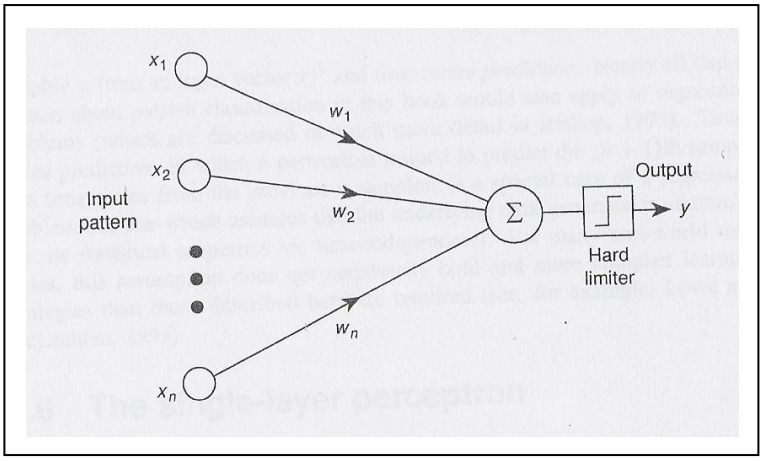

Figure 3.2 Schematic of an Artificial Neural Network (Tarassenko, 1998).

In an artificial neural network, the artificial neuron is called a perceptron. The perceptron is a mathematical model processing unit that represents the biological neuron. Simply described with respect to Figure 3.2, the single perceptron is a summation of weighted inputs (strengths) to which a threshold (hard limiting/activation function) is applied for which an output is obtained. This output, is then sent to other interconnected target processing units. Figure 3.3 and 3.4 clearly shows how the perceptrons are connected to each other in each layer.

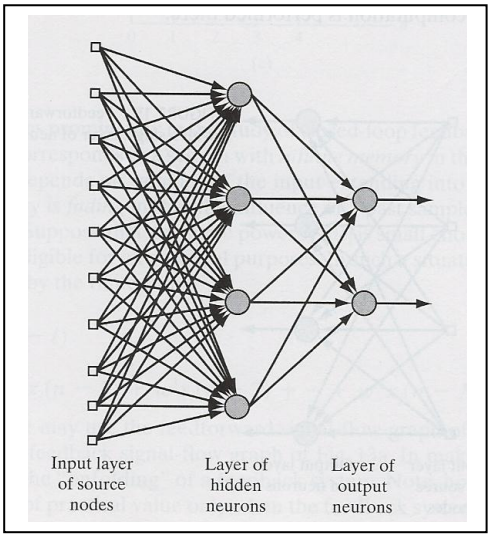

Figure 3.3 Fully connected artificial neural network with one hidden layer of neurons (Haykin, 2009).

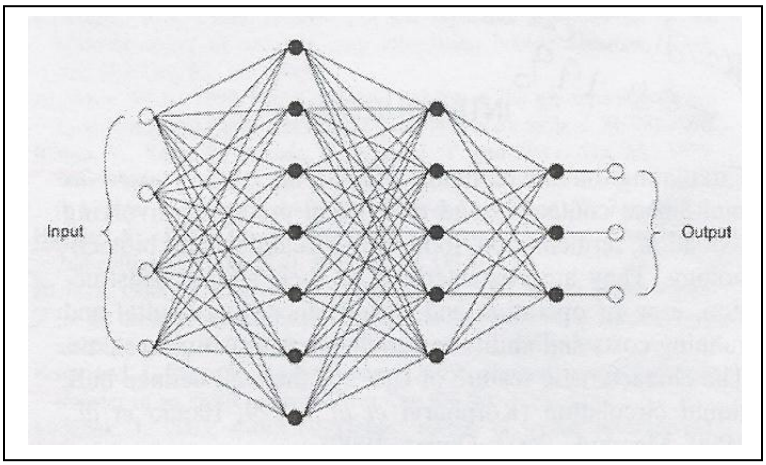

Figure 3.4 Artificial neural network with three hidden layers of neurons (Al-Masry, 2006).

Input data/patterns are introduced into the network as input vectors. There is no processing of data at the input layer in the work of Morris, et al. (1994). The data is then transmitted through the network via interconnections. Each interconnection is weighted. This modifies the strength of the signal. Each perceptron in each layer is connected to every perceptron in adjacent layers (Morris, et al., 1994). The perceptrons in the adjacent layer sums the weighted inputs from the preceding layer. The signal is then passed through a non-linear processing

threshold/hard limiting/activation function. The resulting output is then passed on to the output layer. In addition, a bias weight can also be applied to allow for greater flexibility of the network (Tarassenko, 1998; Morris et al., 1994).

The weights are derived by training the network until the error is minimized. This is achieved by using mathematical techniques were the weights are incrementally adjusted and applied until the error is minimized between a desired response and a weighted actual response such that the problem can be solved or were the output answers closely approximate the target answers. This is called 'training/learning' and is the basis for the back-error propagation algorithm/distributed gradient technique. To train the network using this method, input data is presented to the network to give an output. The error obtained in the prediction is used to update the weights in order to bring the error function to a minimum.

This is referred to as supervised training as the network is supplied with input vectors and related targets/desired outputs/responses. The supervised training technique is applied in this research thesis. Unsupervised learning on the other hand, is when there are no target answers available and the network simply classifies the inputs into categories.

3.4. FEASIBILITY AND APPLICATION OF ARTIFICIAL NEURAL NETWORKS

There are many benefits of using neural networks as opposed to traditional computing methods as summarized in sections 3.4.1 and 3.4.2 from Tarassenko (1998), Haykin (2009), Zhang et al. (1998) and Morris et al. (1994).

3.4.1. FEASIBILITY OF ARTIFICIAL NEURAL NETWORKS

- An artificial neural network is capable of learning from 'experience'. With this 'experience' it is able to recognize patterns and relationships between data, even if they are unknown or difficult to describe. The network is able to adapt to changes in the data. This is referred to as learning from 'experience'.
- The artificial neural network has the ability to generalize. After learning from 'experience', the network is able to perform a prediction with unseen data even if the

data is noisy. Extrapolation of data however cannot be done in an artificial neural network.

- Artificial neural networks are more flexible and functional than traditional statistical computational methods as they assume a relation between the input data and the output data, even though they are data intensive.
- Artificial neural networks are capable of dealing with complex non-linear systems which is often the case in real world situations.
- Although neural networks require intensive computational requirements, once it is fully trained, the network is able to rapidly produce an output for large problems due to its parallel structure.
- Non-numerical data can also be used in artificial neural networks.

3.4.2. APPLICATION OF ARTIFICIAL NEURAL NETWORKS

The feasibility of artificial neural networks is indisputable (Cozma et al., 2014; Cancino, 2013), however the question that arises is when to apply a neural network to a problem? Tarassenko (1998) lists three criterions that need to be met for a neural network to be applied to data.

- The first criterion is that an algorithm, set of equations or rules cannot be used to explicitly describe a solution to a problem. Much research has been done using computational fluid dynamics (Al-Mashhadani et al., 2015; Pourtousi et al., 2015; Davarnejad et al., 2012; Xu et al., 2012; Moraveji, 2012; Zhang et al., 2012; Bannari et al., 2011; Chen et al 2011; Yan et al., 2011; Luo and Al-Dahhan, 2011; Kiambi et al., 2011; Šimčík et al., 2011; Rihani, et al., 2011; Yan et al., 2010; Studely, 2010; Haung et al., 2010; Law, 2010; Jianping et al., 2006; Roy et al., 2006; Talvy et al., 2005; Blažej et al., 2004; Camarasa et al., 2001; Shimizu et al., 2001; Couvert et al., 2001; Mudde et al., 2001; Carvalho et al., 2000; Choi, 1999; Dhaouadi et al., 1997 and 1996; Hinks et al., 1996) to find a generalized prediction model for airlift reactor hydrodynamics and mass transfer. However, the literature has shown that these proposed models are only applicable to the systems under study and have not been verified with other works or on a pilot or industrial scale (Davarnejad et al., 2012;

Zhang et al., 2012; Xu et al., 2012; Chen et al 2011; Kiambi et al., 2011; Yan et al., 2011; Luo and Al-Dahhan, 2011; Bannari et al., 2011; Chen et al 2011; Šimčík et al., 2011; Rihani et al., 2011; Haung et al., 2010; Law, 2010; Yan et al., 2010; Jianping et al., 2006; Roy et al., 2006; Talvy et al., 2005; Blažej et al., 2004; Mudde et al., 2001; Choi, 1999; Dhaouadi et al., 1997 and 1996) and in some cases the data has been adjusted to suit the predictive model (Haung et al., 2010; Freitas, 1999).

- The second criterion stipulates that a mapping/relationship should exist between the input data, *x*, and output data, *y*, such that

$$y = f(x) \tag{3.1}$$

Where f is not known. As mentioned many studies have been done using computational fluid dynamics and a few using neural networks. Although relationships exist, not all variables are varied. The other limitation is that the majority of investigations done on a laboratory scale. By performing pilot plant scale investigations and varying as many parameters as possible a complete picture can be obtained using an artificial neural network.

- The third criterion as stipulated by Tarassenko (1998) is that there should be a large amount of data available to the network. This would ensure that there is sufficient data available for training, validation and testing. Obtaining large amounts of data is time consuming and expensive thus limiting the quantity of data which compromises the ability of the network to generalize. However, having too much of unnecessary data will result in the network being too complex and producing incorrect outputs. Inputs would therefore require some pre-processing to determine significant data that is needed (Laberge, et al., 2000; Gerlach, et al., 1997). In this study investigations were done on three pilot scale external loop airlift reactors. This allowed for a significant amount of data (qualitative and quantitative) to be generated under a wide range of conditions. Some investigations carried out by other researchers would be used as unseen external data to test the network.

3.4.2.1. SOFTWARE

Many neural network software packages are available for use. In this study, Predict version 3.30 by Neuralware was used.

3.4.2.2. DATA REQUIREMENTS

Artificial neural networks allow for the input of different data types, i.e. qualitative, quantitative and descriptive. It is essential to have good quality data that is sufficient for this data-driven modeling approach. Some preprocessing of the data may also be required. Deciding on how much of data is required is important. Although there is no specified quantity as to how much of data is required, too little data may provide incomplete conditions for the network to be trained, validated and tested. It is important to make a measurable estimate of data such that all possible scenarios are covered whether they represent required conditions or error conditions. It is best to have all classes of data represented so that a reliable solution may be found.

The quantity of data also affects the partitioning into training, validation and test sets. Tarassenko (1998) proposes that the data should be of the ratio 1:1:1 for all three sets. However this suggests that three times the amount of data is required. This would impact on cost factors and the ability to actually obtain the data may prove to be an issue. To overcome this Tarassenko (1998) suggests cross validation techniques. This method allows for a large portion of the data to be used for a training set. Of course the data that is input into the network needs to be relevant to the case at hand. To ensure this Tarassenko (1998) suggests using the following conditions,

- The input data must fall within the specified range
- The input data should be consistent
- In a supervised learning application target vectors should be consistent with input vectors

In some cases it would be impossible to obtain complete sets of data as it may not have been available or practical at the time of the investigation. To overcome this, the following methods are employed (Tarassenko, 1998):

- Replace the missing data value by the mean or median throughout the training set and the entire data set.
- Estimate the missing data based on knowledge of the rest of the data
- Use another neural network to predict the data.

3.5. MATHEMATICAL REPRESENTATION OF AN ARTIFICIAL NEURAL NETWORK

3.5.1. BACKGROUND

A perceptron or artificial neuron was initially used for pattern classification from the geometrical perspective (Tarassenko, 1998) but has gradually shifted to statistical pattern recognition. This was made possible by the introduction of algorithms and multilayer perceptrons.

3.5.2. BASIC SINGLE LAYER ARTIFICIAL PERCEPTRON (TARASSENKO, 1998)

As stated previously, the neuron is a summation of the weighted inputs which is then thresholded to give a binary output, *y*, which is either +1 or -1. A mathematical representation of Figure 3.2 is,

$$y = f_n\left(\sum_{i=0}^{n} \omega_i x_i\right) \qquad 3.2$$

The hard limiting/activation/threshold function, f_n, gives an output of +1 when $\sum \omega_i x_i$ is greater than zero or -1 when $\sum \omega_i x_i$ is less than or equal to zero (Tarassenko, 1998).

The learning process is the incremental adjustment of the weights ω_i until the classification is successfully done. The pattern would be classified as class A (+1) or class B (-1) and no flexibility over the separating line.

To allow for flexibility of the separating line, an adaptive bias (increasing or decreasing input to the activation function), weight of +1 is introduced.

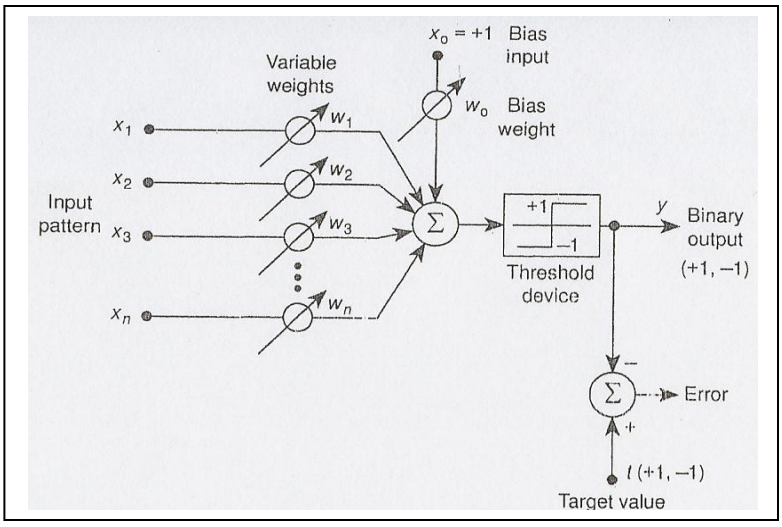

Figure 3.5 Single Layer Perceptron with Bias Weight, ω_o (Tarassenko, 1998).

The output of the perceptron (Figure 3.5) is then

$$y = f_n\left(\sum_{i=0}^{n} \omega_i x_i + \omega_o\right) \qquad 3.3$$

3.5.2.1. TYPES OF ACTIVATION FUNCTIONS

There are two types of activation functions, a threshold function (Figure 3.6) and a sigmoidal function (Figure 3.7) (Haykin, 2009). The threshold function or McCulloh-Pitts model is described as

$$f_n = \begin{cases} 1, & \gamma \geq 0 \\ 0, & \gamma < 0 \end{cases} \qquad 3.4$$

This describes the all or none property of the model.

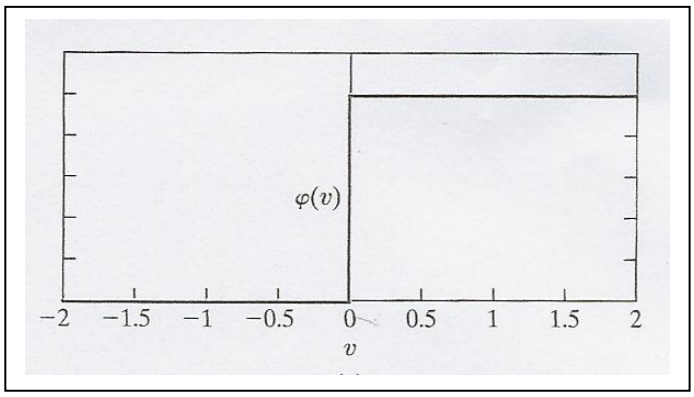

Figure 3.6 Threshold Function (Haykin, 2009).

Nowadays the sigmoidal function is more commonly used in the construction of an artificial neural network (Haykin, 2009) and is represented by

$$f_n = \frac{1}{1 + \exp(-a\gamma)}$$

3.5

Where: a = the slope parameter.

The 'S' shaped sigmoidal curve allows for the generation of different sigmoidal functions with different slopes. The sigmoidal or logistic function provides a better balance between linear and non-linear behaviour (Haykin, 2009).

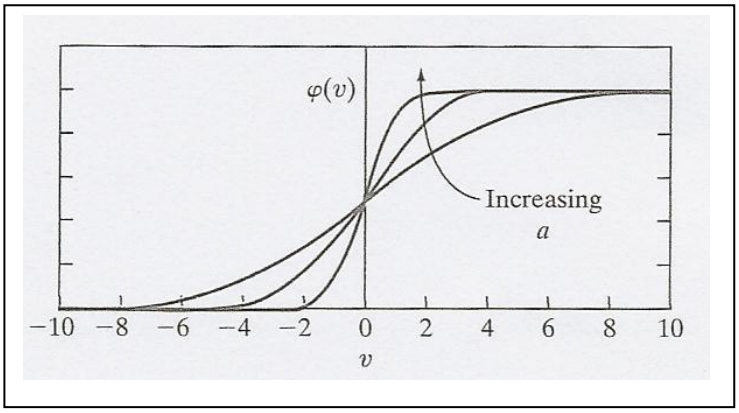

Figure 3.7 'S'-shape Sigmoid Function (Haykin, 2009).

When the activation function ranges between +1 and -1 then the threshold function

$$f_n = \begin{cases} 1, & \gamma > 0 \\ 0, & \gamma = 0 \\ -1, & \gamma < 0 \end{cases}$$

is called the sigmoid function. If the activation function of the sigmoid type is to assume negative values then the hyperbolic tangent function is used, defined by

$$f_n = \tanh(\gamma)$$

3.6

3.5.2.2. ERROR MINIMIZATION (TARASSENKO, 1998)

It is important to reduce the error between the target value and the output value of the artificial network in order to obtain a set of weights which can be used to solve the problem.

In order to do this an error feedback function is used during training. This works when an error, *E*, is measured at the network output. This error is then decreased or minimized by using the gradient descent, i.e. by differentiating every error with respect to every weight, i.e.

$$\Delta\omega_i = -\eta \frac{\partial E}{\partial \omega_i}$$

3.7

Where, η is the step size parameter called the learning rate.

The choice of η is important as a too large value will result in the error correction overshooting resulting in a divergent network. Too small increments and the network would take too long to converge.

For real world noisy data it may sometimes be difficult to classify all the data correctly. The sum of the squares error function is used

$$E = \frac{1}{2} \sum_{p=1}^{p} (y^p - t^p)^2$$

3.8

Where y^p= single output of a multilayer network for the p^{th} pattern

t^p = target value for the p^{th} pattern.

The error function is minimized by gradient descent, the differential with respect to every weight possible. In order to achieve the error minimization, a continuous differentiable function must be used. This is the sigmoid function.

3.5.3. MULTILAYER PERCEPTRON

3.5.3.1. BACK PROPAGATION ALGORITHM (TARASSENKO, 1998)

A multilayer perceptron (MLP) as defined by Tarassenko (1998) refers to the number of layers of weights and not the processing units in a neural network.

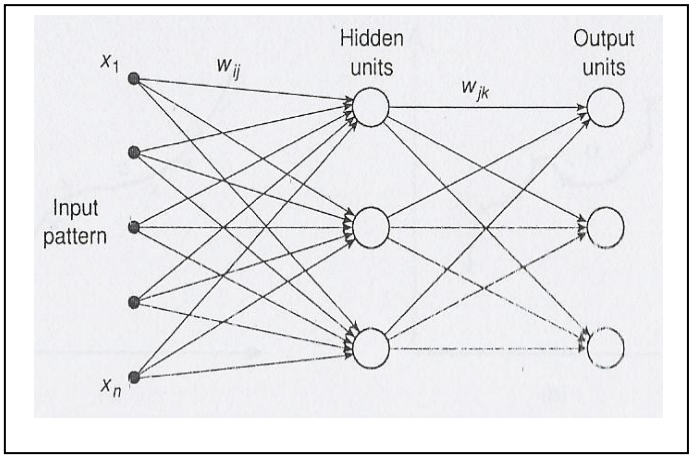

Figure 3.8 Multi-layer Perceptron, 5-3-3 (Tarassenko, 1998).

In Figure 3.8 the two layer perceptron has five inputs, *I*, three hidden units, *J*, and three outputs, *K*. The weights to the hidden units are ω_{ij}, and to the output, ω_{jk}. The error function for this *K*-class problem, where *K* output units are required, is:

$$E = \frac{1}{2}\sum_{p=1}^{P}\sum_{k=1}^{K}\left(y_k^p - t_k^p\right)^2 = \frac{1}{2}\sum_{p}\sum_{k}\left(g\sum_{j}\omega_{jk}\,y_j^p - t_k^p\right)^2 \qquad 3.9$$

As $y_k = g(a_k) = g(\sum \omega_{jk} y_i)$ and $y_j = g(a_j) = g(\sum \omega_{ij} x_i)$, the equation becomes

$$E = \frac{1}{2}\sum_p \sum_k \left(g \sum_j \omega_{jk} g \left(\sum_i \omega_{ij} x_i^p \right) - t_k^p \right)^2$$

3.10

This equation indicates that the error, *E*, is now a continuous differentiable function at every weight such as the sigmoid activation function. Each weight is then continuously updated in a MLP called the error back propagation algorithm. According to Tarassenko (1998), weights for the hidden to output layer is given by:

$$\Delta\omega_{jk} = -\eta \frac{\partial E}{\partial \omega_{jk}}$$

3.11

Where

$$\delta_k = \frac{\partial E}{\partial a_k}$$

3.12

and the input-to-hidden layer weights by:

$$\Delta\omega_{ij} = -\eta \frac{\partial E}{\partial \omega_{ij}}$$

3.13

Where

$$\delta_j = \frac{\partial E}{\partial a_j}$$

3.14

Thus E is minimized using gradient descent which requires the backward propagation of errors (δ_s).

3.5.3.2. NETWORK ARCHITECTURE

The purpose of neural network classification is the generalization ability of the trained network on a set of previously unseen test input data. It is therefore important to select network architecture to give the best generalization performance. Cebenko (1989) and Hornik et al. (1989) (cited in Tarassenko (1998)); Jha (2014) and Zhang et al. (1998) suggested that a two layer MLP with sigmoid non-linearity's is sufficient to approximate any function. The architecture is then defined by increasing the number of hidden units. But this leads to a further problem for complex problems in that too many hidden units leads to over-fitting (Figure 3.9) which results in poor interpolation of data (Tarassenko,1998) by the network.

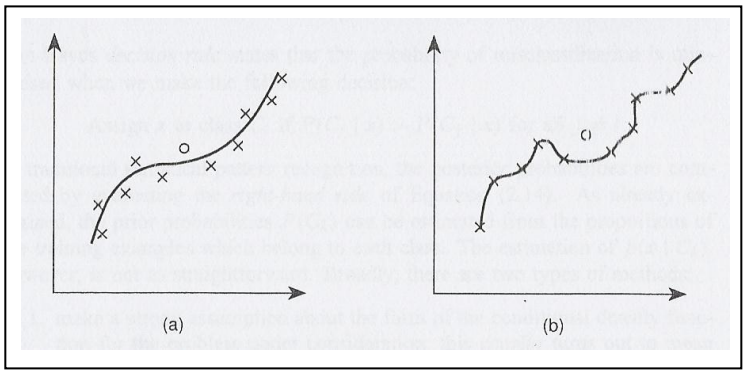

Figure 3.9 Over Fitting of data. (a) Good fit to noisy data (b) Over-fitting (Tarassenko, 1998).

The over-fitting of data needs to be avoided. This is when the network learns the details of the training data rather than the relationship between the input and output units. This happens largely when the network is large but the amount of data is too little (Amiri et al, 2011). Too much of unnecessary data also leads to an inefficient network (Laberge et al., 2000; Gerlach et al., 1998). This would result in an inefficient network that would not be able to perform when given new unseen test data.

With respect to the number of hidden layers, Zhang et al. (1998) suggested that two hidden layers may only be applicable to some types of problems and proposes that only one hidden layer is sufficient for forecasting problems. However, for this type of back propagation training architecture, arriving at the solution or minimal error takes many epochs as every weight has to be initially taken on a random number before each training data set is input into the network one by one. After each training example the output is compared to the actual output and the weights adjusted depending on the amount of error contribution and the network retrained. This may take a long time before a solution can be reached as the weights are constantly changing.

This is referred to as the moving target problem by Fahlman and Lebiere (1989) who proposed the cascade correlation learning architecture to overcome this problem.

3.5.3.3. CASCADE CORRELATION LEARNING ARCHITECTURE (FAHLMAN AND LEBEIRE, 1989)

In supervised learning cascade correlation architecture there are no multiple hidden layers. There is only one hidden layer with many hidden units/neurons/nodes. The network only has input and output data. The output weights are trained until a solution is reached and no further changes to the weights are noted. When this happens a hidden neuron is added to the network from a pool of hidden neurons. This hidden unit that greatly affects the overall error is selected and added to the network. The rest are discarded. The relationship between the new unit and the error is maximized, i.e. the new unit when added results in a significant error reduction of the network. This happens each time a new unit is added.

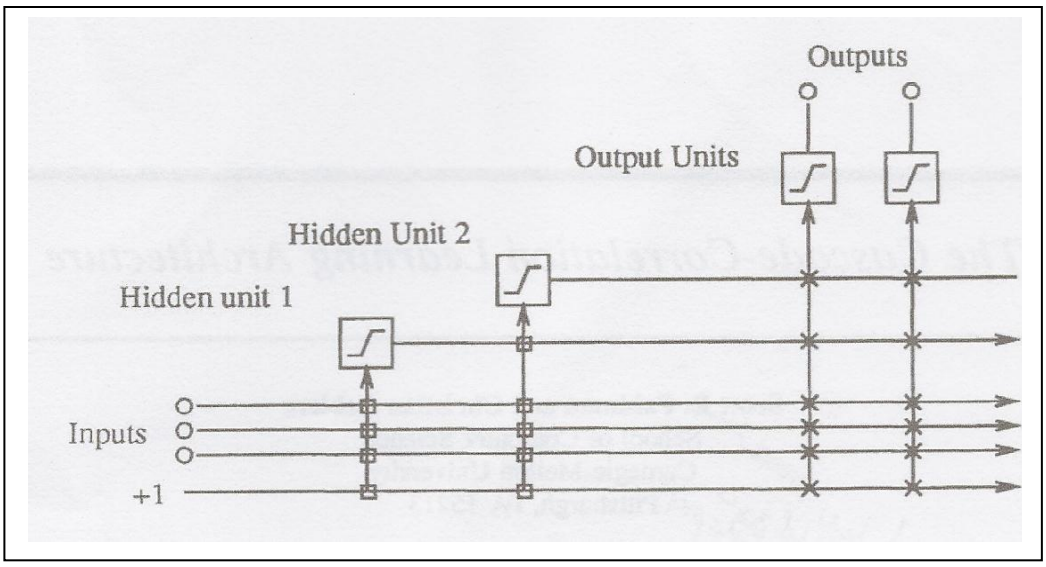

Figure 3.10 Schematic of the Cascade Correlation Architecture (Fahlman and Lebeire, 1989).

Figure 3.10 is an illustration of the cascade correlation architecture. The two hidden units with boxed connections are added and their weights frozen and the 'X' connections are being repeatedly trained until no change is detected (Fahlman and Lebeire, 1989). The number of inputs and outputs dictated by the problem is input into the network. All inputs are connected to all outputs with an adjustable weight and a bias set to +1. Either a linear sum of weighted inputs or a non-linear activation function may be produced by the output units. Hidden units are added to the network one at a time. As illustrated in Figure 3.10, above each new hidden unit is connected to the networks original input and every pre-existing hidden unit. The pre-existing hidden units input is frozen when it is added to the network. Only the output units are repeatedly trained by using either the Widrow-Hoff rule perceptron learning algorithm or any well known learning algorithms that are applicable for single layer networks.

The software, Predict, utilized in this research uses the cascade correlation architecture.

3.5.3.3.1. UNIT CREATION ALGORITHM (FAHLMAN AND LEBEIRE, 1989)

Each new hidden unit that is added to the layer starts off as a candidate unit, *S*. Any trainable unit from all external inputs as well as all pre-existing hidden units is input into the candidate unit. The input weights of candidate units are adjusted each time a pass is made over the

training set. This enables the sum over all the output units *S*, *o*, to be maximized before the candidate unit's value *V* and the residual output error E_o at *o*, represented by:

$$S = \sum_{o} \left| \sum_{p} (V_p - \bar{V}) \left(E_{p,o} - \overline{E_o}\right) \right|$$

3.15

$\bar{V}$ and $\overline{E_o}$ are averaged values of *V* and E_o across all patterns. To maximize *S*, $\frac{\partial S}{\partial \omega_i}$ must be calculated.

$$\frac{\partial S}{\partial \omega_i} = \sum_{p,o} \sigma_o \left(E_{p,o} - \overline{E_o}\right) f_p' I_{i,p}$$

3.16

Where σ_o = correlation between candidates value and output

f_p' = derivative for pattern p of the candidate units activation function with respect to the sum of inputs.

$I_{i,p}$ = input received from unit I for pattern p by candidate unit.

Gradient ascent is applied to maximize *S*. When little to no change occurs to *S*, the new candidate is added to the network and its input weight frozen.

3.6. REVIEW OF ARTIFICIAL NEURAL NETWORK APPLICATIONS IN AIRLIFT REACTORS

3.6.1. INTRODUCTION

Computational fluid dynamics (CFD) is a powerful modeling tool that has been widely applied to airlift reactors to predict gas holdup, liquid velocities and fluid flow patterns (Pourtousi et al., 2015; Manjo, 2014; Moraveji, 2012; Zhang et al., 2012; Xu et al., 2012; Davarnejad et al., 2012; Rihani et al., 2011; Chen et al., 2011; Šimčík et al., 2011; Bannari et al., 2011; Yan et al., 2010; Studley, 2010; Luo and Al-Dahhan, 2008; Roy et al., 2006; Talvy

et al., 2005; Blažej et al., 2004; van Baten et al., 2003; van Baten and Krishna, 2003; Couvert et al., 2001; Mudde and Van Den Akker, 2001; Camarasa et al., 2001; Carvalho et al, 2000; Shimizu et al., 2001; Choi, 1999; Hinks et al., 1996; Dhaouadi et al., 1996); mass transfer (Haung et al., 2010; Jianping et al., 2006; Dhaouadi et al., 1997); particle trajectory (Luo and Al-Dahhan, 2011) residence time (Yan et al., 2011; Luo and Al-Dahhan, 2011) and bubble size (Law, 2010).

The advantage of CFD's often put forward by the researchers listed in the preceding paragraph, is that no equipment has to be initially built as the reactor geometries can be adjusted in the simulation. This however, requires a detailed knowledge of the relationships that exist between variables as well as the effects of the reactor geometry on these relationships. Luo et al. (2008) also states that although extensive work has been done, only global hydrodynamic parameters have been investigated.

A common model used in CFD is the Euler-Euler 2-fluid model or the Euler-Langrian model. In the Euler-Euler model all phases are considered as interpenetrating continuum (Šimčík et al., 2011) while in the Euler-Langrian model where the individual particles are considered in a continuous film (Šimčík et al., 2011). In the Euler-Langrian case, the model can usually be applied to small scale investigations where the gas holdup is low (Šimčík et al., 2011). However, the equation representing the relationships between variables is dependent on researcher choice.

Although all the authors listed in paragraph one of this section repeat that they have achieved 'satisfactory' or 'reusable' approximation between their simulation and experimental results, they have often adjusted their data to achieve this 'reusable' approximation (Freitas et al., 1999). In some cases some parameters have been over estimated while others have been under estimated. Asides from Camarasa et al. (2001) and Carvalho et al. (2000) the published works on CFD's cited in this report are based on bench scale apparatus.

This would prove a challenge when up scaling to pilot plant if in-depth studies are not done to corroborate the experimental with the simulated results. Šimčík et al. (2011) highlights this by stating that although having a CFD does away with building experimental equipment as variations can be done in the simulation, the quality of the CFD is dependent on the model

equations selected that describe the flow phenomena, bearing in mind that flow patterns in an airlift reactor are very complex. He further goes on to state that the studies would be incomplete should the simulations not be validated experimentally.

Although CFD's may be regarded as a powerful modeling tool, it is noted that its applicability in the case of airlift reactors is still limited and is only applicable to each situation (Amiri et al., 2011; Bentifraouine et al., 1997).

3.6.2. NEURAL NETWORKS AND AIRLIFT REACTORS

Neural networks as opposed to CFD's do not require a prior in-depth knowledge of relationships between parameters under investigation. In real-world applications the traditional mathematical approaches used in CFD's may not work as real-world applications are non-linear and change with time (Amiri et al., 2011; Al-Masry, 2006; Morris et al., 1994). In a neural network however, all that is required is the variables/parameters and a large amount of data points to input into the network. There are many neural network software packages that are commercially available to model data, although one can opt to write their own neural network with C-Basic, MATLAB etc. What is crucial is the selection of the algorithm to model the data.

Initial experimentation can be done to obtain data to train and validate the network with some data to be used as test data in conjunction with data from the works of other researchers that is used as unseen data. However, Amiri et al. (2011) warns not to use data from CFD correlations as errors in the correlation will be carried through in the neural network.

3.6.2.1. PREDICTING GAS HOLDUP AND LIQUID VELOCITY WITH NEURAL NETWORKS

Amiri et al. (2011); Kojić et al. (2015) and Al-Masry (2006) used neural networks to predict the gas holdup and liquid velocity with excellent results. Amiri et al. (2011) used emulsified oily solutions to determine the effects of the sparger pore diameter on the gas holdup using compressed air. They used a bench scale bubble column reactor 1.1m in height and 0.95m in

diameter. The type was a perforated plate and the pore sizes varied from 0.02 to 0.3mm in diameter.

Table 3.1 Properties of liquids used (Amiri et al., 2011) ([a,b] Mouza et al., 2005; Kazakis et al. (2007) cited in Amiri et al., 2011).

Material	Density (Kg/m^3)	Kinematic viscosity (10^{-6} m^2/s)	Surface tension (mN/m)	Sparger pore diameter (mm)
Distillated Water	998	1.003	72	0.04[a], 0.1[b], 0.3
Isomax-Diesel	827.09	9.85	29.6	0.3
Kerosene	782.66	1.6	26	0.04[b], 0.1[b], 0.3
HVI-150	874	6.593	32	0.3
HVI-90	867	3.089	31.6	0.3
Diesel (34%) + HVI-150	842.44	3.02	31.5	0.3
Diesel (49%) + HVI-150	837.32	2.06	31	0.3
Kerosene (10%) + HVI-90	844.81	2.22	31	0.3
Diesel (83%) + HVI-150	825.2	1.27	30	0.3
Kerosene (24%) + HVI-90	827.8	1.23	29.5	0.3
Kerosene (46%) + Isomax-Diesel	799.89	3.81	24.8	0.3
Kerosene (69%) + HVI-150	799.85	3.56	26.4	0.3
n-Butanol 0.6% (w/w) in water	994	0.9	60	0.02[a], 0.04[a]
n-Butanol 1.5% (w/w) in water	991	0.9	48	0.02[a], 0.04[a]
Glycerin 33.3% w/w	1081	3.5	70	0.02[a], 0.04[a], 0.1[b]
Glycerin 50.0% w/w	1126	8.2	68	0.02[a], 0.04[a]
Glycerin 66.7% w/w	1173	22.5	67	0.02[a], 0.04[a]
Glycerin 68% w/w	1082	23	67	0.1[b], 0.04[b]
n-Butanol 1.5% (w/w) in water	990	0.9	50	0.1[b], 0.04[b]
n-Butanol 0.75% (w/w) in water	992	0.9	60	0.1[b]

The experimental gas holdup was determined using the empirical volume expansion method at 20 different superficial air velocities. A feed forward back propagation artificial neural network using the sigmoidal function was then used to predict the gas holdup. The input layer to the model consisted of the gas velocity, surface tension, density, kinematic viscosity and sparger pore diameter. Of the 600 results taken, 60% was used for training, 20% for validation and 20% for testing. The neural network model consisted of a single hidden layer with 7 neurons and a trial and error technique was adopted. They investigated several neural network architectures before selecting the model that gave the most accurate comparison between the predicted and experimental values, Figures 3.11a and b.

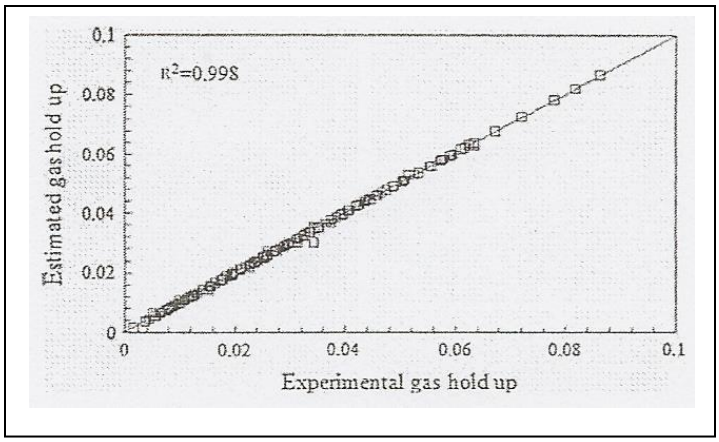

Figure 3.11a Parity plot of estimated and experimental gas holdup, training step (Amiri et al., 2011).

A comparison of the normalized mean square error (NMSE) between the artificial neural network and the correlation by Yazdani (2007) (Correlation A); Mouza et al. (2005) (Correlation B) and Kazakis et al. (2007) (Correlation C) (cited in Amiri et al. (2011)) was done for the gas holdup in Table 3.2.

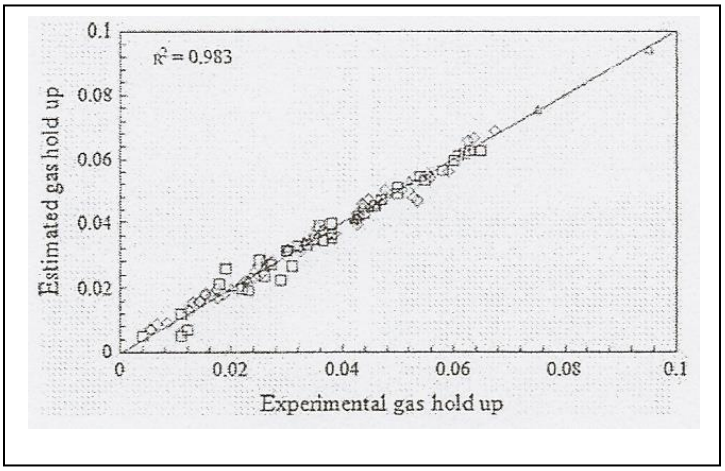

Figure 3.11b Parity plot of estimated and experimental gas holdup, testing step (Amiri et al, 2011).

Table 3.2 NMSE comparison (Amiri et al., 2011).

Material	**ANN**	**Correlation A** (Yazdiani, 2007)	**Correlation B** (Mouza et al., 2005)	**Correlation C** (Kazakis et al., 2007)
Kerosene	0.01	0.17	1.37	0.12
n-Butanol 1.5% v/v in water	0.02	0.3	0.03	0.01
Isomax-Diesel	0.02	0.04	0.01	0.03
Kerosene (10%) + HVI-90	0.05	0.02	0.01	0.03

Yazdani (2007) cited in Amiri et al. (2011) proposed the gas holdup correlation for petroleum based liquids according to

$$\varepsilon_R = 0.469\,[U_{SGR}]^{0.678}\,[\nu]^{-0.022} \tag{3.17}$$

Where $R^2 \approx 0.91$ valid for $0.1 \times 10^{-2} \leq U_{SGR} \leq 1.83 \times 10^{-2}$ m/s.

This correlation showed that the gas holdup is dependent on the gas velocity and the viscosity while the surface tension has no effect. 92% of the data was correlated using this equation with an error of less than 15%.

The second correlation by Mouza et al. (2005) (cited in Amiri et al. (2011)) was for a 1.5% by volume n-butanol water solution:

$$\varepsilon_R = 0.001\left[Fr^{0.5}Ar^{0.1}Eo^{2.2}\left(\frac{d_s}{d_c}\right)\right]^{2/3} \tag{3.18}$$

Where *Fr* is the Froude number

$$Fr = \frac{U_{SGR}^2}{d_c g}$$

Ar the Archimedes number

$$Ar = \frac{d_c^3 \rho_L^2 g}{\mu_L^2}$$

And *Eo* the Eötvös number

$$Eo = \frac{d_c^2 \rho_L}{\sigma_L}$$

And $\left(\frac{d_s}{d_c}\right)$ = ratio of the sparger to the column diameter.

The Froude, Archimedes and Eötvös numbers take into account the gas superficial velocity, liquid density, viscosity and surface tension.

The correlation by Kazakis et al. (2007) (cited in Amiri et al. (2011)) is a modification of the equation proposed by Mouza et al. (2005) (cited in Amiri et al. (2011)) by simply adding the effect of the mean pore diameter to the sparger diameter, $\frac{d_p}{d_s}$.

$$\varepsilon_R = 0.2\left[Fr^{0.8} Ar^{0.2} Eo^{1.6} \left(\frac{d_s}{d_c}\right)^{0.9} \left(\frac{d_p}{d_s}\right)^{0.03}\right]^{2/5}$$

3.19

By plotting the experimental and estimated gas holdups (artificial neural network, correlations by Yazdani (2007); Mouza et al. (2005) and Kazakis et al. (2007) (cited in Amiri et al. (2011))), Amiri et al. (2011) was able to predict the general behaviour of hydrodynamics in the bubble column with a normalized mean square error (NMSE) of less than 0.05 and some cases the neural network provided better estimations than the correlations. Amiri et al. (2011) concluded that the artificial neural network is an excellent tool for predicting as it is purely data driven which allows for more flexibility and adjustment to adapt to the various and varied data ranges.

Al-Masry (2006) used an artificial neural network to predict gas holdup and liquid velocity in two bench scale external loop airlift reactors. The input variables were gas velocity (U_{SGR}), volume ratio (T_{VR}), scale up ratio and viscosity (μ). The liquid systems were air-water and air-glycerol. In the 167L reactor the volume ratio was found to be above 7% for air-water and above 19% for air-glycerol for it not to have an effect on the hydrodynamics of the reactor. The correlation proposed by Al-Masry (2006) to calculate the gas holdup and liquid velocity for this reactor were:

$$\varepsilon_R = 0.34 U_{SGR}^{0.56} T_{VR}^{-0.02} \mu_L^{-0.04} \tag{3.20}$$

$$\varepsilon_D = 0.83 U_{SGR}^{0.38} T_{VR}^{1.42} \mu_L^{-0.2} \tag{3.21}$$

$$U_{SLR} = 0.67 U_{SGR}^{0.39} T_{VR}^{0.08} \mu_L^{-0.03} \tag{3.22}$$

For the smaller volume reactor (135dm^3), the T_{VR} ratio was at 30% for no effects to be detected. The correlations proposed are:

$$\varepsilon_R = 0.023 U_{SGR}^{0.86} T_{VR}^{-0.065} \mu_L^{-0.024} \tag{3.23}$$

$$\varepsilon_D = 0.59 U_{SGR}^{-0.88} T_{VR}^{-0.32} \mu_L^{0.08} \tag{3.24}$$

$$U_{SLR} = 0.003 U_{SGR}^{0.433} T_{VR}^{0.3} \mu_L^{-0.03} \tag{3.25}$$

Al-Masry (2006) further accounted for the area ratio, A_D/A_R, by proposing the following

$$\varepsilon_R = 3.84[(0.73U_{SGR} + 1)^{1.33} - 1]^{1/1.33} \times exp(-0.006T_{VR} - 1.095A_{DR} + 0.084\mu_L)$$

3.26

$$\varepsilon_D = 2.69[(0.47U_{SGR} + 1)^{1.29} - 1]^{1/1.29} \times exp(-0.011T_{VR} - 0.69A_{DR} + 0.075\mu_L)$$

3.27

$$U_{SLR} = 0.42[(0.0547U_{SGR} + 1)^{2.66} - 1]^{1/2.66} \times exp(0.013T_{VR} + 0.59A_{DR} - 0.14\mu_L)$$

3.28

Where $A_{DR} = (A_D + A_R)/A_R$.

He however, noted that these correlations are derived based on assumptions and are linear. In real-life applications hydrodynamics have non-linear characteristics and therefore the traditional mathematical approach is not effective.

Al-Masry (2006) re-analysed his work using a two hidden layer artificial neural network with a feed-forward back propagation algorithm in which the input parameters were US_{GR}, T_{VR}, μ_L and A_D/A_R. The outputs were gas holdup riser (ε_{GR}), gas holdup downcomer (ε_{GD}) and superficial liquid velocity(U_{LR}). The parity plot of Figure 3.12 is a comparison of the model performance using the work of Al-Masry (2004) and Al-Masry (2006). He found that the model gave good approximation between the experimental and predicted downcomer gas holdups with NMSE < 0.01. Al-Masry (2006) used 60% of the data to train the network and 40% to test the network. He concluded that the artificial neural network proposed is an excellent tool for prediction.

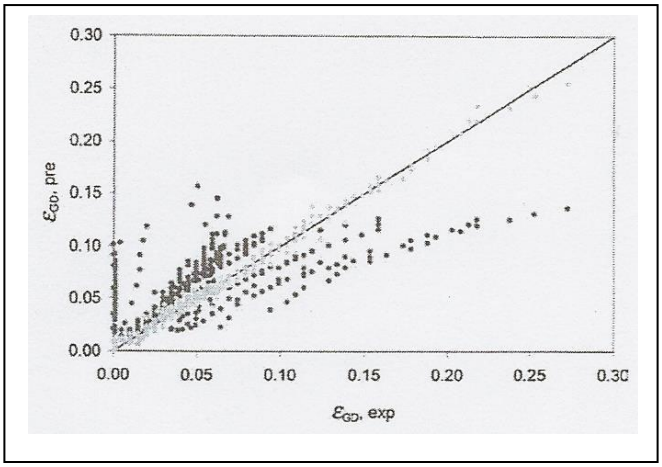

Figure 3.12 Parity plot of downcomer gas holdup (Al-Masry, 2006). A comparison between predicted and experimental results by Al-Masry (2004) (●) and Al-Masry (2006) (◇).

It must be noted that the work of Al-Masry (2004) shows some specific trends both above and below the diagonal as well as a flattening of the curve below the diagonal. This is a possible indication of an omission of input parameters that would be considered important by the network or that parameters were left out by the network in the training phase.

Kojić et al. (2015) investigated the effects of the type of sparger and alcohol concentration in a bench scale external loop airlift reactor on gas holdup. In their investigation three different spargers were used, viz., perforated plate; sintered plate and single orifice sparger. The systems studied were air-water; different concentrations of alcohol-air; 0.01n-butanol-air and 0.0051n-hexanol-air solutions. The conclusions from their experimental investigation was that increasing alcohol concentrations increased the gas holdup and that the perforated and sintered plate spargers provided better gas holdup than the single orifice sparger.

They used an artificial neural network that adopted the Levenberg-Marquardt back propagation algorithm with a sigmoidal transfer function. They used 70% of the 637 data points to train the network, 15% for validation and 15% for testing. The input neurons were superficial gas velocity, sparger orifice diameter, surface tension of liquid and area ratio. The single hidden layer consisted of 8 neurons with one neuron (gas holdup) as the output layer. Their parity plots (Figure 3.13) between predicted and experimental were good.

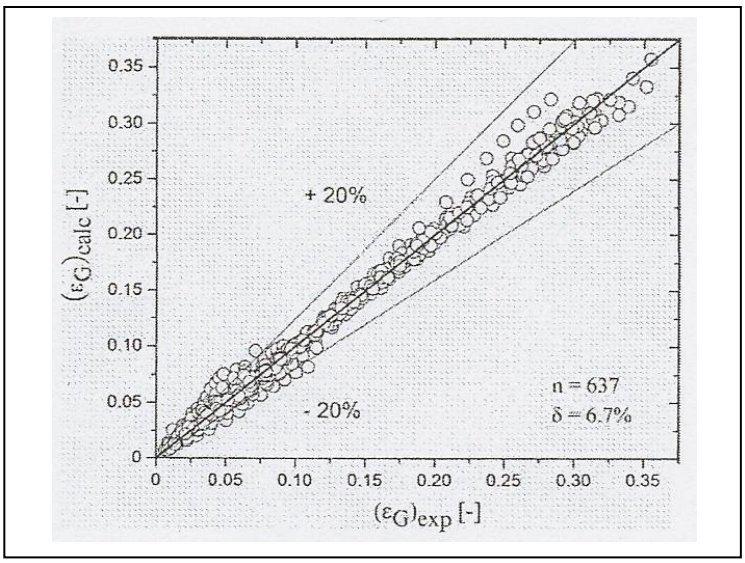

Figure 3.13 Parity plot of gas holdup in the riser using ANN (Kojić et al, 2015).

The general form of the applied power law correlation (equation 3.29) (Figure 3.14), does not give as good a prediction as the neural network (Figure 3.13)

$$(y)_{calc} = AU_{SGR}^{B}\sigma C_{d_o}^{D}\left({}^{A_D}/_{A_R}\right)^{E} \qquad 3.29$$

Where ${}^{A_D}/_{A_R}$ = area ratio

U_{SGR} = superficial gas velocity

σ = surface tension

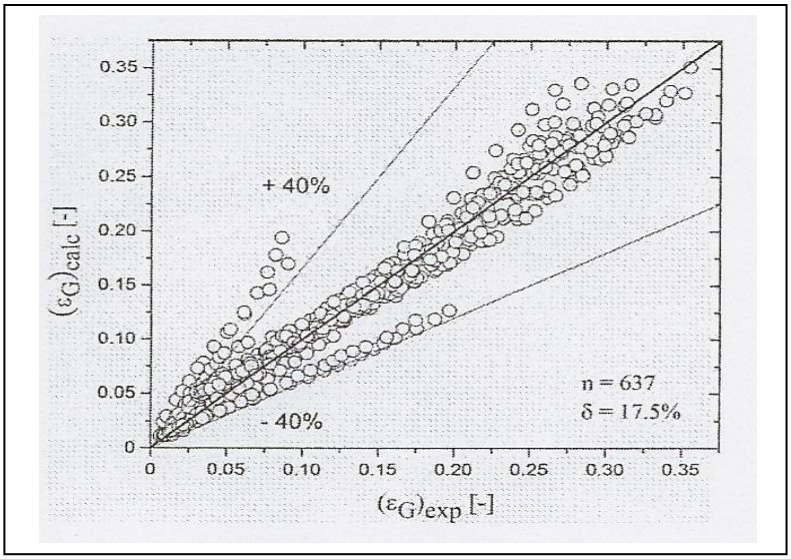

Figure 3.14 Experimental and predicted for ε_R using correlation (Kojić et al, 2015).

They concluded that the neural network predicts the gas holdup with better accuracy than the proposed correlation. Their work raises the same questions as Al-Masry (2004). There are specific trends noted in Figure 3.14 and this could also be the result of incomplete information supplied to the network.

Table 3.3 Correlation Parameters for riser gas holdup and fit statistics (Kojić et al, 2015).

Constants in equation 3.29	**A**	**B**	**C_{do}**	**D**	**E**
y_{cal} (eq. 3.29)	2.35	0.660	-0.47	-0.045	-0.61
Fit Statistics	Correlation		ANN		
Mean relative errors (%)	17.5		6.7		
Mean absolute error	0.51		0.19		
Root mean square error	0.02		0.008		

Behkish et al. (2005) also used a back propagation artificial neural network to predict gas hold up in industrial-scale bubble columns and slurry bubble column reactors for Fischer-Tropsch synthesis. They looked at gas-liquid-solid characteristics, reactor geometry, and sparger type and size and operating variables. The network was initially trained to predict gas holdup which was effectively done after which the network was used to predict the effects of pressure, superficial gas velocity, temperature and catalyst loading on the total synthesis gas holdup for the low-temperature Fisher-Tropsch synthesis. They concluded that the total amount of synthesis gas increased when the reactor was increased together with superficial gas velocity as a result of the increase in gas momentum. The increase in synthesis gas was also a result of the increase in the number of sparger orifices. They also found that catalyst loading above 50wt. % resulted in a decrease in synthesis gas holdup as well as an increase in reactor temperature. The predicted results from their neural network were in agreement with literature trends.

3.6.2.2. FLOW REGIME PREDICTION USING ARTIFICIAL NEURAL NETWORKS (MI et al., 2001)

A self organizing neural network was used in MATLAB to classify the flow regime in air lift reactors. These are bubbly flow, transition zone, churn turbulent and slug flow. The network was able to classify the data using clustering. The traditional impedance method was used to verify the neural network results. The proposed network was able to correctly classify the data.

3.6.2.3. PREDICTING MASS TRANSFER USING ARTIFICIAL NEURAL NETWORKS

Kojić et al. (2015) investigated the effect of an inserted membrane and sparger type on the mass transfer characteristics on a bench scale external loop airlift reactor. From their experimental investigation they concluded that the sintered plate produced a higher mass transfer coefficient value, k_La, than the single orifice sparger and that by increasing the alcohol concentration, the gas holdup increases which in turn increases the mass transfer coefficient. The alcohol effects were due to the non-coalescing characteristics of aliphatics in the alcohol.

The neural network selected by Kojić et al. (2015) was a feed forward back propagation algorithm with four inputs, viz., superficial gas velocity; distributor characteristics; surface tension and overall friction coefficient. The single hidden layer consisted of 13 neurons while the output layer was just one which was the mass transfer coefficient. To obtain the best prediction model, the number of hidden neurons was varied until similar values for trained and predicted data was achieved. Their data set consisted of 479 measurements, of which 70% were used for training, 15% for validation and 15% for testing. The root mean square error obtained was 0.21 while the coefficient of determination (R^2) was 0.97. The parity plots between the experimental and the predicted data showed good agreement. Kojić et al. (2015) concluded that the artificial neural network successfully predicted the mass transfer coefficient in an external loop airlift reactor for different alcohol concentrations and types of spargers.

Reisener et al. (1993) also predicted the mass transfer coefficient with an artificial neural network but in a gas sparged electrolyser. Their comparison with an airlift reactor was also excellent.

3.6.3. CONCLUSION

It can safely be noted that using artificial neural networks to predict the mass transfer coefficient, gas holdup, liquid velocity and regime flow is viable on bench scale apparatus for airlift reactors. This study intends to investigate variations in geometry, sparger type, gas velocity and concentrations of water-glycerin solutions on mass transfer in five configurations of pilot scale external loop airlift reactors. The input parameters, sparger design, area ratio, aspect ratio, superficial gas and liquid velocities, riser and downcomer gas holdup as well as liquid properties will be used as input parameters while the mass transfer coefficient will be the output parameter. The software, Predict (version 3.30) will be used to build the model. Predict uses the cascade correlation architecture to predict the mass transfer coefficient. A parity plot between the predicted and experimental data will be used to ascertain the generalization and accuracy of the network.

CHAPTER FOUR

METHODOLOGY

4.1. INTRODUCTION

The objective of this research was to model the gas holdup, superficial air and liquid velocities, fluid properties, geometric parameters, and visual observations in order to predict the mass transfer coefficients of pilot scale external loop airlift reactors using the neural network software package, Predict version 3.30. To achieve this, five pilot scale external loop airlift devices of varying sizes and similar configuration were used to generate data for the modeling. The developed model would then be applied to data obtained from literature to determine whether it is able to give good approximations. The proposed methodology consisted of the following:

- Preliminary investigations to determine the optimal sparger position, the optimal liquid height in the disengagement tanks, run time and fluid selection.
- Comprehensive experimental studies based on the objectives were done and the results analysed and selected for the neural network.
- Modeling of the experimental data
- Testing of the model using external unseen data from literature (Nayager and Govender, 2016; Fakhari, et al., 2014; Shariati, et al., 2007; Al-Masry, 2004; Al-Masry and Dukkan, 1997; Guo, et al., 1997) and from this work was done to determine how well the network was able to generalize and predict the mass transfer coefficients. The software DigitizeIT 2.3.3 by I Bormann, Am Rohrbruch 41, 38108, Braunnschweig, Germany was used to read the data points from the graphs of the published literature.

4.2. PRELIMINARY INVESTIGATIONS AND PROCEDURES

Prior to the startup of the actual experimentation a few preliminary procedures and investigations were done. These were to ensure correct operation so that reliable results could be achieved.

4.2.1. FLUID SELECTION AND REACTOR CONFIGURATION

Only Newtonian fluids were used in this investigation. Municipal tap water and four concentrations by volume of medical grade glycerin solutions (15%; 22%; 28% and 31.25%) were used, in reactor configuration 1 and 2 (Figure 4.1). In reactor configuration 3 (Figure 4.2), configuration 4 and configuration 5 (Figure 4.3) only municipal tap water was used. The selection of these fluids was based on availability, cost and toxicity. The glycerin solutions were made up in a 1200L storage tank before being pumped into the reactor.

The five reactors were constructed out of QVF borosilicate glass sections with PVC spacers. Table 4.1 contains the dimensions of each of the reactor configurations.

Table 4.1 Reactor dimensions.

Configuration	Riser Diameter (m)	Riser Height (m)	Downcomer Diameter (m)	Downcomer height (m)
1	0.15	2.95	0.15	3.1
2	0.15	2.95	0.1	3.1
3	0.225	5.4	0.225	5.4
4	0.15	4.22	0.15	4.01
5	0.15	4.22	0.1	4.01

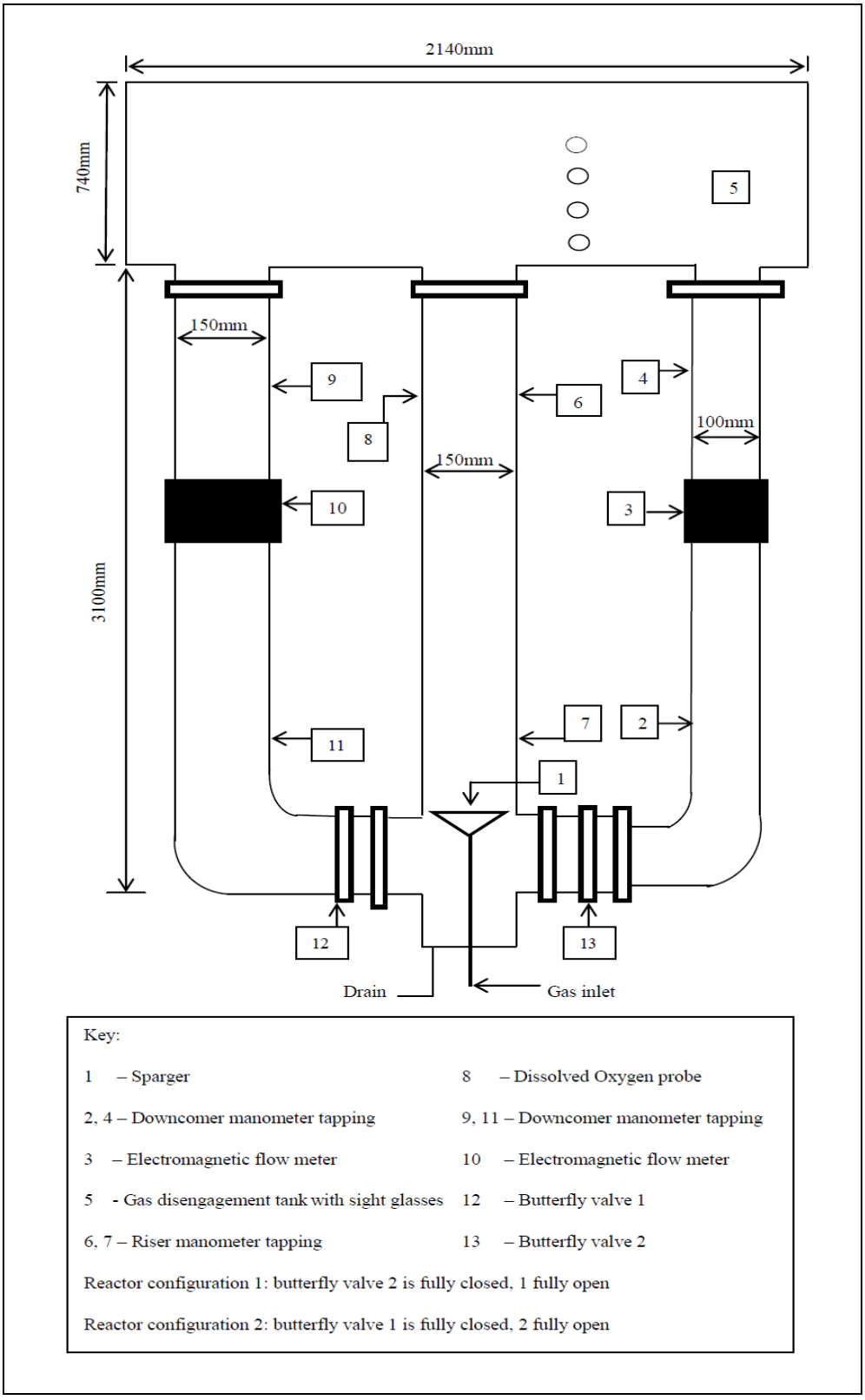

Key:

1 – Sparger	8 – Dissolved Oxygen probe
2, 4 – Downcomer manometer tapping	9, 11 – Downcomer manometer tapping
3 – Electromagnetic flow meter	10 – Electromagnetic flow meter
5 - Gas disengagement tank with sight glasses	12 – Butterfly valve 1
6, 7 – Riser manometer tapping	13 – Butterfly valve 2

Reactor configuration 1: butterfly valve 2 is fully closed, 1 fully open

Reactor configuration 2: butterfly valve 1 is fully closed, 2 fully open

Figure 4.1 Schematic of reactor configuration 1 and configuration 2.

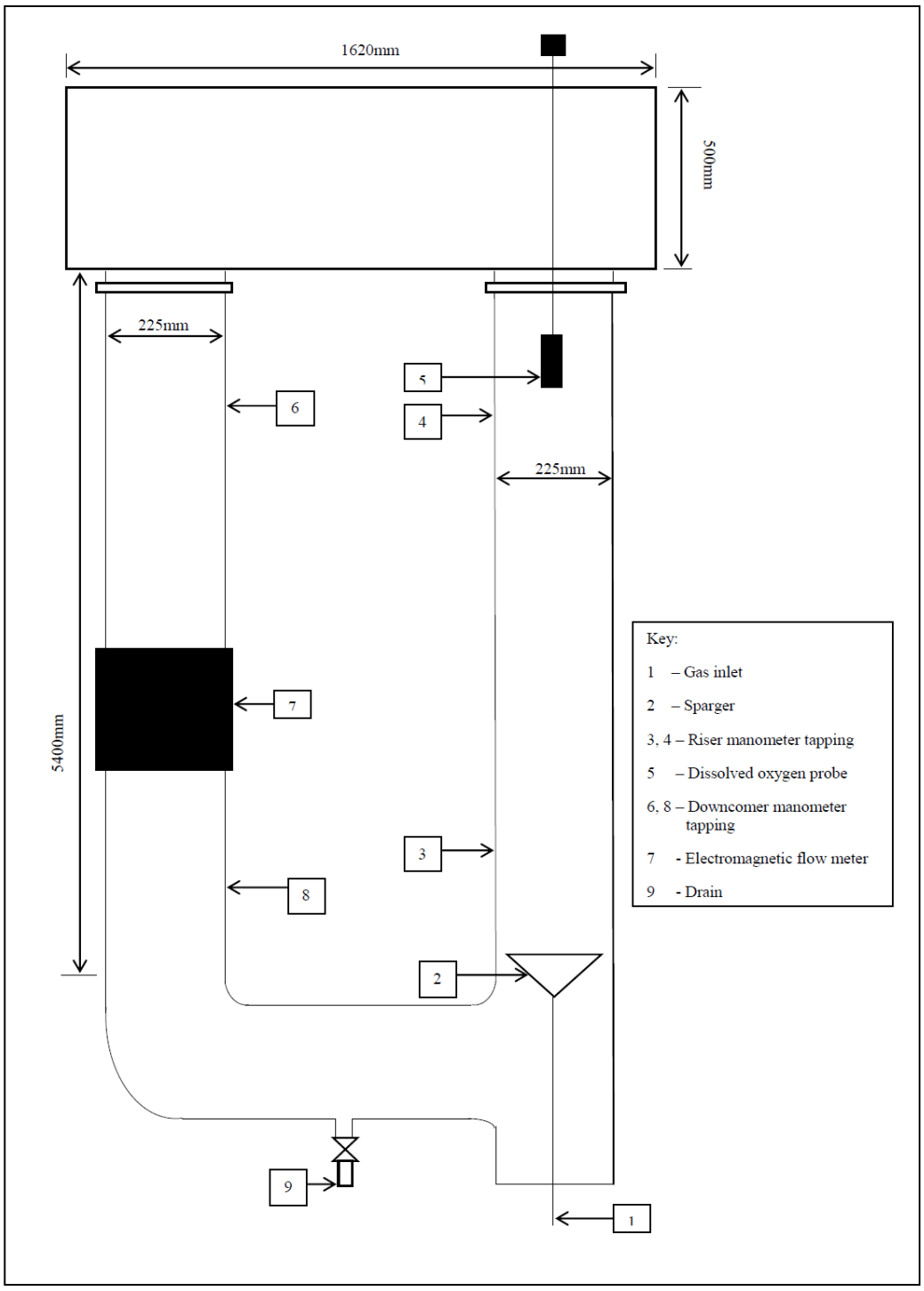

Figure 4.2 Schematic of reactor configuration 3.

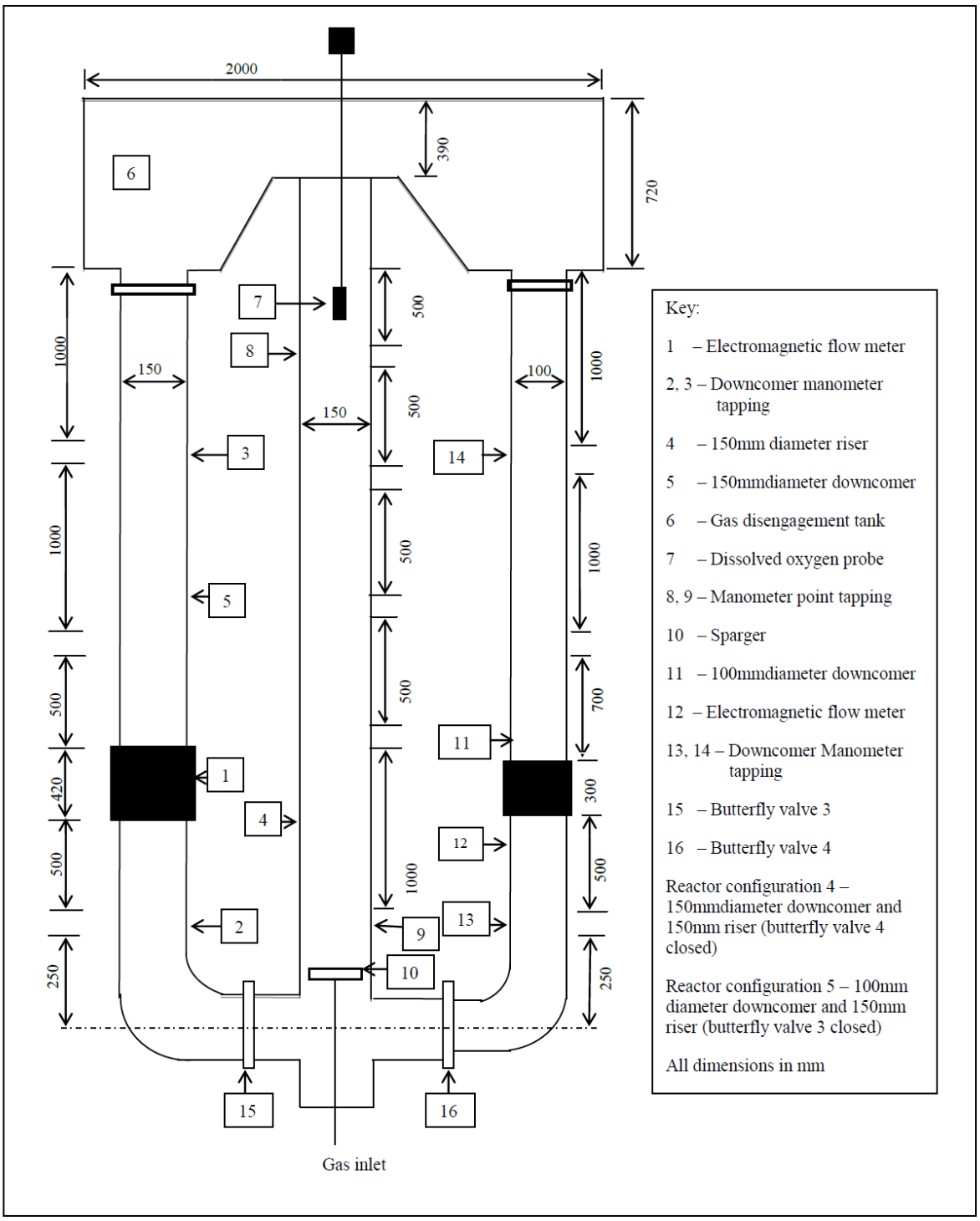

Figure 4.3 Schematic of reactor configuration 4 and configuration 5.

4.2.1.1. VISCOSITY, DENSITY AND SURFACE TENSION TESTING

The glycerin solutions and tap water samples were sent for testing and analysis. Standard procedures were followed by this laboratory to carry out the analysis. The Kruss Tensiometer Instrument method was used to determine surface tension. The Haake Viscometer method with a variable temperature water-bath was used to determine viscosity and density of the solutions was determined by the Anton Paar DMA 500 density meter method. The results appear in Table 4.2.

Table 4.2 Fluid properties.

FLUID	DENSITY (kg/m^3)	SURFACE TENSION (mN/m)	VISCOSITY (mPas)
Municipal tap water	997.05	72	1.08
15% glycerin solution	1032.9	64.5	1.68
22% glycerin solution	1046.9	73.1	2.136
28% glycerin solution	1059.1	72.8	2.28
31.25% glycerin solution	1065.9	67.2	2.76

4.2.2. SPARGER SELECTION

Although five different sparger designs were used in this investigation, the spargers were classified into three broad categories. These were perforated plate (A) (Figure 4.4 and Figure 4.7), perforated disk (B) (Figure 4.5 and Figure 4.8) and perforated pipe (C) (Figure 4.6). Assigning the spargers labels of type A, type B and type C was done for ease of use in the neural network model.

The individual sparger's characteristics are noted in Table 4.3.:

Table 4.3 Sparger classification.

Sparger type	**n_h (number of holes)**	**d_o (diameter of pore)**	**Diameter of sparger**
Perforated Plate (Type A)	21	4.5mm	140mm
Perforated Disk (Type B)	20	4.5mm	100mm
Perforated Pipe (Type C)	21	4.5mm	120mm
Perforated Plate (Type A)	210	1mm	198mm
Perforated Disk (Type B)	56	1mm	100mm

Figure 4.4 Perforated Plate (A) (used in reactor configuration 1 and configuration 2).

Figure 4.5 Perforated Disk (B) (used in reactor configuration 1 and configuration 2).

Figure 4.6 Perforated Pipe (C) (used in reactor configuration 1 and configuration 2).

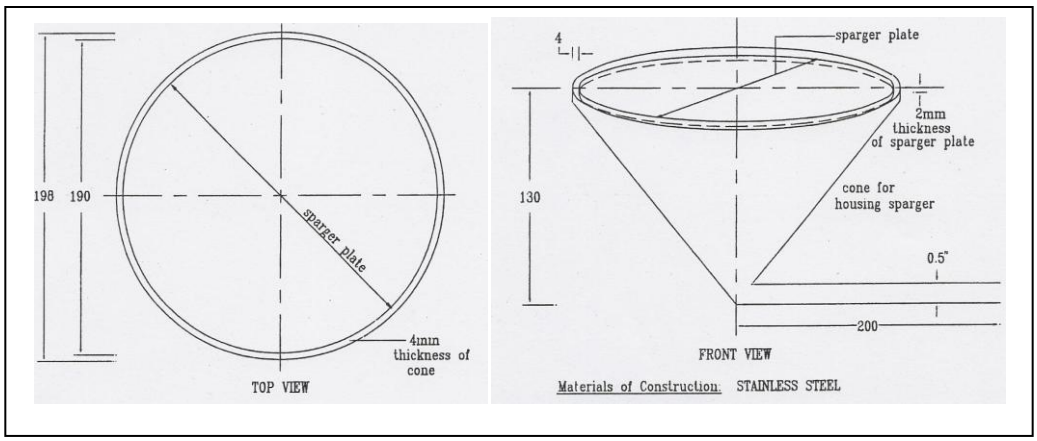

Figure 4.7 Perforated Plate (A) (used in reactor configuration 3) (Al-Masry and Dukkan, 1997).

Figure 4.8 Perforated Disk (B) (used in reactor configuration 4 and configuration 5).

4.2.2.1. SPARGER POSITIONING

Sparger positioning in the airlift reactor is important as reported by Chisti and Moo-Young (1987). In this investigation, it was found that the optimal position for the sparger was at the entrance of the riser. This prevented any deflection (Figure 4.9) of the entering air bubbles from the sparger by the returning liquid from the downcomer as illustrated in Figure 4.10.

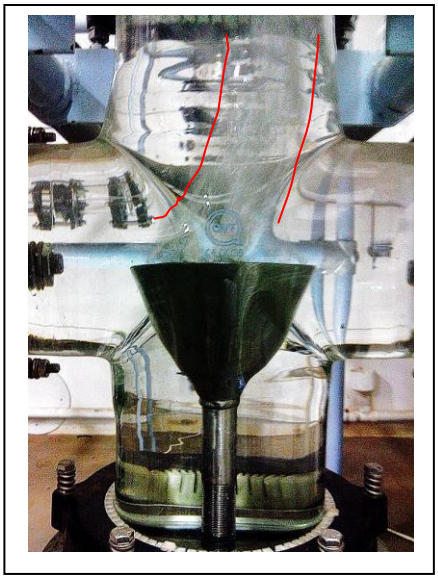

Figure 4.9 Deflection of entering bubbles with sparger on the central horizontal axis of the base.

Figure 4.10 Sparger positioned at the entrance to the riser – no deflection of bubbles.

In reactor configuration 1, configuration 2 and configuration 3, the sparger was positioned at the entrance to the riser however in reactor configuration 4 and configuration 5, the sparger was positioned 23cm above the entrance of the riser. Unfortunately the positioning for the sparger in reactor configuration 4 and configuration 5 were preset and could not be adjusted.

4.2.3. DISSOLVED OXYGEN PROBE POSITIONING AND READINGS

Due to the turbulence created by the entering air lower down in the riser, the possibility of bubble impingement on the dissolved oxygen probe was highly likely. To avoid this it was recommended that the dissolved oxygen probe be positioned at the highest possible sampling point in the risers of each reactor configuration. The distance as measured from the entrance to the riser to the probe position:

Table 4.4 Dissolved oxygen probe position for each reactor configuration.

Reactor Configuration	Dissolved oxygen probe position in relation to riser height (m)
1	2.53
2	2.53
3	5.915
4	3.425
5	3.425

4.2.3.1 DYNAMIC DE-AERATION

The dynamic de-aeration method was used to carry out the mass transfer coefficient investigation. This involved sparging the reactor with technical grade nitrogen until the dissolved oxygen reading was as close to zero as possible. In this investigation that value ranged between 0.005ppm and 0.96ppm. This range was found to be the zero reading for a de-aerated liquid in this investigation. After a steady reading from the dissolved oxygen probe, the nitrogen was turned off. Nitrogen bubbles were allowed to disengage completely from the liquid, especially at higher viscosities, before air was sparged into the reactor. Mass transfer coefficient calculations were done according to the method described in Section 2.4.4.

4.2.4. LIQUID HEIGHT IN THE DISENGAGEMENT TANK

In Section 2.6.2 of this thesis, a detailed discussion of the effects of the liquid height in the disengagement tank was presented. To minimize the adverse effects of bubble entrainment

into the downcomers of the reactors, the following liquid heights (Table 4.5) in the disengagement tanks directly above the riser outlets were used. This was done by observation.

Table 4.5 Liquid heights in disengagement tanks.

Reactor configuration	**Disengagement tank liquid level (m)**
1	0.3
2	0.3
3	0.19
4	0.1
5	0.1

Although a significant percentage of the returning bubbles to the downcomer were greatly reduced, some very fine bubbles were entrained in the returning liquid to the downcomers.

4.2.5. GAS HOLDUP MEASUREMENTS

The gas holdup could either be determined manometrically or using the volume expansion method. The volume expansion method required the static height of the liquid and dispersed height of the liquid. The volume expansion method is more suitable for a laboratory scale airlift reactors although there is no difference in the measurements. For ease of investigation the manometric method was used to determine the gas holdup in the reactors in this study.

The manometric method (Figure 4.11) as described by Chisti (1989) was used to determine the gas holdup in the riser (ε_R) and the downcomer (ε_D) according to equation 2.22:

$$\varepsilon = \frac{\rho_L}{\rho_L - \rho_G} \frac{dh_m}{d\hat{z}}$$

2.22

Where ε - represents ε_R and ε_D

ρ_L – density of the liquid

ρ_G - density of the gas

dh_m – difference in liquid level (m)

$d\hat{z}$- distance between manometer tappings (refer to Figure 4.11) (Table 4.6).

The risers and downcomers were fitted with independent inverted U-tube manometers. To measure the gas holdup across the length of the riser and downcomer, pressure tappings were made at the extreme ends of the columns and connected to the manometers using flexible plastic hose. The manometers were then filled with the liquid from the column by bleeding the lines. This also ensures that there are no air bubbles in the lines that would affect the pressure readings. To get the air bubble in the manometer, one arm of the manometer was sealed while the other was bled of most of its liquid. The line was then reconnected to the manometer arm. Prior to startup, the liquid levels in the arms of the manometer must be at the same heights. Any discrepancies are indicative of air bubbles in the lines connecting the manometer. Once air is sparged into the reactor the levels on the arms change and readings are taken. The gas holdup was calculated according to equation 2.22.

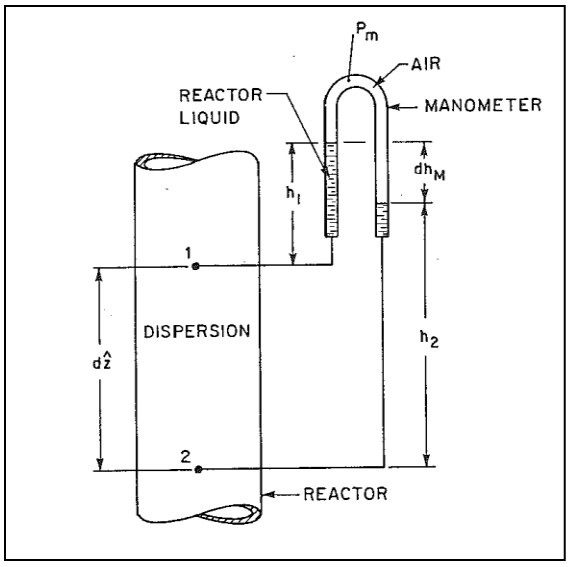

Figure 4.11 Inverted U-tube manometer (Chisti, 1989).

Table 4.6 Distance between manometer tappings.

Reactor Configuration	Riser (m)	Downcomer (m)
1	2.33	2.14
2	2.33	2.01
3	3.31	3.74
4	3.13	2.64
5	3.13	2.67

4.2.6. VISUALIZATION STUDIES

Flow visualization studies are vitally important in helping to understand the flow dynamics in an external loop airlift reactor. By noting the changing behaviour of the fluid and bubbles with changes in gas velocity, type of sparger and downcomer diameter, changes in flow regimes can be better explained as well as behaviour of the system that should be expected when transitions between regimes occurs. This would assist in providing a clearer explanation for reactor operating parameters and their effect on mass transfer. In this investigation a high

speed camera (Nikon D5100) was used for still photographs as well video recordings to better understand the behaviour of the fluid in the reactors.

4.2.7. AIRLIFT REACTOR SOFTWARE AND HARDWARE

Airlift reactor configuration 1 and configuration 2 (Figure 4.1) was automated using LabVIEW version 14 software, by National Instruments Software. From extensive initial pretesting, it was found that the liquid velocity stabilised after a few seconds and the dissolved oxygen remained unchanged after 12 minutes or less for all experiments. However, for completeness each experiment had a run time of 20 minutes. Considering the run time for each experiment and the amount of data that would be logged, by adopting a sampling time of 20 seconds, sufficient data was logged to comfortably calculate the mass transfer coefficient as described in section 2.4.4. The data recorded every 20 seconds was captured directly into an Excel spreadsheet:

- Dissolved oxygen (8 in Figure 4.1) using a Hanna Galvanic DO Probe (HI 76410/10) and Hanna Dissolved Oxygen Process Controller (HI 8410)
- Liquid flowrate using a SAFMAG Flowmetrix SA electromagnetic flowmeter (10 and 3 in Figure 4.1)
- Gas flowrate and incoming gas temperature using an ALICAT MCS series mass flow meter

The manometer readings were taken manually. In reactor configuration 3, configuration 4, and configuration 5 all readings were taken manually. The dissolved oxygen was detected using a HACH HQ 440d benchtop dual input multi-parameter meter with HACH IntelliCAL^{TM} LDO101 rugged luminescent/optical dissolved oxygen (LDO) probe. The liquid flowrates were measured using a SAFMAG Flowmetrix SA electromagnetic flowmeters. The manometer readings were recorded manually.

4.3. SUPERFICIAL LIQUID VELOCITY MEASUREMENTS

Liquid flowrate was measured with a SAFMAG Flowmetrix SA electromagnetic flow meter positioned on the downcomers (see Figure 4.1, Figure 4.2 and Figure 4.3). The liquid

flowrate was then converted into the superficial liquid velocity by dividing the value by the cross sectional area of the respective downcomer:

$$U_{SLD} = \frac{Q_{LD}}{A_D} \quad 4.1$$

Where Q_{LD} = liquid flowrate (L/min).

4.4. SUPERFICIAL GAS VELOCITY MEASUREMENTS

The incoming gas flowrate was measured using an ALICAT MCS series mass flow meter for reactor configuration 1 and 2 and KDG 2000 rotameters for reactor configurations 3, 4 and 5. The measured gas flowrate was converted into superficial gas velocity by dividing the value by the cross sectional area of the respective riser:

$$U_{SGR} = \frac{Q_{LR}}{A_R} \quad 4.2$$

Where Q_{LR} = the gas flowrate (L/min).

4.5. OPERATIONAL PROCEDURE

The following operational procedure applied to all configurations of reactors asides from the filling of the reactors which differed as will be further explained.

- The reactors were filled to the required gas disengagement tank levels as follows:
    - For reactor configuration 1 and 2, the liquid was pumped to the reactor. The glycerin mixtures were mixed in the tank before being pumped to the reactor.
    - Reactor configurations 3, 4 and 5 were filled with water using a hose directly attached to a tap.
- Entrained bubbles were allowed to disengage.
- The manometers were then set according to the procedure in section 4.2.6.

- Depending on the configuration under investigation, butterfly valves 1, 2, 3 and 4 were closed (see Figure 4.1; Figure 4.2; Figure 4.3).
    - For configuration 1, butterfly valve 2 was fully closed, while valve 1 was fully opened.
    - For configuration 2, butterfly valve 1 was fully closed, while valve 2 was fully opened.
    - For configuration 4, butterfly valve 4 was fully closed, while valve 3 was fully opened.
    - For configuration 5, butterfly valve 3 was fully closed, while valve 4 was fully opened.
- The liquids were dynamically de-aerated with technical grade nitrogen until the dissolved oxygen range of between 0.0054ppm to 0.96ppm (C_{LO}) (zero range) was reached.
- Once the required 'zero' dissolved oxygen was reached the nitrogen was shut off and the manometers were re-inspected for any changes in levels and corrected if any were found.
- Compressed gas (air) was then sparged into the risers.
- For reactor configuration 1 and 2, the data logging software was started simultaneously with the sparged gas. For reactor configuration 3, 4 and 5, the readings from the dissolved oxygen probed was immediately recorded and continually logged (C_L) at every 10 second interval.
- The manometer readings were manually recorded when the liquid flowrates reached stability. This occurred after approximately 1minute for all reactor configurations.
- During the course of a run:
    - Visual observations were made noting approximate riser bubble size according to the following categories:
        - ❖ Small bubble diameter (S) – 1mm to 1cm.
        - ❖ Medium bubble diameter (M) range greater than 1cm but less than 3cm.
        - ❖ Large bubble diameter (L) range greater than 3cm but less than 5cm.
        - ❖ Extra-large bubble diameter (XL) range greater than 5cm.

    - Coalescence of bubbles in the riser.
    - Flow patterns in the riser taking into consideration level of turbulence.
    - Downcomer bubble size using the same bubble size category as for the riser bubble sizes.
- The compressed gas was stopped when the dissolved oxygen (C^*) change became minimal for each run.
- Entrained bubbles were allowed to disengage completely.
- Point 5 through to point 12 was repeated for each predetermined gas flowrate (Appendix A1).

4.6. THE NEURAL NETWORK

In this research the computer system consisted of an Intel(R) Core (TM) iS-7500 CPU @ 3.40GHz processor with 4.00GB RAM using Windows 10 Pro edition. The neural network software, Predict version 3.30 by Neuralware (Pensylvania, United States of America) was used to model the experimental data. In this investigation 663 experimental runs were initially carried out after which 12 more were added to reactor configuration 3. From this set, 32 points were set aside as an external validation set together with data from literature. These points were selected using the round robin technique. Of the remaining data set, 70% was used as training data in the network, 15% for validation (internal) and 15% for testing (internal). The final input variables (Appendix A1) into the model were:

- Sparger type
- Area ratio
- Aspect ratio
- Density, surface tension and viscosity of the fluid
- Riser bubble size
- Bubble flow pattern
- Riser height
- Downcomer height
- Riser diameter

- Downcomer diameter
- Downcomer bubble size
- Superficial gas velocity
- Superficial liquid velocity
- Riser gas holdup
- Downcomer gas holdup
- Bubble flow pattern

The output variable was the mass transfer coefficient.

The model was then ‘Trained’ and ‘Run’ to determine the predicted output. Optimisation took a maximum of two minutes. To determine how well the model can generalize and to what degree of accuracy, the model was then ‘Tested’. The model that was built was then validated with external data from the works of Nayager and Govender (2016), Fakhari et al. (2014), Shariati et al. (2007), Al-Masry and Dukkan (1997), Guo et al. (1997) and the 32 unseen data points from this work. This was done to determine how well the model could approximate the mass transfer coefficients of systems with different geometries and fluids.

CHAPTER FIVE

RESULTS AND DISCUSSION

5.1. INTRODUCTION

The artificial neural network with its ability to provide solutions where the traditional algorithms and models fail is highly data driven in order to effectively model complex non-linear systems. To this end the first part of this investigation involved the study of the effects of reactor and sparger geometry and fluid properties on the mass transfer characteristics of 5 configurations of pilot scale external loop airlift reactors to generate data. Initially six hundred and sixty three data points or records were experimentally generated after which a further 12 records were added for reactor configuration 3. From the initial records, 32 records were selected using the round robin technique, and set aside to form part of the validation record set with records from literature. After an analysis of the experimental data from the initial investigation, parameters that were considered important were used as inputs into the model. This was done progressively so that assumptions from literature with respect to significant and insignificant parameters could be resolved resulting in a progressively improving model.

5.2. FLOW VISUALIZATION STUDIES

Visual observations with regards to sparger location, bubble flow patterns, approximate bubble sizes and distribution during an investigation are very important as they provide another perspective to understanding, to some degree the complex behaviour patterns within

an airlift reactor as well as providing some insight into the mass transfer characteristics of the reactor. However, the availability of flow visualization studies in literature is lacking. This is in agreement with Chisti (1989) who also states that flow visualization studies are important and comments on the lack thereof in literature. He also reports that the flow visualization studies will assist in understanding the behaviour within an airlift reactor. He investigated the correct positioning of a sparger in an airlift reactor and was able to only come to a conclusion based on his visual observations. In this investigation, observations were made with respect to sparger design and location, area ratio, aspect ratio and fluid properties on the bubble flow patterns, size, distribution, coalescence and weeping in the five reactor configurations.

5.2.1. EFFECT OF SPARGER DESIGN, AREA RATIO AND FLUID PROPERTIES ON BUBBLE FLOW BEHAVIOUR

The optimum sparger location was found to be at the entrance of riser as discussed in Section 2.6.1.1 and is in agreement with Chisti (1989). Sparger design followed by the area ratio (A_D/A_R) had the most significant effect on bubble flow pattern, distribution and coalescence while the sparger pore size influenced the bubble size exiting the sparger. The following visual observations (described in Sections 5.2.1.1.; 5.2.1.2.; 5.2.1.3.; 5.2.1.4.; 5.2.1.5. and 5.2.1.6.) were not available in literature and were important in helping to further understand the mass transfer characteristics in all the reactors used in this investigation.

5.2.1.1. REACTOR CONFIGURATIONS 1 AND 2 WITH A PERFORATED PLATE SPARGER (TYPE A) DESIGN

When using the perforated plate sparger for reactor configuration 1, i.e. $A_D/A_R = 1$ (downcomer diameter 150mm), the bubbles followed a fairly ‘straight’ path up the riser (Figure 5.1) even though at above 0.04m/s it was noted that the bubble flow patterns had started to become slightly chaotic for all solutions. The bubble sizes were approximately 5mm in diameter. Slight weeping was noted for superficial gas velocities of 0.019 and 0.021m/s after which flow was consistent through all pores of the sparger (Figure 5.2). The manometer remained stable even though Kulkarni et al. (2009) reported that an unstable manometer is the result of weeping at the sparger. Coalescence of bubbles for the gas-water

system and the 15% and 31.25% glycerin-gas systems began at a superficial velocity of approximately 0.028 – 0.033m/s but there was always rapid breakup of these irregularly shaped bubbles. The 22% and 28% glycerin-gas systems had very little to no coalescence respectively although the 28% glycerin-gas system produced a slightly bigger bubble size as compared to the other systems which had no effect on the mass transfer (see Section 5.3.2.4).

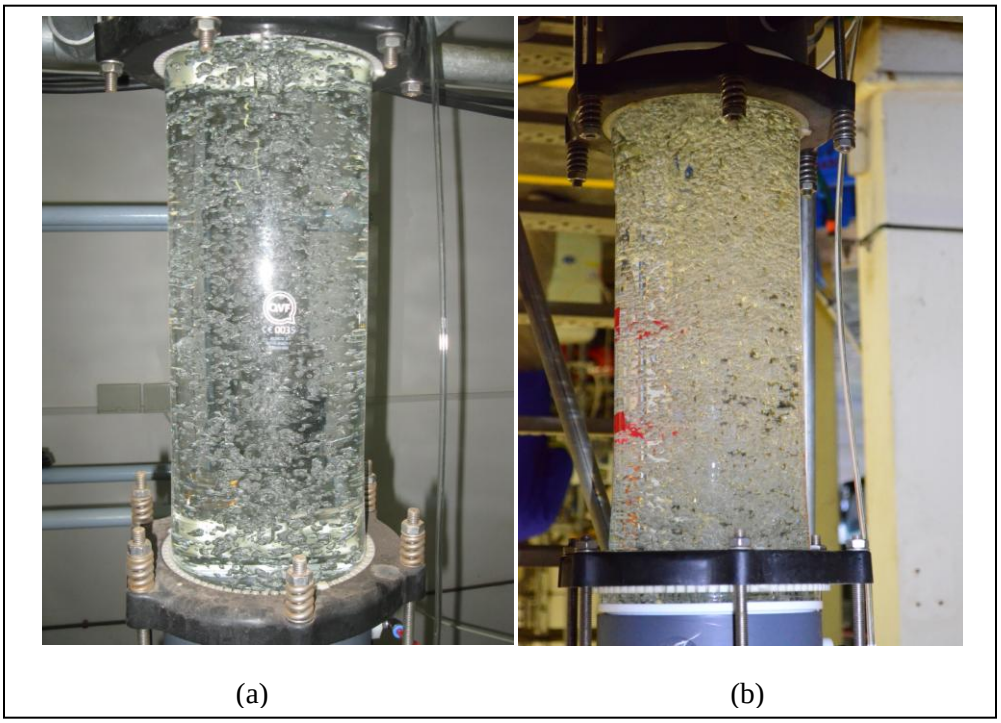

(a) (b)

Figure 5.1 Fairly uniform flows at low (a) and high velocities (b) for a perforated plate sparger.

(a) (b)

Figure 5.2 Weeping at initial gas velocity (a) no weeping at higher velocity (b).

Bubbles in the downcomer were so small (< 1mm diameter) that from a 20cm distance away from the column they were not visible. Downcomer bubbles were noted at the start of each run. The only manner with which to observe these bubbles was to shine a light into the downcomer at the back of the column. The very fine bubbles could be observed returning to the riser. This finding contradicts the report by Albijanic et al. (2007) (cited in Fakhari et al. (2014)), who reported that at superficial gas velocities higher than 0.012m/s, the bubbles in the downcomer do not return to the riser.

When the area ratio was less than 1, i.e. the downcomer diameter was 100mm (configuration 2, Figure 4.1), the bubble flow pattern took on a slightly wavy path (Figure 5.3) with the perforated plate sparger. This phenomenon was evident for a distance of approximately 0.5m up the riser from the sparger after which the bubbles followed a fairly 'straight' path up the riser. There was always a good distribution of bubbles across the cross section and length of the riser.

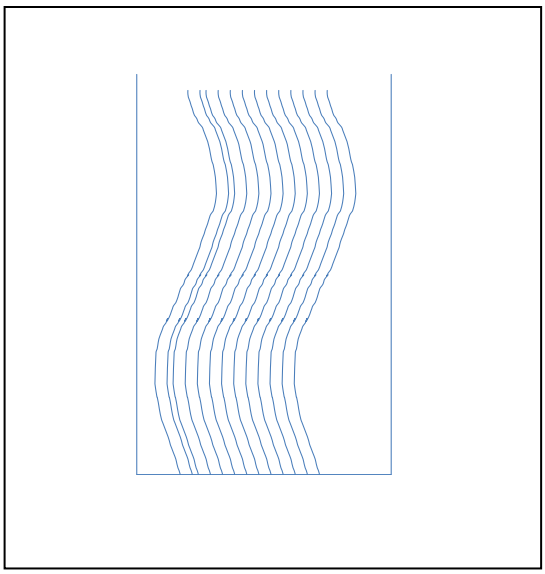

Figure 5.3 Schematic of initial bubble flow pattern ($A_D/A_R < 1$; perforated plate sparger; configurations 1, 2, 4 and 5).

This phenomenon became more pronounced as the superficial gas velocity increased beyond 0.04m/s and was evident for all systems. Coalescence for the gas-water system was noted from a superficial gas velocity of 0.042m/s whereas for the 15% glycerin-gas system occasional coalescence was noted at this velocity. However coalescence was prevalent from a superficial gas velocity of 0.045m/s for the 15% glycerin-gas system. These coalesced bubbles rapidly broke up. A phenomenon similar to pulsing was noted. This can be described as the very quick congregation and dispersion of bubbles similar to the illustration in Figure 5.4.

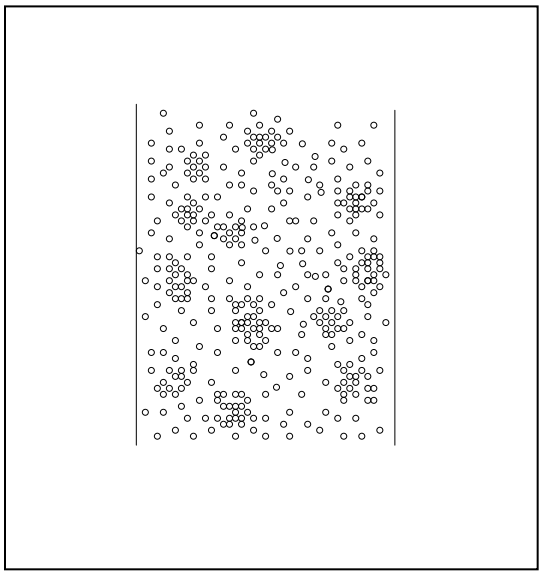

Figure 5.4 Schematic of congregation and dispersion of bubbles.

Coalescence was prevalent from a superficial gas velocity of 0.026m/s for the 22% and 31.25% glycerin-gas systems. Surprisingly coalescence was only noted at 0.05m/s for the 28% glycerin-gas system. The fine bubbles in the downcomer was again barely visible at a distance as stated for when A_D/A_R =1.

5.2.1.2. REACTOR CONFIGURATIONS 1 AND 2 WITH A PERFORATED DISK SPARGER (TYPE B) DESIGN

When the perforated disk sparger was used in reactor configuration 1, the bubble patterns for approximately 0.5m up the riser followed a slightly wavy path (Figure 5.5).

This was evident at all superficial gas velocities and for all systems. However, even though this flow pattern was noted, there was always an even distribution of bubbles within this 0.5m and beyond. Coalescence for all systems began before the superficial gas velocity range of 0.028 – 0.033m/s. However, these highly irregularly shaped coalesced bubbles rapidly broke up. Between the superficial velocity of 0.038 and 0.042m/s the bubble pattern appeared chaotic for the 0 -28% glycerin-gas systems but for the 31.25% glycerin-gas system, chaotic behaviour was only noted at a superficial gas velocity of 0.05m/s.

Figure 5.5 Bubble paths slightly wavy for perforated disk spargers. Bubbles are coalesced. Bubbles flow toward central vertical axis of riser.

When the area ratio decreased, i.e. A_D/A_R <1, the wavy pattern became more prominent and began to take on a swirling effect or helical effect as the body of bubbles moved together (Figure 5.6) for all systems for reactor configurations 2 and 5. The bubbles exiting the sparger also appeared as elongated coalesced bubbles (Figure 5.6) for a short period.

This flow pattern was evident for a distance of approximately 1m up the riser from the sparger. After this distance, the bubbles began to follow a fairly 'straight' path up the column. In addition to this phenomenon, the bubbles tended to concentrate toward the central axis of the riser as illustrated in Figure 5.5.

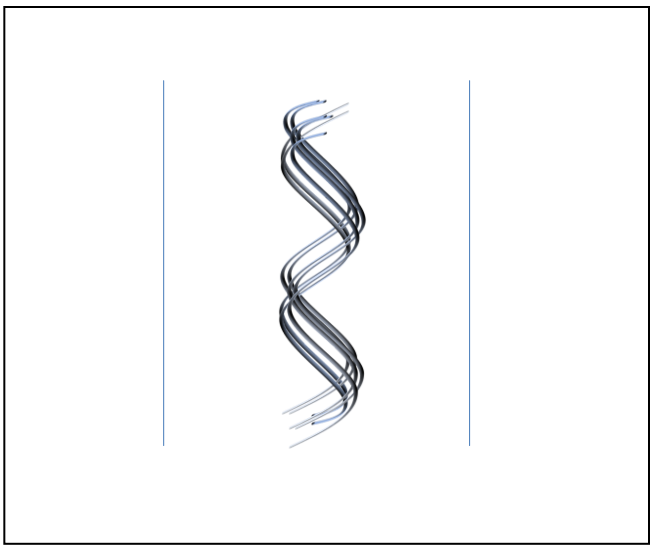

Figure 5.6 Schematic of helical effect.

Coalescence for this sparger type and reactor configuration 2 began at a superficial gas velocity of approximately 0.023m/s for water-gas; 0.03m/s for the 15% and 22% glycerin-gas system. However, for the 28% and 31.25% glycerin-gas system, coalescence of bubbles began at the initial superficial gas velocity of 0.019m/s. Poor bubble dispersion was noted for the 22%, 28% and 31.25% glycerin-gas systems across the length of the riser. At approximately 0.038m/s the bubble flow pattern for all systems became chaotic except for the 31.25% glycerin-gas system which became chaotic at approximately 0.048m/s. The pulsing effect was noted at approximately 0.042m/s whereas this was only noted at 0.048m/s for the 31.25% glycerin-gas system.

5.2.1.3. REACTOR CONFIGURATIONS 1 AND 2 WITH A PERFORATED PIPE SPARGER (TYPE C) DESIGN

When the perforated pipe sparger was used for reactor configuration 1, i.e. A_D/A_R = 1, the bubble flow pattern tended toward the central vertical axis of the riser for the water-gas system as described in Section 5.2.1.2 following a slightly wavy path. This phenomenon occurred for approximately 1.5m into the riser after which the bubbles dispersed evenly across the cross section of the riser. This was prevalent for all water-gas systems for configuration 1 and was indicative of very poor dispersion for this design of sparger. The bubbles exiting the sparger appeared to also be elongated coalesced bubbles (Figure 5.5).

For the glycerin-gas systems, the bubbles were deflected toward the wall of the riser away from the downcomer for approximately 0.5m into the riser (Figure 5.7) before dispersing fairly evenly across the cross section of the riser. A possible explanation for this was the increased presence of entrained bubbles returning to the riser from the downcomer which created a possible deflection of the bubbles exiting the sparger. Another possibility could be due to the bubbles exiting the sparger were also intermittent while there were no bubbles exiting the sparger on the half opposite to the downcomer (see Section 5.2.2.1).

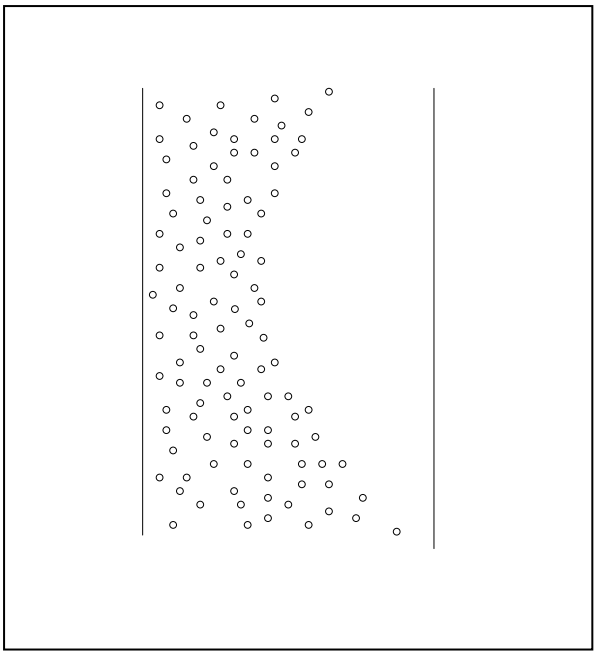

Figure 5.7 Schematic of gas bubbles deflected to wall of riser.

Coalesced bubbles for the water-gas system began at a superficial gas velocity of approximately 0.048m/s whereas coalescing for the glycerin-gas system began at a superficial gas velocity of 0.019m/s. These coalesced bubbles took slightly longer to breakup as compared to the bubbles produced by the other sparger designs. Chaotic behaviour of bubbles was noted at a superficial gas velocity of approximately 0.038m/s for all systems.

By decreasing the area ratio to 0.44, the bubble flow pattern became a prominent swirl up the riser. This pattern became more significant as the superficial gas velocity increased for all systems. There was a slight deflection of the body of bubbles in the riser toward the wall opposite the downcomer that was in use. This deflection was evident for approximately 1m in

length into the riser after which the bubbles dispersed evenly across the cross section of the riser. Coalescence for the water-gas system began at a superficial gas velocity of approximately 0.028m/s while for the glycerin-gas systems, coalescence of bubbles occurred at 0.019m/s. These coalesced bubbles were always quick to break up. The combination of a perforated pipe and configuration 2 appeared to give the worst dispersion of bubble behaviour when compared to the other combinations.

5.2.1.4. REACTOR CONFIGURATION 3

For reactor configuration 3 (downcomer diameter 225mm, A_D/A_R =1), a perforated plate sparger was used. The key difference between the perforated plate sparger used in configuration 1 and 2 is the sparger pore size for configuration 3. The sparger pore size for configuration 3 was 1mm in diameter whereas the pore size for configuration 1 and 2 was 4.5mm. This influenced the size of the bubbles in the riser as the sparger with the pore diameter of 1mm produced bubbles smaller in size than the sparger with pore size 4.5mm although both produced bubbles in the same bubble size range. This contradicts the findings of Ruen-ngam et al. (2008) cited in Kadic and Heindel (2014), who reported that bubble diameter increases with reactor size. The bubble diameter is more dependent on the sparger pore size and design as observed in this investigation and reported by Kadic and Heindel (2014).

This reactor and sparger combination produced a uniform bubble size and flow up to a superficial gas velocity of 0.045m/s. Beyond this gas velocity in the range of 0.05-0.068m/s the bubble sizes were a combination of bubbles with diameters ranging from 1mm to 5cm. The coalesced bubbles were in the range 3cm to 5cm. In this superficial gas velocity range, the fluid had a pulsing movement created by the congregation and dispersion of the bubbles (Figure 5.4) whereas at the very low superficial gas velocity there was slight deflection of the bubbles to riser wall opposite the downcomer (Figure 5.8).

This behaviour was over a very short distance after which the bubbles were evenly dispersed across the cross section of the riser. Although there were some 0.5mm diameter bubbles in the downcomer, this was due mainly to the very small disengagement tank. This

configuration produced the best flow patterns and bubble size. The riser manometer for this reactor was slightly unstable and varied at a maximum of 5mm either side of a central point at the maximum superficial gas velocity. This was not indicative of any weeping at the sparger as reported by Kulkarni et al (2009). It was due in fact to the very large amount of bubbles present in the riser due to the sparger design.

Figure 5.8 Deflection of bubbles at low velocity for reactor configuration 3.

5.2.1.5. REACTOR CONFIGURATIONS 4 AND 5

Reactor configuration 4, A_D/A_R = 1 (downcomer diameter = 150mm, H_R = 4.2m), a perforated disk sparger was used with pore diameter 1mm. Good distribution of bubbles throughout the riser was noted across all superficial gas velocities. The bubble sizes were small with coalesced bubbles beginning to appear at a superficial gas velocity of 0.061m/s. Slightly chaotic behaviour was noted from 0.05m/s to 0.072m/s after which the bubble flow patterns became chaotic. From a superficial gas velocity of 0.114m/s to 0.125m/s, very turbulent and

chaotic behaviour of bubbles was noted. Very fine bubbles were detected in the downcomer by shining a light behind the column. These bubbles were not easily visible from a distance.

By reducing the area ratio to 0.44 (reactor configuration 5: D_D = 100mm, H_R = 4.2m), the bubble flow path was slightly wavy (Figure 5.3). This was very much like the behaviour observed for reactor configuration 2 with the bubbles initially congregating toward the centre of the riser (Figure 5.9). In fact the behaviour patterns at all superficial gas velocities were similar to that observed for reactor configuration 2.

Figure 5.9 Bubbles congregating to the central axis of the riser when area ratio is less than 1 for reactor configuration 5 with a perforated disk sparger. Similar behaviour was noted for reactor configurations 1 and 2 with the perforated disk sparger.

5.2.1.6. OBSERVATIONS OF EFFECTS OF SPARGER DESIGN AND FLUID PROPERTIES

At low superficial gas velocities, i.e. below 0.028m/s, for reactor configuration 1 and 2, all spargers exhibited weeping. This behaviour got progressively worse from the perforated plate sparger to the perforated pipe sparger for reactor configuration 1 but was worse still for reactor configuration 2 for the perforated disk and perforated pipe sparger. Weeping occurs when there is non-uniform flow distribution of bubbles exiting the sparger as shown in Figure 5.9 for the perforated pipe sparger.

Kulkarni et al. (2009) reported that weeping is most prevalent in perforated pipe spargers and is due to the complex flow found within the sparger and is dependent on the sparger design and inlet kinetic energy. According to Kulkarni et al. (2009), this non-uniform flow is primarily the result of the kinetic energy of the gas through the sparger pores being insufficient to support the liquid head above the sparger pores. In this investigation this phenomenon disappeared at a superficial gas velocity of 0.028m/s for the perforated plate sparger for reactor configuration 1 and 2; at 0.028m/s for the perforated disk for configuration 1 and at 0.048m/s for reactor configuration 2 while for the perforated pipe sparger this phenomenon disappeared at 0.033m/s for reactor configuration 1 and 2. However, it must be noted that the perforated pipe sparger for reactor configuration 1 and 2, in addition to weeping the sparger displayed behaviour unique to its design. The bubbles continually exited the sparger closest to the downcomer being used (Figure 5.10a) but exited the pores on the opposite half, intermittently only at very high superficial gas velocities i.e. 0.06 – 0.076m/s (Figure 5.10b and 5.10c.).

This phenomenon influenced the distribution and dispersion of the bubbles within the riser. The bubbles were deflected to the riser wall opposite the downcomer in use for reactor configurations 1 and 2.

Although the non-uniform or intermittent flow of bubbles through the perforated pipe sparger was explained by Kulkarni et al. (2009), as being due to the friction of the fluid against the internal surface of the pipe allows the pressure to fall in the direction of flow and a decrease in the momentum of the gas due to the deceleration of the fluid as it escapes out of the pore, no explanation was found for the behaviour noted in this investigation for the perforated pipe

sparger. What can be proposed as an explanation of the phenomenon is the returning bubble laden fluid from the downcomer created a change in density of the fluid across that half of the perforated pipe sparger closest to the downcomer being used. This resulted in a decrease in the density of the fluid in this immediate region and allowed the bubbles to exit the sparger pores whereas at the opposite half of the sparger, the liquid density was too high and the incoming gas could not overcome the pressure caused by the fluid. This phenomenon became more pronounced as the density of the fluid increased.

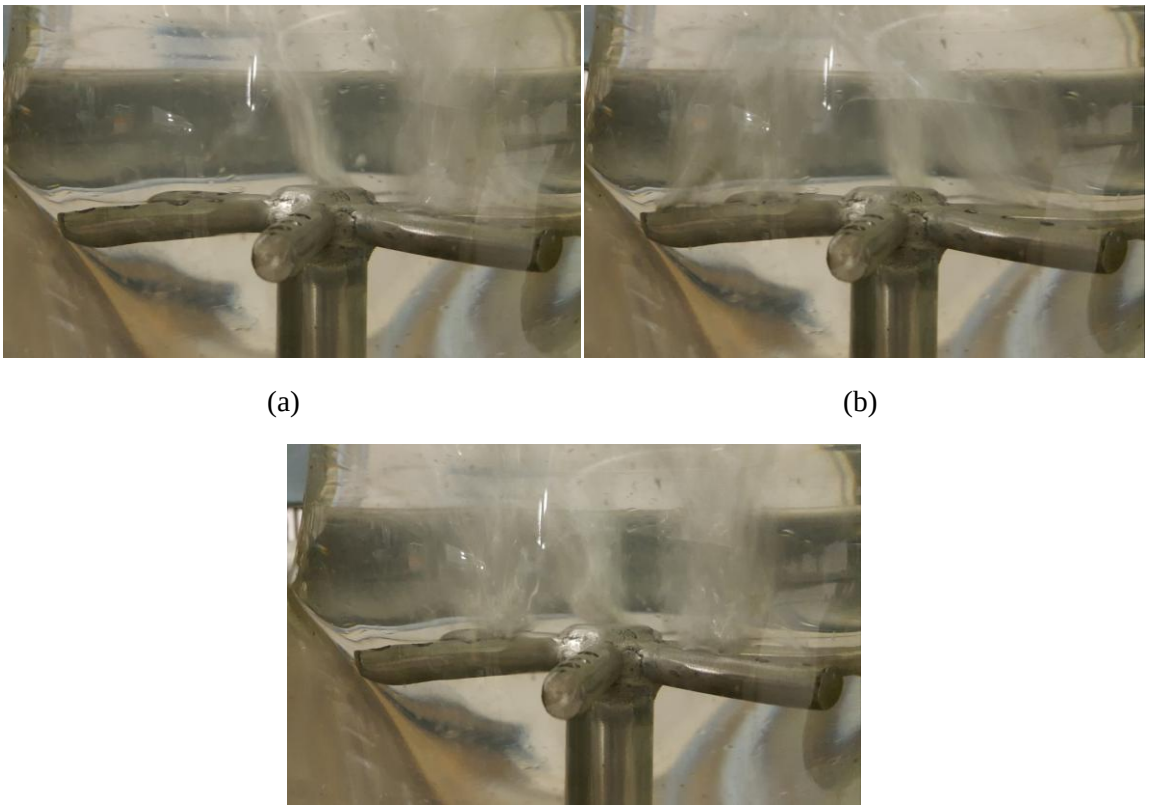

Figure 5.10 Weeping in a perforated pipe sparger.

This explanation may seem close to that of Kulkarni et al. (2009). However the difference lies in the fact at certain superficial gas velocities the non-uniform flow was overcome according to Kulkarni et al. (2009) whereas in this investigation although it was overcome on the half of

the sparger closest to the downcomer in use, it did not account for the other half where no bubbles leave the sparger at all gas velocities. More investigative work is required on the perforated pipe sparger design but if the results of the following Section are read, the perforated pipe design gives the worst mass transfer coefficient and should be omitted. The riser manometer was also unstable for very high superficial gas velocities for the perforated pipe sparger and varied to a maximum of 3mm either side of a central point. This however, could not be attributed to the weeping at the sparger as when weeping was evident, the manometer was stable. This is in direct contradiction of the statement made by Kulkarni et al. (2009). A possible and logical cause of this effect would be due to the large amount of bubbles present in the riser and high liquid flows in the riser.

5.2.2. CONCLUSION

From the visual observations it can be concluded that the area ratio and sparger design play a major role in the bubble flow patterns and distribution in the riser. An area ratio of less than 1 creates an opposition to the smooth flow of the fluid, which is in agreement with Jones and Heindel (2010); Al-Masry (2004); Yazdian et al. (2009); Lu et al. (2000); Korpijarvi et al. (1999); Gavrilescu and Tudose (1998 and 1997a); Kawase and Hashiguchi (1995); Chisti et al. (1994); Merchuk (1986 and 1984); and Merchuk and Stein (1981). These authors however, did not provide a description of the bubble flow patterns and distribution when the area ratio was less than 1. In this investigation it was noted that the opposition to flow due to a decrease in area ratio resulted in unsteady bubble flow patterns and poor distribution in the riser. Later in this Chapter, the effects of area ratio on mass transfer coefficient, gas holdup and superficial liquid velocity will be discussed. This discussion will further justify the pointless nature of using an area ratio of less than 1 for the external loop airlift reactors.

With respect to the sparger design for the two configurations, the ideal sparger design would be the perforated plate sparger with 1mm pore diameter combined with an area ratio of 1, but in this part of the investigation the best sparger design was the perforated plate sparger with 4.5mm pore size. Although the perforated plate sparger with 4.5mm pores gives good flow patterns and mass transfer, the perforated plate sparger used in reactor configuration 3 with 1mm pore diameter had minimal coalescence even at high velocities. Also it must be noted

that weeping does not necessarily produce an unstable manometer as reported by Kulkarni et al. (2009). In this investigation an unstable manometer was only noted for the perforated pipe sparger at very high superficial gas velocities and for reactor configuration 3. The unstable manometer was due to the high bubble density and the high fluid velocity. It can be concluded that a perforated plate sparger with 1mm pore diameter and a reactor with an area ratio of 1 will provide the best flow patterns and bubble distribution.

5.3. EFFECTS OF REACTOR GEOMETRY AND SPARGER DESIGN ON GAS HOLDUP, SUPERFICIAL LIQUID VELOCITY AND MASS TRANSFER

The gas holdup and superficial liquid velocity play a significant role in influencing the mass transfer characteristics in an airlift loop reactor as discussed in Section 2.5. Ensuring complete or significant gas disengagement in the gas disengagement tank results in a very low downcomer gas holdup of non-nutrient rich bubbles which do not contribute to enhancing mass transfer but only to increasing the gas holdup in the riser. In this investigation, the downcomer gas holdup values were significantly lower in comparison to the riser gas holdup (Figure 5.11) although it does show a slight increase as the superficial gas velocity increases.

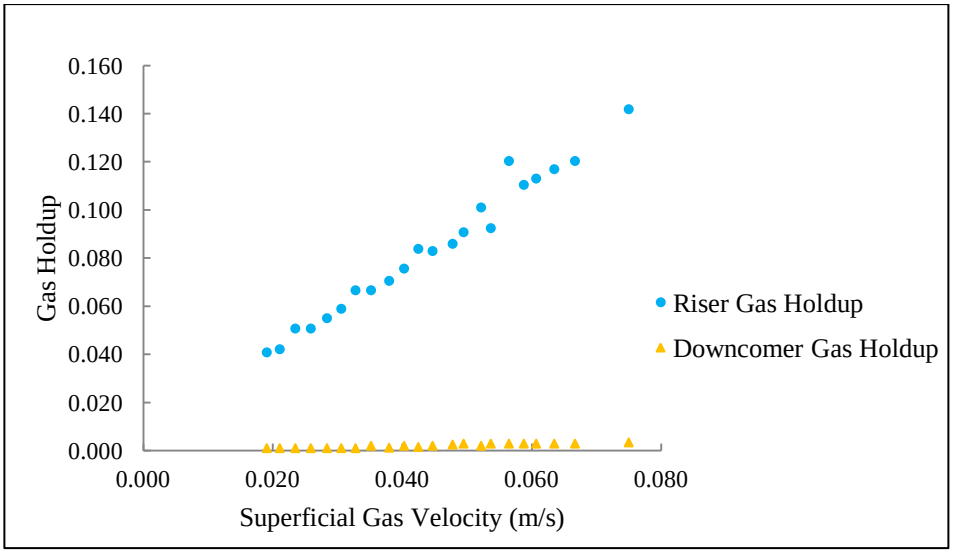

Figure 5.11 Comparison of riser to downcomer gas holdup in reactor configuration 1 for a water-gas system.

The effects of geometry of the reactor (area and aspect ratio), sparger design and fluid properties on the riser gas holdup, superficial liquid velocity and mass transfer will be discussed in detail to clarify the conflicting views in Section 2.6.1.2 and to confirm the behaviour noted in Sections 2.6.3 and 2.6.2.1 as well as to clarify the disagreement with the statement made by Kulkarni et al. (2009) with respect to weeping and an unstable manometer.

5.3.1. EFFECTS OF SPARGER DESIGN, AREA RATIO AND ASPECT RATIO ON RISER GAS HOLDUP, SUPERFICIAL LIQUID VELOCITY AND MASS TRANSFER

5.3.1.1. REACTOR CONFIGURATIONS 1 AND 2 FOR THE WATER-GAS SYSTEM

In reactor configurations 1 and 2, the riser diameter was consistent at 0.15m with a height of 2.95m while the downcomer diameters were 0.15m (configuration 1) and 0.1m (configuration 2). Both the downcomer heights were 2.95m. Figures 5.12, 5.13 and 5.14 show that the sparger design played a significant role on the gas holdup, mass transfer and superficial liquid velocity characteristics of the external loop airlift reactor. This is in direct contradiction of the findings by Kojić et al. (2015), Lin et al. (2004), Contreras et al. (1999), Gavrilescu and Tudose (1998 Part 1), Merchuk (1996a), Kemblowski et al. (1993) and Chisti (1989).

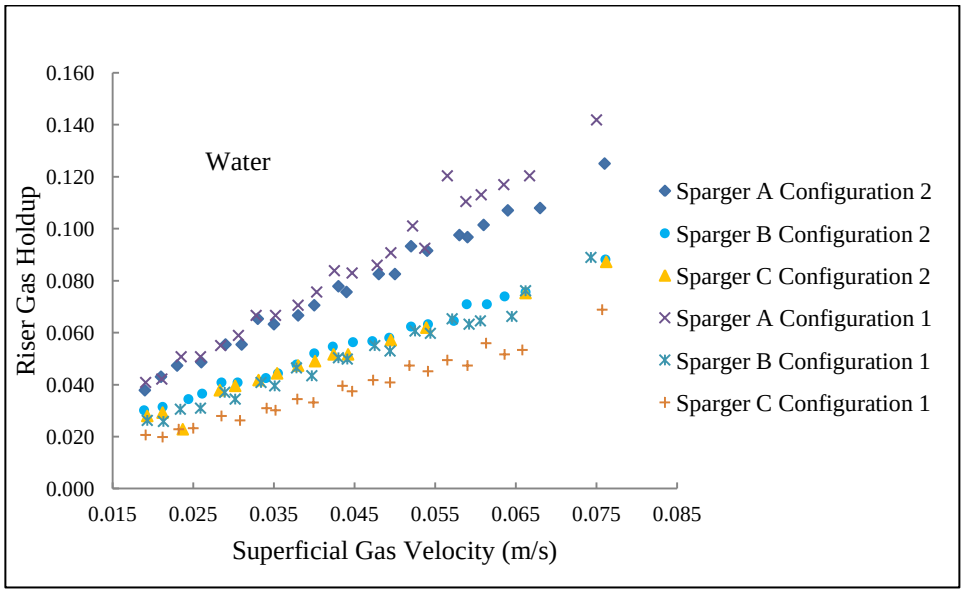

Figure 5.12 Sparger effects on riser gas holdup in reactor configurations 1 and 2 using a gas-water system (Table 5.1. - sparger classification).

However, it must be noted that these authors did report that the reactor design and area ratio played a more important role on the gas holdup, superficial liquid velocity and mass transfer but that they were not specific as to which had the most significant influence. In this investigation, it was found that the sparger effects could not be discarded completely as the design of the perforated plate (Sparger A) (refer to Table 5.1. for sparger classification) and perforated disk (Sparger B) spargers influenced the gas holdup, superficial liquid velocity and mass transfer more than the area ratio. Whereas for the perforated pipe (Sparger C) sparger, the area ratio effects as well as the sparger effects influenced the mass transfer, superficial liquid velocity and gas holdup.

In Figure 5.12 and Figure 5.13, the perforated plate (A) sparger produced a higher gas holdup and mass transfer than the perforated disk (B) sparger. Whereas the perforated pipe (C) sparger produced the worst gas holdup and mass transfer characteristics. From the visual observations the perforated plate sparger, displayed the best bubble size and distribution (Figure 5.1) with fairly 'linear' bubble flow patterns when compared to the perforated disk and perforated pipe spargers. This contributed to significantly better mass transfer when compared to the perforated disk and perforated pipe spargers for both configurations. Although it must be noted that reactor configuration 1 produced a slightly better gas holdup from a superficial gas velocity of approximately, 0.055m/s than reactor configuration 2. From the visual observations, these characteristics were expected due to the non-uniform flows experienced for the perforated disk and perforated pipe spargers as well as for the restricted flows when the area ratio was reduced.

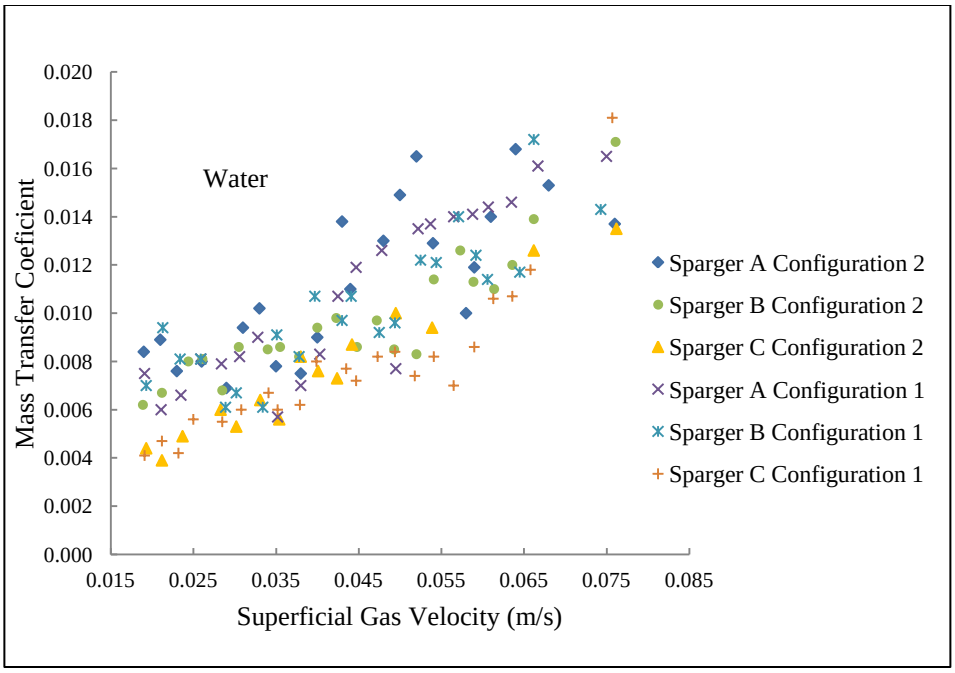

Figure 5.13 Sparger effects on the mass transfer coefficient in reactor configurations 1 and 2 using a gas-water system.

The mass transfer coefficient in Figure 5.13 for reactor configuration 2 is very varied and unstable as compared to reactor configuration 1. In fact it gets more scattered as the superficial gas velocity increases which is in keeping with the visual observations which indicate increasingly poor dispersion and erratic bubble flow patterns with the increased presence of coalesced bubbles. Whereas for reactor configuration 1 the coalesced bubbles broke up almost immediately even though they were occasionally present from prior to 0.028m/s for configuration 1 and 0.042m/s for configuration 2. The bubbles also tended to take on an elongated shape thus reducing the mass transfer area.

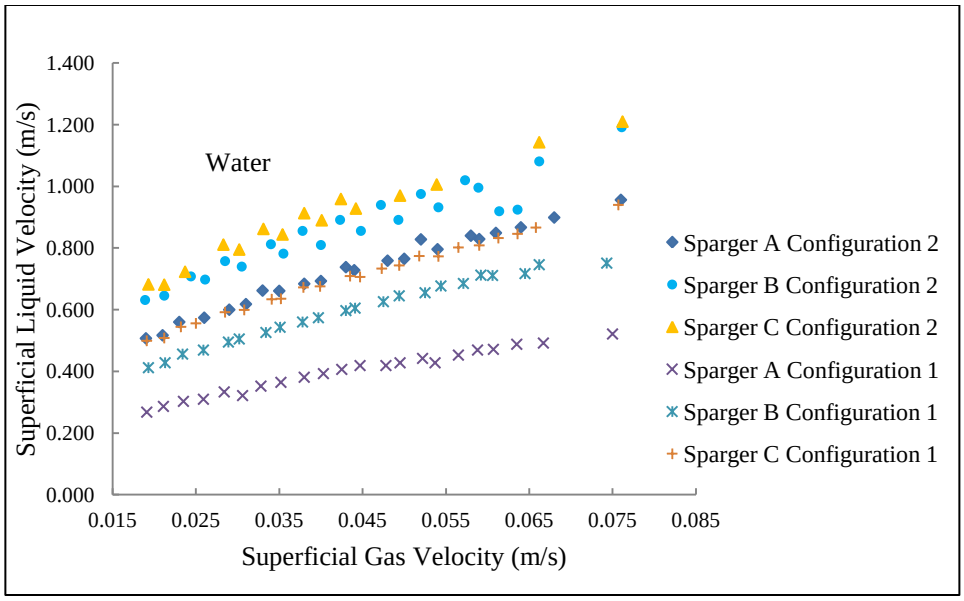

Figure 5.14 Sparger effects on the downcomer superficial liquid velocity in reactor configurations 1 and 2 using a gas-water system.

When using the perforated disk sparger (B) in reactor configuration 1 and 2, the gas holdup and mass transfer are lower when compared to the gas holdup and mass transfer for the perforated plate sparger (A). However both the gas holdup and mass transfer show very similar behavioral trends and results for both configurations even though there is slight scatter for the mass transfer for reactor configuration 1 and 2. It was anticipated that the gas holdup and mass transfer would be lower after noting the visual observations. There was poor bubble dispersion and inconsistent bubble size as a result of slight weeping.

The perforated pipe (C) sparger produced the worst gas holdup and mass transfer results when compared to the perforated plate (A) and perforated disk (B) spargers. This sparger was significantly affected by the weeping effect (Figure 5.10) as reported by Kulkarni et al. (2009) as well as uneven sparging. Figure 5.10a shows that the weeping effect is significant at low superficial gas velocities up to 0.047m/s after which the bubbles come through intermittently on the side opposite to the downcomer in use (Figure 5.10b and c).

The area ratio also played a more significant part with this sparger combination as compared to the perforated plate and perforated disk spargers for the gas holdup due to the reduced flow

path created by the downcomer of configuration 2. This contributed significantly to the poor gas holdup and mass transfer (Figure 5.12 and Figure 5.13).

It would be expected that the gas holdup for reactor configuration 1 would be lower than for reactor configuration 2 for all spargers. However, this is not the case for the perforated plate sparger where the gas holdup is the same for a superficial gas velocity up to 0.05m/s after which the gas holdup for reactor configuration 1 increases slightly instead of the gas holdup for reactor configuration 2. The perforated disk sparger and the perforated pipe sparger exhibit this behaviour as it is indicative of the reduced flow path of the liquid thereby increasing the residence time of the gas bubbles in the riser. It is evident that the gas holdup is influenced by the design of the perforated disk and perforated pipe spargers when the area ratio is less than 1. This is also reflected in the mass transfer (Figure 5.13). The superficial liquid velocity is mainly affected by the area ratio but also by the sparger design (Figure 5.14). The perforated plate sparger had the lowest liquid circulation velocity which allowed for increased bubble residence time which resulted in a high gas holdup for reactor configuration 1 while the perforated pipe sparger had the highest liquid circulation velocity and therefore the lowest gas holdup. The residence time of the bubbles was substantially decreased. The low gas holdup can also be attributed to the uneven discharge of bubbles from the sparger.

The perforated pipe sparger design produced the higher superficial liquid velocities for both reactor configuration 1 and 2. This led to lower gas holdups and mass transfer as well as to an unstable manometer at very high superficial gas velocities. However, by decreasing the area ratio, even though the liquid circulation velocity is higher the gas holdup is higher for the perforated pipe sparger (Figure 5.12 and Figure 5.14) for reactor configuration 2 than for reactor configuration 1.

5.3.1.1.1 CONCLUSION

It can be concluded that the sparger design does influence the gas holdup, mass transfer and superficial liquid velocity in external loop airlift reactors and needs to be considered as an important design parameter. In the case of the perforated pipe (C) sparger the effects were compounded by the decrease in area ratio as well. The perforated pipe sparger is considered the worst design in this investigation as it produces the lowest mass transfer coefficient.

However Kulkarni et al. (2009) reported that perforated pipe design spargers are the most widely used in industrial scale airlift reactors. Kadic and Heindel (2014) reported that the area ratio greater than 0.25 has no effect on the superficial liquid velocity. This was not observed in this investigation.

5.3.1.2. A COMPARISON BETWEEN REACTOR CONFIGURATIONS 1, 2 AND 3 FOR WATER-GAS SYSTEMS

When comparing the effects of the area ratio, aspect ratio and sparger design for reactor configurations 1, 2 and 3, it is interesting to note that all three parameters have no significant effect on the gas holdup at the lower superficial gas velocities (Figure 5.15).

It is also important to note that although the area ratio is 1 for reactor configuration 1 and 3, the actual size and volume of the reactors differ significantly yet the gas holdups are similar. However, the mass transfer for reactor configuration 3 is far higher compared to reactor configurations 1 and 2 (Figure 5.16). This can be attributed to the aspect ratio which allows for a longer residence time in the riser as compared to reactor configurations 1 and 2 as well as an increase in density of nutrient-rich bubbles due to the sparger design. Another factor which also contributed to this effect is noted from the flow visualization studies. In reactor configuration 3, the bubble size is fairly constant up to 0.05m/s with minimal to no coalescence. The bulk of the bubble size in reactor configuration 3 was 1cm or less in diameter. Reactor configuration 2 had more turbulence and coalescence due to the reduced area ratio when compared to reactor configurations 1 and 3 which is reflected in a more erratic mass transfer coefficient (Figure 5.16).

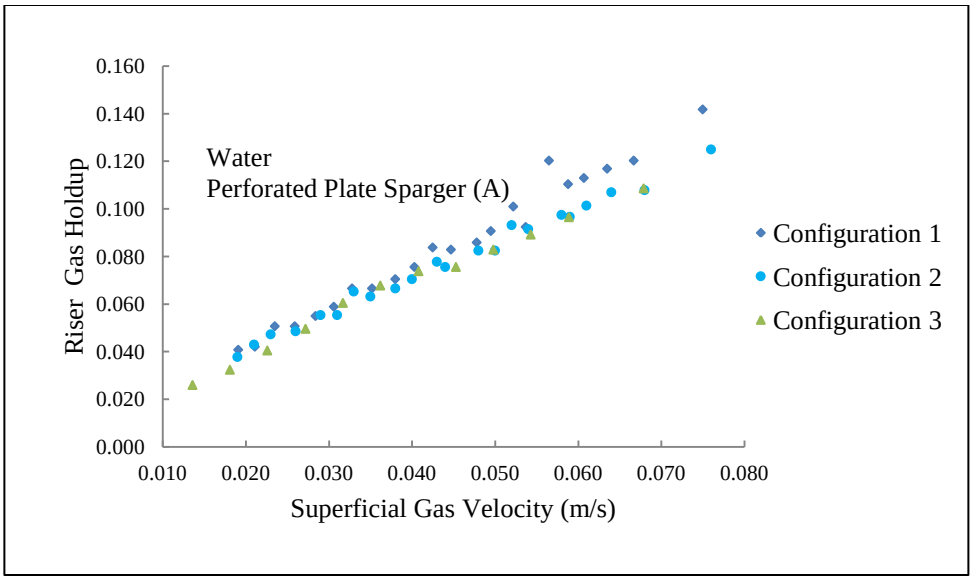

Figure 5.15 Area ratio effects on riser gas holdup in reactor configurations 1, 2 and 3 using a gas-water system (Configuration 1: 0.15m diameter downcomer (A_D/A_R =1); configuration 2: 0.1m diameter downcomer (A_D/A_R =0.44); configuration 3: 0.225m diameter downcomer (A_D/A_R =1)).

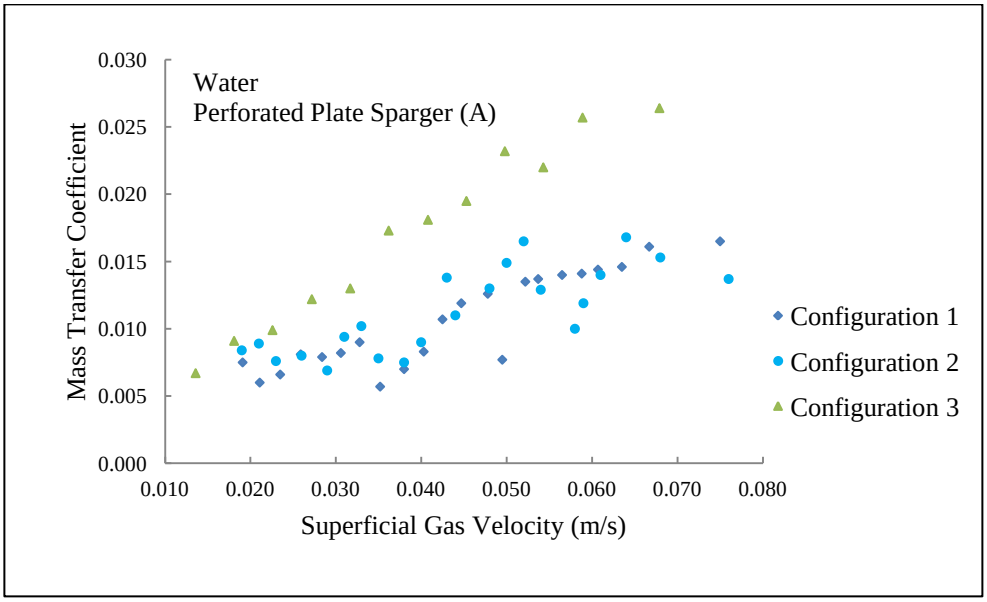

Figure 5.16 Area ratio effects on mass transfer in reactor configurations 1, 2 and 3 using a gas-water system.

These findings are in agreement with Fakhari et al. (2014) and Gavrilescu and Tudose (1997a) who reported that increasing area ratio increases the mass transfer coefficient. Their statement however, failed to take into consideration the actual dimensions of the reactor as in this investigation although the area ratio is 1 for both reactor configurations 1 and 3, their actual dimensions differ significantly to each other. This means that the area ratio on its own cannot be used conclusively when describing the gas holdup and mass transfer trends within an airlift reactor.

In reactor configuration 3, the superficial liquid velocity should be below the superficial liquid velocity of reactor configuration 1, but it lies between the superficial liquid velocities of reactor configurations 1 and 2 (Figure 5.17).

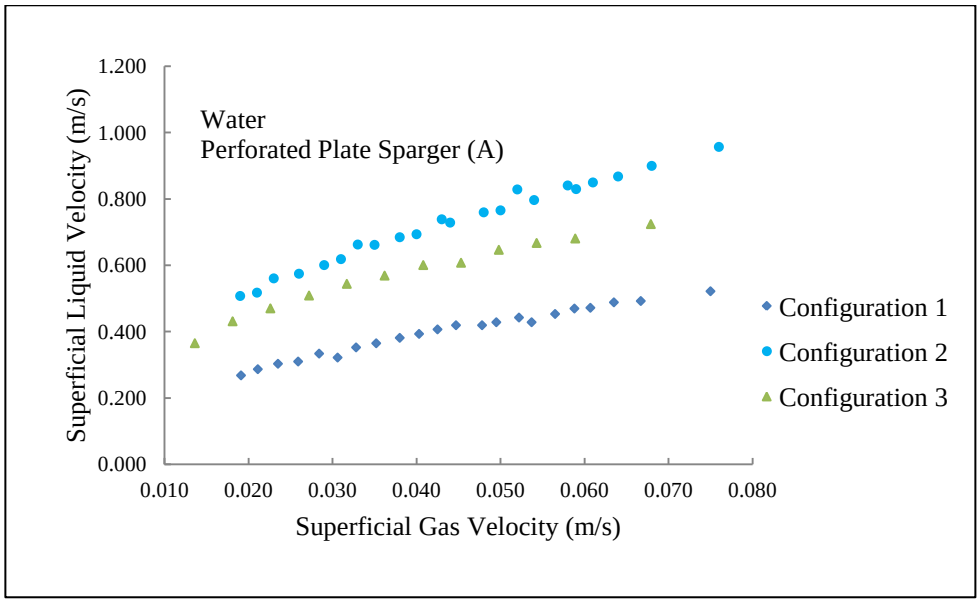

Figure 5.17 Area ratio effects on the downcomer superficial liquid velocity in reactor configurations 1, 2 and 3 using a gas-water system.

One conclusion to arrive at for this trend is the difference in size of the disengagement tanks for both reactors. The disengagement tank for reactor configurations 1 and 2 was of total volume 0.966m^3 while the total volume of the disengagement tank for reactor configuration 3 was 0.324m^3. This would mean that the size of the disengagement tank would also affect the downcomer gas holdup but in Figure 5.20, the downcomer gas holdup is similar for reactor

configuration 1 and 3. This contradicts the findings by Al-Masry and Dukkan (1997) that the disengagement tank size influences the bubble entrainment to the downcomer.

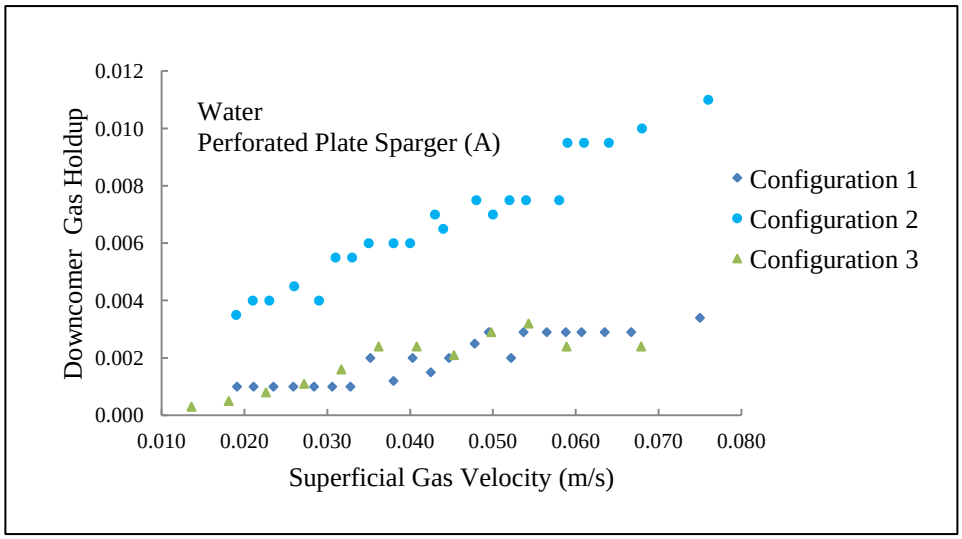

Figure 5.18 Aspect ratio effects on the downcomer gas holdup in reactor configurations 1, 2 and 3 using a gas-water system.

This implies that the size of the gas disengagement tank does not play a significant role in the gas disengagement but that the actual diameter of the riser and downcomer as well as the static liquid height appears to have a more significant role. This phenomenon experienced with the superficial liquid velocity for reactor configuration 3 could also be due to the sparger design as is indicative in Figure 5.19 but not so evident in Figure 5.18.

5.3.1.2.1. CONCLUSION

Aspect ratio and area ratio play a significant role in mass transfer. However, instead of using only the area ratio, the actual diameters need to be used to have any real meaning as reactor configurations 1 and 3 have the same area ratio of 1. Generally an increase in the superficial liquid velocity results in a decrease in the residence (mixing) time of the bubbles but by having an increase in aspect ratio and riser diameter it increases the residence time of the nutrient rich bubbles with an increase in superficial gas velocity thereby increasing mass transfer. The sparger design again comes through as an important parameter to consider in the overall design of an airlift reactor as illustrated in Figures 5.16, 5.17 and 5.18. This means

that area ratio, aspect ratio and riser and downcomer diameter as well as sparger details are important input parameters for a neural network.

5.3.1.3. A COMPARISON BETWEEN REACTOR CONFIGURATIONS 4 AND 5 FOR A WATER-GAS SYSTEM

Reactor configurations 4 (A_D/A_R = 1, downcomer diameter 0.15m, H_R = 4.2m) and 5 (A_D/A_R = 0.44, downcomer diameter 0.1m, H_R = 4.2m) differed from reactor configurations 1 (A_D/A_R = 1, downcomer diameter 0.15m, H_R = 3.1m) and 2 (A_D/A_R = 0.44, downcomer diameter 0.15m, H_R = 3.1m) in terms of the riser height or aspect ratio. Although the spargers differed in pore size and position it is noted that this has no effect on the gas holdup and mass transfer as indicated in Figures 5.19 to 5.22.

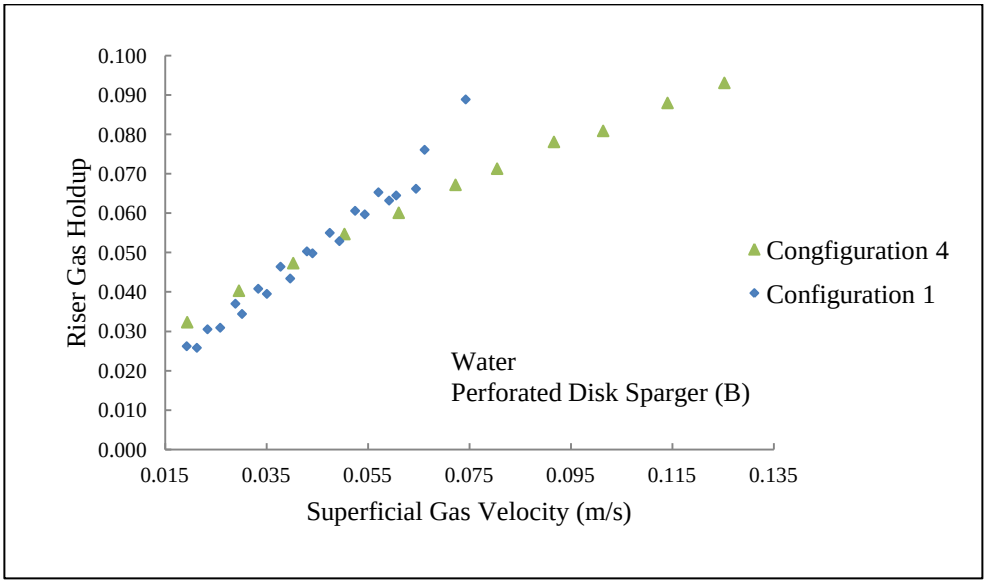

Figure 5.19 Aspect ratio effects on gas holdup in reactor configurations 1 and 4 using a gas-water system.

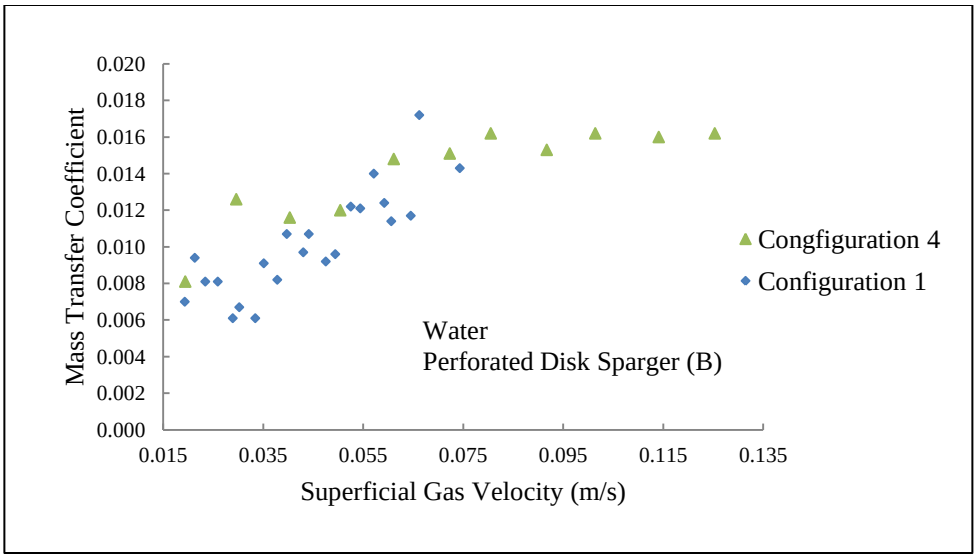

Figure 5.20 Aspect ratio effects on mass transfer in reactor configurations 1 and 4 using a gas-water system.

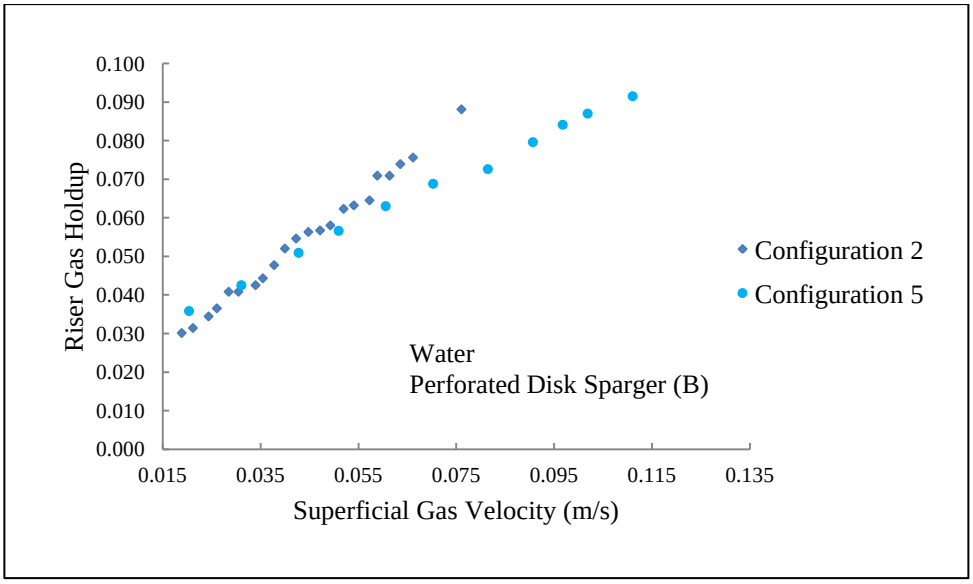

Figure 5.21 Aspect ratio effects on gas holdup in reactor configurations 2 and 5 using a gas-water system.

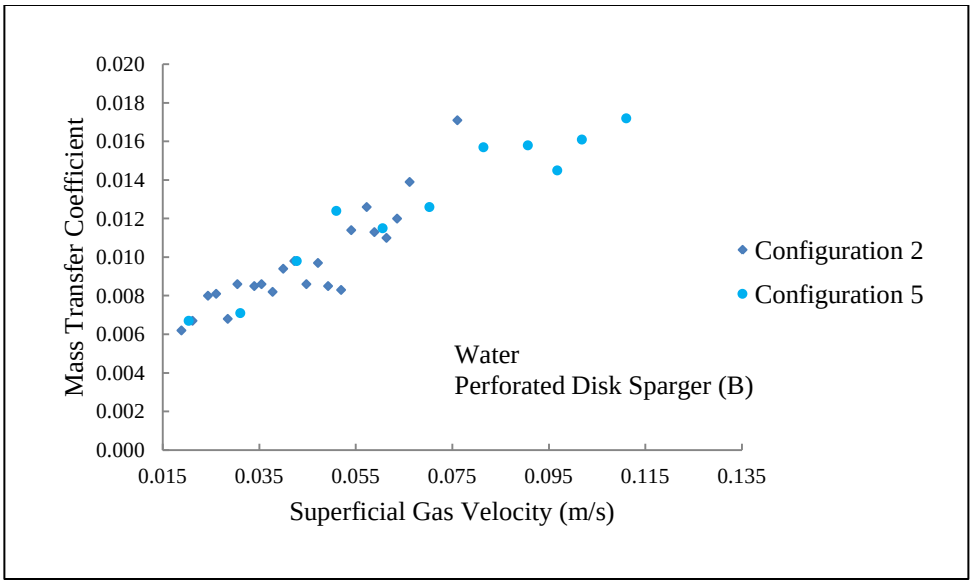

Figure 5.22 Aspect ratio effects on mass transfer in reactor configurations 2 and 5 using a gas-water system.

As with reactor configuration 1 and 2, the area ratio had no effect on the riser gas holdup but for the mass transfer it had a slight effect as the A_D/A_R increased (Figure 5.23 and Figure 5.24).

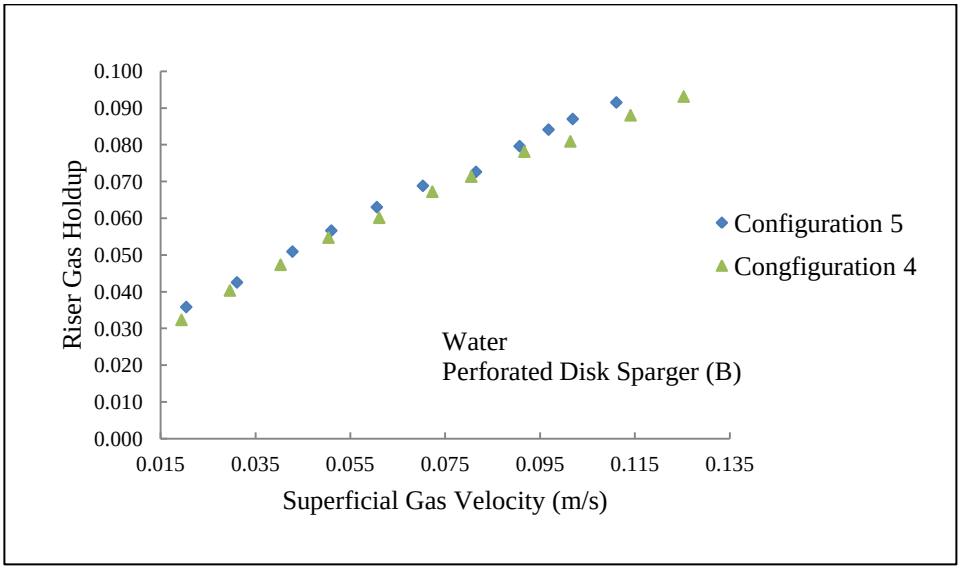

Figure 5.23 Area ratio effects on the riser gas holdup in reactor configurations 4 and 5 using a gas-water system.

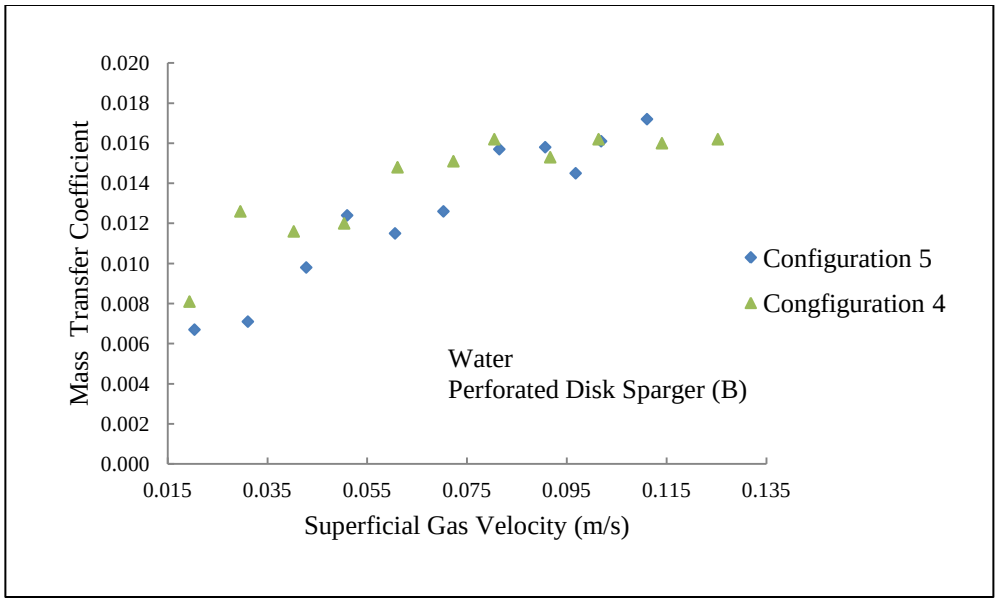

Figure 5.24 Area ratio effects on the mass transfer in reactor configurations 4 and 5 using a gas-water system.

When comparing reactor configurations 1 and 4 and 2 and 5, the aspect ratio had no effect for an area ratio of less than 1 but for A_D/A_R equivalent to 1, the aspect ratio does play a role in the mass transfer by allowing a longer residence time for nutrient rich bubbles. This effect is only noticeable up to $U_{SGR} \geq 0.075$m/s after which it has no effect as the mass transfer does not show any further increase with increasing U_{SGR}. From the flow visualization studies for reactor configuration 4, the bubble patterns become very chaotic and turbulent at approximately this velocity. However for a lower aspect ratio the riser gas holdup is higher when compared to reactor configuration 2 and 5 and 1 and 4 with a significant deviation starting to occur at 0.06m/s.

5.3.1.4. EFFECTS OF SPARGER DESIGN, AREA RATIO AND ASPECT RATIO ON RISER GAS HOLDUP, SUPERFICIAL LIQUID VELOCITY AND MASS TRANSFER GLYCERIN-GAS SYSTEMS

The glycerin-gas systems were only investigated using reactor configurations 1 and 2 with the perforated plate sparger, perforated disk sparger and the perforated pipe sparger.

5.3.1.4.1. EFFECTS OF GLYCERIN CONCENTRATIONS

The glycerin-gas systems displayed a slightly higher riser gas holdup than the water-gas system as illustrated in Figure 5.25 to Figure 5.30 for the perforated plate sparger type while there was not much difference for the perforated disk and perforated pipe type spargers.

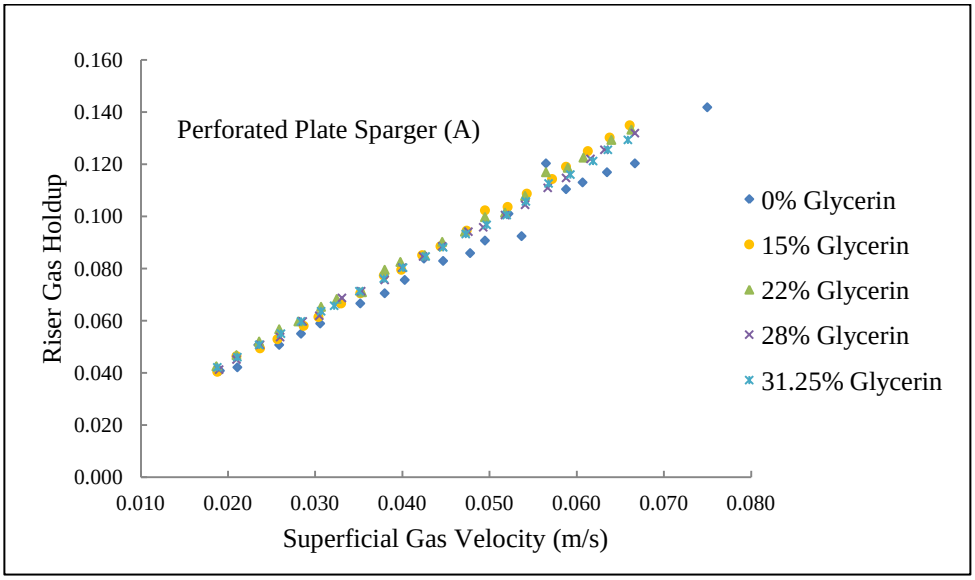

Figure 5.25 Effects of glycerin concentrations on the riser gas holdup for reactor configuration 1 using a perforated plate sparger (A).

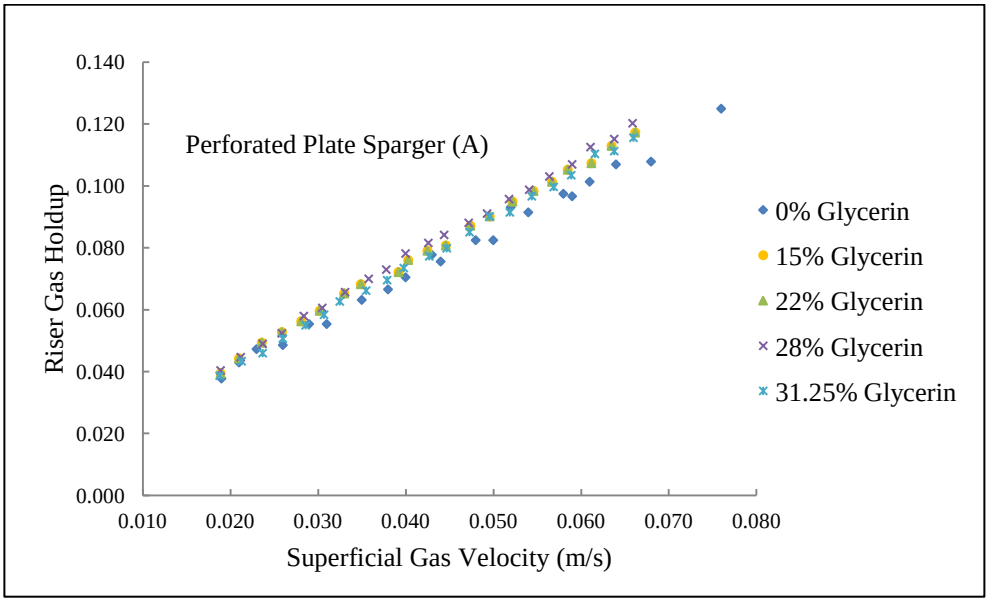

Figure 5.26 Effects of glycerin concentrations on the riser gas holdup for reactor configuration 2 using a perforated plate sparger (A).

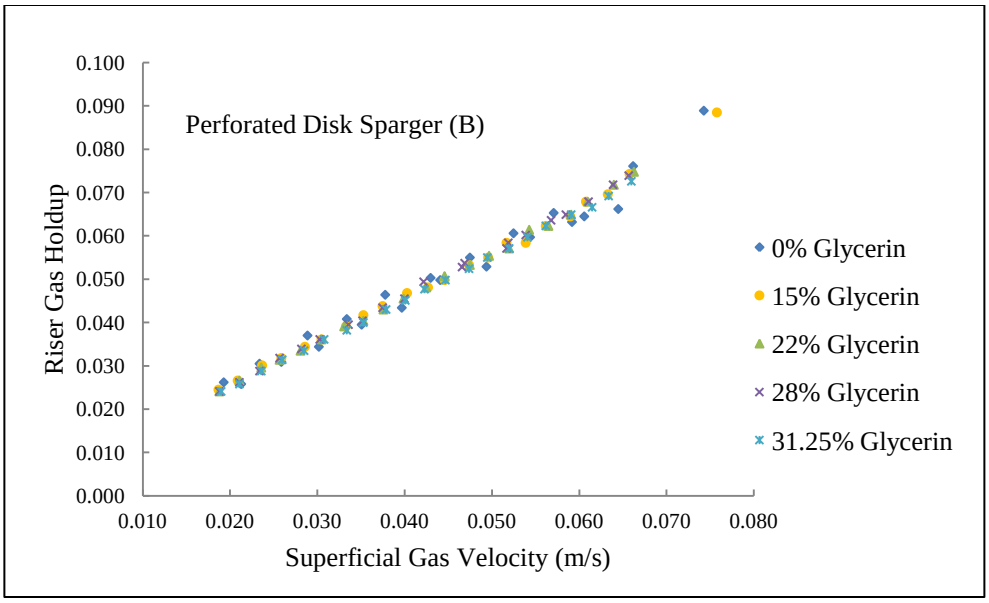

Figure 5.27 Effects of glycerin concentrations on the riser gas holdup for reactor configuration 2 using a perforated disk sparger (B).

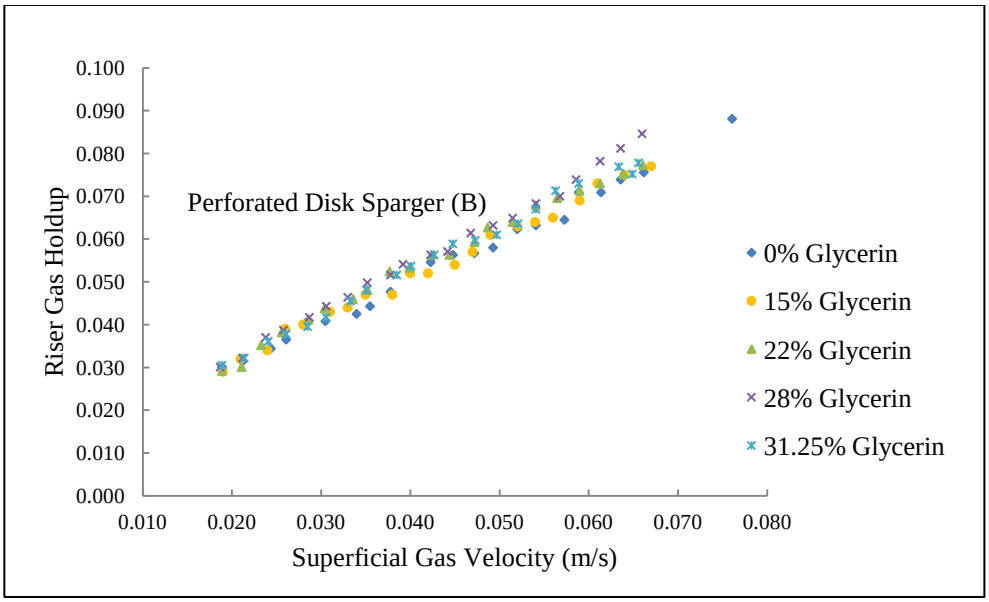

Figure 5.28 Effects of glycerin concentrations on the riser gas holdup for reactor configuration 2 using a perforated disk sparger (B).

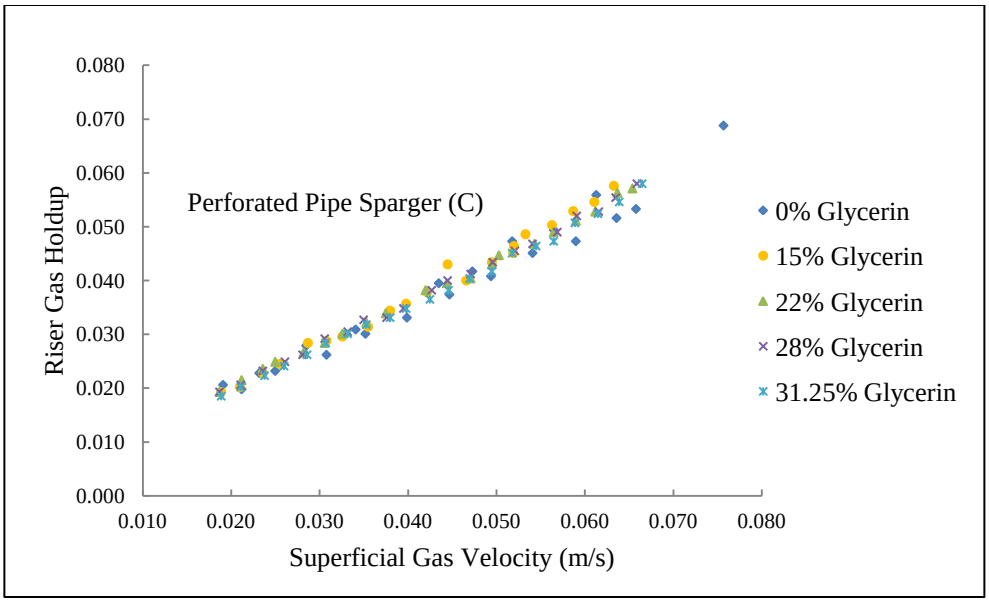

Figure 5.29 Effects of glycerin concentrations on the riser gas holdup for reactor configuration 2 using a perforated pipe sparger (C).

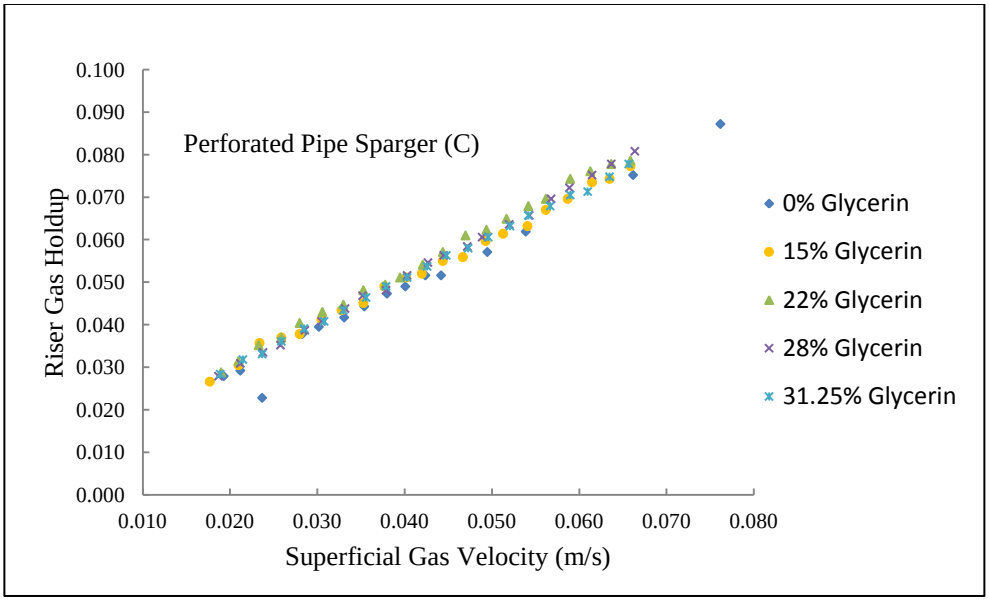

Figure 5.30 Effects of glycerin concentrations on the riser gas holdup for reactor configuration 2 using a perforated pipe sparger (C).

However from Figure 5.31 to Figure 5.36 for mass transfer the opposite is true. An increase in the concentration results in a decrease in mass transfer irrespective of the sparger type used.

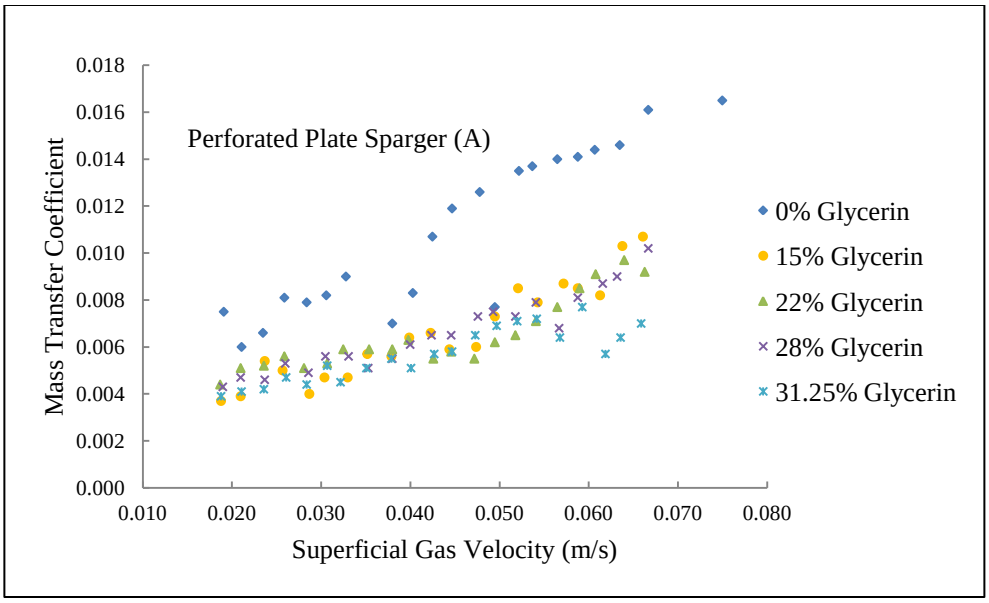

Figure 5.31 Effects of glycerin concentrations on the mass transfer coefficient for reactor configuration 1 using a perforated plate sparger (A).

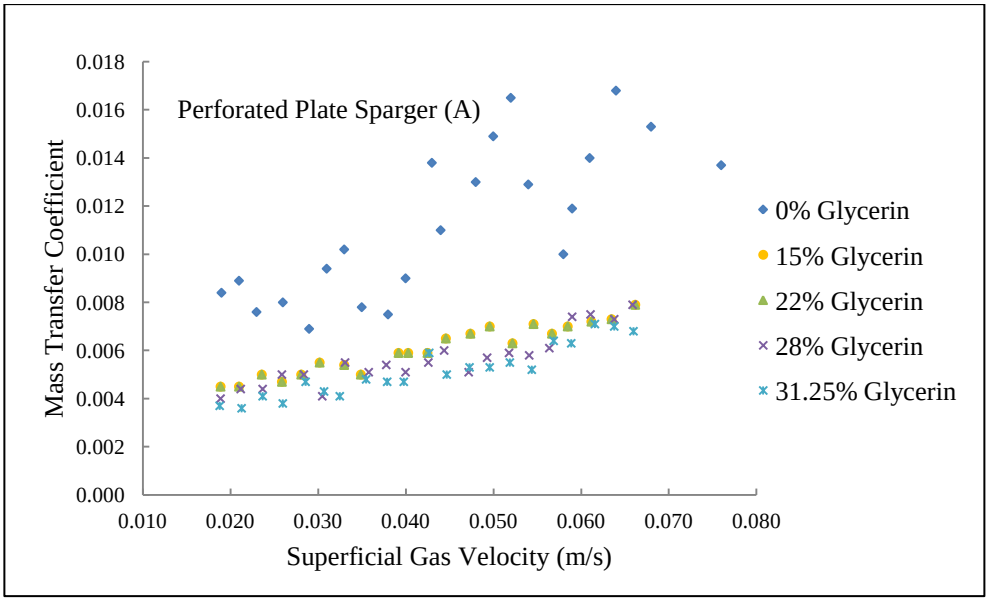

Figure 5.32 Effects of glycerin concentrations on the mass transfer coefficient for reactor configuration 2 using a perforated plate sparger (A).

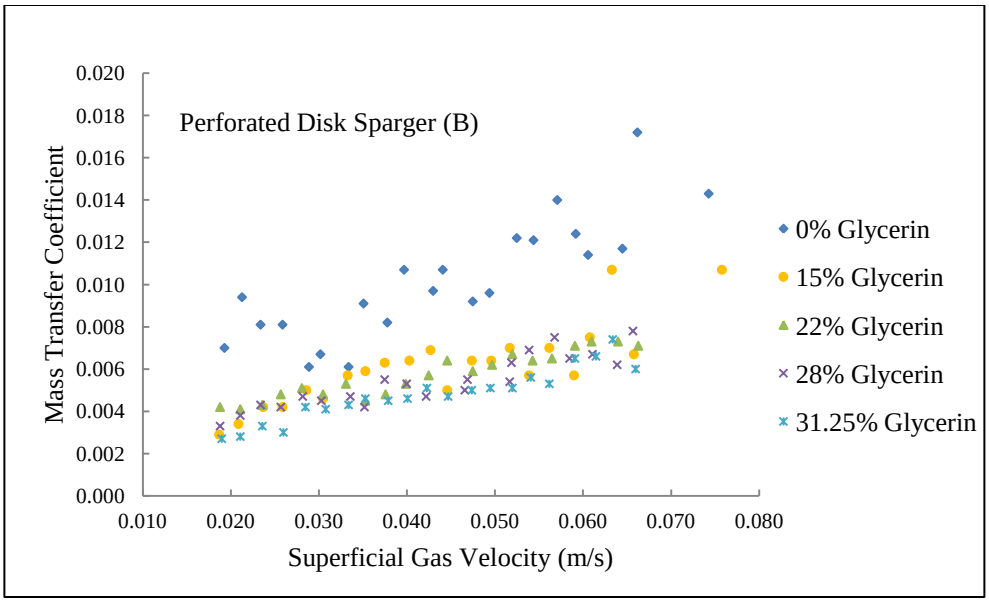

Figure 5.33 Effects of glycerin concentrations on the mass transfer coefficient for reactor configuration 1 using a perforated disk sparger (B).

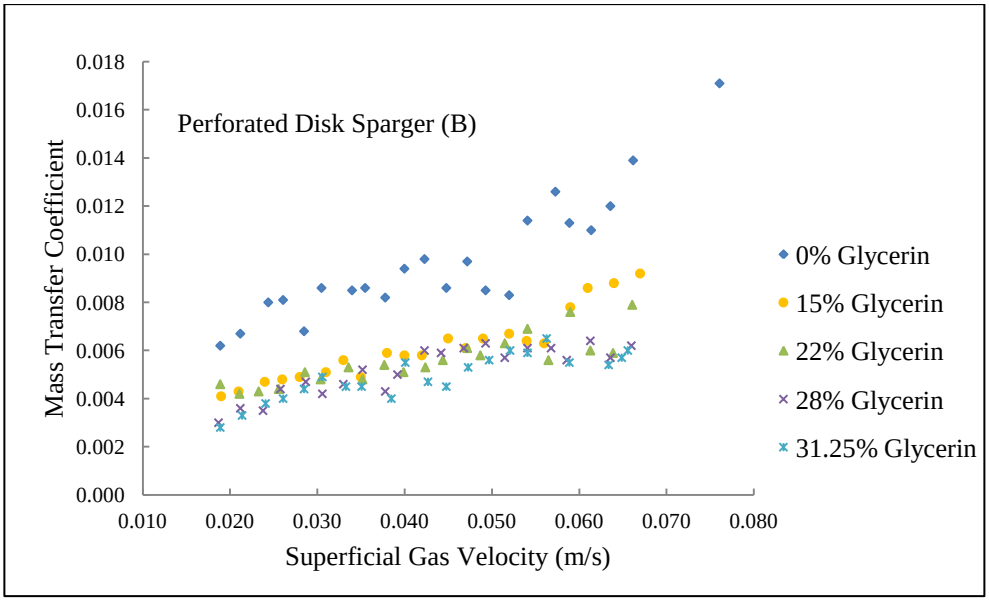

Figure 5.34 Effects of glycerin concentrations on the mass transfer coefficient for reactor configuration 2 using a perforated disk sparger (B).

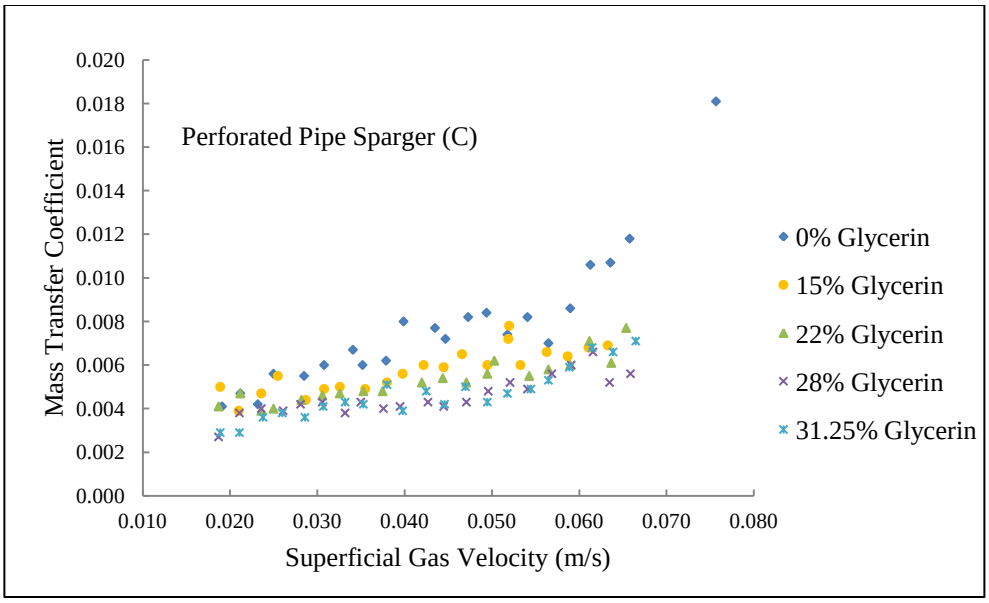

Figure 5.35 Effects of glycerin concentrations on the mass transfer coefficient for reactor configuration 1 using a perforated pipe sparger (C).

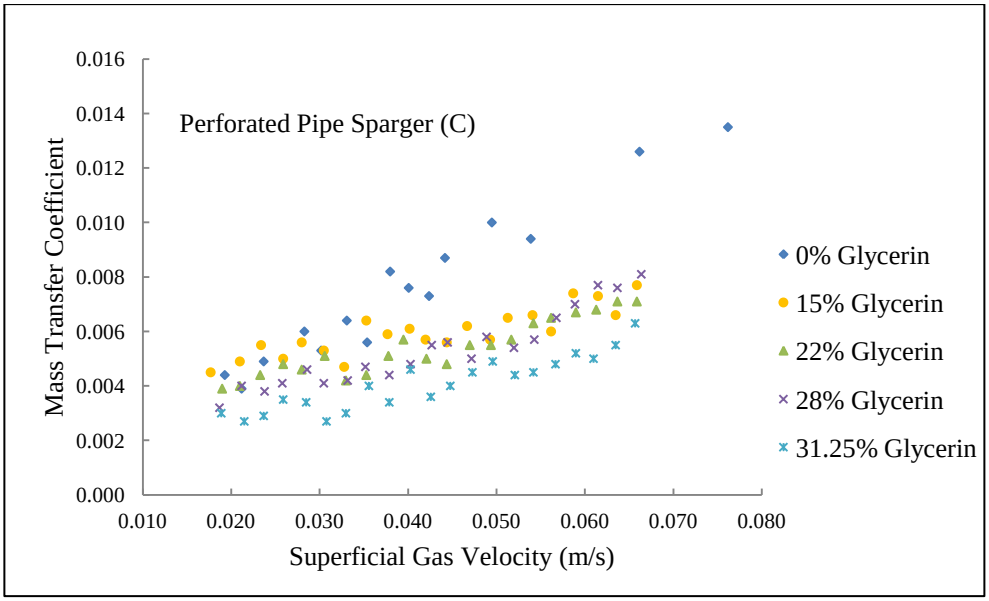

Figure 5.36 Effects of glycerin concentrations on the mass transfer coefficient for reactor configuration 2 using a perforated pipe sparger (C).

This is due to the surface tension and increasing viscosity of the glycerin solutions which presents a greater drag force on the rising bubbles in higher viscosity solutions. This increase in drag force reduces the bubble rise velocity which results in an increase in the riser gas

holdup. This is in agreement with Fakhari et al. (2014); Rahman-Al-Ezzi and Najmuldeen (2013); Yazdian et al. (2009); Sivasubramnium et al. (2008); Shariati et al. (2007). However, Nakao et al. (1988) cited in Fakhari et al. (2014) found that the mass transfer increased due to an increase in viscosity.

From the visual observations it is noted that as the concentrations increased, coalescence of bubbles began at very low superficial gas velocities. Increased coalescence results in a decrease in surface area for mass transfer. Wilke and Chang (1955) cited in Fakhari et al. (2014) reported that this is also due to the increasing thickness of the liquid boundary layer or lower solute diffusivity due to an increase in viscosity.

With respect to the sparger effects, the same behaviour was noted as for water. The perforated plate sparger for an area ratio of 1 provides the best mass transfer with an increasing concentration of glycerin and the highest riser gas holdup (Figure 5.37 to Figure 5.43).

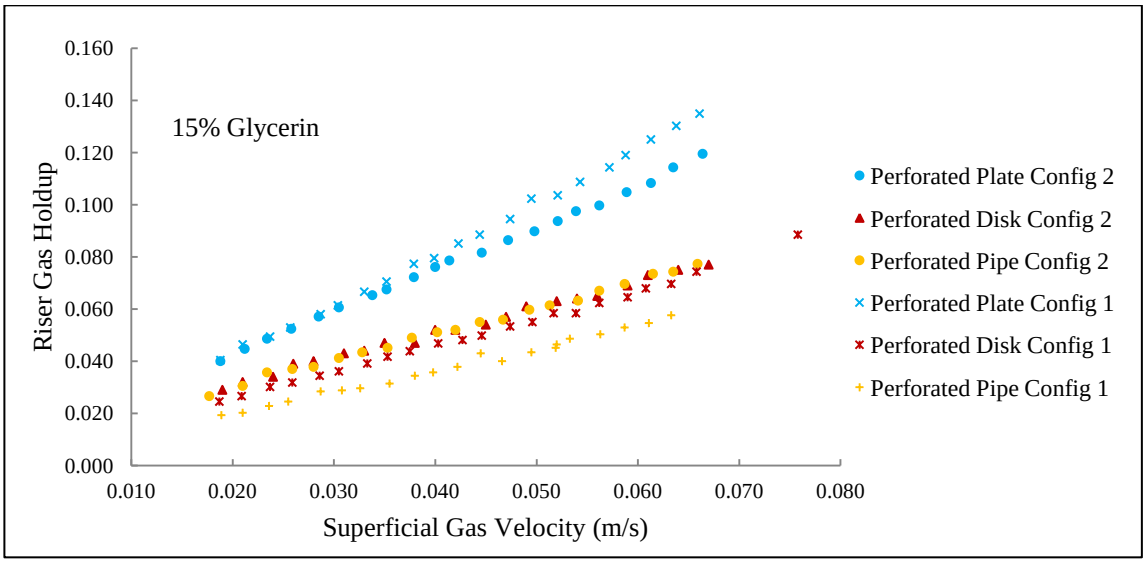

Figure 5.37 Comparison of area ratio effects on the riser gas holdup using different sparger types for a 15% glycerin solution in reactor configurations 1 and 2.

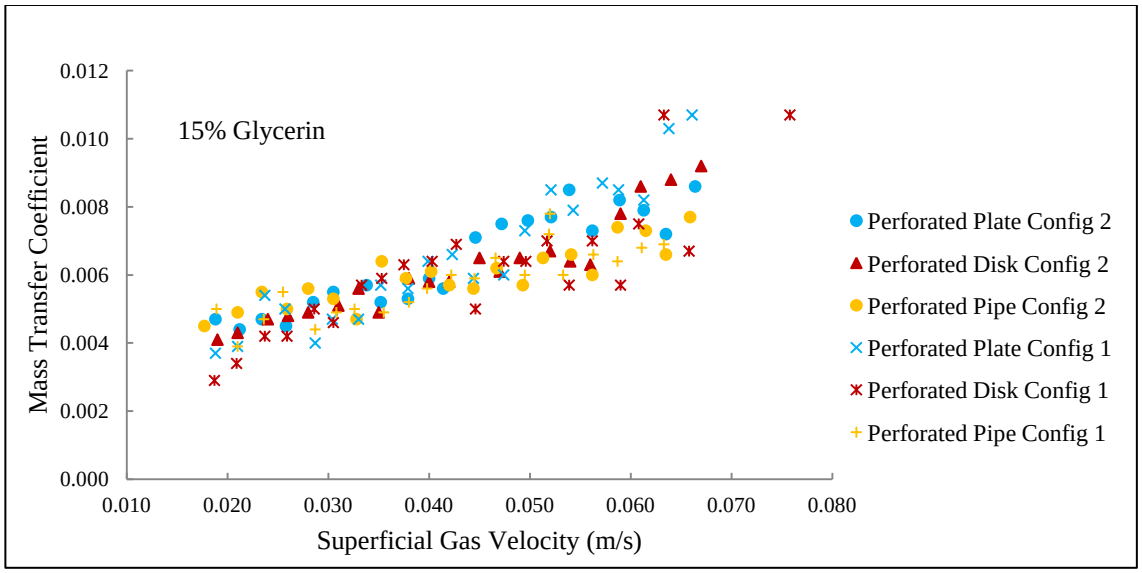

Figure 5.38 Comparison of area ratio effects on the mass transfer coefficient using different sparger types for a 15% glycerin solution in reactor configurations 1 and 2.

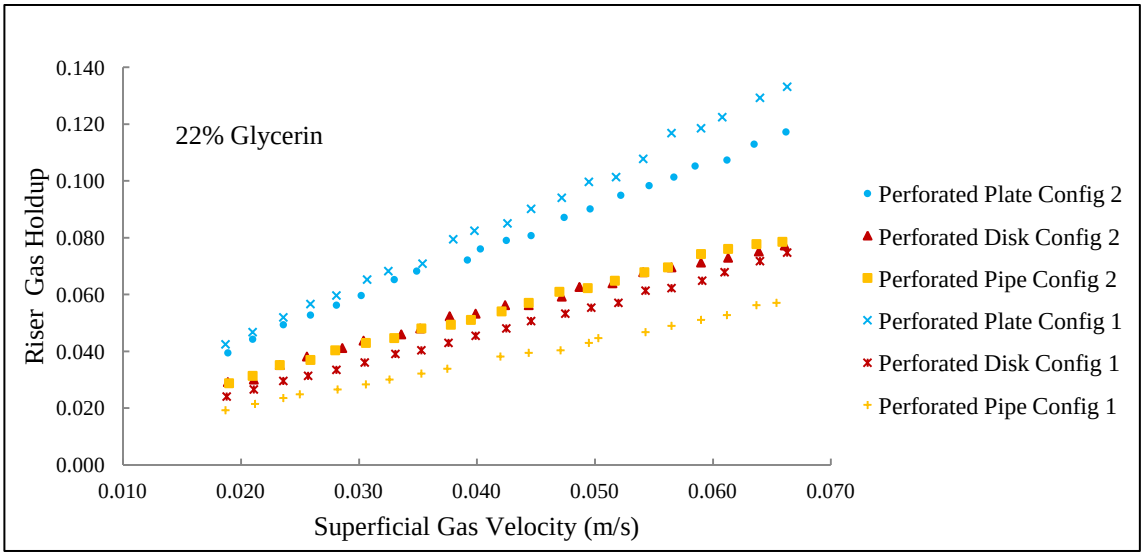

Figure 5.39 Comparison of area ratio effects on the riser gas holdup using different sparger types for a 22% glycerin solution in reactor configurations 1 and 2.

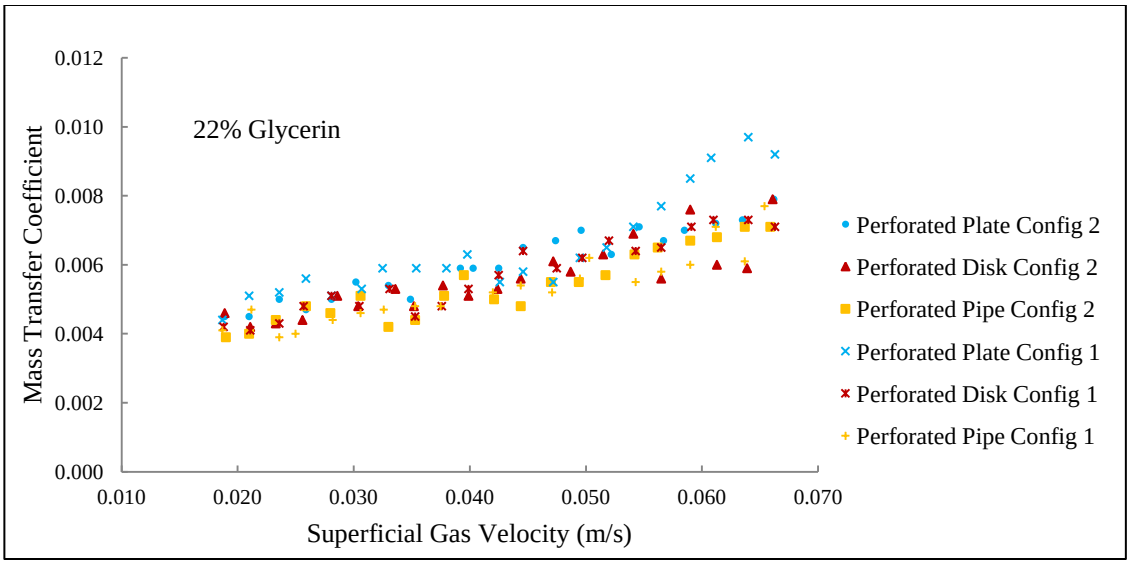

Figure 5.40 Comparison of area ratio effects on the mass transfer coefficient using different sparger types for a 22% glycerin solution in reactor configurations 1 and 2.

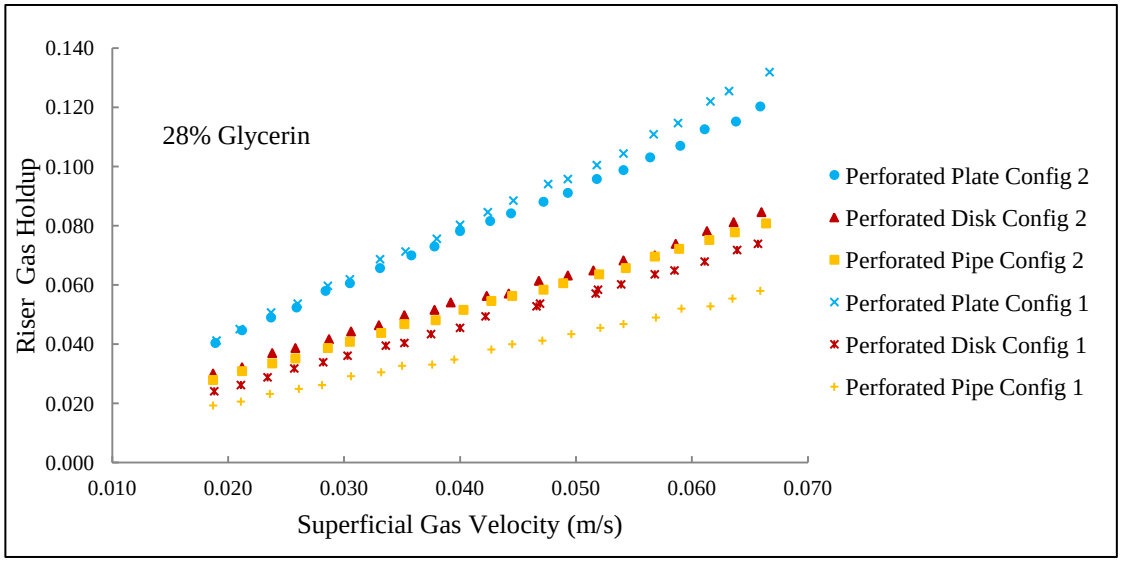

Figure 5.41 Comparison of area ratio effects on the riser gas holdup using different sparger types for a 28% glycerin solution in reactor configurations 1 and 2.

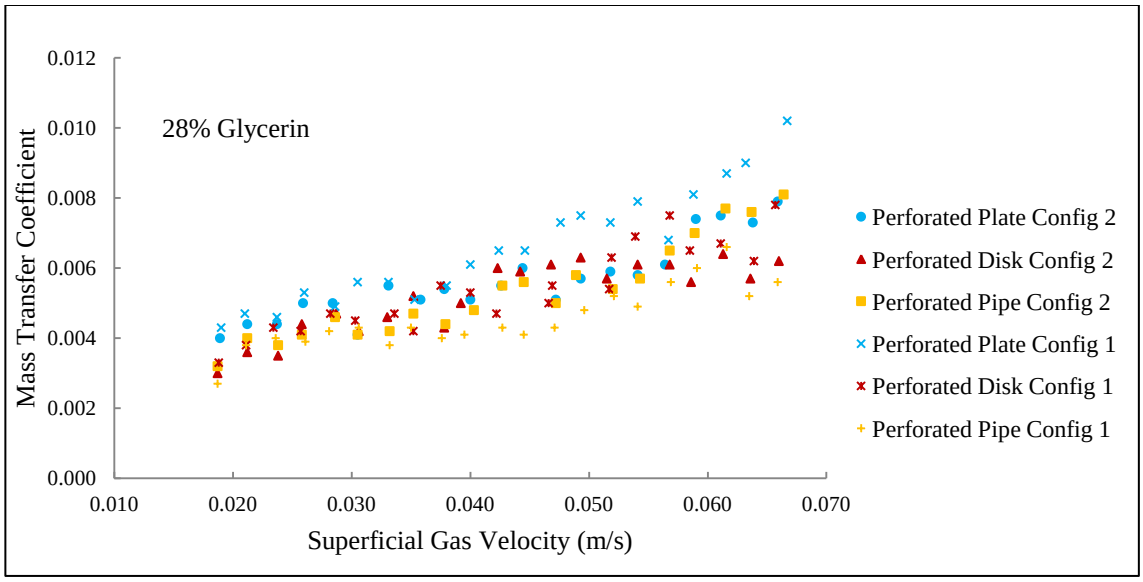

Figure 5.42 Comparison of area ratio effects on the mass transfer coefficient using different sparger types for a 28% glycerin solution in reactor configurations 1 and 2.

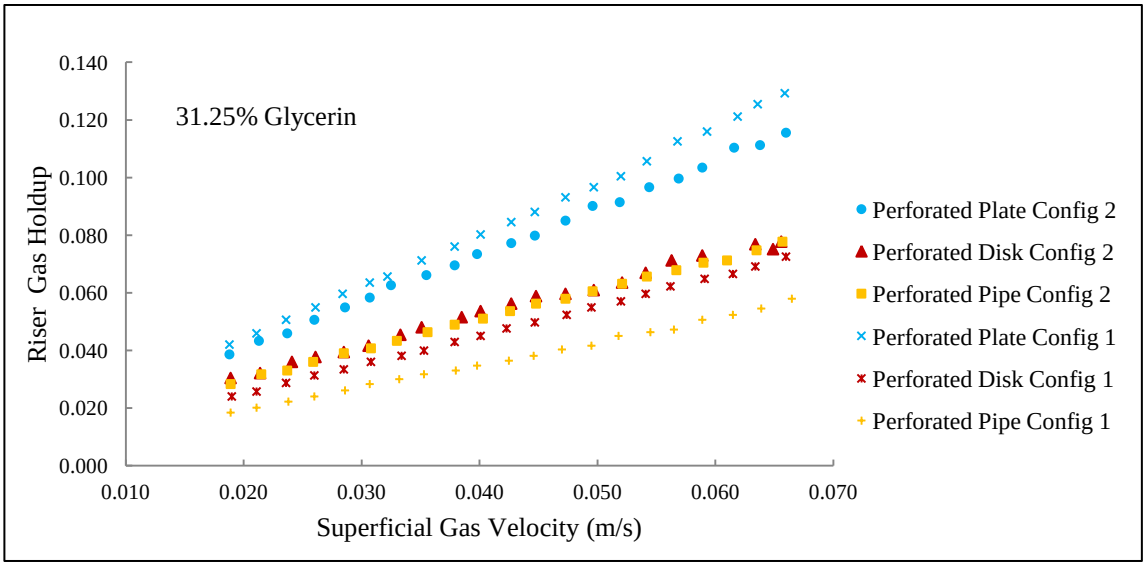

Figure 5.43 Comparison of area ratio effects on the riser gas holdup using different sparger types for a 31.25% glycerin solution in reactor configurations 1 and 2.

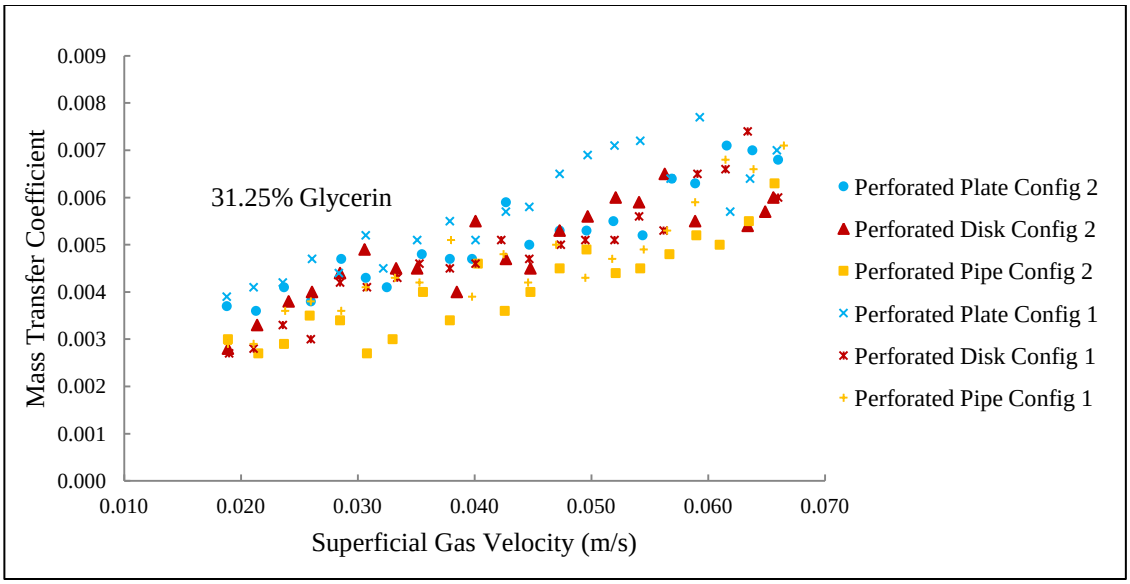

Figure 5.44 Comparison of area ratio effects on the mass transfer coefficient using different sparger types for a 31.25% glycerin solution in reactor configurations 1 and 2.

It is apparent that the liquid properties of a solution, especially the surface tension, viscosity and density, play an important role in the mass transfer characteristics and need to be considered as design parameters for airlift reactors.

5.3.2. CONCLUSION

The result of the investigation into the mass transfer characteristics of the five reactor configurations of pilot scale external loop airlift reactors has yielded some interesting results and conclusions. Visual observations are of paramount importance as they contribute significantly to understanding why trends with respect to mass transfer are experienced in the external loop airlift reactor. In this investigation it was found that the sparger does play a significant role in the mass transfer characteristics of an external loop airlift reactor and that this effect can be compounded by the area ratio of the reactor depending on the actual design of the sparger. This is in direct contradiction of the reports by the following authors, Kojić et al. (2015), Lin et al. (2004), Contreras et al. (1999), Gavrilescu and Tudose (1998 Part 1), Merchuk (1996a), Kemblowski et al. (1993) and Chisti (1989). It was also found that the although the area ratio is an important parameter to consider in external loop airlift reactors, using the actual diameters of the riser and downcomer provides a more realistic and

appropriate approach to analyzing the mass transfer characteristics in the reactor. This is important as in this investigation although reactor configurations 1 and 3 had the same area ratio of 1 their actual diameters were very different viz., 0.15m and 0.225m respectively. By only taking the area ratio into consideration, a valid conclusion with regards to mass transfer and gas holdup cannot be done. Although it may be argued that the area ratio represents to some extent the reactor geometry, it is done implicitly and does not give a true indication of the actual geometry and what is actually present. In the investigation of the effects of the aspect ratio, it was found that a clearer analysis of the mass transfer characteristics could be drawn if it is done together with the reactor diameters. The liquid properties as well are important as they contribute significantly to the behaviour of the bubbles within the column which impact on the mass transfer characteristics in the reactors.

From this initial investigation, it can be concluded that all important parameters need to be taken into consideration in the neural network model as they are interdependent and no one parameter is more significant than the other. Ratios may be significant but having the actual parameters expressed explicitly would be more reliable. An all-inclusive model should contribute to a network that should give a better generalization.

5.4. NEURAL NETWORK MODELING

An artificial neural network was used to model the data generated experimentally from 5 pilot scale external loop airlift reactor configurations. The artificial neural network was selected due to its ability to model highly complex non-linear data as discussed in Chapter 3. From the initial study of the literature (Chapter 3) it was found that the traditional approach to modeling using computational fluid dynamics, although good for the systems at hand, could not be successfully applied to all other systems as detailed knowledge of relationships between parameters are first required. Computational fluid dynamics could also not be applied if non-numeric data inputs were being used to describe an airlift reactor system. The computational fluid dynamics were also non-adaptive and could not be applied to complex non-linear systems. The artificial neural network on the other hand satisfied all these criteria but only required a large amount of data inputs to provide a good generalization. Unfortunately generating substantial amounts of data is often constrained by time and resources.

5.4.1. DATA CLASSIFICATION AND PARTITIONING

The input variables sparger type, bubble size range and type of bubble flow pattern were reclassified for ease of use as model inputs. The sparger type was reclassified according to Table 5.1 based on the overall geometric shape only. The bubble sizes were classified according to Table 5.2. This classification included the presence of coalesced bubbles irrespective of whether they were present instantly or for long periods of time. The bubble flow patterns were classified according to Table 5.3. The bubble flow patterns described whether the flow path was linear, slightly random and chaotic or very random and highly turbulent based on visual observations.

Table 5.1 Reclassification of sparger type for the neural network model.

Sparger type (Initial Classification)	**Reactor Configuration Used**	**n_h (number of holes)**	**d_o (diameter of pore)**	**Diameter of sparger**	**Reclassified Sparger Type for the Neural Network**
Perforated Plate	1; 2	21	4.5mm	140mm	A
Perforated Disk	1; 2	20	4.5mm	100mm	B
Perforated Pipe	1; 2	21	4.5mm	120mm	C
Perforated Plate	3	210	1mm	198mm	A
Perforated Disk	4; 5	56	1mm	100mm	B

Table 5.2 Classification of bubble size for the neural network model.

Size Range	**1mm – 1cm**	**3cm≥ bubble size > 1cm**	**5cm ≥ bubble size > 1cm**	**Bubble size > 5cm**
Classification	S	M	L	XL

Table 5.3 Classification of bubble flow patterns for the neural network model.

Bubble Flow Pattern	**Linear/straight**	**Slightly Random**	**Random/ Turbulent**	**Highly Random/Highly Turbulent**
Classification	Good (G)	Average (A)	Poor (P)	Very Poor (VP)

The final model input parameters were reclassified sparger type; sparger pore size; riser diameter; downcomer diameter; area ratio; aspect ratio; riser height; downcomer height; static liquid height; bubble size range; bubble flow pattern; fluid density; viscosity; surface tension; superficial gas velocity; superficial downcomer liquid velocity; riser gas holdup; downcomer gas holdup. The output was always the mass transfer coefficient.

5.4.2. BUILDING THE NEURAL NETWORK MODEL

In this investigation the neural network software, Predict (Version 3.30) by Neuralware was used to build the model. Predict uses the cascade correlation learning architecture technique. This type of architecture only has one hidden layer and can have multiple hidden units also known as neurons or nodes within this hidden layer depending on the significant reduction of error obtained after each hidden unit is added to the model.

Predict allowed for numeric and non-numeric inputs which in the case of this investigation were important. No prior relationships between parameters were required to be known and all calculations for some of the input variables were done from first principles.

The data was partitioned by the software. Seventy percent was used as the training data while 15% was used for internal validation and 15% for testing. The internal validation data was selected according to the "round robin technique" parameter and did not constitute either the training or the test data. In Predict, the test data is used to test the model after training. The internal validation data is unseen by the model and is used to determine whether the model is able to give a good generalization.

When selecting the input variables for the model, the conclusions derived from Chapter 2 and Sections 5.2 and 5.3 of this Chapter were considered. From the discussion in Chapter 2, with respect to significant parameters in an airlift reactor design for mass transfer, there were conflicting views amongst authors. Consolidation of available information before continuation of further research is almost non-existent. If comparisons were done to develop correlations, often the equipment used was not similarly built and although the proposed correlations may be useful they are very limited as they are mostly empirical and are often reactor dependant. The same view is expressed by Kadic and Heindel (2014).

In the building of the neural network model for this investigation all these factors had to be taken into consideration. The first model proposed considered all the parameters that were deemed important in literature, even the sparger, although there were many conflicting viewpoints on this in literature. The output was always only the mass transfer coefficient *(k_La (s^{-1})).*

The input variables in the initial model were area ratio, aspect ratio, fluid density, surface tension, viscosity, superficial gas velocity, downcomer superficial liquid velocity, riser gas holdup and downcomer gas holdup. The sparger type, bubble size riser and downcomer were included at this stage based on the results and conclusions obtained during this experimental investigation. The parity plot of Figure 5.45 shows the relation between all the predicted and experimental mass transfer data with a 95% confidence interval and a correlation coefficient (R) of 0.94.

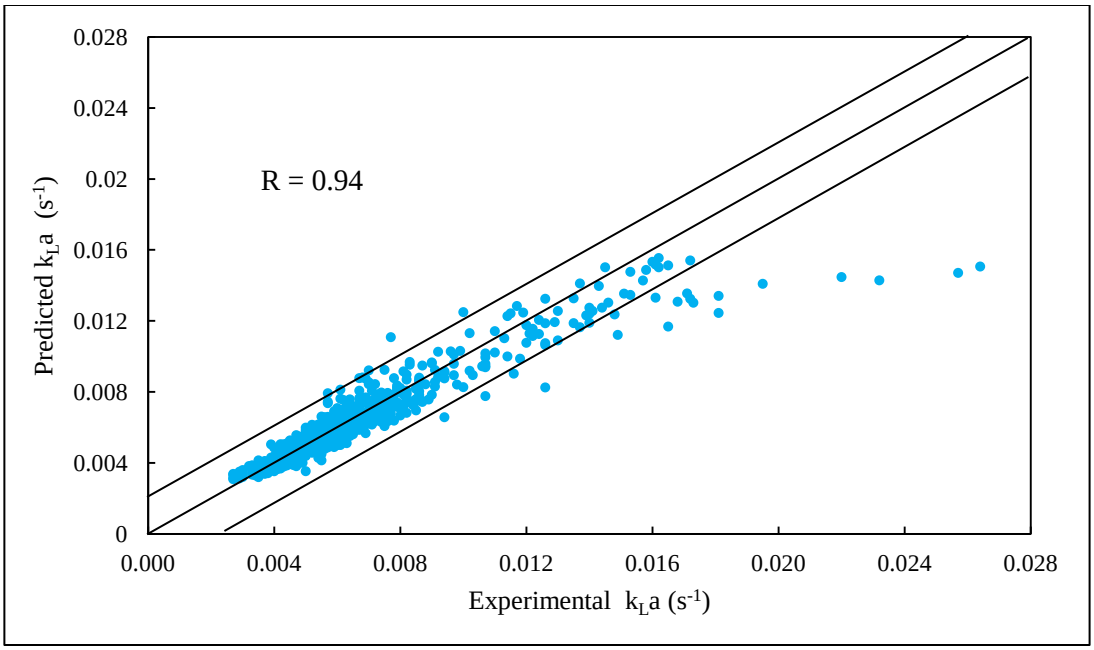

Figure 5.45 Parity plot of all predicted and experimental mass transfer coefficient data for neural network model 1.

From this parity plot, it is noted that although the model is able to make good predictions at lower values of mass transfer, at high mass transfer coefficient values, i.e. above 0.012, the curve flattens out. This flattening of the curve is an indication that the model is unable to make predictions and does not work. Upon investigation, these outlying points were found to correspond to the mass transfer coefficients at very high superficial gas velocities in reactor configuration 3. To improve the model's reliability, the numbers of significant input variables were increased as it was concluded that some input parameter was missing which was the reason for the model not able to predict at the higher mass transfer values. Each of the original variables was re-examined. The sparger type, aspect ratio and area ratio although important, have information which is implicit. Making this hidden information available to the model in its explicit form was considered important. This was based especially on the conclusions in Sections 5.3.1.2 and 5.3.2. The area ratio was not representative enough as it was the same for reactor configurations 1 and 3. Yet these reactors differed significantly in their geometrical characteristics. To rectify this misrepresentation, the actual riser diameter was added as a variable into the model.

The sparger type was also considered to be insufficiently represented as the pore sizes for the spargers were different. The sparger pore size was added to the model as an input variable. Building the model with these two additional input variables, i.e. riser diameter and sparger pore size, yielded the parity plot of Figure 5.46.

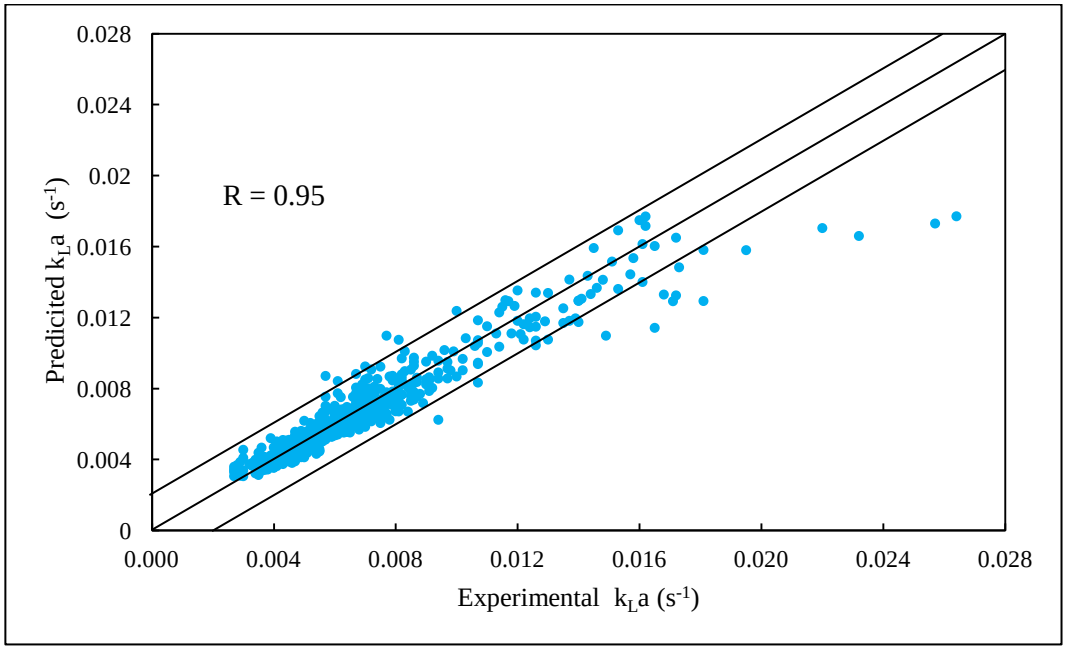

Figure 5.46 Parity plot of all predicted and experimental mass transfer coefficient data for neural network model 2.

From the parity plot of the experimental and predicted mass transfer coefficient data of Figure 5.46, it is noted that there is a slight improvement in the ability of the 2nd model to generalize at these same high mass transfer coefficients when compared to the first model (Figure 5.45). The number of outlying points decreased and lies closer to the diagonal or within the 95% confidence interval while the correlation coefficient (R) was 0.95.

It can be inferred that in model 1, the information contained implicitly in the area ratio and the sparger shape was not recognized by the artificial neural network. Explicit information was required which resulted in an improved approximation in model 2. With this inference, to further improve model 2, the riser height was included as an input variable into model 3. The resulting change in the parity plot (Figure 5.47; model 3) shows some improvement at low

mass transfer coefficient values but this 3rd model appeared again to poorly predict for the four outlying points from reactor configuration 3.

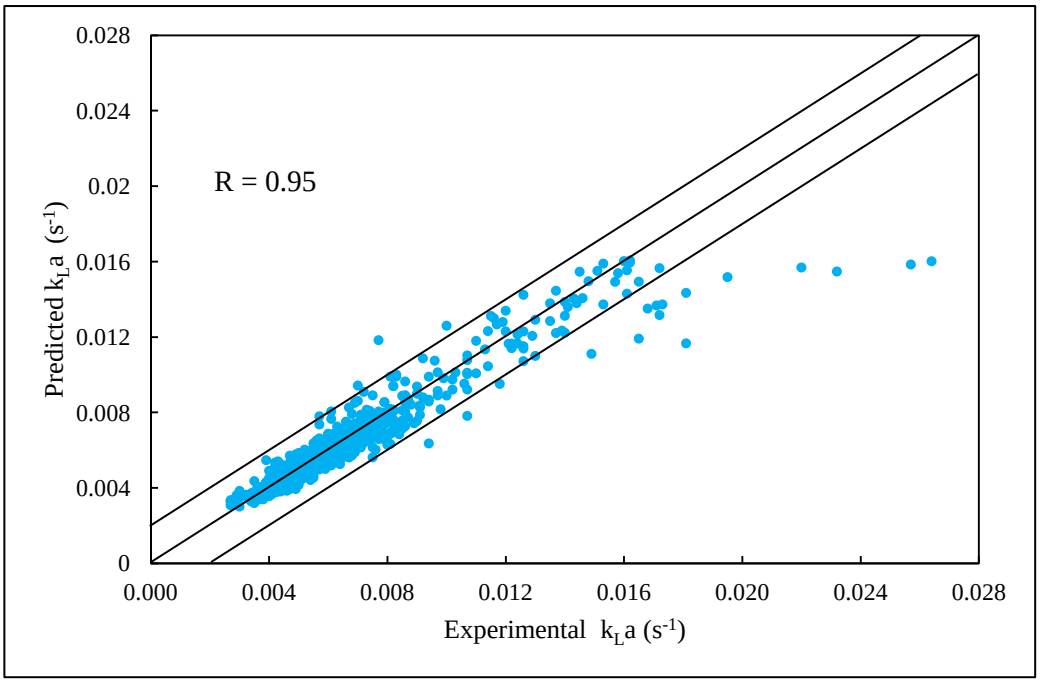

Figure 5.47 Parity plot of all predicted and experimental mass transfer coefficient data for neural network model 3.

This prompted the use of the downcomer diameter as an input to complete the implicit variables represented by the area ratio as it was concluded that there was still some input parameter missing in the model. The addition of the downcomer diameter had no real influence on the model 3's ability to predict (R = 0.95) (Figure 5.48) at higher mass transfer values (the four highlighted outliers related to reactor configuration 3) but for the lower mass transfer values, although the scatter appears slightly more than in Figure 5.47, model 4 does seem to give very slightly better approximations.

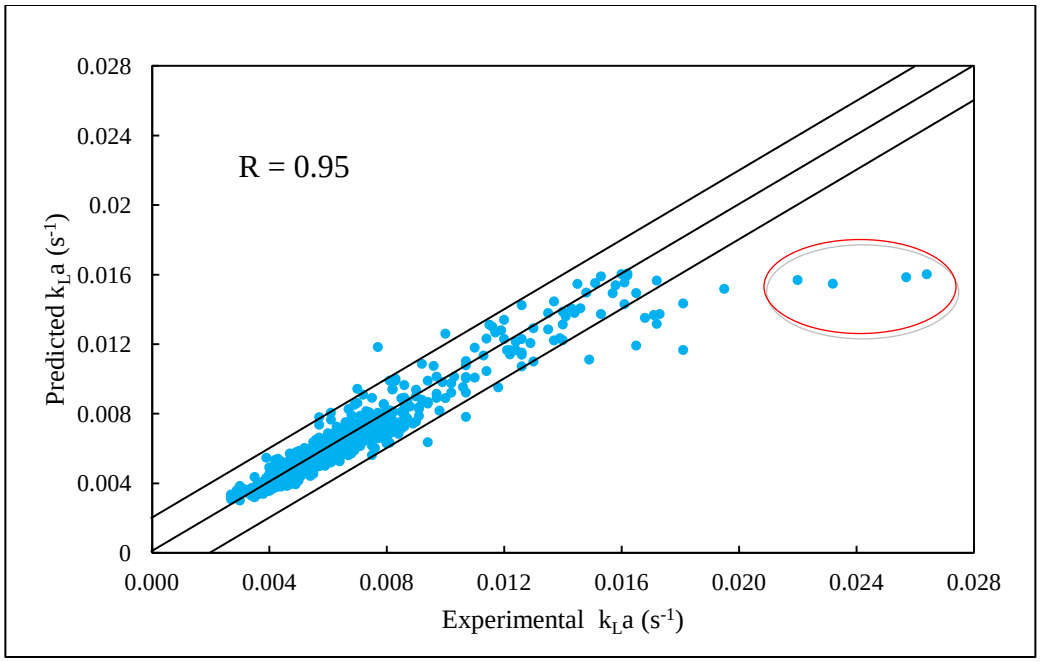

Figure 5.48 Parity plot of all predicted and experimental mass transfer coefficient data for neural network model 4.

Based on further conclusions from Section 5.2.2, the mass transfer was affected by the bubble flow patterns in the riser. This was included as an input variable in the model with the bubble behaviour classified according to visual observations. The classification according to Table 5.2 was added as a new input variable to model 5. This immediately resulted in an improvement in model 5's ability to make predictions (Figure 5.49 although the R value is slightly lower at 0.94) for the four outliers highlighted in Figure 5.48 at the higher superficial gas velocities that were related to reactor configuration 3.

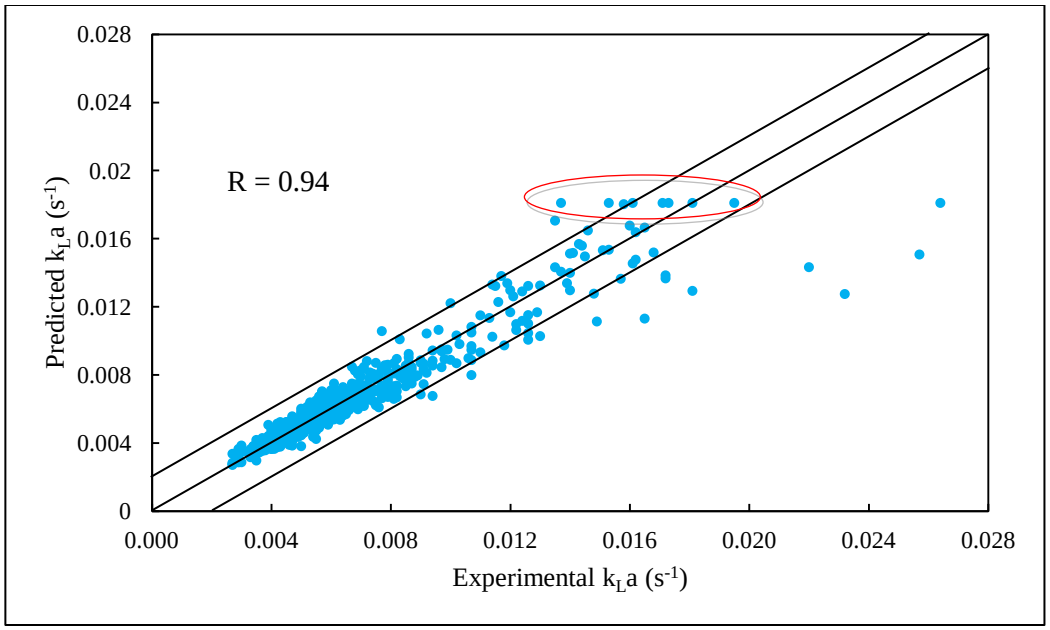

Figure 5.49 Parity plot of all predicted and experimental mass transfer coefficient data for neural network model 5.

Although the few points highlighted in Figure 5.49 (range 0.014 to 0.02) display a flattening of the curve, these highlighted point's do not all belong to any one reactor or system condition. These points (Figure 5.49) are unrelated to each other whereas the points highlighted in Figure 5.48 all belonged to reactor configuration 3 from a particular system condition. However, to further improve the ability of model 5 to give better generalizations, the downcomer height was added as an input variable into the 6th model. It was done with the assumption that the four outliers would possibly move closer to the diagonal and that the model would be able to continue to make better predictions. Figure 5.50 (model 6) shows that the addition of the downcomer height results in a slight increase in the scatter of the data points.

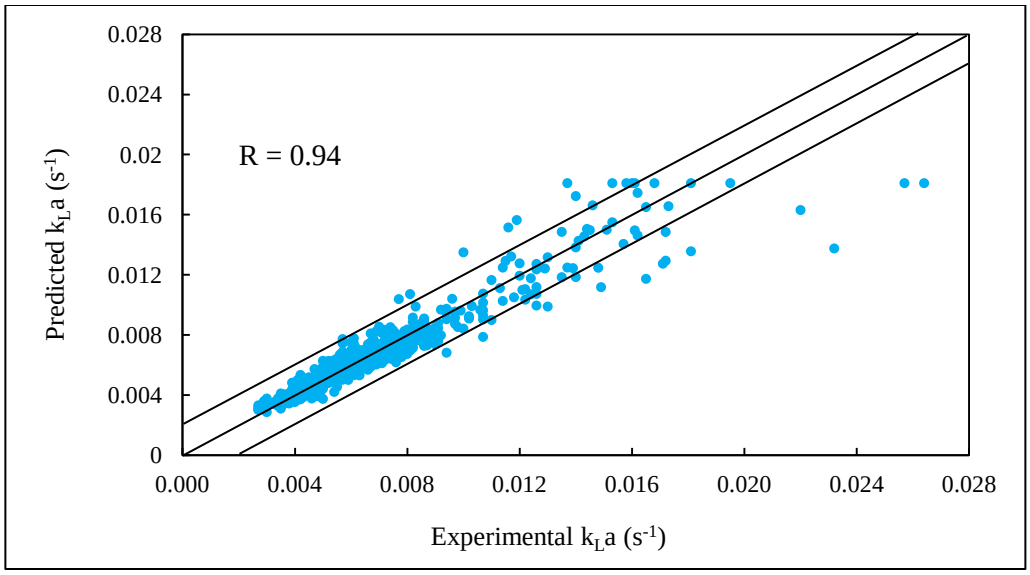

Figure 5.50 Parity plot of all predicted and experimental mass transfer coefficient data for neural network model 6.

This also resulted in the model not being able to predict at the very high end of mass transfer values as it flattens out again. To resolve this, the static liquid height was added as an input with the resulting graph in Figure 5.51 (model 7).

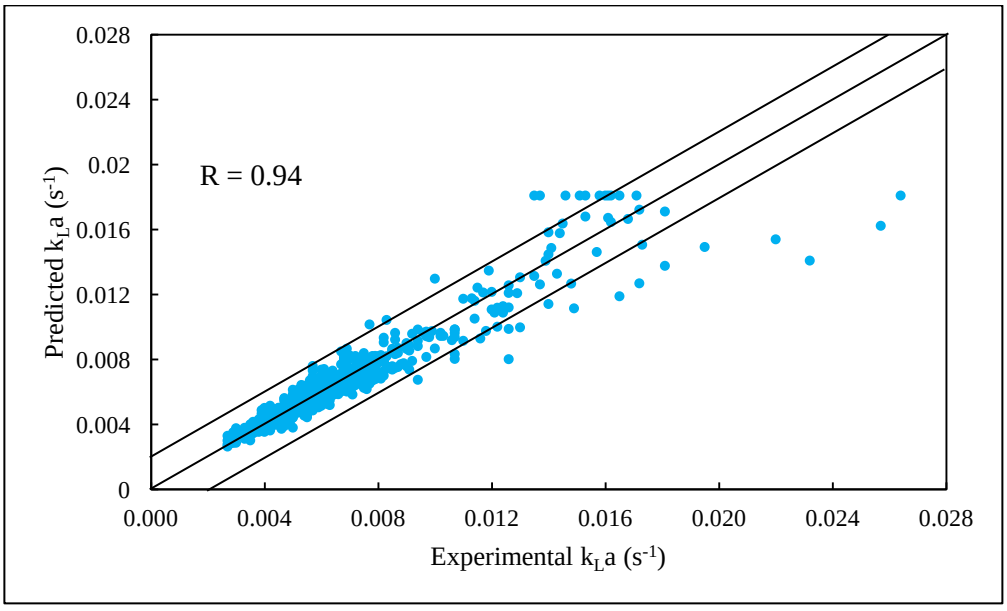

Figure 5.51 Parity plot of all predicted and experimental mass transfer coefficient data for neural network model 7.

Although this resulted in a seemingly improved model, the outliers were still of concern together with the few unrelated points between 0.013 and 0.017 where the model was unable to make predictions. This suggested that the static liquid height appeared to not be as important an input variable in the model. Considering that all physical parameters that could be measured or observed were already used as input variables in the model, more data points for reactor configuration 3 from superficial gas velocity 0.05m/s were added to the model during training. This resulted in a highly significant improvement in the models ability to predict (Figure 5.52; model 8).

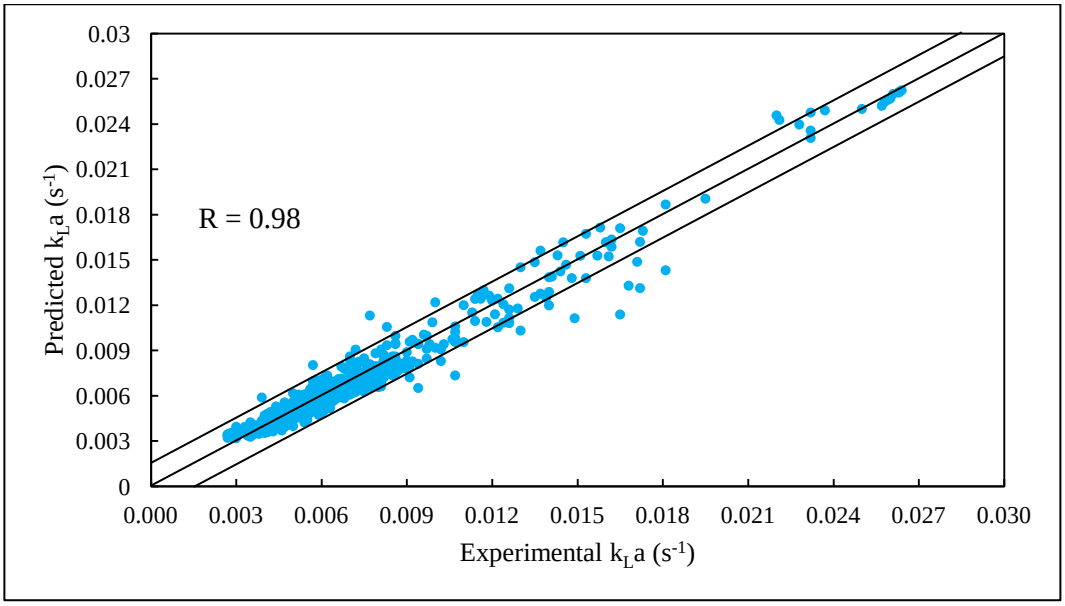

Figure 5.52 Parity plot of all predicted and experimental mass transfer coefficient data for neural network model 8.

The few outliers in the range 0.015 to 0.018 were unrelated to each other. This final model selected had 7 hidden units within the single hidden layer. When analyzing the weighting applied by the model in Table 5.4 (Appendix A3 - detailed variable weighting table with transformations) to the input variables for each hidden node, it is apparent that the superficial gas velocity is consistently significant at each node. The superficial gas velocity is the driving force in airlift reactors and therefore should indeed be the dominant variable. However, it must be noted that the sparger type, bubble size in the riser, bubble flow pattern, superficial liquid velocity and riser and downcomer gas holdup are also significant variables in all hidden nodes as well as the surface tension and the bubble size in the downcomer. The sparger type

had a direct influence on the bubble flow patterns in the riser as observed during the visualization study which affected the mass transfer characteristics of the reactors. The bubble size influenced the available area for mass transfer. The riser and downcomer gas holdup together with the superficial liquid velocity also impacts on the mass transfer. Entrained non-nutritive bubbles in the liquid return to the riser via the downcomer if the superficial liquid velocity is high as not enough time is allowed for disengagement of bubbles. These non-nutritive bubbles may increase the riser gas holdup but will not result in an increase in the mass transfer. The surface tension and viscosity are also considered significant as they influence the residence time of the bubbles in the riser due to the resistance provided by the liquid. The bubble size in the downcomer will influence the riser gas holdup which does not increase mass transfer.

By analyzing the weighting of the 8^{th} model (sparger pore size; riser diameter; downcomer diameter; area ratio; riser height; downcomer height; aspect ratio; static liquid height and fluid density) model the remaining variables are also significant. It can be concluded that every input is significant to some degree in the model and cannot be completely omitted. This is in agreement with the conclusion in Section 5.3.2. All possible parameters are important in airlift reactors as they are interdependent and that they are best expressed in their component form while ratios are kept to a minimum.

Table 5.4 Weights (ω_{xi}) applied by the model from the input variables to the hidden layer.

Name	**Hidden Units**						
	1	**2**	**3**	**4**	**5**	**6**	**7**
Sparger type	-0.17	0.940	0.467	-0.657	0.11	0.393	0.475
Sparger pore size	0.0066	-0.123	-0.103	-0.007	-0.031	-0.129	0.187
Riser diameter	-0.294	-0.0895	0.259	0.014	0.089	0.137	0.421
Downcomer diameter	0.03	-0.197	0.236	-0.085	0.0797	0.082	0.284
Area ratio	-0.058	-0.207	-0.055	-0.138	0.0369	-0.0717	-0.083
Riser height	-0.09	0.049	0.116	0.0297	-0.041	-0.122	0.30
Downcomer height	-0.056	-0.0637	0.0659	0.0298	0.0348	-0.121	0.316
Aspect ratio	-0.189	0.059	-0.087	0.028	-0.091	-0.198	0.165
Static liquid height	0.157	-0.121	0.024	0.029	-0.039	-0.114	0.295
Fluid density	0.084	-0.036	0.304	0.231	0.06	0.121	-0.192
Surface tension	-0.178	0.704	-0.027	0.716	-0.158	-0.213	0.222
Viscosity	-0.047	-0.201	-0.213	0.27	0.032	0.2176	0.291
Bubble size riser	0.176	0.291	0.554	-0.713	-0.303	0.393	0.766
Bubble size downcomer	-0.281	0.323	-0.513	0.454	-0.217	0.057	-0.135
Bubble flow patterns	0.208	0.179	0.565	-0.474	0.134	0.453	0.288
Superficial gas velocity	-0.736	-0.248	-0.435	0.552	-0.578	0.723	0.97
Superficial liquid velocity	0.164	0.199	0.196	0.407	0.202	0.235	0.439
Riser gas holdup	-0.485	-0.369	-0.261	-0.480	-0.638	0.664	-0.654
Downcomer gas holdup	0.295	0.133	0.291	0.878	-0.495	0.312	0.453

5.4.3. VALIDATION OF THE ARTIFICIAL NEURAL NETWORK

To validate the selected artificial neural network model, unseen data from literature as well as unseen experimental data from the author's own investigation was input into the model. Complete sets of data inputs were obtained from Nayager and Govender (2016), Shariati et al. (2007) and Guo et al. (1997). The data from Fakhari et al. (2014) was incomplete with only the confirmed sparger design information missing. To complete this data set, it was decided that the three types of sparger designs classified in this research would be used as substitute information. The perforated plate was the first choice as this sparger design type is commonly used in literature followed by the perforated disk sparger and lastly the perforated pipe sparger. From Al-Masry and Dukkan (1997) the bubble flow patterns were easily inferred as the reactor setup was similar to that used in this investigation.

5.4.3.1. PREDICTIONS WITHIN THE RANGE OF THE TRAINING DATA

The airlift reactor and system used by Nayager and Govender (2016) was the same as that used in the author's own investigation (reactor configuration 4 and 5 with a gas–water system and perforated disk sparger), different superficial gas velocities were used. From Figure 5.53, the model gives a reasonable correlation for the data from Nayager and Govender (2016), which although appearing approximately linear, there is a distinct offset from the $y = x$ line. It was discovered that this was related to a methodological error throughout the work carried out by Nayager and Govender (2016).

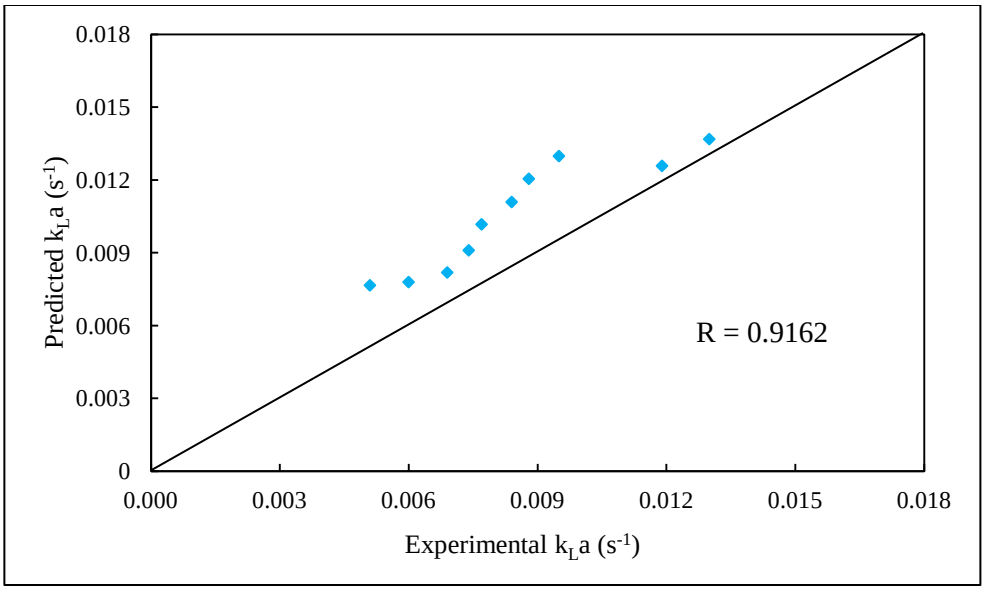

Figure 5.53 Prediction of mass transfer coefficient data, Nayager and Govender (2016).

The model gave very good predictions for the 32 unseen data points from the author's own investigation with the R value of 0.9896 (Figure 5.54) and the majority of points lying close to the diagonal and within the 95% confidence interval.

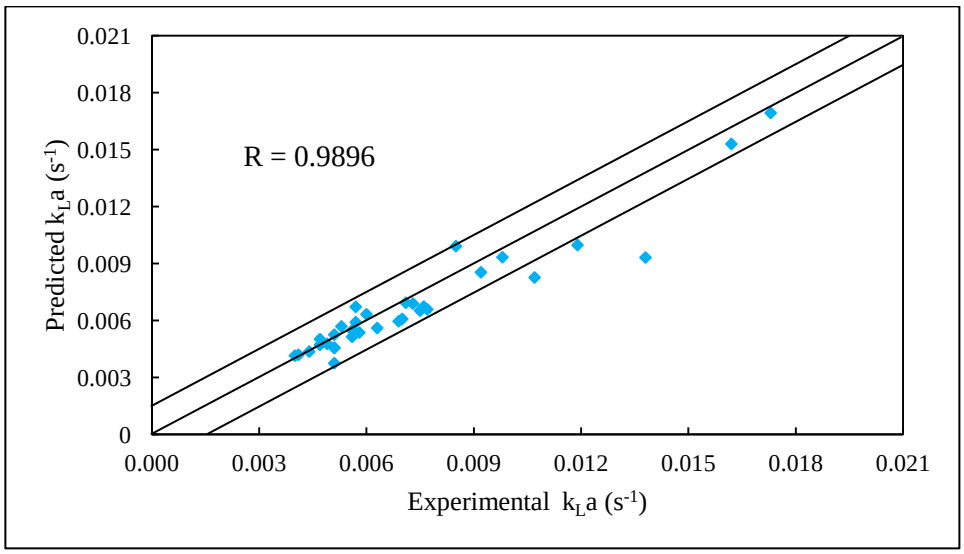

Figure 5.54 Prediction of the 32 unseen mass transfer coefficient data points from the author's own investigation.

5.4.3.2. PREDICTIONS OUTSIDE THE RANGE OF TRAINING DATA

In the investigation by Guo et al. (1997) a laboratory scale modified fluidized bed external loop airlift reactor with a perforated disk sparger and an air-water system was used. The fluidized bed was located below the sparger. There was complete gas disengagement which resulted in no entrainment of bubbles into the downcomer. Although the riser and downcomer diameters and heights were below the range of the training data, the superficial gas velocity, sparger design and fluid properties were within the range of the training data. The model was still able to make good predictions with an R value of 0.9525 (Figure 5.55).

This suggests that the modifications made to the reactor were not significant to the model as the model was still able to make good predictions. From Figure 5.55, it also suggests that if the reactor geometric size (riser and downcomer diameters and heights) is within or smaller than the size used in the training data the model will still be able to make predictions if the superficial gas velocity, sparger design and fluid properties are within the range of the training data.

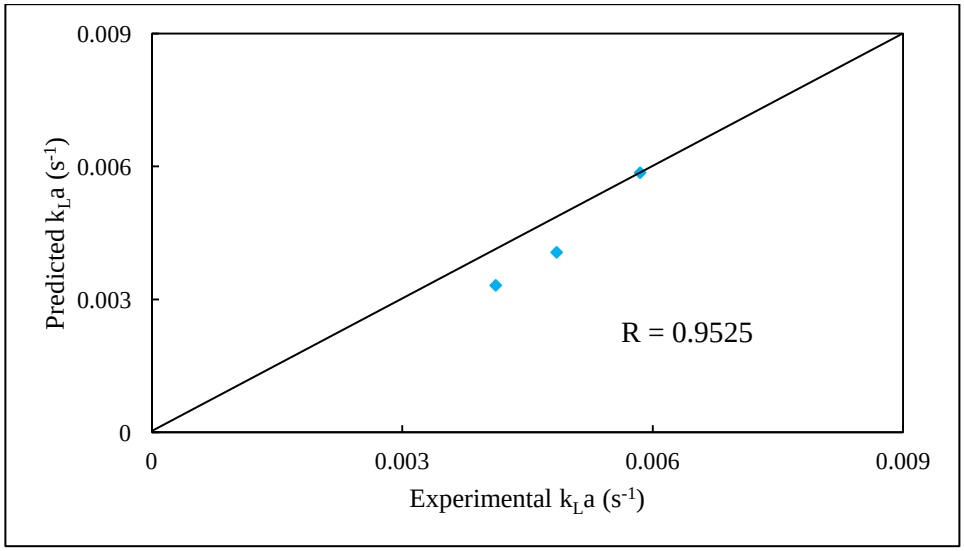

Figure 5.55 Prediction of mass transfer coefficient data, Guo et al. (1997).

In the case of Al-Masry and Dukkan (1997) a pilot scale external loop airlift reactor was used with an air-water system. The perforated plate sparger and riser and downcomer diameters were identical to that used in this investigation (reactor configuration 3, D_R and D_D = 0.225m). The reactor height (7m) was much taller than reactor configuration 3 and the superficial gas

velocity exceeded the highest velocity (0.068m/s) used in this investigation for reactor configuration 3. Although the model was able to make predictions (R value 0.8523) within the superficial gas velocity range of the training data (Figure 5.56), the model under predicted the mass transfer coefficient indicating sensitivity to the reactor height. This suggests that the riser height does play an important role in the mass transfer characteristics of the reactor as it influences the residence time of the nutrient rich bubbles in the reactor. A longer residence time of nutrient rich bubbles in the riser results in an increase in mass transfer. It can be inferred that the model was unable to make good predictions within the training data range as the predicted mass transfer coefficients were lower than the experimental mass transfer coefficients. This was due to the reactor height of Al-Masry and Dukkan (1997) being above the range of the training data used.

However, in the preceding case of Guo et al. (1997) the model was able to make predictions with the reactor height and riser and downcomer diameters below the training data range (Figure 5.55). This implies that the model will work if the superficial gas velocity is within the training data range even though the reactor height and riser and downcomer diameters are below the training data range for the model. However, from Figure 5.56 the model was unable to make any predictions at superficial gas velocities above the training data range of the model as the curve flattens out. This suggests that the model is unable to extrapolate above the training data range of the model for the superficial gas velocity indicating the more dominant role of the superficial gas velocity in airlift reactors.

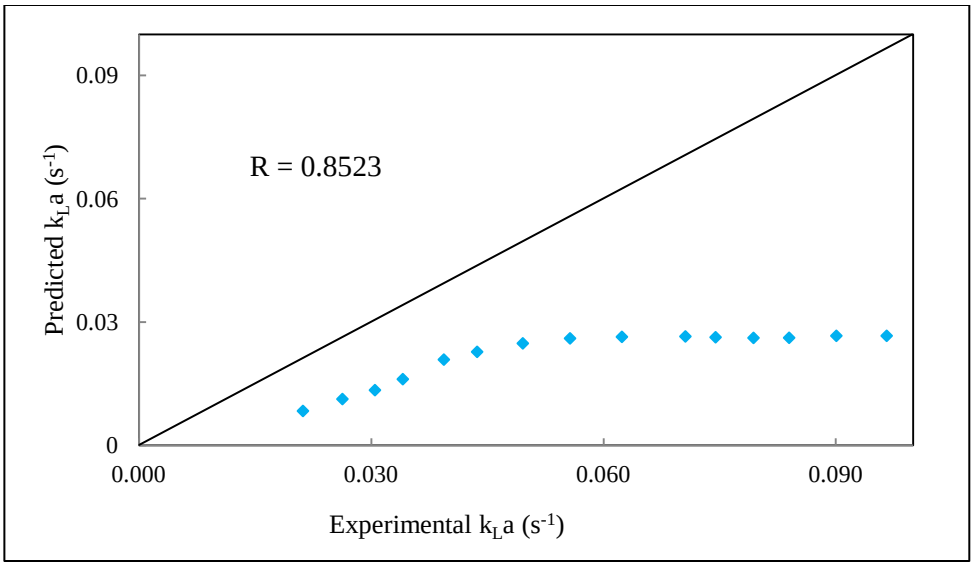

Figure 5.56 Prediction of mass transfer coefficient data, Al-Masry and Dukkan (1997).

In the case of Fakhari et al. (2014) a laboratory scale external loop airlift reactor with a tube separator and a water-air system was used. The data from Fakhari et al. (2014) was possibly obtained using a tennis ball type sparger with 1mm pore size as inferred from Moraveji et al. (2012) and Fakhari et al. (2014).

The superficial gas velocities and the geometric dimensions of the reactor (i.e. riser and downcomer diameters and reactor height) were well below the range of the training data. The sparger input was classified each time as a perforated plate (A), perforated disk (B) and perforated pipe (C) sparger before the data was input into the model. The model was unable to make good predictions as noted in Figure 5.57 (R value 0.6692, sparger A), Figure 5.58 (R value 0.6740, sparger B) while in Figure 5.59 (R value 0.8557, sparger C) the model starts to show an over prediction of mass transfer. This shows the sensitivity of the model to the sparger as an input parameter even though the superficial gas velocity is below the training data range as will be discussed in the following Section 5.4.3.3. This suggests that the model is less sensitive to the lower end of the superficial gas velocity (Section 5.4.3.3) which is in the bubble/laminar flow regime (Figure 2.7a.) as opposed to the very high end of the superficial gas velocity range which is highly turbulent and disruptive in the airlift reactor. In the case of Fakhari et al. (2014), there were too many variables outside the range of the

training data as compared to Al-Masry and Dukkan (1997) and Guo et al. (1997). However, the model should have been able to make some good predictions based on the range of the reactor geometric data and fluid properties as in the case of Guo et al. (1997) as well as the sparger input data.

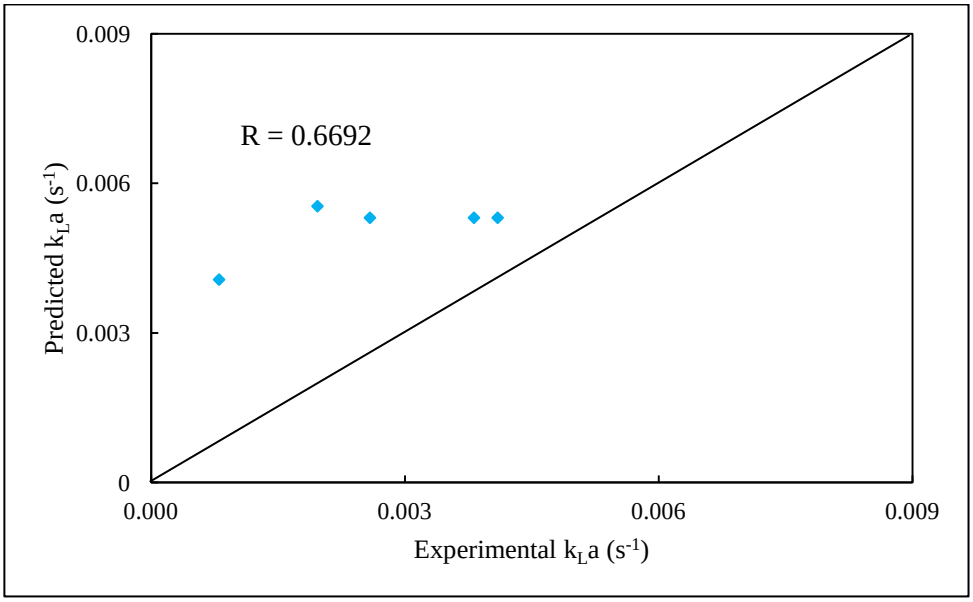

Figure 5.57 Prediction of mass transfer coefficient data, Fakhari et al. (2014) using a perforated plate sparger (A).

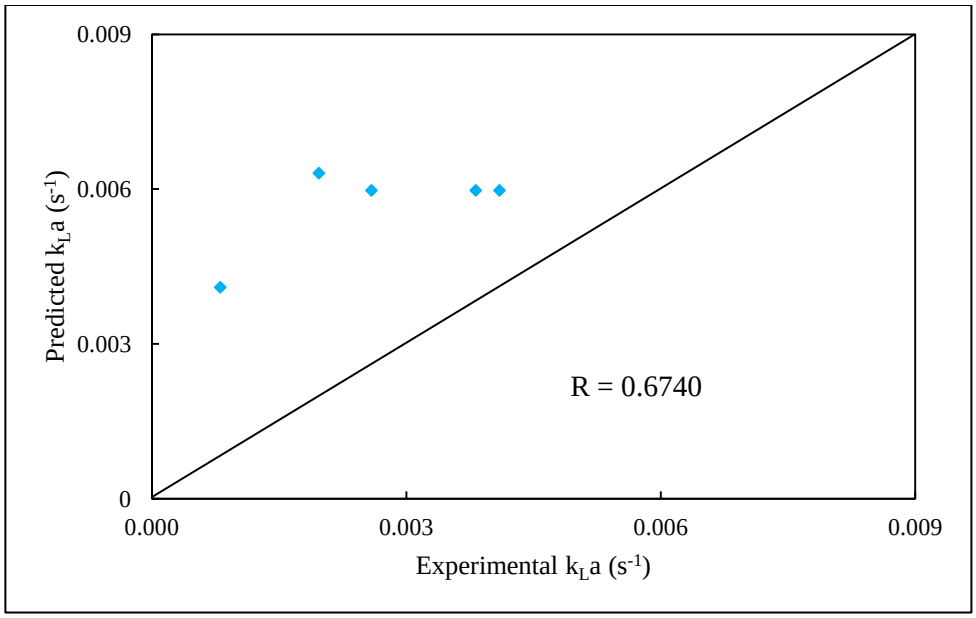

Figure 5.58 Prediction of mass transfer coefficient data, Fakhari et al. (2014) using a perforated disk sparger (B).

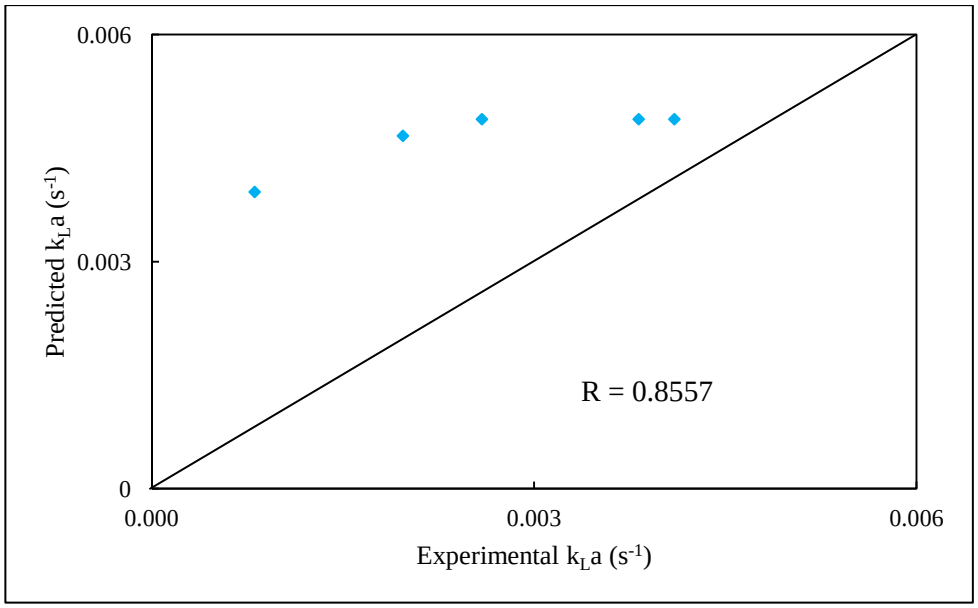

Figure 5.59 Prediction of mass transfer coefficient data, Fakhari et al. (2014) using a perforated pipe sparger (C).

The model shows sensitivity to the sparger as an input variable which is in keeping with the conclusions made in this study (Section 5.3.2) with respect to sparger influence on the mass transfer characteristics in an airlift reactor which is contrary to the findings by Kojić et al.

(2015), Lin et al. (2004), Contreras et al. (1999), Gavrilescu and Tudose (1998 Part 1), Merchuk (1996a), Kemblowski et al. (1993) and Chisti (1989).

In summary, it can be inferred from the model predictions from the data of Guo et al. (1997) (Figure 5.55) that the model is not sensitive to the geometric dimensions of the riser and downcomer heights and diameters below the training data range nor the modifications made to the reactor. The predictions from the data of Al-Masry and Dukkan (1997) (Figure 5.56) however, suggests that the model will under predict if the height of the reactor is above the training data range and that the model will not be able to make predictions if the superficial gas velocities exceed the training data range. From the predictions of the data from Fakhari et al. (2014), it suggests that the model is sensitive to the sparger design (Figure 5.57, Figure 5.58 and Figure 5.59) even though the superficial gas velocities were below the training data range. In the following Section (Section 5.4.3.3.) the model was able to make predictions with the superficial gas velocities below the training data range and a type C sparger. It can therefore be inferred that the sparger design also does play an important role in an airlift reactor.

5.4.3.3. APPLICATION OF THE NEURAL NETWORK TO THE DATA SET OF AN INTERNAL LOOP AIRLIFT REACTOR

To further test the reliability of the model, the neural network model was applied to the data from Shariati et al. (2007). Shariati et al. (2007) used a laboratory scale internal loop airlift reactor with a ladder type sparger. The systems under investigation were water-diesel micro-emulsions. This sparger fell within the type C classification of this investigation but the reactor design itself was completely different to the reactor design used in the model during training. The first two data points also fell outside the range of training data for superficial gas velocity but this appeared not to affect the networks ability to generalize. The geometric dimensions of the reactor were also below the range of the training data.

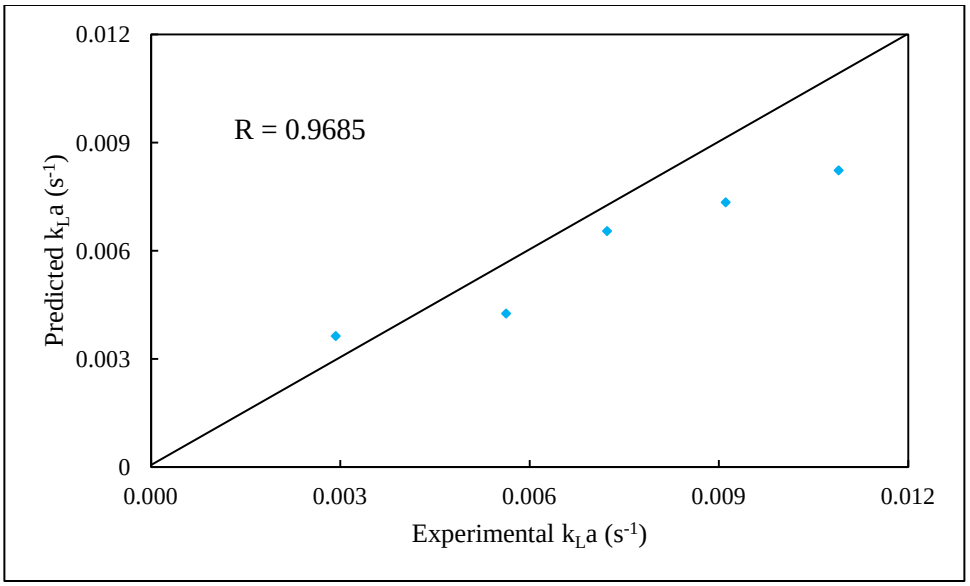

Figure 5.60 Prediction of mass transfer coefficient data, Shariati et al. (2007).

However, from Figure 5.60, the selected model was still able to give good predictions (R = 0.9685) of the data from Shariati et al. (2007) even though an internal loop airlift reactor was used in their investigation and not in the training of the neural network model of this investigation. The classification of the sparger type for this investigation is also validated as the model was still able to make good predictions for data from Shariati et al. (2007) even though the geometric design was different to the sparger type and design used in the training of the model. This shows that the model was able to make a good approximation although the reactor used was an internal loop airlift reactor. This also shows the ability of the model to make predictions with the superficial gas velocities below the training data range.

5.4.4. CONCLUSION

The neural network model built was able to give a good generalization of the unseen data that was within the range of the data used during training. This was achieved after ensuring that all important geometric data of the airlift reactors and visual observations from the investigation were included as input variables into the model.

From the predictions of the data from Guo et al. (1997), Al-Masry and Dukkan (1997), Fakhari et al. (2014) and Shariati et al. (2007) it can be inferred that the model is not sensitive

to the riser and downcomer diameters and heights below the training data range nor any modifications to the reactor. The predictions however suggest the models sensitivity to the superficial gas velocities, riser and downcomer heights exceeding the training data range. The predictions also infer the models sensitivity to the sparger design and it relative importance after the superficial gas velocity. The models sensitivity to the sparger design supports the conclusion reached in Section 5.3.2 of this thesis although this may not be in agreement with other authors.

The use of ratios as input variables are insufficient for a neural network model to give a good generalization and should be broken down into their component form to give a reliable output. However, they should not be entirely left out of the model input parameters.

CHAPTER SIX

GENERAL CONCLUSIONS AND RECOMMENDATIONS

6.1. GENERAL CONCLUSIONS

Airlift reactors can provide a viable means for the treatment of waste water and increasingly the production of microorganisms. However, although there is a large body of knowledge available pertaining to airlift reactors, there is still no definitive all encompassing correlation available that easily describes the behaviour and the mass transfer characteristics in these reactors. Although CFD's have been extensively used previously their applicability is very limited when compared to artificial neural networks which offer a more flexible learning approach to modeling but require large amounts of data.

To generate data for this investigation, experimental work was carried out on 5 configurations of pilot scale external loop airlift reactors. Three sparger design categories were used. The effects of the geometry of the reactors and sparger designs as well as the fluid properties (density, surface tension and viscosity) and superficial gas velocities on mass transfer coefficients were investigated and a data base of 663 runs was produced.

The results and visual observations were streamlined and used as input variables (sparger classification; sparger pore size; riser diameter and height; downcomer diameter and height; aspect ratio; area ratio; static liquid height; bubble sizes in the riser and downcomer; bubble flow patterns; liquid density, viscosity and surface tension, superficial gas and liquid velocities, riser and downcomer gas holdup) that were used to train the neural network model to predict the mass transfer coefficients. The model was tested with external data available from literature and unseen external data from the author's own investigation.

The following conclusions were drawn from this research:

- It was found that the model was able to give better approximations if the actual geometries of the reactors were used as inputs instead of only ratios.
- Inputs of the visual observations with respect to actual bubble flow patterns and average bubble size were also found to improve the models reliability.
- From the author's own experimental investigation the importance of the sparger design and parameters was noted and therefore used as an input variable in the model. The sensitivity of the model to the sparger design is confirmed in the application of the model to the data from Fakhari et al. (2014). The application of the model to this data base also confirmed that the sparger was a very significant input variable in the design of airlift reactors after the superficial gas velocity and could not be omitted.
- It was also found from the visual observations of the author's own investigation that the sparger pore sizes should be kept to 1mm with the perforated plate sparger being the recommended design. This combination provided the best bubble size and distribution.
- The area ratio of 1 is recommended for airlift reactors to prevent poor dispersion and bubble behaviour when it is less than 1.
- From the experimental investigation it was also found that the parameters of an airlift reactor were interdependent although some were more dominant than others. Analyzing the weighting of the input variables by the model also revealed that all input variables into the model were important to some degree.
- Ratios as well are required to be represented explicitly for the model to make good predictions.
- The applicability of the final neural network model to the unseen external data from literature and the author's own investigation showed a model that was highly capable of making predictions on reactors with different unseen configurations as long as the data remained within or below the training data range. However, in dealing with the unseen data it was not possible for the model to extrapolate to dimensions above the training data range.

- The neural network model was able to model other systems from literature even though there were differences in the internal arrangements and construction. A modification made to an airlift reactor does not affect the ability of the model to predict as in Guo et al. (1997) and Shariati et al. (2007).
- The model was also able to make predictions for internal loop and external loop airlift reactors. This indicates that the actual measurable geometric parameters (diameters and heights) of the reactor are important.
- The need for an increased data base extrapolated to higher dimensions was also highlighted from this application. This would allow for a broader range of predictions.
- The importance of visual observations is also highlighted as an important input variable by the model.

The model emphasizes the interdependence of the parameters in airlift reactors highlighting the complexity that cannot be easily interpreted by traditional means. The artificial neural network model is highly capable to perform predictions for external and internal loop airlift reactors irrespective of their geometries without prior knowledge of any relations between parameters.

6.2. RECOMMENDATIONS FOR FURTHER WORK

1. This study represents a start at the attempt to consolidate the research data available on airlift reactors. Further consolidation is required as this would address the areas where there is a lack of information and prevent an overlap of information.
2. The data base at higher gas velocities, larger airlift reactors and the inclusion of synthetic waste-water systems (from industry and municipalities) need to be increased. This would enable the artificial neural network model to provide a wider range of predictions which would be more suitable for industrial applications.
3. An important conclusion arrived at in this investigation is the significant influence of the sparger and its design on the mass transfer. A greater quantification of the parameters of the sparger design is required.

REFERENCES

Albijanic, B., Havran, V., Petrovic, L., Duric, M., Tekic, M.N., 2007. Hydrodynamics and mass transfer in a draft tube airlift reactor with dilute alcohol solutions. *AIChE Journal*, 53(11), pp 2987-2904.

Al-Mashhadani, M.K.H., Wilkinson, S.J., Zimmerman, W.B., 2015. Airlift bioreactor for biological applications with microbubble mediated transport processes. *Chemical Engineering Science*, 137, pp 243-253.

Al-Masry, W. A. 2006. Analysis of hydrodynamics of external loop circulating bubble columns with open channel gas separators using neural networks. *Chemical Engineering Research and Design*, 84 (A6), pp 483-486.

Al-Masry, W. A. Dukkan, A. R. 1997. The role of gas disengagement and surface active agents on hydrodynamic and mass transfer characteristics of airlift reactors. *Chemical Engineering Journal*, 65, pp 263-271.

Al-Masry, W.A., 2004. Influence of gas separator and scale up on the hydrodynamics of external loop circulating bubble columns. *Chemical Engineering Research and Design*, 82 (A3), pp 381-389.

Amiri, S., Mehrnia, M.R., Barzegari, D., Yazdani, A., 2011. An artificial neural network for prediction of gas holdup in bubble columns with oily solutions. *Neural Computing and Application*, 20, pp 487 – 494

Anon, n.d. Artificial neural networks – Cornell Computer Science. www.cs.cornell.edu>lectures>13_Ann.pdf (Access date: 16 May 2017).

Bannari, R., Bannari, A., Selma, B., Proulx, P., 2011. Mass transfer and shear in an airlift bioreactor: using a mathematical model to improve reactor design and performance. *Chemical Engineering Science*, 66, pp 2057 – 2067.

Behin, J., 2012. Deinking in bubble column and airlift reactors: influence of wastewater Merox unit as pulping liquor. *Chemical Engineering Research and Design*, 90, pp 1045-1051.

Behkish, A., Lemoine, R., Sehabiague, L., Oukaci, R., Morsi, B.I., 2005. Prediction of gas holdup in industrial-scale bubble columns and slurry bubble column reactors using back-propagation neural networks. *International Journal of Chemical Reactor Engineering*, 3 (A53), pp 1-35.

Bennajah, M., Gourich, B., Essadki, A.H., Vial, Ch., Delmas, H., 2009. Deflouridation of Morocco drinking water by electrocoagulation/electroflottation in an electrochemical external-loop airlift reactor. *Chemical Engineering Journal*, 148(1), pp 122-131. ISSN 1385-8947.

Bentifraouine, C. Xuereb, C. Riba, J-P. 1997. Effect of gas liquid separator and liquid height on the global hydrodynamic parameters of an external loop airlift contactor. *Chemical Engineering Journal*, 66, pp 91-95.

Bentifraouine, C. Xuereb, C. Riba, J.P. 1999. Local gas hydrodynamics in an external-loop airlift reactor: newtonian and non-newtonian fluids. *Bioprocess Engineering*, 20:303-307.

Blažej, M. Cartland Glover, G. M. Generalis, S. C. Markoš, J. 2004. Gas-liquid simulation of an airlift bubble column reactor. *Chemical Engineering and Processing*, 43, pp 137-144.

Camarasa, E. Carvalho, E. Meleiro, L. A. C. Maciel Filho, R. Domingues, A. Wild, G. Poncin, S. Midoux, N. Bouillard, J. 2001. A hydrodynamic model for air-lift reactors. *Chemical Engineering and Processing*, 40, pp 121-128.

Cancino, M.L., 2013. Artificial neural network modeling of phenol adsorption onto barley husks activated carbon in an airlift reactor. *PhD Thesis*. Facultad De Ciencias Químicas, Universidad Autónoma De Nuevo León.

Carvalho, E. Camarasa, E. Meleiro, L. A. C. Maciel Filho, R. Domingues, A. Vial, Ch. Wild, G. Poncin, S. Midoux, N. Bouillard, J. 2000. Development of a hydrodynamic model for air-lift reactors. *Brazilian Journal of Chemical Engineering*, 17 (4-7).

Carvalho, E., Camarasa, E., Meleiro, L.A.C., Maciel Filho, R., Domingues, A., Vial, Ch., Wild, G., Poncin, S., Midous, N., Bouillard, J., 2000. Development of a hydrodynamic model for air-lift reactors. *Brazilian Journal of Chemical Engineering*, 17 (4-7).

Chen, X.Z., Shi, D.P., Gao, X., Luo, Z.H., 2011. A fundamental CFD study of the gas-solid flow field in fluidized bed polymerization reactors. *Powder Technology*, 205, pp 276-288.

Chisti, M. Moo-Young, M. 1993. Improve the performance of airlift reactors. *Chemical Engineering Progress*, 38-45.

Chisti, M.Y. 1989. Airlift Bioreactors. *Elsevier Science Publishers Ltd. London and New York*.

Chisti, M.Y., Moo-Young, M., 1987. Airlift reactors: characteristics, applications and design considerations. *Chemical Engineering Communications*, 60, pp 195-242.

Chisti, Y., Wenge, F., Moo-Young, M., 1995. Relationship between riser and downcomer gas hold-up in internal-loop airlift reactors without gas-liquid separators. *The Chemical Engineering Journal*, 57, pp B7-B13.

Choi, K.H., 1999. A mathematical model for unsteady-state oxygen transfer in an external-loop airlift reactor. *Korean Journal of Chemical Engineering*, 16(4), pp 441-448.

Contreras, A., Chisti, Y., Molina, E., 1998. The reassessment of relationship between riser and downcomer gas holdups in airlift reactors. Shorter Communications. *Chemical Engineering Science*, 53(24), pp 4151-4154.

Contreras, A., Garcia, F., Molina, E., Merchuk, J.C., 1999. Influence of sparger in energy dissipation, shear rate, and mass transfer to sea water in a concentric-tube airlift bioreactor. *Enzyme and Microbial Technology*, 25, pp 820-830.

Couvert, A. Bastoul, D. Roustan, M. Line, A. Chatellier, P. 2001. Prediction of liquid velocity and gas holdup in rectangular air-lift reactors of different scales. *Chemical Engineering and Processing*, 40, pp 113-119.

Cozma, P., Drăgoi, E.N., Mămăliga, I., Curteanu, S., Wukovits, W., Friedl, A., Gavrilescu, M., 2015. Modelling and optimization of CO_2 absorption in pneumatic contactors using artificial neural networks developed with clonal selection based algorithm. *International Journal of Nonlinear Sciences and Numerical Simulation*. Available at: http://mc.manuscriptcentral.com/ijnsns.2014.0052. (Access date: 15 July 2015).

Cybenko, G., 1989. Approximation by superpositions of a sigmoidal function. *Math. Control, Signals and Systems*, 2, pp 304-314.

Davarnejad, R., Bagheripoor, E., Sahraei, A., 2012. CFD simulation of scale influence on the hydrodynamics of an internal loop airlift reactor. Engineering, 4, pp 668-674. DOI: http://dx.doi.org.10.4236/eng.2012.410085.

Dhaouadi, H. Poncin, S. Hornut, J. M. Wild, G. Oinas, P. 1996. Hydrodynamics of an airlift reactor: experiments and modeling. *Chemical Engineering Science*, 51, pp 2625-2630.

Dhaouadi, H. Poncin, S. Hornut, J. M. Wild, G. Oinas, P. Korpijarvi, J. 1997. Mass transfer in an external-loop airlift reactor: experiments and modelling. *Chemical Engineering Science*, 52 (21/22), pp 3909-3917.

Fahlman, S.E., Lebiere, C., 1989. http://papers.nips.cc/paper/207-the-cascade-correlation-learning-architecture. (Access date: 30 January 2016).

Fakhari, M.E., Moraveji, M.K., Davarnejad, R., 2014. Hydrodynamics and mass transfer of oily –micro-emulsions in an external loop airlift reactor. *Fluid Dynamics and Transport Phenomena, Chinese Journal of Chemical Engineering*, 22 (3), pp 267-273.

Finn, R.K., 1967. Agitation and aeration. In: S. Blakebrough, ed. *Biochemical and Biological Engineering Science*, Academic Press: London, pp 69-99.

Fogler, H.S. 1995. Elements of chemical reaction engineering. 2nd Ed. Prentice Hall. India.

Freitas, C. Teixeira, J.A. 1998. Hydrodynamic studies in an airlift reactor with an enlarged degassing zone. *Bioprocess Engineering*, 18, pp 267-279.

Freitas, C., Fialová, M., Zahradnik, J., Teixeira, J.A., 1999. Hydrodynamic model for three-phase internal- and external-loop airlift reactors. Chemical Engineering Science, 54, pp 5253-5258.

Gaddis, E.S., 1999. Mass transfer in gas-liquid contactors. *Chemical Engineering and Processing*, 38, pp 503 – 510.

Gajbhiye, N.K. Khadse, J.B. Dawande, S.D. 2012. Hydrodynamics of multi-stage air lift reactor (MSALR). *International Journal of Engineering Research and Technology*, 1(5), pp 1-9.

Gavrilescu, M. Tudose, R.Z. 1997b. The specific interfacial area in external-loop airlift bioreactors. *Bioprocess Engineering*, 16, 127-133.

Gavrilescu, M. Tudose, R.Z. 1998 Part 1. Hydrodynamics of non-newtonian liquids in external-loop airlift bioreactors, part 1: study of the gas holdup. *Bioprocess Engineering*, 18: 17-26.

Gavrilescu, M. Tudose, R.Z. 1998 Part 2. Hydrodynamics of non-newtonian liquids in external-loop airlift bioreactors, part 2: study of the liquid circulation velocity. *Bioprocess Engineering*, 18: 83-89.

Gavrilescu, M. Tudose, R.Z., 1997a. Mixing studies in external-loop airlift reactors. Chemical Engineering Journal, 66, pp 97-104.

Gavrilescu, M., Tudose, R.Z., 1999. Residence time distribution of the liquid phase in a concentric-tube airlift reactor. *Chemical Engineering and Processing*, 38, pp 225-238.

Geankoplis, C.J. 2009. Transport process and separation process principles. 4th Ed. Prentice Hall.

Gerlach, S.R., Siedenberg, D., Gerlach, D., Schürgerl, K., Giuseppin, M.L.F., Hunik, J., 1998. Influence of reactor systems on the morphology of Apergillus awamori. Application of neural network and cluster analysis for characterization of fungal morphology. *Process Biochemistry*, 33 (6), pp 601-615.

Gharib, J., Moraveji, M.K., Davarnejad, R., 2013. Hydrodynamics and mass transfer study of aliphatic alcohols in airlift reactors. *Chemical Engineering Research and Design*, 91, 925-932.

Ghosh, T.K., Bhattacharyya, D., Kim, T.H., 2010. To study yeast growth kinetics in a specially designed external loop airlift bioreactor. *International Journal of Bio-Science and Bio-Technology*, 2(1), pp 47-58.

Ghosh, T.K., Bhattacharyya, D., Kim, T.K., 2010. Gas holdup characteristics of an external loop airlift contactor. International Journal of Hybrid Information Technology, 3 (2), pp 25-32.

Guo, Y.X., Rathor, M.N., Ti, H.C., 1997. Hydrodynamics and mass transfer studies in a novel external loop airlift reactor. *Chemical Engineering Journal*, 67, pp 205-214.

Haykin, S. 2009. Neural Networks and Learning Machines. 3rd Edition. Pearson International Edition. Upper Saddle River, New Jersey.

Hinks, J.W. Cawte, H. Sanders, D.A. Hudson, A. Dockree, C.N. 1996. Prediction of flowrates and stability in large scale airlift reactors. *Wat. Sci. Tech*., 34(5-6), pp 51-57.

Hopfield, J.J., 1988. Artificial neural networks. IEEE Circuits and Designs Magazine, 4(5). DOI 10.1109/101.8118. http://ieeexplore.ieee.org/document/8118/?arnurber=81184tag=1 (Access date: 30 November 2016).

Hornik, K., Stinchcombe, M., White, H., 1989. Multilayer feedforward networks are universal approximators. *Neural Networks*, 2, pp 359-366.

Huang, Q., Yang, C., Yu, G., Mao, Z.S., 2010. CFD simulation of hydrodynamics and mass transfer in an internal airlift loop reactor using a steady two-fluid model. *Chemical Engineering Science*, 65, pp 5527-5536.

Jha, G.K., 2014. Artificial neural networks and its applications. Available at: https://www.researchgate.net. (Access date: 16 March 2016).

Jianping, W. Xiaoqiang, J. Guozhu, M. 2006. Local liquid side mass transfer model in airlift loop reactor and self-aspirated reversed flow jet loop reactor. *Chemical Engineering Communication*, 193, pp 417-426.

Jin, B. Van Leeuwen, J. Doelle, H.W. Yu, Q. 1999. The influence of geometry on hydrodynamic and mass transfer characteristics in an external airlift reactor for the cultivation of filamentous fungi. *World Journal of Microbiology and Biotechnology*, 15, pp 73-79.

Jones, S.T., Heindel, T.J., 2010. Hydrodynamic considerations in an external loop airlift reactor with a modified downcomer. *Ind. Eng. Chem. Res*., 49, pp 1931-1936.

Kadic, E., Heindel, T.J., 2014. An Introduction to bioreactor hydrodynamics and gas-liquid mass transfer. *John Wiley and Sons, Inc, Hoboken New Jersey*.

Kawase, Y., Hashiguchi, N., 1996. Gas-liquid mass transfer in external loop airlift columns with newtonian and non-newtonian fluids. *The Chemical Engineering Journal*, 62, pp 35-42.

Kazakis, N.A., Papdopoulos, S.V., Mouza, A.A., 2007. Bubble columns with fine pore sparger operatinig in the pseudo-homogenous regime: gas holdup prediction and a criterion for the transition to heterogeneous regime. Chemical Engineering Science, 62, pp 3092-3103.

Kemblowski, Z. Przywarski, J. Diab, A. 1993. An average gas hold-up and liquid circulation velocity in airlift reactors with external loop. *Chemical Engineering Science*, 48 (23), pp 4023-4035.

Ketheesan, B., Nirmalakhandan, N., 2011. Development of a new airlift-driven raceway reactor for algal cultivation. *Applied Energy*, 88, pp 3370-3376.

Khondee, N., Tathong, S., Pinyakong, O., Powtongsook, S., Chatchupong, T., Ruangchainikom, C., Luepromchai, E., 2012. Airlift bioreactor containing chitosan-immobilised Sphingobium sp. P2 for treatment of lubricants in wastewater. *Journal of Hazardous Materials*, 213-214, pp 466-473.

Kiambi, S.L., Kiriamiti, H.K., Kumar, A., 2011. Characterization of two phase flows in chemical engineering reactors. *Flow Measurement and Instrumentation*, 22, pp 265-271.

Kilonzo, P.M., Margaritis, A., 2004. The effects of non-Newtonian fermentation broth viscosity and small bubble segregation on oxygen mass transfer in gas-lift bioreactors: a critical review. *Biochemical Engineering Journal*, 17, pp 27-40.

Kojić, P.S., Šijački, I.M., Lukić, N.Lj., Jovičević, D.Z., Popović, S.S., 2015a. Volumetric gas-liquid mass transfer coefficient in an external-loop airlift reactor with inserted membrane. Available at: www.doiserbia.nb.rs/ft.aspx.id=1451-93721500041K. Access date: 26 October /2015.

Kojić, P.S., Tokić, M.S., Šijački, I.M., Lukić, N.Lj., Jovičević, D.Z., Popović, S.S., 2015b. Influence of the sparger type and added alcohol on the gas holdup of an external loop airlift reactor. *Chemical Engineering Technology*, 38 (4), pp 701-708.

Korpijarvi, J., Oinas, P., Reunanen, J., 1999. Hydrodynamics and mass transfer in an airlift reactor. *Chemical Engineering Science*, 54, pp 2255-2262.

Kulkarni, A.A., 2005. Effect of sparger design on the local flow field in a bubble column analysis using LDA. *Chemical Engineering Research and Design*, 83(A1), pp 59 – 66.

Kulkarni, A.V., Badgandi, S.V., Joshi, J.B., 2009. Design of ring and spider type spargers for bubble column reactor: Experimental measurements and CFD simulation of flow and weeping. *Chemical Engineering Research and Design*, 87, pp 1612 – 1630.

Kulkarni, A.V., Joshi, J.B., 2011. Design and selection of sparger for bubble column reactor. Part II: Optimum sparger type and design. *Chemical Engineering Research and Design*, 89, pp 1986 – 1995.

Laberge, C., Cluis, D., Mercier, G., 2000. Metal bioleaching prediction in continuous processing of municipal sewage with *thiobacillus ferrooxidans* using neural networks. *Water Research*, 34 (4), pp 1145 – 1156.

Law, D., 2010. *Computational modeling and simulations of hydrodynamics for air-water external loop airlift reactors*. Ph.D. Blacksburg, Virginia: Virginia Polytechnic Institute and State University.

León-Becerril, E., Cockx, A., Liné, A., 2002. Effect of bubble deformation on stability and mixing in bubble columns. *Chemical Engineering Science*, 56(21-22), pp 6135 – 6141.

Lin, J. Han, M. Wang, T. Zhang, T. Wang, J. Jin, Y. 2004. Influence of the gas distributor on the local hydrodynamic behaviour of an external loop airlift reactor. *Chemical Engineering Journal*, 102, pp 51-59.

Lu, X., Ding, J., Wang, Y., Shi, J., 2000. Comparison of the hydrodynamics and mass transfer characteristics of a modified square airlift reactor with common airlift reactors. *Chemical Engineering Science*, 55, pp 2257-2263.

Luo, H. Al-Dahhan, M. H. 2011. Verification and validation of CFD simulations for local flow dynamics in a draft tube airlift bioreactor. *Chemical Engineering Science*, 66, pp 907-923.

Luo, H. Al-Dahhan, M. H. 2008. Local characteristics of hydrodynamics in draft tube airlift bioreactor. *Chemical Engineering Science*, 63, pp 3057-3068.

Luo, L. Liu, F. Xu, Y. Yaun, J. 2011. Hydrodynamics and mass transfer characteristics in an internal loop airlift reactor with different spargers. *Chemical Engineering Journal*, 175, pp 494-504.

Luo, L., Yuan, J., Xie, P., Sun, J., Guo, W., 2013. Hydrodynamics and mass transfer characteristics in an internal loop airlift reactor with sieve plates. *Chemical Engineering Research and Design*, 91, pp 2377-2388.

Manipura, A., Barbosa, V.L., Burgess, J.E., 2007. Comparison of biological ammonium removal from synthetic metal refinery wastewater using three different types of reactor. *Minerals Engineering*, 20, pp 617-620.

Manjo, P.Y., 2014. *Fundamental approach to predicting mass transfer coefficients in bubble column reactors*. MSc. Cape Town: University of Cape Town, South Africa.

Martínez, A. M. M. Silva, E. M. E., 2013. *Airlift bioreactors: hydrodynamics and rheology application to secondary metabolites production* (online). Available at: http://dx.doi.org/10.5772/53711. Access date: 22 January 2014.

Merchuk, J., 1986a. Gas holdup and liquid velocity in a two dimensional air lift reactor. *Chemical Engineering Science*, 41 (1), pp 11-16.

Merchuk, J.C, Gluz, M. 2002. Airlift Reactors. In: *Encyclopedia of Bioprocess Technology* 320-353. M. C. Flickinger and S. W. Drew eds. John Wiley & Sons, New York. http://www.bioreactorsciences.com/uploads/1/8/5/9/18594674/bioreactors_air-lift_reactors_merchuk_gluz.pdf. Access date: 24 November 2016.

Merchuk, J.C., 1986b. Hydrodynamics and holdup in airlift reactors. In: *Encyclopedia of Fluid Mechanics, Gas-Liquid flows*, 3, pp 1485-1511. Cheremisinoff, N.P., Ed. Gulf Publishing Company.

Merchuk, J.C., Stein, Y., 1981. Local holdup and liquid velocity in airlift reactors. *AIChE Journal*, 27 (3), pp 377-388.

Mi, Y. Ishii, M. Tsoukalas, L. H. 2001. Flow regime identification methodology with neural networks and two-phase flow models. *Nuclear Engineering and Design*, 204, pp 87-100.

Mohanty, K., Das, D., Biswas, M.N., 2008. Treatment of phenolic wastewater in a novel multi-stage external loop airlift reactor using activated carbon. *Separation and Purification Technology*, 58, pp 311-319.

Moraveji, M. K. 2012. Hydrodynamic analysis of a concentric draft tube airlift reactor using computational fluid dynamics. *Middle-East Journal of Scientific Research*, 12 (10), pp 1420-1425.

Moraveji, M.K., Mohsenzadeh, E., Fakhari, M.E., 2012. Effects of surface active agents on hydrodynamics and mass transfer characteristics in a split-cylinder airlift bioreactor with packed bed. *Chemical Engineering Research and Design*, 90, pp 899-905.

Morris, A.J., Montague, G.A., Willis, M.J., 1994. Artificial neural networks: studies in process modeling and control. *Chemical Engineering Research and Design*, 72a, pp 3-19.

Moutafchieva, D., Popova, D., Dimitrova, M., Tchaoushev, S., 2013. Experimental determination of the volumetric mass transfer coefficient. *Journal of Chemical Technology and Metallurgy*, 48, pp 351-356.

Mouza, A.A., Dalakoglou, G.K., Paras, S.V., 2005. Effect of liquid properties on the performance of bubble column reactors with fine pore spargers. *Chemical Engineering Science*, 60(50), pp 1465-1475.

Mudde, R.F., Van Den Akker, H.E.A., 2001. 2D and 3D simulations of an internal airlift loop reactor on the basis of a two-fluid model. *Chemical Engineering Science*, 56, pp 6351-6358.

Nakao, K., Suenaga, S., Takeda, K., Kimura, M., Robinson, C.W., 1988. Mass transfer in a bubble column with external liquid circulation. *First German-Japanese Symposium Bubble Columns*, Schwerte, Germany, pp 153-158.

Naveen Prasad, B.S., Velan, M., 2009. Mass transfer studies on external loop airlift reactor. *International Journal on Applied Bioengineering*, 4 (2), pp 21 – 25.

Nayager, K., Govender C., 2016. Modelling of Mass Transfer Characteristics of a Two-Phase External Loop Airlift Reactor. *Laboratory Project: University of KwaZulu Natal*.

Nikakhtari, H., Hill, G.A., 2005. Hydrodynamic and oxygen mass transfer in an external loop airlift bioreactor with a packed bed. *Biochemical Engineering Journal*, 27, pp 138-145.

Pauck, W.J., 2011. *Neural network modeling and prediction of the flotation deinking behaviour of complex recycled paper mixes*. Ph.D. Durban: University of KwaZulu Natal.

Poutousi, M., Sahu, J.N., Ganesan, P., Shamshirband, S., Redzwan, G., 2015. A combination of computational fluid dynamics (CFD) and adaptive neuro-fuzzy system (ANFIS) for prediction of the bubble column hydrodynamics. *Powder Technology*, 274, pp 466-481.

Rahman-Al Ezzi, A.A., Najmuldeen, G.F., 2013. The effects of superficial gas velocity and liquid phase properties on gas holdup and mass transfer in an airlift reactor. *American Journal of Engineering Research*, 02 (11), pp 25-32.

Rajarajan, J., Pollard, D., Ison, A.P., Shamlou, P.A., 1996. Gas holdup and liquid velocity in airlift bioreactors containing viscous newtonian liquids. *Bioprocess Engineering*, 14, pp 311-315.

Reisener, J., Reuter, M.A., Krüger, J., 1993. Modelling of the mass transfer in gas sparged electrolysers with neural nets. *Chemical Engineering Science*, 48 (6), pp 1089 – 1101.

Rengel, A., Zoughaib, A., Dron, D., Clodic, D., 2012. Hydrodynamic study of an internal airlift reactor for microalgae culture. *Applied Microbiol Biotechnology*, 93, pp 117-129.

Rihani, R. Guerri, O. Legrand, J. 2011. Three dimensional CFD simulations of gas-liquid flow in milli torus reactor without agitation. *Chemical Engineering and Processing: Process Intensification*, 50, pp 369-376.

Roy, S., Dhotre, M.T., Joshi, J.B., 2006. CFD simulation of flow and axial dispersion in external loop airlift reactor. *Chemical Engineering Research and Design*, 84(A8), pp 677 – 690

Ruff, K., Pilhofer, T., Mersmann, A., 1978. Ensuring flow through all the openings of perforated plates for fluid dispersion. *International Journal of Chemical Engineering*, 18, pp 395 – 401.

Salehi, M. A. Amanifard, N. Mirnezami, Z. 2011. Experimental study of geometrical effects with internal loop on gas hold up and flow pattern in gas-liquid bubble column reactor. *Australian Journal of Basic and Applied Sciences*, 5(9), pp 1514-1516.

Sánchez Mirón, A. Cerón Garcia, M.C. Garcia Camacho, F. Molina Grima, E. Chisti, Y. 2004. Mixing in bubble column and airlift reactors. *Chemical Engineering Research and Design*, 82(A), pp 1367-1374.

Sánchez Mirón, A., Cerón Garcia, M.C., Contreras Gómez, A., Garcia Camacho, F., Molina Grima, E. Chisti, Y. 2003. Shear stress tolerance and biochemical characterization of Phaeodactylum tricornutum in a quasi steady-state continuous culture in outdoor photobioreactors. Biochemical Engineering Journal, 16, pp 287-297.

Schürgerl, K, Lübbert, A. 1995. Pneumatically Agitated Bioreactors. In: *Bioreactor Design System* 257-303. J. A. Asenjo and J. C. Merchuk eds. Marcel Dekker Inc., New York.

Shariati, F.P., Bonakdarpour, B., Mehrnia, M.R., 2007. Hydrodynamics and oxygen transfer behaviour of water in diesel microemulsions in a draft tube airlift bioreactor. *Chemical Engineering and Processing*, 46, pp 334-342.

Shimizu, K., Takada, S., Takahashi, T., Yoshinori, K., 2001. Phenomenological simulation model for gas hold-ups and volumetric mass transfer coefficients in external-loop airlift reactors. *Chemical Engineering Journal*, 84, pp 599-603.

Šijački, I.M., Radmilo, R.C., Milenko, S.T., Kojič, P.S., 2009. Simple correlation for bubble columns and draft tube airlift reactors with dilute alcohol solutions. *BIBLID*, 40, pp 183-192. DOI: 10.2298/APT0940183S.

Šimičík, M. Mota, A. Ruzicka, M. C. Vicente, A. Teixeira, J. 2011. CFD simulation and experimental measurement of gas holdup and liquid interstitial velocity in internal loop airlift reactor. *Chemical Engineering Science*, 66: 3268-3279.

Sivasubramanian, V., Naveen Prasad, B.S., 2009. Effects of superficial gas velocity and fluid property on the hydrodynamic performance of an airlift column with alcohol solution. *International Journal of Engineering, Science and Technology*, 1 (1), pp 245-253.

Sivasubramanian, V., Naveen Prasad, B.S., Velan, M., 2008. Mass transfer studies in an external loop airlift bioreactor for wastewater treatment. Available at: https://www.researchgate.net/publication/259173848. Access date: February 2016.

Snape, J. B. Zahradník, J. Fialová, M. Thomas, N. H., 1995. Liquid-phase properties and sparger design effects in an external-loop airlift reactor. *Chemical Engineering Science*, 50 (20), pp 3175-3186.

Somnath, N., Someshwar, J.J., 2015. Hydrodynamics of pilot plant scale airlift reactor in presence of alcohols. Polish Journal of Chemical Technology, 17 (3), pp 118-123.

Studley, A. F., 2010. *Numerical modelling of air-water flows in bubble columns and airlift reactors.* M. Sc. (Mechanical Engineering). Blacksburg, Virgina: Virginia Polytechnic Institute and State University.

Talvy, S. Cockx, A. Line, A. 2005. Global modelling of a gas-liquid-solid airlift reactor. *Chemical Engineering Science*, 60, pp 5991-6003.

Tarassenko, L., 1998. *A guide to neural computing applications*. London: Arnold.

Van Baten, J. M. Ellenberger, J. Krishna, R. 2003. Hydrodynamics of internal air-lift reactors: experiments versus CFD simulations. *Chemical Engineering and Processing*, 42, pp 733-742.

Van Baten, J.M., Krishna, R., 2003. Comparison of hydrodynamics and mass transfer in airlift and bubble column reactors using CFD. *Chemical Engineering Technology*, 26, pp 1074-1079.

Venkatachalam, S. Palaniappan, A. Kandasamy, S. Kandasamy, K. 2011. Prediction of gas hold-up in a combined loop air lift fluidized bed reactor using newtonian and non-newtonian liquids. *Chem. Ind. Chem. Eng.*, 17(3), pp 375-383.

Vial, C. Poncin, S. Wild, G. Midoux, N. 2001. A simple method for regime identification and flow characterisation in bubble columns and airlift reactors. *Chemical Engineering and Processing*, 40, pp 135-151.

Vial, C., Camarasa, E., Poncin, S., Wild, G., Midoux, N., Bouillard, J., 2000. Study of hydrodynamic behaviour in bubble columns and external loop airlift reactors through analysis of pressure fluctuations. *Chemical Engineering Science*, 55, pp2957-2973.

Vial, Ch., Poncin, S., Wild, G., Midoux, N., 2002. Experimental and theoretical analysis of the hydrodynamics in the riser of an external loop airlift reactor. *Chemical Engineering Science*, 57, pp 4745-4762.

Viswanathan, K. 1986. Flow Patterns in bubble columns. In: Cheremisinoff, N. Ed. *Encyclopaedia of fluid mechanics.* Vol. 3: Gas liquid flows, pp 1180-1215.

Wang, F. Yang, F. Zhang, X. Lui, Y. Zhang, H. Zhou, J. 2005. Effects of cycle time on properties of aerobic granules in sequencing batch airlift reactors. *World Journal of Microbiology and Biotechnology*, 21, pp 1379-1384.

Wang, S., Arimatsu, Y., Koumatsu, K., Furumoto, K., Yoshimoto, M., Fukunaga, K., Nakao, K., 2003. Gas holdup, liquid circulating velocity and mass transfer properties in a mini-scale external loop airlift bubble column. *Chemical Engineering Science*, 58, pp 3353-3360.

Whitman, W.G., 1923. The two-film theory of gas absorption. *Chemical and metallurgical engineering*, 29 (4), pp 1460–148. Available at: http://www.chemeng.in.coocan.jp/CR/WhitmanCME1923.pdf. Access date: 17 August 2015.

Wilke, C.R. and Chang, P., 1955. Correlation of diffusion coefficients in dilute solutions. *Journal of the American Institute of Chemical Engineers*, 1, pp 264-270.

Xianling, L., Jianping, W., Qing, Y., Xueming, Z., 2005. The pilot study for oil refinery waste water treatment using a gas-liquid-solid three phase flow airlift loop bioreactor. *Biochemical Engineering Journal*, 27, pp 40-44.

Xu, L., Liu, R., Wang, F., Liu, C.Z., 2012. Development of a draft tube airlift bioreactor for Botryococcus braunii with an optimized inner structure using computational fluid dynamics. *Bioresource Technology*. DOI: http://dx.doi.org/10.1016/j.biortech.2012.05.123. Access date: 21 March 2015.

Yan, C. Lu, C. Fan, Y. Cao, R. Lui, Y. 2011. Experiments and simulations of gas-solid flow in an airlift loop reactor. *Particuology*, 9, pp 130-138.

Yan, C. Lu, C. Zhang, Y. Wang, D. Liu, M. 2010. Profiles of solid fraction and heterogeneous phase structure in a gas-solid airlift loop reactor. *Chemical Engineering Science*, 65, pp 2707-2726.

Yazdani, A., 2007. Hydrodynamic behaviour of bubble column with oily solutions. MSc. Thesis, University of Tehran, Iran.

Yazdian, F. Shojaosadati, S. A. Nosrati, M. Pesaran Hajiabbas, M. Vasheghani-Farahani, E. 2009. Investigation of gas properties, design and operational parameters on hydrodynamic characteristics, mass transfer, and biomass production from natural gas in an external airlift loop bioreactor. *Chemical Engineering Science*, 64: 2455-2465.

Zhang, G., Patuwo, B.E., Hu, M.Y., 1998. Forecasting with artificial neural networks: the state of the art. *International Journal of Forecasting*, 14, pp 35-62.

Zhang, T., Wei, C., Feng, C., Zhu, J., 2012. A novel airlift reactor enhanced by funnel internals and hydrodynamics prediction by the CFD method. *Bioresource Technology*, 104, pp 600-607.

Zuber,N., Findlay, J.A., 1965. Average volumetric concentration in two-phase flow systems. American Journal of Mechanical Engineers, 87 (4), pp 453-468.

APPENDIX

APPENDIX A1 – NEURAL NETWORK MODEL INPUTS AND PREDICTIONS

SPARGER TYPE	SPARGER PORE SIZE	D_R	D_D	A_D/A_R	H_R	H_D	H_R/D_R	h_L	ρ	σ	μ	BS_R	BS_D	BFP	U_{SGR}	U_{SLD}	ε_R	ε_D	k_La_L (EXP)	k_La_L (PRED)	FLAGS
A	L	0.15	0.1	0.44	3	3	19.67	3.4	997.05	72	1.08	S	NONE	G	0.019	0.507	0.038	0.004	0.008	0.008	____V
A	L	0.15	0.1	0.44	3	3	19.67	3.4	997.05	72	1.08	S	NONE	G	0.021	0.517	0.043	0.004	0.009	0.008	AWT__
A	L	0.15	0.1	0.44	3	3	19.67	3.4	997.05	72	1.08	S	NONE	G	0.023	0.560	0.047	0.004	0.008	0.008	AW_S_
A	L	0.15	0.1	0.44	3	3	19.67	3.4	997.05	72	1.08	S	NONE	G	0.026	0.574	0.049	0.005	0.008	0.008	AWT__
A	L	0.15	0.1	0.44	3	3	19.67	3.4	997.05	72	1.08	S	NONE	G	0.029	0.600	0.055	0.004	0.007	0.008	AWT__
A	L	0.15	0.1	0.44	3	3	19.67	3.4	997.05	72	1.08	S	NONE	G	0.031	0.618	0.055	0.006	0.009	0.008	____V
A	L	0.15	0.1	0.44	3	3	19.67	3.4	997.05	72	1.08	S	NONE	G	0.033	0.662	0.065	0.006	0.010	0.008	AWT__
A	L	0.15	0.1	0.44	3	3	19.67	3.4	997.05	72	1.08	S	S	G	0.035	0.661	0.063	0.006	0.008	0.008	AWT__
A	L	0.15	0.1	0.44	3	3	19.67	3.4	997.05	72	1.08	SML	S	A	0.038	0.684	0.067	0.006	0.008	0.008	AWT__
A	L	0.15	0.1	0.44	3	3	19.67	3.4	997.05	72	1.08	SML	S	A	0.040	0.693	0.071	0.006	0.009	0.009	AWT__
A	L	0.15	0.1	0.44	3	3	19.67	3.4	997.05	72	1.08	SML	S	A	0.044	0.728	0.076	0.007	0.011	0.010	AW_S_
A	L	0.15	0.1	0.44	3	3	19.67	3.4	997.05	72	1.08	SML	S	A	0.048	0.759	0.083	0.008	0.013	0.010	AW_S_
A	L	0.15	0.1	0.44	3	3	19.67	3.4	997.05	72	1.08	SML	S	P	0.050	0.765	0.083	0.007	0.015	0.011	____V
A	L	0.15	0.1	0.44	3	3	19.67	3.4	997.05	72	1.08	SML	S	P	0.052	0.828	0.093	0.008	0.017	0.011	AW_S_
A	L	0.15	0.1	0.44	3	3	19.67	3.4	997.05	72	1.08	SML	S	P	0.054	0.796	0.092	0.008	0.013	0.012	AWT__
A	L	0.15	0.1	0.44	3	3	19.67	3.4	997.05	72	1.08	SML	S	P	0.058	0.840	0.098	0.008	0.010	0.012	AW_S_
A	L	0.15	0.1	0.44	3	3	19.67	3.4	997.05	72	1.08	SML	S	P	0.059	0.829	0.097	0.010	0.012	0.013	AWT__
A	L	0.15	0.1	0.44	3	3	19.67	3.4	997.05	72	1.08	SML	S	P	0.061	0.849	0.101	0.010	0.014	0.013	AW_S_
A	L	0.15	0.1	0.44	3	3	19.67	3.4	997.05	72	1.08	SML	S	P	0.064	0.867	0.107	0.010	0.017	0.013	____V
A	L	0.15	0.1	0.44	3	3	19.67	3.4	997.05	72	1.08	SML	S	P	0.068	0.899	0.108	0.010	0.015	0.014	AWT__
A	L	0.15	0.1	0.44	3	3	19.67	3.4	997.05	72	1.08	SML	S	VP	0.076	0.956	0.125	0.011	0.014	0.016	AW_S_
C	L	0.15	0.1	0.44	3	3	19.67	3.4	997.05	72	1.08	S	S	G	0.019	0.682	0.028	0.006	0.004	0.005	____V
C	L	0.15	0.1	0.44	3	3	19.67	3.4	997.05	72	1.08	S	S	G	0.021	0.681	0.029	0.006	0.004	0.006	AW_S_
C	L	0.15	0.1	0.44	3	3	19.67	3.4	997.05	72	1.08	S	S	G	0.024	0.723	0.023	0.003	0.005	0.005	AWT__

C	L	0.15	0.1	0.44	3	3	19.67	3.4	997.05	72	1.08	SML	S	G	0.028	0.811	0.038	0.009	0.006	0.006	AW_S_
C	L	0.15	0.1	0.44	3	3	19.67	3.4	997.05	72	1.08	SML	S	G	0.030	0.795	0.040	0.006	0.005	0.006	AWT__
C	L	0.15	0.1	0.44	3	3	19.67	3.4	997.05	72	1.08	SML	S	G	0.033	0.862	0.042	0.009	0.006	0.006	AWT__
C	L	0.15	0.1	0.44	3	3	19.67	3.4	997.05	72	1.08	SML	S	A	0.035	0.844	0.044	0.008	0.006	0.006	AWT__
C	L	0.15	0.1	0.44	3	3	19.67	3.4	997.05	72	1.08	SML	S	A	0.038	0.913	0.047	0.010	0.008	0.007	AWT__
C	L	0.15	0.1	0.44	3	3	19.67	3.4	997.05	72	1.08	SML	S	A	0.042	0.959	0.052	0.011	0.007	0.008	____V
C	L	0.15	0.1	0.44	3	3	19.67	3.4	997.05	72	1.08	SML	S	A	0.044	0.928	0.052	0.008	0.009	0.008	____V
C	L	0.15	0.1	0.44	3	3	19.67	3.4	997.05	72	1.08	SML	S	A	0.050	0.970	0.057	0.010	0.010	0.009	AWT__
C	L	0.15	0.1	0.44	3	3	19.67	3.4	997.05	72	1.08	SML	S	P	0.054	1.006	0.062	0.012	0.009	0.009	AWT__
C	L	0.15	0.1	0.44	3	3	19.67	3.4	997.05	72	1.08	SML	S	P	0.066	1.143	0.075	0.013	0.013	0.012	AWT__
C	L	0.15	0.1	0.44	3	3	19.67	3.4	997.05	72	1.08	SML	S	VP	0.076	1.210	0.087	0.016	0.014	0.015	____V
B	L	0.15	0.1	0.44	3	3	19.67	3.4	997.05	72	1.08	S	S	G	0.019	0.632	0.030	0.005	0.006	0.006	AW_S_
B	L	0.15	0.1	0.44	3	3	19.67	3.4	997.05	72	1.08	S	S	G	0.021	0.646	0.031	0.006	0.007	0.007	AW_S_
B	L	0.15	0.1	0.44	3	3	19.67	3.4	997.05	72	1.08	SM	S	G	0.024	0.708	0.034	0.006	0.008	0.007	AW_S_
B	L	0.15	0.1	0.44	3	3	19.67	3.4	997.05	72	1.08	SM	S	G	0.026	0.698	0.037	0.007	0.008	0.008	AWT__
B	L	0.15	0.1	0.44	3	3	19.67	3.4	997.05	72	1.08	SM	S	G	0.029	0.758	0.041	0.007	0.007	0.008	AW_S_
B	L	0.15	0.1	0.44	3	3	19.67	3.4	997.05	72	1.08	SM	S	G	0.031	0.740	0.041	0.008	0.009	0.008	AWT__
B	L	0.15	0.1	0.44	3	3	19.67	3.4	997.05	72	1.08	SM	S	G	0.034	0.812	0.043	0.008	0.009	0.009	AWT__
B	L	0.15	0.1	0.44	3	3	19.67	3.4	997.05	72	1.08	SM	S	A	0.036	0.782	0.044	0.009	0.009	0.009	AWT__
B	L	0.15	0.1	0.44	3	3	19.67	3.4	997.05	72	1.08	SM	S	A	0.038	0.856	0.048	0.009	0.008	0.009	AWT__
B	L	0.15	0.1	0.44	3	3	19.67	3.4	997.05	72	1.08	SM	S	A	0.040	0.810	0.052	0.010	0.009	0.009	AW_S_
B	L	0.15	0.1	0.44	3	3	19.67	3.4	997.05	72	1.08	SML	S	P	0.042	0.891	0.055	0.010	0.010	0.009	AWT__
B	L	0.15	0.1	0.44	3	3	19.67	3.4	997.05	72	1.08	SML	S	P	0.045	0.856	0.056	0.011	0.009	0.010	AW_S_
B	L	0.15	0.1	0.44	3	3	19.67	3.4	997.05	72	1.08	SML	S	P	0.047	0.940	0.057	0.011	0.010	0.010	AWT__
B	L	0.15	0.1	0.44	3	3	19.67	3.4	997.05	72	1.08	SML	S	P	0.052	0.975	0.062	0.012	0.008	0.011	AWT__
B	L	0.15	0.1	0.44	3	3	19.67	3.4	997.05	72	1.08	SML	S	P	0.054	0.932	0.063	0.013	0.011	0.011	AW_S_
B	L	0.15	0.1	0.44	3	3	19.67	3.4	997.05	72	1.08	SML	S	P	0.057	1.020	0.065	0.013	0.013	0.011	AW_S_
B	L	0.15	0.1	0.44	3	3	19.67	3.4	997.05	72	1.08	SML	S	P	0.059	0.996	0.071	0.013	0.011	0.012	AWT__
B	L	0.15	0.1	0.44	3	3	19.67	3.4	997.05	72	1.08	SML	S	P	0.061	0.919	0.071	0.013	0.011	0.012	AWT__

B	L	0.15	0.1	0.44	3	3	19.67	3.4	997.05	72	1.08	SML	S	P	0.064	0.924	0.074	0.014	0.012	0.012	AWT__
B	L	0.15	0.1	0.44	3	3	19.67	3.4	997.05	72	1.08	SML	S	P	0.066	1.081	0.076	0.014	0.014	0.012	AWT__
B	L	0.15	0.1	0.44	3	3	19.67	3.4	997.05	72	1.08	SML	S	VP	0.076	1.192	0.088	0.017	0.017	0.015	AWT__
A	L	0.15	0.2	1	3	3	19.67	3.4	997.05	72	1.08	S	S	G	0.019	0.268	0.041	0.001	0.008	0.006	____V
A	L	0.15	0.2	1	3	3	19.67	3.4	997.05	72	1.08	S	S	G	0.021	0.286	0.042	0.001	0.006	0.007	AWT__
A	L	0.15	0.2	1	3	3	19.67	3.4	997.05	72	1.08	S	S	G	0.024	0.303	0.051	0.001	0.007	0.007	AWT__
A	L	0.15	0.2	1	3	3	19.67	3.4	997.05	72	1.08	S	S	G	0.026	0.310	0.051	0.001	0.008	0.007	AWT__
A	L	0.15	0.2	1	3	3	19.67	3.4	997.05	72	1.08	S	S	G	0.028	0.333	0.055	0.001	0.008	0.008	____V
A	L	0.15	0.2	1	3	3	19.67	3.4	997.05	72	1.08	S	S	G	0.031	0.321	0.059	0.001	0.008	0.008	AW_S_
A	L	0.15	0.2	1	3	3	19.67	3.4	997.05	72	1.08	S	S	G	0.033	0.352	0.067	0.001	0.009	0.008	AWT__
A	L	0.15	0.2	1	3	3	19.67	3.4	997.05	72	1.08	S	S	G	0.035	0.364	0.067	0.002	0.006	0.008	AWT__
A	L	0.15	0.2	1	3	3	19.67	3.4	997.05	72	1.08	SML	S	G	0.038	0.381	0.071	0.001	0.007	0.008	AWT__
A	L	0.15	0.2	1	3	3	19.67	3.4	997.05	72	1.08	SML	S	G	0.040	0.393	0.076	0.002	0.008	0.009	AWT__
A	L	0.15	0.2	1	3	3	19.67	3.4	997.05	72	1.08	SML	S	A	0.043	0.406	0.084	0.002	0.011	0.010	AWT__
A	L	0.15	0.2	1	3	3	19.67	3.4	997.05	72	1.08	SML	S	A	0.048	0.419	0.086	0.003	0.013	0.011	____V
A	L	0.15	0.2	1	3	3	19.67	3.4	997.05	72	1.08	SML	S	A	0.050	0.428	0.091	0.003	0.008	0.011	AW_S_
A	L	0.15	0.2	1	3	3	19.67	3.4	997.05	72	1.08	SML	S	P	0.052	0.442	0.101	0.002	0.014	0.013	AWT__
A	L	0.15	0.2	1	3	3	19.67	3.4	997.05	72	1.08	SML	S	P	0.054	0.428	0.092	0.003	0.014	0.013	AWT__
A	L	0.15	0.2	1	3	3	19.67	3.4	997.05	72	1.08	SML	S	P	0.057	0.453	0.120	0.003	0.014	0.014	AWT__
A	L	0.15	0.2	1	3	3	19.67	3.4	997.05	72	1.08	SML	S	P	0.059	0.469	0.110	0.003	0.014	0.014	AWT__
A	L	0.15	0.2	1	3	3	19.67	3.4	997.05	72	1.08	SML	S	P	0.061	0.471	0.113	0.003	0.014	0.014	AW_S_
A	L	0.15	0.2	1	3	3	19.67	3.4	997.05	72	1.08	SML	S	P	0.064	0.488	0.117	0.003	0.015	0.015	AWT__
A	L	0.15	0.2	1	3	3	19.67	3.4	997.05	72	1.08	SML	S	P	0.067	0.492	0.120	0.003	0.016	0.015	AWT__
A	L	0.15	0.2	1	3	3	19.67	3.4	997.05	72	1.08	SML	S	VP	0.075	0.521	0.142	0.003	0.017	0.017	AWT__
B	L	0.15	0.2	1	3	3	19.67	3.4	997.05	72	1.08	S	S	G	0.019	0.412	0.026	0.001	0.007	0.006	AW_S_
B	L	0.15	0.2	1	3	3	19.67	3.4	997.05	72	1.08	S	S	G	0.021	0.428	0.026	0.002	0.009	0.007	AWT__
B	L	0.15	0.2	1	3	3	19.67	3.4	997.05	72	1.08	S	S	G	0.023	0.456	0.031	0.002	0.008	0.007	AW_S_
B	L	0.15	0.2	1	3	3	19.67	3.4	997.05	72	1.08	S	S	G	0.026	0.469	0.031	0.002	0.008	0.007	____V
B	L	0.15	0.2	1	3	3	19.67	3.4	997.05	72	1.08	S	S	G	0.029	0.495	0.037	0.003	0.006	0.007	AW_S_

B	L	0.15	0.2	1	3	3	19.67	3.4	997.05	72	1.08	S	S	G	0.030	0.505	0.034	0.003	0.007	0.007	____V
B	L	0.15	0.2	1	3	3	19.67	3.4	997.05	72	1.08	S	S	G	0.033	0.526	0.041	0.003	0.006	0.007	AWT__
B	L	0.15	0.2	1	3	3	19.67	3.4	997.05	72	1.08	S	S	G	0.035	0.543	0.040	0.003	0.009	0.007	AW_S_
B	L	0.15	0.2	1	3	3	19.67	3.4	997.05	72	1.08	SML	S	G	0.038	0.560	0.046	0.003	0.008	0.008	____V
B	L	0.15	0.2	1	3	3	19.67	3.4	997.05	72	1.08	SML	S	G	0.043	0.597	0.050	0.003	0.010	0.009	AW_S_
B	L	0.15	0.2	1	3	3	19.67	3.4	997.05	72	1.08	SML	S	G	0.044	0.605	0.050	0.005	0.011	0.010	AWT__
B	L	0.15	0.2	1	3	3	19.67	3.4	997.05	72	1.08	SML	S	A	0.048	0.626	0.055	0.004	0.009	0.010	AW_S_
B	L	0.15	0.2	1	3	3	19.67	3.4	997.05	72	1.08	SML	S	A	0.049	0.645	0.053	0.005	0.010	0.010	AWT__
B	L	0.15	0.2	1	3	3	19.67	3.4	997.05	72	1.08	SML	S	A	0.053	0.655	0.061	0.004	0.012	0.011	AWT__
B	L	0.15	0.2	1	3	3	19.67	3.4	997.05	72	1.08	SML	S	P	0.054	0.677	0.060	0.005	0.012	0.011	____V
B	L	0.15	0.2	1	3	3	19.67	3.4	997.05	72	1.08	SML	S	P	0.057	0.685	0.065	0.005	0.014	0.012	____V
B	L	0.15	0.2	1	3	3	19.67	3.4	997.05	72	1.08	SML	S	P	0.059	0.712	0.063	0.005	0.012	0.012	AW_S_
B	L	0.15	0.2	1	3	3	19.67	3.4	997.05	72	1.08	SML	S	P	0.061	0.711	0.065	0.006	0.011	0.012	AWT__
B	L	0.15	0.2	1	3	3	19.67	3.4	997.05	72	1.08	SML	S	P	0.065	0.717	0.066	0.006	0.012	0.013	AW_S_
B	L	0.15	0.2	1	3	3	19.67	3.4	997.05	72	1.08	SML	S	P	0.066	0.746	0.076	0.005	0.017	0.013	AW_S_
B	L	0.15	0.2	1	3	3	19.67	3.4	997.05	72	1.08	SML	S	VP	0.074	0.751	0.089	0.007	0.014	0.015	AWT__
C	L	0.15	0.2	1	3	3	19.67	3.4	997.05	72	1.08	S	S	G	0.019	0.499	0.021	0.002	0.004	0.004	AWT__
C	L	0.15	0.2	1	3	3	19.67	3.4	997.05	72	1.08	S	S	G	0.021	0.508	0.020	0.003	0.005	0.005	AW_S_
C	L	0.15	0.2	1	3	3	19.67	3.4	997.05	72	1.08	S	S	G	0.023	0.544	0.023	0.003	0.004	0.005	AW_S_
C	L	0.15	0.2	1	3	3	19.67	3.4	997.05	72	1.08	S	S	G	0.025	0.556	0.023	0.003	0.006	0.005	AW_S_
C	L	0.15	0.2	1	3	3	19.67	3.4	997.05	72	1.08	S	S	G	0.029	0.592	0.028	0.002	0.006	0.005	AWT__
C	L	0.15	0.2	1	3	3	19.67	3.4	997.05	72	1.08	S	S	G	0.031	0.599	0.026	0.004	0.006	0.006	____V
C	L	0.15	0.2	1	3	3	19.67	3.4	997.05	72	1.08	S	S	G	0.034	0.634	0.031	0.004	0.007	0.006	AWT__
C	L	0.15	0.2	1	3	3	19.67	3.4	997.05	72	1.08	SML	S	G	0.038	0.672	0.034	0.005	0.006	0.006	AWT__
C	L	0.15	0.2	1	3	3	19.67	3.4	997.05	72	1.08	SML	S	G	0.040	0.676	0.033	0.005	0.008	0.007	AWT__
C	L	0.15	0.2	1	3	3	19.67	3.4	997.05	72	1.08	SML	S	G	0.044	0.709	0.040	0.004	0.008	0.007	AWT__
C	L	0.15	0.2	1	3	3	19.67	3.4	997.05	72	1.08	SML	S	A	0.045	0.706	0.037	0.005	0.007	0.007	AWT__
C	L	0.15	0.2	1	3	3	19.67	3.4	997.05	72	1.08	SML	S	A	0.047	0.733	0.042	0.005	0.008	0.007	AWT__
C	L	0.15	0.2	1	3	3	19.67	3.4	997.05	72	1.08	SML	S	A	0.049	0.744	0.041	0.006	0.008	0.008	AW_S_

C	L	0.15	0.2	1	3	3	19.67	3.4	997.05	72	1.08	SML	S	A	0.052	0.774	0.047	0.006	0.007	0.008	AWT__
C	L	0.15	0.2	1	3	3	19.67	3.4	997.05	72	1.08	SML	S	P	0.054	0.773	0.045	0.006	0.008	0.008	AWT__
C	L	0.15	0.2	1	3	3	19.67	3.4	997.05	72	1.08	SML	S	P	0.057	0.802	0.049	0.006	0.007	0.009	AWT__
C	L	0.15	0.2	1	3	3	19.67	3.4	997.05	72	1.08	SML	S	P	0.059	0.809	0.047	0.007	0.009	0.009	AWT__
C	L	0.15	0.2	1	3	3	19.67	3.4	997.05	72	1.08	SML	S	P	0.061	0.832	0.056	0.007	0.011	0.010	AWT__
C	L	0.15	0.2	1	3	3	19.67	3.4	997.05	72	1.08	SML	S	P	0.064	0.846	0.052	0.008	0.011	0.011	AW_S_
C	L	0.15	0.2	1	3	3	19.67	3.4	997.05	72	1.08	SML	S	P	0.066	0.866	0.053	0.008	0.012	0.011	AWT__
C	L	0.15	0.2	1	3	3	19.67	3.4	997.05	72	1.08	SML	S	VP	0.076	0.940	0.069	0.009	0.018	0.014	AWT__
A	S	0.23	0.2	1	5.4	5.4	24	5.8	997.05	72	1.08	S	S	G	0.014	0.365	0.026	0.000	0.007	0.006	AWT__
A	S	0.23	0.2	1	5.4	5.4	24	5.8	997.05	72	1.08	S	S	G	0.018	0.431	0.032	0.001	0.009	0.010	AWT__
A	S	0.23	0.2	1	5.4	5.4	24	5.8	997.05	72	1.08	S	S	G	0.023	0.470	0.041	0.001	0.010	0.011	AWT__
A	S	0.23	0.2	1	5.4	5.4	24	5.8	997.05	72	1.08	S	S	G	0.027	0.508	0.050	0.001	0.012	0.012	AWT__
A	S	0.23	0.2	1	5.4	5.4	24	5.8	997.05	72	1.08	S	S	G	0.032	0.544	0.061	0.002	0.013	0.015	AWT__
A	S	0.23	0.2	1	5.4	5.4	24	5.8	997.05	72	1.08	S	S	G	0.036	0.568	0.068	0.002	0.017	0.017	AWT__
A	S	0.23	0.2	1	5.4	5.4	24	5.8	997.05	72	1.08	S	S	G	0.041	0.600	0.074	0.002	0.018	0.019	AW_S_
A	S	0.23	0.2	1	5.4	5.4	24	5.8	997.05	72	1.08	SML	S	G	0.045	0.607	0.076	0.002	0.020	0.019	____V
A	S	0.23	0.2	1	5.4	5.4	24	5.8	997.05	72	1.08	SML	S	P	0.050	0.646	0.083	0.003	0.023	0.023	AWT__
A	S	0.23	0.2	1	5.4	5.4	24	5.8	997.05	72	1.08	SML	S	P	0.051	0.656	0.084	0.003	0.023	0.024	AWT__
A	S	0.23	0.2	1	5.4	5.4	24	5.8	997.05	72	1.08	SML	S	P	0.052	0.661	0.086	0.003	0.023	0.024	AW_S_
A	S	0.23	0.2	1	5.4	5.4	24	5.8	997.05	72	1.08	SML	S	P	0.053	0.666	0.087	0.003	0.022	0.024	AWT__
A	S	0.23	0.2	1	5.4	5.4	24	5.8	997.05	72	1.08	SML	S	P	0.054	0.667	0.089	0.003	0.022	0.025	AWT__
A	S	0.23	0.2	1	5.4	5.4	24	5.8	997.05	72	1.08	SML	S	P	0.056	0.676	0.091	0.003	0.023	0.025	____V
A	S	0.23	0.2	1	5.4	5.4	24	5.8	997.05	72	1.08	SML	S	P	0.057	0.677	0.093	0.003	0.024	0.025	AW_S_
A	S	0.23	0.2	1	5.4	5.4	24	5.8	997.05	72	1.08	SML	S	P	0.058	0.679	0.095	0.003	0.025	0.025	AWT__
A	S	0.23	0.2	1	5.4	5.4	24	5.8	997.05	72	1.08	SML	S	P	0.059	0.680	0.097	0.002	0.026	0.025	AWT__
A	S	0.23	0.2	1	5.4	5.4	24	5.8	997.05	72	1.08	SML	S	P	0.061	0.692	0.098	0.002	0.026	0.025	AWT__
A	S	0.23	0.2	1	5.4	5.4	24	5.8	997.05	72	1.08	SML	S	P	0.061	0.699	0.099	0.003	0.026	0.026	AW_S_
A	S	0.23	0.2	1	5.4	5.4	24	5.8	997.05	72	1.08	SML	S	P	0.062	0.703	0.100	0.003	0.026	0.026	AWT__
A	S	0.23	0.2	1	5.4	5.4	24	5.8	997.05	72	1.08	SML	S	P	0.065	0.716	0.103	0.003	0.026	0.026	____V

A	S	0.23	0.2	1	5.4	5.4	24	5.8	997.05	72	1.08	SML	S	P	0.066	0.719	0.105	0.003	0.026	0.026	AWT__
A	S	0.23	0.2	1	5.4	5.4	24	5.8	997.05	72	1.08	SML	S	P	0.067	0.724	0.106	0.003	0.026	0.026	AW_S_
A	S	0.23	0.2	1	5.4	5.4	24	5.8	997.05	72	1.08	SML	S	P	0.068	0.724	0.109	0.002	0.026	0.026	AWT__
B	S	0.15	0.2	1	4.2	4	28.13	4.7	997.05	72	1.08	S	NONE	G	0.019	0.504	0.032	0.010	0.008	0.009	AWT__
B	S	0.15	0.2	1	4.2	4	28.13	4.7	997.05	72	1.08	S	NONE	G	0.030	0.571	0.040	0.011	0.013	0.011	AWT__
B	S	0.15	0.2	1	4.2	4	28.13	4.7	997.05	72	1.08	S	NONE	G	0.040	0.628	0.047	0.014	0.012	0.012	AWT__
B	S	0.15	0.2	1	4.2	4	28.13	4.7	997.05	72	1.08	S	S	A	0.050	0.661	0.055	0.017	0.012	0.012	AW_S_
B	S	0.15	0.2	1	4.2	4	28.13	4.7	997.05	72	1.08	SM	S	A	0.061	0.714	0.060	0.021	0.015	0.014	AW_S_
B	S	0.15	0.2	1	4.2	4	28.13	4.7	997.05	72	1.08	SM	S	A	0.072	0.753	0.067	0.022	0.015	0.015	AWT__
B	S	0.15	0.2	1	4.2	4	28.13	4.7	997.05	72	1.08	SML	S	P	0.092	0.813	0.078	0.028	0.015	0.017	AW_S_
B	S	0.15	0.2	1	4.2	4	28.13	4.7	997.05	72	1.08	SML	S	P	0.101	0.834	0.081	0.028	0.016	0.016	AWT__
B	S	0.15	0.2	1	4.2	4	28.13	4.7	997.05	72	1.08	SML	S	VP	0.114	0.867	0.088	0.032	0.016	0.016	____V
B	S	0.15	0.2	1	4.2	4	28.13	4.7	997.05	72	1.08	SML	S	VP	0.125	0.915	0.093	0.035	0.016	0.016	AWT__
B	S	0.15	0.1	0.44	4.2	4	28.13	4.7	997.05	72	1.08	SML	S	G	0.020	1.022	0.036	0.014	0.007	0.007	AWT__
B	S	0.15	0.1	0.44	4.2	4	28.13	4.7	997.05	72	1.08	SML	S	G	0.031	1.142	0.043	0.017	0.007	0.008	AW_S_
B	S	0.15	0.1	0.44	4.2	4	28.13	4.7	997.05	72	1.08	SML	S	G	0.051	1.323	0.057	0.024	0.012	0.011	AWT__
B	S	0.15	0.1	0.44	4.2	4	28.13	4.7	997.05	72	1.08	SML	S	G	0.061	1.416	0.063	0.024	0.012	0.013	____V
B	S	0.15	0.1	0.44	4.2	4	28.13	4.7	997.05	72	1.08	SML	S	P	0.070	1.473	0.069	0.028	0.013	0.013	AWT__
B	S	0.15	0.1	0.44	4.2	4	28.13	4.7	997.05	72	1.08	SML	S	P	0.082	1.559	0.073	0.030	0.016	0.015	AWT__
B	S	0.15	0.1	0.44	4.2	4	28.13	4.7	997.05	72	1.08	SML	S	P	0.091	1.627	0.080	0.031	0.016	0.017	AWT__
B	S	0.15	0.1	0.44	4.2	4	28.13	4.7	997.05	72	1.08	SMLX	S	VP	0.097	1.661	0.084	0.033	0.015	0.016	AWT__
B	S	0.15	0.1	0.44	4.2	4	28.13	4.7	997.05	72	1.08	SMLX	S	VP	0.102	1.698	0.087	0.034	0.016	0.016	AW_S_
B	S	0.15	0.1	0.44	4.2	4	28.13	4.7	997.05	72	1.08	SMLX	S	VP	0.111	1.766	0.092	0.038	0.017	0.016	AWT__
A	L	0.15	0.1	0.44	3	3	19.67	3.4	1033	65	1.68	S	S	G	0.019	0.504	0.040	0.004	0.005	0.004	AWT__
A	L	0.15	0.1	0.44	3	3	19.67	3.4	1033	65	1.68	S	S	G	0.021	0.532	0.045	0.004	0.004	0.004	AWT__
A	L	0.15	0.1	0.44	3	3	19.67	3.4	1033	65	1.68	S	S	G	0.023	0.559	0.049	0.004	0.005	0.005	AWT__
A	L	0.15	0.1	0.44	3	3	19.67	3.4	1033	65	1.68	S	S	G	0.026	0.586	0.052	0.005	0.005	0.005	AW_S_
A	L	0.15	0.1	0.44	3	3	19.67	3.4	1033	65	1.68	S	S	G	0.029	0.615	0.057	0.005	0.005	0.005	AWT__
A	L	0.15	0.1	0.44	3	3	19.67	3.4	1033	65	1.68	S	S	G	0.031	0.634	0.061	0.005	0.006	0.005	AWT__

A	L	0.15	0.1	0.44	3	3	19.67	3.4	1033	65	1.68	S	S	G	0.034	0.630	0.065	0.006	0.006	0.006	AWT__
A	L	0.15	0.1	0.44	3	3	19.67	3.4	1033	65	1.68	S	S	G	0.035	0.675	0.068	0.006	0.005	0.006	AW_S_
A	L	0.15	0.1	0.44	3	3	19.67	3.4	1033	65	1.68	S	S	G	0.038	0.694	0.072	0.006	0.005	0.006	AW_S_
A	L	0.15	0.1	0.44	3	3	19.67	3.4	1033	65	1.68	S	S	G	0.040	0.716	0.076	0.007	0.006	0.006	AWT__
A	L	0.15	0.1	0.44	3	3	19.67	3.4	1033	65	1.68	S	S	A	0.041	0.726	0.079	0.007	0.006	0.006	____V
A	L	0.15	0.1	0.44	3	3	19.67	3.4	1033	65	1.68	SM	S	A	0.047	0.772	0.086	0.008	0.008	0.008	AW_S_
A	L	0.15	0.1	0.44	3	3	19.67	3.4	1033	65	1.68	SM	S	A	0.050	0.774	0.090	0.008	0.008	0.008	____V
A	L	0.15	0.1	0.44	3	3	19.67	3.4	1033	65	1.68	SM	S	A	0.052	0.806	0.094	0.008	0.008	0.008	AWT__
A	L	0.15	0.1	0.44	3	3	19.67	3.4	1033	65	1.68	SM	S	P	0.054	0.819	0.098	0.008	0.009	0.008	AWT__
A	L	0.15	0.1	0.44	3	3	19.67	3.4	1033	65	1.68	SM	S	P	0.056	0.831	0.100	0.009	0.007	0.008	AWT__
A	L	0.15	0.1	0.44	3	3	19.67	3.4	1033	65	1.68	SM	S	P	0.059	0.842	0.105	0.009	0.008	0.008	AWT__
A	L	0.15	0.1	0.44	3	3	19.67	3.4	1033	65	1.68	SM	S	P	0.061	0.859	0.108	0.010	0.008	0.009	AW_S_
A	L	0.15	0.1	0.44	3	3	19.67	3.4	1033	65	1.68	SM	S	P	0.064	0.880	0.114	0.010	0.007	0.009	AW_S_
A	L	0.15	0.1	0.44	3	3	19.67	3.4	1033	65	1.68	SM	S	P	0.066	0.891	0.120	0.010	0.009	0.009	AWT__
C	L	0.15	0.1	0.44	3	3	19.67	3.4	1033	65	1.68	SM	S	G	0.018	0.638	0.027	0.004	0.005	0.004	AWT__
C	L	0.15	0.1	0.44	3	3	19.67	3.4	1033	65	1.68	SM	S	G	0.021	0.697	0.031	0.007	0.005	0.005	AWT__
C	L	0.15	0.1	0.44	3	3	19.67	3.4	1033	65	1.68	SM	S	G	0.023	0.722	0.036	0.007	0.006	0.005	AW_S_
C	L	0.15	0.1	0.44	3	3	19.67	3.4	1033	65	1.68	SM	S	G	0.026	0.763	0.037	0.007	0.005	0.005	AW_S_
C	L	0.15	0.1	0.44	3	3	19.67	3.4	1033	65	1.68	SM	S	G	0.028	0.781	0.038	0.007	0.006	0.005	AWT__
C	L	0.15	0.1	0.44	3	3	19.67	3.4	1033	65	1.68	SM	S	G	0.031	0.811	0.041	0.008	0.005	0.005	AWT__
C	L	0.15	0.1	0.44	3	3	19.67	3.4	1033	65	1.68	SM	S	A	0.033	0.839	0.043	0.008	0.005	0.006	____V
C	L	0.15	0.1	0.44	3	3	19.67	3.4	1033	65	1.68	SM	S	A	0.035	0.842	0.045	0.009	0.006	0.006	AWT__
C	L	0.15	0.1	0.44	3	3	19.67	3.4	1033	65	1.68	SM	S	A	0.038	0.887	0.049	0.010	0.006	0.006	____V
C	L	0.15	0.1	0.44	3	3	19.67	3.4	1033	65	1.68	SM	S	A	0.040	0.916	0.051	0.010	0.006	0.006	AWT__
C	L	0.15	0.1	0.44	3	3	19.67	3.4	1033	65	1.68	SM	S	P	0.044	0.958	0.055	0.010	0.006	0.006	AWT__
C	L	0.15	0.1	0.44	3	3	19.67	3.4	1033	65	1.68	SM	S	P	0.047	0.978	0.056	0.011	0.006	0.006	____V
C	L	0.15	0.1	0.44	3	3	19.67	3.4	1033	65	1.68	SM	S	P	0.049	0.975	0.060	0.011	0.006	0.006	AW_S_
C	L	0.15	0.1	0.44	3	3	19.67	3.4	1033	65	1.68	SM	S	P	0.051	0.997	0.061	0.011	0.007	0.006	AW_S_
C	L	0.15	0.1	0.44	3	3	19.67	3.4	1033	65	1.68	SM	S	P	0.054	1.019	0.063	0.011	0.007	0.006	AW_S_

C	L	0.15	0.1	0.44	3	3	19.67	3.4	1033	65	1.68	SM	S	P	0.056	1.039	0.067	0.012	0.006	0.007	AWT__
C	L	0.15	0.1	0.44	3	3	19.67	3.4	1033	65	1.68	SM	S	P	0.059	1.053	0.070	0.013	0.007	0.007	AWT__
C	L	0.15	0.1	0.44	3	3	19.67	3.4	1033	65	1.68	SM	S	P	0.062	1.078	0.074	0.013	0.007	0.007	AWT__
C	L	0.15	0.1	0.44	3	3	19.67	3.4	1033	65	1.68	SML	S	P	0.064	1.098	0.074	0.013	0.007	0.007	AWT__
C	L	0.15	0.1	0.44	3	3	19.67	3.4	1033	65	1.68	SML	S	P	0.066	1.114	0.077	0.015	0.008	0.007	AW_S_
B	L	0.15	0.1	0.44	3	3	19.67	3.4	1033	65	1.68	S	NONE	G	0.019	0.620	0.029	0.004	0.004	0.004	____V
B	L	0.15	0.1	0.44	3	3	19.67	3.4	1033	65	1.68	S	NONE	G	0.021	0.650	0.032	0.005	0.004	0.005	____V
B	L	0.15	0.1	0.44	3	3	19.67	3.4	1033	65	1.68	S	NONE	G	0.024	0.680	0.034	0.006	0.005	0.005	AW_S_
B	L	0.15	0.1	0.44	3	3	19.67	3.4	1033	65	1.68	S	NONE	G	0.026	0.720	0.039	0.006	0.005	0.005	AWT__
B	L	0.15	0.1	0.44	3	3	19.67	3.4	1033	65	1.68	SM	NONE	G	0.028	0.730	0.040	0.006	0.005	0.005	AW_S_
B	L	0.15	0.1	0.44	3	3	19.67	3.4	1033	65	1.68	SM	NONE	G	0.031	0.760	0.043	0.007	0.005	0.005	AW_S_
B	L	0.15	0.1	0.44	3	3	19.67	3.4	1033	65	1.68	SM	NONE	G	0.033	0.780	0.044	0.008	0.006	0.005	AW_S_
B	L	0.15	0.1	0.44	3	3	19.67	3.4	1033	65	1.68	SM	NONE	G	0.035	0.800	0.047	0.009	0.005	0.005	AWT__
B	L	0.15	0.1	0.44	3	3	19.67	3.4	1033	65	1.68	SM	NONE	A	0.038	0.830	0.047	0.009	0.006	0.006	AWT__
B	L	0.15	0.1	0.44	3	3	19.67	3.4	1033	65	1.68	SM	NONE	A	0.042	0.860	0.052	0.010	0.006	0.006	AWT__
B	L	0.15	0.1	0.44	3	3	19.67	3.4	1033	65	1.68	SML	S	A	0.045	0.890	0.054	0.010	0.007	0.006	AWT__
B	L	0.15	0.1	0.44	3	3	19.67	3.4	1033	65	1.68	SML	S	A	0.047	0.910	0.057	0.010	0.006	0.007	AW_S_
B	L	0.15	0.1	0.44	3	3	19.67	3.4	1033	65	1.68	SML	S	P	0.049	0.920	0.061	0.011	0.007	0.006	AWT__
B	L	0.15	0.1	0.44	3	3	19.67	3.4	1033	65	1.68	SML	S	P	0.052	0.940	0.063	0.011	0.007	0.006	AW_S_
B	L	0.15	0.1	0.44	3	3	19.67	3.4	1033	65	1.68	SML	S	P	0.054	0.950	0.064	0.011	0.006	0.007	AW_S_
B	L	0.15	0.1	0.44	3	3	19.67	3.4	1033	65	1.68	SML	S	P	0.056	0.950	0.065	0.012	0.006	0.007	AWT__
B	L	0.15	0.1	0.44	3	3	19.67	3.4	1033	65	1.68	SML	S	P	0.059	1.000	0.069	0.012	0.008	0.007	AW_S_
B	L	0.15	0.1	0.44	3	3	19.67	3.4	1033	65	1.68	SML	S	P	0.061	1.020	0.073	0.013	0.009	0.007	AW_S_
B	L	0.15	0.1	0.44	3	3	19.67	3.4	1033	65	1.68	SML	S	P	0.064	1.040	0.075	0.013	0.009	0.008	AW_S_
B	L	0.15	0.1	0.44	3	3	19.67	3.4	1033	65	1.68	SML	S	P	0.067	1.050	0.077	0.013	0.009	0.008	AWT__
B	L	0.15	0.2	1	3	3	19.67	3.4	1033	65	1.68	S	S	G	0.019	0.417	0.025	0.002	0.003	0.004	AWT__
B	L	0.15	0.2	1	3	3	19.67	3.4	1033	65	1.68	S	S	G	0.021	0.433	0.027	0.002	0.003	0.004	AWT__
B	L	0.15	0.2	1	3	3	19.67	3.4	1033	65	1.68	S	S	G	0.024	0.465	0.030	0.003	0.004	0.004	AWT__
B	L	0.15	0.2	1	3	3	19.67	3.4	1033	65	1.68	S	S	G	0.026	0.477	0.032	0.003	0.004	0.004	____V

B	L	0.15	0.2	1	3	3	19.67	3.4	1033	65	1.68	S	S	G	0.029	0.501	0.034	0.003	0.005	0.005	AWT__
B	L	0.15	0.2	1	3	3	19.67	3.4	1033	65	1.68	S	S	G	0.031	0.519	0.036	0.003	0.005	0.005	AWT__
B	L	0.15	0.2	1	3	3	19.67	3.4	1033	65	1.68	S	S	G	0.033	0.535	0.039	0.004	0.006	0.005	AWT__
B	L	0.15	0.2	1	3	3	19.67	3.4	1033	65	1.68	S	S	G	0.035	0.548	0.042	0.004	0.006	0.006	AW_S_
B	L	0.15	0.2	1	3	3	19.67	3.4	1033	65	1.68	S	S	A	0.040	0.585	0.047	0.004	0.006	0.006	AWT__
B	L	0.15	0.2	1	3	3	19.67	3.4	1033	65	1.68	S	S	A	0.043	0.599	0.048	0.005	0.007	0.006	AWT__
B	L	0.15	0.2	1	3	3	19.67	3.4	1033	65	1.68	S	S	A	0.045	0.615	0.050	0.004	0.005	0.006	AWT__
B	L	0.15	0.2	1	3	3	19.67	3.4	1033	65	1.68	SML	S	A	0.047	0.633	0.053	0.005	0.006	0.007	AWT__
B	L	0.15	0.2	1	3	3	19.67	3.4	1033	65	1.68	SML	S	P	0.050	0.651	0.055	0.006	0.006	0.007	____V
B	L	0.15	0.2	1	3	3	19.67	3.4	1033	65	1.68	SML	S	P	0.052	0.666	0.058	0.006	0.007	0.007	AWT__
B	L	0.15	0.2	1	3	3	19.67	3.4	1033	65	1.68	SML	S	P	0.054	0.690	0.058	0.007	0.006	0.007	____V
B	L	0.15	0.2	1	3	3	19.67	3.4	1033	65	1.68	SML	S	P	0.056	0.695	0.062	0.006	0.007	0.007	AW_S_
B	L	0.15	0.2	1	3	3	19.67	3.4	1033	65	1.68	SML	S	P	0.059	0.707	0.065	0.005	0.006	0.006	AWT__
B	L	0.15	0.2	1	3	3	19.67	3.4	1033	65	1.68	SML	S	P	0.061	0.724	0.068	0.007	0.008	0.007	AWT__
B	L	0.15	0.2	1	3	3	19.67	3.4	1033	65	1.68	SML	S	P	0.063	0.739	0.070	0.007	0.011	0.007	AWT__
B	L	0.15	0.2	1	3	3	19.67	3.4	1033	65	1.68	SML	S	P	0.066	0.763	0.074	0.008	0.007	0.008	AWT__
B	L	0.15	0.2	1	3	3	19.67	3.4	1033	65	1.68	SML	S	P	0.076	0.826	0.089	0.009	0.011	0.010	____V
A	L	0.15	0.2	1	3	3	19.67	3.4	1033	65	1.68	S	NONE	G	0.019	0.272	0.040	0.001	0.004	0.004	AW_S_
A	L	0.15	0.2	1	3	3	19.67	3.4	1033	65	1.68	SML	S	G	0.021	0.286	0.046	0.001	0.004	0.004	AWT__
A	L	0.15	0.2	1	3	3	19.67	3.4	1033	65	1.68	SML	S	G	0.024	0.302	0.049	0.001	0.005	0.004	AWT__
A	L	0.15	0.2	1	3	3	19.67	3.4	1033	65	1.68	SML	S	G	0.026	0.312	0.053	0.001	0.005	0.004	____V
A	L	0.15	0.2	1	3	3	19.67	3.4	1033	65	1.68	SML	S	G	0.029	0.335	0.058	0.002	0.004	0.005	AW_S_
A	L	0.15	0.2	1	3	3	19.67	3.4	1033	65	1.68	SML	S	G	0.030	0.340	0.061	0.002	0.005	0.005	AWT__
A	L	0.15	0.2	1	3	3	19.67	3.4	1033	65	1.68	SML	S	G	0.035	0.365	0.071	0.002	0.006	0.005	AWT__
A	L	0.15	0.2	1	3	3	19.67	3.4	1033	65	1.68	SML	S	G	0.038	0.378	0.077	0.002	0.006	0.006	AWT__
A	L	0.15	0.2	1	3	3	19.67	3.4	1033	65	1.68	SML	S	G	0.040	0.391	0.080	0.002	0.006	0.006	AWT__
A	L	0.15	0.2	1	3	3	19.67	3.4	1033	65	1.68	SML	S	G	0.042	0.385	0.085	0.003	0.007	0.006	____V
A	L	0.15	0.2	1	3	3	19.67	3.4	1033	65	1.68	SML	S	A	0.044	0.412	0.089	0.003	0.006	0.007	AWT__
A	L	0.15	0.2	1	3	3	19.67	3.4	1033	65	1.68	SML	S	A	0.047	0.424	0.095	0.003	0.006	0.007	AW_S_

A	L	0.15	0.2	1	3	3	19.67	3.4	1033	65	1.68	SML	S	A	0.050	0.433	0.102	0.003	0.007	0.007	AW_S_
A	L	0.15	0.2	1	3	3	19.67	3.4	1033	65	1.68	SML	S	A	0.052	0.445	0.104	0.003	0.009	0.007	AW_S_
A	L	0.15	0.2	1	3	3	19.67	3.4	1033	65	1.68	SML	S	A	0.054	0.453	0.109	0.003	0.008	0.008	AWT__
A	L	0.15	0.2	1	3	3	19.67	3.4	1033	65	1.68	SML	S	P	0.057	0.461	0.114	0.003	0.009	0.008	AWT__
A	L	0.15	0.2	1	3	3	19.67	3.4	1033	65	1.68	SML	S	P	0.059	0.467	0.119	0.003	0.009	0.008	AWT__
A	L	0.15	0.2	1	3	3	19.67	3.4	1033	65	1.68	SML	S	P	0.061	0.484	0.125	0.003	0.008	0.009	AW_S_
A	L	0.15	0.2	1	3	3	19.67	3.4	1033	65	1.68	SML	S	P	0.064	0.491	0.130	0.003	0.010	0.009	____V
A	L	0.15	0.2	1	3	3	19.67	3.4	1033	65	1.68	SML	S	P	0.066	0.500	0.135	0.003	0.011	0.010	AWT__
C	L	0.15	0.2	1	3	3	19.67	3.4	1033	65	1.68	S	S	G	0.019	0.487	0.019	0.003	0.005	0.004	AW_S_
C	L	0.15	0.2	1	3	3	19.67	3.4	1033	65	1.68	S	S	A	0.021	0.510	0.020	0.003	0.004	0.004	AWT__
C	L	0.15	0.2	1	3	3	19.67	3.4	1033	65	1.68	S	S	A	0.024	0.517	0.023	0.003	0.005	0.004	AWT__
C	L	0.15	0.2	1	3	3	19.67	3.4	1033	65	1.68	S	S	A	0.026	0.555	0.025	0.003	0.006	0.004	____V
C	L	0.15	0.2	1	3	3	19.67	3.4	1033	65	1.68	S	S	A	0.029	0.582	0.028	0.003	0.004	0.005	AW_S_
C	L	0.15	0.2	1	3	3	19.67	3.4	1033	65	1.68	S	S	A	0.033	0.620	0.030	0.004	0.005	0.005	AWT__
C	L	0.15	0.2	1	3	3	19.67	3.4	1033	65	1.68	S	S	A	0.036	0.630	0.031	0.004	0.005	0.005	AWT__
C	L	0.15	0.2	1	3	3	19.67	3.4	1033	65	1.68	S	S	A	0.038	0.658	0.034	0.004	0.005	0.005	AWT__
C	L	0.15	0.2	1	3	3	19.67	3.4	1033	65	1.68	S	S	A	0.040	0.676	0.036	0.005	0.006	0.005	AWT__
C	L	0.15	0.2	1	3	3	19.67	3.4	1033	65	1.68	S	S	P	0.042	0.697	0.038	0.005	0.006	0.006	AWT__
C	L	0.15	0.2	1	3	3	19.67	3.4	1033	65	1.68	S	S	P	0.045	0.713	0.043	0.005	0.006	0.006	AWT__
C	L	0.15	0.2	1	3	3	19.67	3.4	1033	65	1.68	S	S	P	0.047	0.725	0.040	0.006	0.007	0.006	AWT__
C	L	0.15	0.2	1	3	3	19.67	3.4	1033	65	1.68	S	S	P	0.050	0.744	0.043	0.006	0.006	0.007	AWT__
C	L	0.15	0.2	1	3	3	19.67	3.4	1033	65	1.68	S	S	P	0.052	0.761	0.045	0.006	0.007	0.007	AWT__
C	L	0.15	0.2	1	3	3	19.67	3.4	1033	65	1.68	S	S	P	0.052	0.758	0.046	0.007	0.008	0.007	AWT__
C	L	0.15	0.2	1	3	3	19.67	3.4	1033	65	1.68	S	S	P	0.053	0.786	0.049	0.007	0.006	0.007	AW_S_
C	L	0.15	0.2	1	3	3	19.67	3.4	1033	65	1.68	S	S	P	0.056	0.800	0.050	0.007	0.007	0.007	AWT__
C	L	0.15	0.2	1	3	3	19.67	3.4	1033	65	1.68	S	S	P	0.059	0.827	0.053	0.008	0.006	0.007	AW_S_
C	L	0.15	0.2	1	3	3	19.67	3.4	1033	65	1.68	S	S	P	0.061	0.840	0.055	0.008	0.007	0.007	AWT__
C	L	0.15	0.2	1	3	3	19.67	3.4	1033	65	1.68	S	S	P	0.063	0.851	0.058	0.009	0.007	0.007	AW_S_
B	L	0.15	0.1	0.44	3	3	19.67	3.4	1047	73	2.14	SM	S	G	0.019	0.612	0.029	0.005	0.005	0.004	AWT__

B	L	0.15	0.1	0.44	3	3	19.67	3.4	1047	73	2.14	SM	S	G	0.021	0.639	0.030	0.005	0.004	0.004	AWT__
B	L	0.15	0.1	0.44	3	3	19.67	3.4	1047	73	2.14	SM	S	G	0.023	0.670	0.035	0.006	0.004	0.005	AW_S_
B	L	0.15	0.1	0.44	3	3	19.67	3.4	1047	73	2.14	SM	S	G	0.026	0.698	0.038	0.007	0.004	0.005	AWT__
B	L	0.15	0.1	0.44	3	3	19.67	3.4	1047	73	2.14	SM	S	A	0.030	0.750	0.044	0.008	0.005	0.005	____V
B	L	0.15	0.1	0.44	3	3	19.67	3.4	1047	73	2.14	SM	S	A	0.034	0.784	0.046	0.008	0.005	0.005	AWT__
B	L	0.15	0.1	0.44	3	3	19.67	3.4	1047	73	2.14	SM	S	A	0.035	0.802	0.048	0.009	0.005	0.005	AW_S_
B	L	0.15	0.1	0.44	3	3	19.67	3.4	1047	73	2.14	SM	S	P	0.038	0.824	0.052	0.009	0.005	0.005	AWT__
B	L	0.15	0.1	0.44	3	3	19.67	3.4	1047	73	2.14	SM	S	P	0.040	0.842	0.053	0.010	0.005	0.005	AWT__
B	L	0.15	0.1	0.44	3	3	19.67	3.4	1047	73	2.14	SM	S	P	0.042	0.857	0.056	0.010	0.005	0.005	AWT__
B	L	0.15	0.1	0.44	3	3	19.67	3.4	1047	73	2.14	SM	S	P	0.044	0.885	0.056	0.010	0.006	0.006	____V
B	L	0.15	0.1	0.44	3	3	19.67	3.4	1047	73	2.14	SM	S	P	0.047	0.904	0.059	0.011	0.006	0.006	AWT__
B	L	0.15	0.1	0.44	3	3	19.67	3.4	1047	73	2.14	SM	S	P	0.049	0.916	0.063	0.012	0.006	0.006	____V
B	L	0.15	0.1	0.44	3	3	19.67	3.4	1047	73	2.14	SM	S	P	0.052	0.942	0.064	0.012	0.006	0.006	____V
B	L	0.15	0.1	0.44	3	3	19.67	3.4	1047	73	2.14	SM	S	VP	0.054	0.966	0.068	0.013	0.007	0.007	AWT__
B	L	0.15	0.1	0.44	3	3	19.67	3.4	1047	73	2.14	SML	S	VP	0.057	0.984	0.070	0.013	0.006	0.006	AWT__
B	L	0.15	0.1	0.44	3	3	19.67	3.4	1047	73	2.14	SML	S	VP	0.059	0.992	0.071	0.013	0.008	0.006	AWT__
B	L	0.15	0.1	0.44	3	3	19.67	3.4	1047	73	2.14	SML	S	VP	0.061	1.019	0.073	0.013	0.006	0.007	AWT__
B	L	0.15	0.1	0.44	3	3	19.67	3.4	1047	73	2.14	SML	S	VP	0.064	1.029	0.075	0.013	0.006	0.007	AWT__
B	L	0.15	0.1	0.44	3	3	19.67	3.4	1047	73	2.14	SML	S	VP	0.066	1.053	0.077	0.013	0.008	0.007	AWT__
A	L	0.15	0.1	0.44	3	3	19.67	3.4	1047	73	2.14	S	S	G	0.019	0.512	0.040	0.003	0.005	0.004	AWT__
A	L	0.15	0.1	0.44	3	3	19.67	3.4	1047	73	2.14	S	S	G	0.021	0.532	0.044	0.003	0.005	0.004	AW_S_
A	L	0.15	0.1	0.44	3	3	19.67	3.4	1047	73	2.14	S	S	G	0.024	0.565	0.049	0.003	0.005	0.005	AWT__
A	L	0.15	0.1	0.44	3	3	19.67	3.4	1047	73	2.14	SM	S	G	0.028	0.614	0.056	0.004	0.005	0.005	AW_S_
A	L	0.15	0.1	0.44	3	3	19.67	3.4	1047	73	2.14	SM	S	G	0.030	0.624	0.060	0.005	0.006	0.005	AWT__
A	L	0.15	0.1	0.44	3	3	19.67	3.4	1047	73	2.14	SM	S	G	0.033	0.648	0.065	0.005	0.005	0.005	AWT__
A	L	0.15	0.1	0.44	3	3	19.67	3.4	1047	73	2.14	SM	S	G	0.035	0.667	0.068	0.005	0.005	0.006	AWT__
A	L	0.15	0.1	0.44	3	3	19.67	3.4	1047	73	2.14	SM	S	G	0.039	0.703	0.072	0.005	0.006	0.006	AW_S_
A	L	0.15	0.1	0.44	3	3	19.67	3.4	1047	73	2.14	SM	S	A	0.040	0.707	0.076	0.005	0.006	0.006	____V
A	L	0.15	0.1	0.44	3	3	19.67	3.4	1047	73	2.14	SM	S	A	0.043	0.728	0.079	0.006	0.006	0.006	AWT__

A	L	0.15	0.1	0.44	3	3	19.67	3.4	1047	73	2.14	SM	S	A	0.045	0.744	0.081	0.006	0.007	0.006	____V
A	L	0.15	0.1	0.44	3	3	19.67	3.4	1047	73	2.14	SM	S	A	0.047	0.769	0.087	0.006	0.007	0.006	AWT__
A	L	0.15	0.1	0.44	3	3	19.67	3.4	1047	73	2.14	SM	S	A	0.050	0.782	0.090	0.007	0.007	0.007	____V
A	L	0.15	0.1	0.44	3	3	19.67	3.4	1047	73	2.14	SM	S	A	0.052	0.806	0.095	0.007	0.006	0.007	AWT__
A	L	0.15	0.1	0.44	3	3	19.67	3.4	1047	73	2.14	SM	S	P	0.055	0.820	0.098	0.007	0.007	0.007	AWT__
A	L	0.15	0.1	0.44	3	3	19.67	3.4	1047	73	2.14	SM	S	P	0.057	0.829	0.101	0.007	0.007	0.007	____V
A	L	0.15	0.1	0.44	3	3	19.67	3.4	1047	73	2.14	SM	S	P	0.059	0.844	0.105	0.008	0.007	0.007	AWT__
A	L	0.15	0.1	0.44	3	3	19.67	3.4	1047	73	2.14	SM	S	P	0.061	0.856	0.107	0.008	0.007	0.007	AWT__
A	L	0.15	0.1	0.44	3	3	19.67	3.4	1047	73	2.14	SM	S	P	0.064	0.870	0.113	0.009	0.007	0.008	AWT__
A	L	0.15	0.1	0.44	3	3	19.67	3.4	1047	73	2.14	SM	S	P	0.066	0.885	0.117	0.009	0.008	0.008	AW_S_
C	L	0.15	0.1	0.44	3	3	19.67	3.4	1047	73	2.14	SM	S	A	0.019	0.637	0.029	0.006	0.004	0.004	AW_S_
C	L	0.15	0.1	0.44	3	3	19.67	3.4	1047	73	2.14	SM	S	A	0.021	0.667	0.031	0.006	0.004	0.004	AWT__
C	L	0.15	0.1	0.44	3	3	19.67	3.4	1047	73	2.14	SM	S	A	0.026	0.728	0.037	0.007	0.005	0.004	AWT__
C	L	0.15	0.1	0.44	3	3	19.67	3.4	1047	73	2.14	SM	S	A	0.028	0.755	0.040	0.008	0.005	0.005	AW_S_
C	L	0.15	0.1	0.44	3	3	19.67	3.4	1047	73	2.14	SM	S	A	0.031	0.784	0.043	0.008	0.005	0.005	AWT__
C	L	0.15	0.1	0.44	3	3	19.67	3.4	1047	73	2.14	SM	S	A	0.033	0.812	0.045	0.009	0.004	0.005	AW_S_
C	L	0.15	0.1	0.44	3	3	19.67	3.4	1047	73	2.14	SM	S	A	0.035	0.829	0.048	0.009	0.004	0.005	AWT__
C	L	0.15	0.1	0.44	3	3	19.67	3.4	1047	73	2.14	SM	S	A	0.038	0.857	0.049	0.010	0.005	0.005	AWT__
C	L	0.15	0.1	0.44	3	3	19.67	3.4	1047	73	2.14	SM	S	A	0.040	0.872	0.051	0.010	0.006	0.005	AW_S_
C	L	0.15	0.1	0.44	3	3	19.67	3.4	1047	73	2.14	SML	S	A	0.042	0.894	0.054	0.011	0.005	0.005	____V
C	L	0.15	0.1	0.44	3	3	19.67	3.4	1047	73	2.14	SML	S	A	0.044	0.918	0.057	0.011	0.005	0.005	AWT__
C	L	0.15	0.1	0.44	3	3	19.67	3.4	1047	73	2.14	SML	S	A	0.047	0.940	0.061	0.012	0.006	0.005	AWT__
C	L	0.15	0.1	0.44	3	3	19.67	3.4	1047	73	2.14	SML	S	A	0.049	0.955	0.062	0.013	0.006	0.006	AWT__
C	L	0.15	0.1	0.44	3	3	19.67	3.4	1047	73	2.14	SML	S	A	0.052	0.982	0.065	0.013	0.006	0.006	AWT__
C	L	0.15	0.1	0.44	3	3	19.67	3.4	1047	73	2.14	SML	S	P	0.054	0.998	0.068	0.013	0.006	0.006	AWT__
C	L	0.15	0.1	0.44	3	3	19.67	3.4	1047	73	2.14	SML	S	P	0.056	1.016	0.070	0.014	0.007	0.006	AW_S_
C	L	0.15	0.1	0.44	3	3	19.67	3.4	1047	73	2.14	SML	S	P	0.059	1.040	0.074	0.014	0.007	0.007	AW_S_
C	L	0.15	0.1	0.44	3	3	19.67	3.4	1047	73	2.14	SML	S	VP	0.061	1.056	0.076	0.014	0.007	0.007	AWT__
C	L	0.15	0.1	0.44	3	3	19.67	3.4	1047	73	2.14	SML	S	VP	0.064	1.114	0.078	0.016	0.007	0.007	AWT__

C	L	0.15	0.1	0.44	3	3	19.67	3.4	1047	73	2.14	SML	S	VP	0.066	1.133	0.079	0.016	0.007	0.007	____V
B	L	0.15	0.2	1	3	3	19.67	3.4	1047	73	2.14	S	S	G	0.019	0.410	0.024	0.002	0.004	0.004	AWT__
B	L	0.15	0.2	1	3	3	19.67	3.4	1047	73	2.14	S	S	G	0.024	0.455	0.030	0.002	0.004	0.004	AWT__
B	L	0.15	0.2	1	3	3	19.67	3.4	1047	73	2.14	S	S	G	0.026	0.468	0.031	0.003	0.005	0.005	AW_S_
B	L	0.15	0.2	1	3	3	19.67	3.4	1047	73	2.14	SML	S	G	0.028	0.491	0.034	0.002	0.005	0.005	____V
B	L	0.15	0.2	1	3	3	19.67	3.4	1047	73	2.14	SML	S	G	0.031	0.509	0.036	0.002	0.005	0.005	AWT__
B	L	0.15	0.2	1	3	3	19.67	3.4	1047	73	2.14	SML	S	G	0.033	0.527	0.039	0.003	0.005	0.005	____V
B	L	0.15	0.2	1	3	3	19.67	3.4	1047	73	2.14	SML	S	G	0.035	0.545	0.040	0.003	0.005	0.005	AWT__
B	L	0.15	0.2	1	3	3	19.67	3.4	1047	73	2.14	SML	S	G	0.038	0.563	0.043	0.004	0.005	0.005	AWT__
B	L	0.15	0.2	1	3	3	19.67	3.4	1047	73	2.14	SML	S	G	0.040	0.574	0.046	0.004	0.005	0.005	AW_S_
B	L	0.15	0.2	1	3	3	19.67	3.4	1047	73	2.14	SML	S	G	0.043	0.595	0.048	0.004	0.006	0.006	AWT__
B	L	0.15	0.2	1	3	3	19.67	3.4	1047	73	2.14	SML	S	A	0.045	0.607	0.051	0.004	0.006	0.006	AWT__
B	L	0.15	0.2	1	3	3	19.67	3.4	1047	73	2.14	SML	S	A	0.048	0.628	0.053	0.005	0.006	0.006	AWT__
B	L	0.15	0.2	1	3	3	19.67	3.4	1047	73	2.14	SML	S	A	0.050	0.641	0.055	0.005	0.006	0.006	AWT__
B	L	0.15	0.2	1	3	3	19.67	3.4	1047	73	2.14	SML	S	A	0.052	0.651	0.057	0.005	0.007	0.006	AWT__
B	L	0.15	0.2	1	3	3	19.67	3.4	1047	73	2.14	SML	S	A	0.054	0.675	0.061	0.005	0.006	0.006	AWT__
B	L	0.15	0.2	1	3	3	19.67	3.4	1047	73	2.14	SML	S	A	0.057	0.687	0.062	0.006	0.007	0.007	AWT__
B	L	0.15	0.2	1	3	3	19.67	3.4	1047	73	2.14	SML	S	P	0.059	0.699	0.065	0.006	0.007	0.006	AW_S_
B	L	0.15	0.2	1	3	3	19.67	3.4	1047	73	2.14	SML	S	P	0.061	0.711	0.068	0.006	0.007	0.007	AWT__
B	L	0.15	0.2	1	3	3	19.67	3.4	1047	73	2.14	SML	S	P	0.064	0.728	0.072	0.006	0.007	0.007	AWT__
B	L	0.15	0.2	1	3	3	19.67	3.4	1047	73	2.14	SML	S	P	0.066	0.750	0.075	0.007	0.007	0.007	AWT__
A	L	0.15	0.2	1	3	3	19.67	3.4	1047	73	2.14	S	NONE	G	0.019	0.269	0.043	0.001	0.004	0.004	AW_S_
A	L	0.15	0.2	1	3	3	19.67	3.4	1047	73	2.14	S	NONE	G	0.021	0.286	0.047	0.001	0.005	0.005	AW_S_
A	L	0.15	0.2	1	3	3	19.67	3.4	1047	73	2.14	S	S	G	0.024	0.301	0.052	0.001	0.005	0.005	____V
A	L	0.15	0.2	1	3	3	19.67	3.4	1047	73	2.14	S	S	G	0.026	0.308	0.057	0.001	0.006	0.005	AW_S_
A	L	0.15	0.2	1	3	3	19.67	3.4	1047	73	2.14	S	S	G	0.028	0.328	0.060	0.001	0.005	0.005	AWT__
A	L	0.15	0.2	1	3	3	19.67	3.4	1047	73	2.14	S	S	G	0.031	0.340	0.065	0.002	0.005	0.005	AWT__
A	L	0.15	0.2	1	3	3	19.67	3.4	1047	73	2.14	S	S	G	0.033	0.352	0.068	0.002	0.006	0.005	AW_S_
A	L	0.15	0.2	1	3	3	19.67	3.4	1047	73	2.14	S	S	G	0.035	0.365	0.071	0.002	0.006	0.005	AWT__

A	L	0.15	0.2	1	3	3	19.67	3.4	1047	73	2.14	S	S	G	0.038	0.370	0.080	0.002	0.006	0.006	AWT__
A	L	0.15	0.2	1	3	3	19.67	3.4	1047	73	2.14	S	S	G	0.040	0.388	0.083	0.002	0.006	0.006	AW_S_
A	L	0.15	0.2	1	3	3	19.67	3.4	1047	73	2.14	S	S	G	0.043	0.398	0.085	0.002	0.006	0.006	AW_S_
A	L	0.15	0.2	1	3	3	19.67	3.4	1047	73	2.14	S	S	A	0.045	0.413	0.090	0.002	0.006	0.006	AWT__
A	L	0.15	0.2	1	3	3	19.67	3.4	1047	73	2.14	S	S	A	0.047	0.418	0.094	0.003	0.006	0.006	AWT__
A	L	0.15	0.2	1	3	3	19.67	3.4	1047	73	2.14	S	S	A	0.050	0.430	0.100	0.003	0.006	0.006	AW_S_
A	L	0.15	0.2	1	3	3	19.67	3.4	1047	73	2.14	S	S	A	0.052	0.439	0.101	0.003	0.007	0.007	AWT__
A	L	0.15	0.2	1	3	3	19.67	3.4	1047	73	2.14	S	S	A	0.054	0.451	0.108	0.003	0.007	0.007	AWT__
A	L	0.15	0.2	1	3	3	19.67	3.4	1047	73	2.14	S	S	A	0.057	0.460	0.117	0.003	0.008	0.008	____V
A	L	0.15	0.2	1	3	3	19.67	3.4	1047	73	2.14	S	S	P	0.059	0.461	0.119	0.003	0.009	0.008	____V
A	L	0.15	0.2	1	3	3	19.67	3.4	1047	73	2.14	S	S	P	0.061	0.482	0.123	0.003	0.009	0.008	AWT__
A	L	0.15	0.2	1	3	3	19.67	3.4	1047	73	2.14	S	S	P	0.064	0.490	0.129	0.003	0.010	0.008	____V
C	L	0.15	0.2	1	3	3	19.67	3.4	1047	73	2.14	SM	S	G	0.019	0.487	0.019	0.002	0.004	0.004	AW_S_
C	L	0.15	0.2	1	3	3	19.67	3.4	1047	73	2.14	SM	S	G	0.021	0.510	0.022	0.002	0.005	0.004	AWT__
C	L	0.15	0.2	1	3	3	19.67	3.4	1047	73	2.14	SM	S	G	0.024	0.534	0.024	0.003	0.004	0.004	AWT__
C	L	0.15	0.2	1	3	3	19.67	3.4	1047	73	2.14	SM	S	G	0.025	0.543	0.025	0.003	0.004	0.004	AWT__
C	L	0.15	0.2	1	3	3	19.67	3.4	1047	73	2.14	SM	S	G	0.028	0.576	0.027	0.004	0.004	0.005	____V
C	L	0.15	0.2	1	3	3	19.67	3.4	1047	73	2.14	SM	S	G	0.031	0.597	0.028	0.004	0.005	0.005	AWT__
C	L	0.15	0.2	1	3	3	19.67	3.4	1047	73	2.14	SM	S	A	0.033	0.616	0.030	0.004	0.005	0.005	AW_S_
C	L	0.15	0.2	1	3	3	19.67	3.4	1047	73	2.14	SM	S	A	0.035	0.636	0.032	0.004	0.005	0.005	____V
C	L	0.15	0.2	1	3	3	19.67	3.4	1047	73	2.14	SM	S	P	0.038	0.653	0.034	0.004	0.005	0.005	AW_S_
C	L	0.15	0.2	1	3	3	19.67	3.4	1047	73	2.14	SM	S	P	0.042	0.688	0.038	0.005	0.005	0.005	AWT__
C	L	0.15	0.2	1	3	3	19.67	3.4	1047	73	2.14	SM	S	P	0.044	0.707	0.040	0.005	0.005	0.005	AW_S_
C	L	0.15	0.2	1	3	3	19.67	3.4	1047	73	2.14	SM	S	P	0.047	0.727	0.040	0.006	0.005	0.005	AWT__
C	L	0.15	0.2	1	3	3	19.67	3.4	1047	73	2.14	SML	S	P	0.050	0.742	0.043	0.006	0.006	0.005	AWT__
C	L	0.15	0.2	1	3	3	19.67	3.4	1047	73	2.14	SML	S	P	0.050	0.731	0.045	0.007	0.006	0.006	AWT__
C	L	0.15	0.2	1	3	3	19.67	3.4	1047	73	2.14	SML	S	P	0.054	0.778	0.047	0.007	0.006	0.006	____V
C	L	0.15	0.2	1	3	3	19.67	3.4	1047	73	2.14	SML	S	P	0.057	0.791	0.049	0.007	0.006	0.006	AW_S_
C	L	0.15	0.2	1	3	3	19.67	3.4	1047	73	2.14	SML	S	P	0.059	0.809	0.051	0.008	0.006	0.006	____V

C	L	0.15	0.2	1	3	3	19.67	3.4	1047	73	2.14	SML	S	P	0.061	0.828	0.053	0.008	0.007	0.006	AW_S_
C	L	0.15	0.2	1	3	3	19.67	3.4	1047	73	2.14	SML	S	P	0.064	0.844	0.056	0.008	0.006	0.007	AWT__
B	L	0.15	0.1	0.44	3	3	19.67	3.4	1059	73	2.28	S	S	G	0.019	0.609	0.030	0.005	0.003	0.004	____V
B	L	0.15	0.1	0.44	3	3	19.67	3.4	1059	73	2.28	S	S	G	0.021	0.637	0.032	0.005	0.004	0.004	____V
B	L	0.15	0.1	0.44	3	3	19.67	3.4	1059	73	2.28	SM	S	A	0.024	0.671	0.037	0.005	0.004	0.004	AW_S_
B	L	0.15	0.1	0.44	3	3	19.67	3.4	1059	73	2.28	SM	S	A	0.026	0.700	0.039	0.006	0.004	0.004	AWT__
B	L	0.15	0.1	0.44	3	3	19.67	3.4	1059	73	2.28	SM	S	A	0.029	0.731	0.042	0.007	0.005	0.004	AWT__
B	L	0.15	0.1	0.44	3	3	19.67	3.4	1059	73	2.28	SM	S	A	0.031	0.750	0.044	0.007	0.004	0.004	AWT__
B	L	0.15	0.1	0.44	3	3	19.67	3.4	1059	73	2.28	SM	S	A	0.033	0.777	0.046	0.007	0.005	0.004	AWT__
B	L	0.15	0.1	0.44	3	3	19.67	3.4	1059	73	2.28	SM	S	A	0.035	0.801	0.050	0.008	0.005	0.005	AW_S_
B	L	0.15	0.1	0.44	3	3	19.67	3.4	1059	73	2.28	SM	S	A	0.038	0.823	0.052	0.009	0.004	0.005	AWT__
B	L	0.15	0.1	0.44	3	3	19.67	3.4	1059	73	2.28	SM	S	A	0.039	0.831	0.054	0.009	0.005	0.005	AWT__
B	L	0.15	0.1	0.44	3	3	19.67	3.4	1059	73	2.28	SM	S	A	0.042	0.859	0.056	0.009	0.006	0.005	AWT__
B	L	0.15	0.1	0.44	3	3	19.67	3.4	1059	73	2.28	SML	S	A	0.044	0.880	0.057	0.009	0.006	0.005	____V
B	L	0.15	0.1	0.44	3	3	19.67	3.4	1059	73	2.28	SML	S	A	0.047	0.899	0.061	0.010	0.006	0.005	____V
B	L	0.15	0.1	0.44	3	3	19.67	3.4	1059	73	2.28	SML	S	A	0.049	0.924	0.063	0.011	0.006	0.005	AWT__
B	L	0.15	0.1	0.44	3	3	19.67	3.4	1059	73	2.28	SML	S	A	0.052	0.940	0.065	0.011	0.006	0.005	AW_S_
B	L	0.15	0.1	0.44	3	3	19.67	3.4	1059	73	2.28	SML	S	A	0.054	0.959	0.068	0.012	0.006	0.006	AWT__
B	L	0.15	0.1	0.44	3	3	19.67	3.4	1059	73	2.28	SML	S	P	0.057	0.983	0.070	0.012	0.006	0.006	AW_S_
B	L	0.15	0.1	0.44	3	3	19.67	3.4	1059	73	2.28	SML	S	P	0.059	1.000	0.074	0.013	0.006	0.006	AWT__
B	L	0.15	0.1	0.44	3	3	19.67	3.4	1059	73	2.28	SML	S	P	0.061	1.034	0.078	0.015	0.006	0.007	AW_S_
B	L	0.15	0.1	0.44	3	3	19.67	3.4	1059	73	2.28	SML	S	P	0.066	1.080	0.085	0.016	0.006	0.007	AWT__
A	L	0.15	0.1	0.44	3	3	19.67	3.4	1059	73	2.28	SM	S	G	0.019	0.509	0.040	0.004	0.004	0.004	AW_S_
A	L	0.15	0.1	0.44	3	3	19.67	3.4	1059	73	2.28	SM	S	A	0.021	0.535	0.045	0.004	0.004	0.004	AWT__
A	L	0.15	0.1	0.44	3	3	19.67	3.4	1059	73	2.28	SM	S	A	0.024	0.565	0.049	0.004	0.004	0.005	AWT__
A	L	0.15	0.1	0.44	3	3	19.67	3.4	1059	73	2.28	SML	S	A	0.026	0.588	0.052	0.004	0.005	0.005	AWT__
A	L	0.15	0.1	0.44	3	3	19.67	3.4	1059	73	2.28	SML	S	A	0.028	0.612	0.058	0.005	0.005	0.005	AW_S_
A	L	0.15	0.1	0.44	3	3	19.67	3.4	1059	73	2.28	SML	S	A	0.031	0.632	0.061	0.005	0.004	0.005	AWT__
A	L	0.15	0.1	0.44	3	3	19.67	3.4	1059	73	2.28	SML	S	A	0.033	0.660	0.066	0.006	0.006	0.005	AWT__

A	L	0.15	0.1	0.44	3	3	19.67	3.4	1059	73	2.28	SML	S	A	0.036	0.662	0.070	0.006	0.005	0.005	AWT__
A	L	0.15	0.1	0.44	3	3	19.67	3.4	1059	73	2.28	SML	S	A	0.038	0.695	0.073	0.007	0.005	0.005	____V
A	L	0.15	0.1	0.44	3	3	19.67	3.4	1059	73	2.28	SML	S	A	0.040	0.716	0.078	0.007	0.005	0.005	AW_S_
A	L	0.15	0.1	0.44	3	3	19.67	3.4	1059	73	2.28	SML	S	A	0.043	0.735	0.082	0.007	0.006	0.005	AW_S_
A	L	0.15	0.1	0.44	3	3	19.67	3.4	1059	73	2.28	SML	S	A	0.044	0.753	0.084	0.008	0.006	0.005	AWT__
A	L	0.15	0.1	0.44	3	3	19.67	3.4	1059	73	2.28	SML	S	A	0.047	0.773	0.088	0.008	0.005	0.006	AWT__
A	L	0.15	0.1	0.44	3	3	19.67	3.4	1059	73	2.28	SML	S	A	0.049	0.782	0.091	0.009	0.006	0.006	____V
A	L	0.15	0.1	0.44	3	3	19.67	3.4	1059	73	2.28	SML	S	P	0.052	0.798	0.096	0.009	0.006	0.006	AW_S_
A	L	0.15	0.1	0.44	3	3	19.67	3.4	1059	73	2.28	SML	S	P	0.054	0.820	0.099	0.009	0.006	0.006	AWT__
A	L	0.15	0.1	0.44	3	3	19.67	3.4	1059	73	2.28	SML	S	P	0.056	0.839	0.103	0.010	0.006	0.006	AWT__
A	L	0.15	0.1	0.44	3	3	19.67	3.4	1059	73	2.28	SML	S	P	0.059	0.857	0.107	0.010	0.007	0.006	AW_S_
A	L	0.15	0.1	0.44	3	3	19.67	3.4	1059	73	2.28	SML	S	P	0.064	0.885	0.115	0.011	0.007	0.007	____V
A	L	0.15	0.1	0.44	3	3	19.67	3.4	1059	73	2.28	SML	S	P	0.066	0.908	0.120	0.011	0.008	0.007	AWT__
C	L	0.15	0.1	0.44	3	3	19.67	3.4	1059	73	2.28	SM	S	G	0.019	0.644	0.028	0.006	0.003	0.004	AWT__
C	L	0.15	0.1	0.44	3	3	19.67	3.4	1059	73	2.28	SML	S	A	0.021	0.676	0.031	0.007	0.004	0.004	AWT__
C	L	0.15	0.1	0.44	3	3	19.67	3.4	1059	73	2.28	SML	S	A	0.024	0.713	0.034	0.007	0.004	0.004	____V
C	L	0.15	0.1	0.44	3	3	19.67	3.4	1059	73	2.28	SML	S	A	0.026	0.740	0.035	0.007	0.004	0.004	AWT__
C	L	0.15	0.1	0.44	3	3	19.67	3.4	1059	73	2.28	SML	S	A	0.029	0.765	0.039	0.007	0.005	0.004	AWT__
C	L	0.15	0.1	0.44	3	3	19.67	3.4	1059	73	2.28	SML	S	A	0.031	0.789	0.041	0.007	0.004	0.004	AW_S_
C	L	0.15	0.1	0.44	3	3	19.67	3.4	1059	73	2.28	SML	S	A	0.033	0.823	0.044	0.008	0.004	0.004	AW_S_
C	L	0.15	0.1	0.44	3	3	19.67	3.4	1059	73	2.28	SML	S	A	0.035	0.843	0.047	0.009	0.005	0.005	____V
C	L	0.15	0.1	0.44	3	3	19.67	3.4	1059	73	2.28	SML	S	A	0.038	0.872	0.048	0.009	0.004	0.005	AW_S_
C	L	0.15	0.1	0.44	3	3	19.67	3.4	1059	73	2.28	SML	S	P	0.040	0.894	0.052	0.010	0.005	0.005	AWT__
C	L	0.15	0.1	0.44	3	3	19.67	3.4	1059	73	2.28	SML	S	P	0.043	0.919	0.055	0.010	0.006	0.005	AWT__
C	L	0.15	0.1	0.44	3	3	19.67	3.4	1059	73	2.28	SML	S	P	0.045	0.936	0.056	0.011	0.006	0.005	AW_S_
C	L	0.15	0.1	0.44	3	3	19.67	3.4	1059	73	2.28	SML	S	P	0.047	0.961	0.058	0.012	0.005	0.005	AWT__
C	L	0.15	0.1	0.44	3	3	19.67	3.4	1059	73	2.28	SML	S	P	0.049	0.975	0.061	0.013	0.006	0.005	AWT__
C	L	0.15	0.1	0.44	3	3	19.67	3.4	1059	73	2.28	SML	S	P	0.052	1.000	0.064	0.013	0.005	0.006	AWT__
C	L	0.15	0.1	0.44	3	3	19.67	3.4	1059	73	2.28	SML	S	P	0.054	1.021	0.066	0.013	0.006	0.006	AWT__

C	L	0.15	0.1	0.44	3	3	19.67	3.4	1059	73	2.28	SML	S	P	0.057	1.043	0.070	0.013	0.007	0.006	AW_S_
C	L	0.15	0.1	0.44	3	3	19.67	3.4	1059	73	2.28	SML	S	P	0.062	1.084	0.075	0.015	0.008	0.007	AWT__
C	L	0.15	0.1	0.44	3	3	19.67	3.4	1059	73	2.28	SML	S	P	0.064	1.110	0.078	0.015	0.008	0.007	AWT__
C	L	0.15	0.1	0.44	3	3	19.67	3.4	1059	73	2.28	SML	S	P	0.066	1.131	0.081	0.015	0.008	0.007	AWT__
C	L	0.15	0.2	1	3	3	19.67	3.4	1059	73	2.28	S	S	G	0.019	0.478	0.019	0.003	0.003	0.003	AWT__
C	L	0.15	0.2	1	3	3	19.67	3.4	1059	73	2.28	S	S	A	0.021	0.507	0.021	0.003	0.004	0.004	AWT__
C	L	0.15	0.2	1	3	3	19.67	3.4	1059	73	2.28	S	S	A	0.024	0.528	0.023	0.003	0.004	0.004	____V
C	L	0.15	0.2	1	3	3	19.67	3.4	1059	73	2.28	S	S	A	0.026	0.553	0.025	0.003	0.004	0.004	AWT__
C	L	0.15	0.2	1	3	3	19.67	3.4	1059	73	2.28	SML	S	A	0.028	0.573	0.026	0.003	0.004	0.004	AWT__
C	L	0.15	0.2	1	3	3	19.67	3.4	1059	73	2.28	SML	S	A	0.031	0.599	0.029	0.004	0.004	0.004	AW_S_
C	L	0.15	0.2	1	3	3	19.67	3.4	1059	73	2.28	SML	S	A	0.033	0.617	0.031	0.004	0.004	0.004	AWT__
C	L	0.15	0.2	1	3	3	19.67	3.4	1059	73	2.28	SML	S	A	0.035	0.626	0.033	0.004	0.004	0.004	AWT__
C	L	0.15	0.2	1	3	3	19.67	3.4	1059	73	2.28	SML	S	A	0.038	0.649	0.033	0.005	0.004	0.004	AWT__
C	L	0.15	0.2	1	3	3	19.67	3.4	1059	73	2.28	SML	S	P	0.040	0.665	0.035	0.005	0.004	0.004	AWT__
C	L	0.15	0.2	1	3	3	19.67	3.4	1059	73	2.28	SML	S	P	0.043	0.680	0.038	0.005	0.004	0.004	AWT__
C	L	0.15	0.2	1	3	3	19.67	3.4	1059	73	2.28	SML	S	P	0.045	0.703	0.040	0.005	0.004	0.004	AWT__
C	L	0.15	0.2	1	3	3	19.67	3.4	1059	73	2.28	SML	S	P	0.047	0.718	0.041	0.006	0.004	0.004	____V
C	L	0.15	0.2	1	3	3	19.67	3.4	1059	73	2.28	SML	S	P	0.050	0.737	0.043	0.006	0.005	0.005	AWT__
C	L	0.15	0.2	1	3	3	19.67	3.4	1059	73	2.28	SML	S	P	0.052	0.750	0.046	0.007	0.005	0.005	AWT__
C	L	0.15	0.2	1	3	3	19.67	3.4	1059	73	2.28	SML	S	P	0.054	0.760	0.047	0.007	0.005	0.005	AW_S_
C	L	0.15	0.2	1	3	3	19.67	3.4	1059	73	2.28	SML	S	P	0.059	0.801	0.052	0.008	0.006	0.006	AW_S_
C	L	0.15	0.2	1	3	3	19.67	3.4	1059	73	2.28	SML	S	P	0.062	0.823	0.053	0.009	0.007	0.006	AW_S_
C	L	0.15	0.2	1	3	3	19.67	3.4	1059	73	2.28	SML	S	P	0.064	0.835	0.055	0.009	0.005	0.006	AWT__
C	L	0.15	0.2	1	3	3	19.67	3.4	1059	73	2.28	SML	S	P	0.066	0.855	0.058	0.009	0.006	0.006	AWT__
B	L	0.15	0.2	1	3	3	19.67	3.4	1059	73	2.28	S	S	G	0.019	0.411	0.024	0.003	0.003	0.004	AWT__
B	L	0.15	0.2	1	3	3	19.67	3.4	1059	73	2.28	S	S	G	0.021	0.431	0.026	0.003	0.004	0.004	AW_S_
B	L	0.15	0.2	1	3	3	19.67	3.4	1059	73	2.28	S	S	G	0.023	0.456	0.029	0.003	0.004	0.004	AW_S_
B	L	0.15	0.2	1	3	3	19.67	3.4	1059	73	2.28	S	S	G	0.026	0.469	0.032	0.003	0.004	0.004	____V
B	L	0.15	0.2	1	3	3	19.67	3.4	1059	73	2.28	S	S	G	0.028	0.495	0.034	0.003	0.005	0.005	AWT__

B	L	0.15	0.2	1	3	3	19.67	3.4	1059	73	2.28	S	S	G	0.030	0.509	0.036	0.003	0.005	0.005	AWT__
B	L	0.15	0.2	1	3	3	19.67	3.4	1059	73	2.28	S	S	G	0.034	0.531	0.040	0.003	0.005	0.005	AW_S_
B	L	0.15	0.2	1	3	3	19.67	3.4	1059	73	2.28	SM	S	G	0.035	0.547	0.040	0.003	0.004	0.005	AWT__
B	L	0.15	0.2	1	3	3	19.67	3.4	1059	73	2.28	SM	S	G	0.038	0.564	0.043	0.003	0.006	0.005	AWT__
B	L	0.15	0.2	1	3	3	19.67	3.4	1059	73	2.28	SM	S	G	0.040	0.576	0.046	0.004	0.005	0.005	AWT__
B	L	0.15	0.2	1	3	3	19.67	3.4	1059	73	2.28	SM	S	A	0.042	0.596	0.049	0.004	0.005	0.005	AWT__
B	L	0.15	0.2	1	3	3	19.67	3.4	1059	73	2.28	SM	S	A	0.047	0.626	0.053	0.005	0.005	0.005	AWT__
B	L	0.15	0.2	1	3	3	19.67	3.4	1059	73	2.28	SM	S	P	0.047	0.626	0.054	0.005	0.006	0.005	AW_S_
B	L	0.15	0.2	1	3	3	19.67	3.4	1059	73	2.28	SM	S	P	0.052	0.657	0.057	0.005	0.005	0.006	AWT__
B	L	0.15	0.2	1	3	3	19.67	3.4	1059	73	2.28	SM	S	P	0.052	0.662	0.058	0.005	0.006	0.006	AWT__
B	L	0.15	0.2	1	3	3	19.67	3.4	1059	73	2.28	SM	S	P	0.057	0.696	0.064	0.006	0.008	0.006	AWT__
B	L	0.15	0.2	1	3	3	19.67	3.4	1059	73	2.28	SM	S	P	0.059	0.704	0.065	0.006	0.007	0.007	AWT__
B	L	0.15	0.2	1	3	3	19.67	3.4	1059	73	2.28	SM	S	P	0.061	0.723	0.068	0.006	0.007	0.007	AWT__
B	L	0.15	0.2	1	3	3	19.67	3.4	1059	73	2.28	SM	S	P	0.064	0.737	0.072	0.007	0.006	0.007	AW_S_
B	L	0.15	0.2	1	3	3	19.67	3.4	1059	73	2.28	SM	S	P	0.066	0.755	0.074	0.007	0.008	0.008	AWT__
A	L	0.15	0.2	1	3	3	19.67	3.4	1059	73	2.28	SML	S	G	0.019	0.274	0.041	0.001	0.004	0.004	AWT__
A	L	0.15	0.2	1	3	3	19.67	3.4	1059	73	2.28	SML	S	G	0.021	0.287	0.045	0.001	0.005	0.004	AWT__
A	L	0.15	0.2	1	3	3	19.67	3.4	1059	73	2.28	SM	S	G	0.024	0.304	0.051	0.001	0.005	0.005	____V
A	L	0.15	0.2	1	3	3	19.67	3.4	1059	73	2.28	SM	S	G	0.026	0.315	0.054	0.001	0.005	0.005	AW_S_
A	L	0.15	0.2	1	3	3	19.67	3.4	1059	73	2.28	SM	S	G	0.029	0.332	0.060	0.001	0.005	0.005	____V
A	L	0.15	0.2	1	3	3	19.67	3.4	1059	73	2.28	SML	S	G	0.031	0.339	0.062	0.002	0.006	0.005	____V
A	L	0.15	0.2	1	3	3	19.67	3.4	1059	73	2.28	SML	S	G	0.033	0.360	0.069	0.002	0.006	0.005	AWT__
A	L	0.15	0.2	1	3	3	19.67	3.4	1059	73	2.28	SML	S	G	0.035	0.364	0.071	0.002	0.005	0.005	____V
A	L	0.15	0.2	1	3	3	19.67	3.4	1059	73	2.28	SM	S	G	0.038	0.376	0.076	0.002	0.006	0.006	AWT__
A	L	0.15	0.2	1	3	3	19.67	3.4	1059	73	2.28	SM	S	G	0.040	0.388	0.080	0.002	0.006	0.006	AWT__
A	L	0.15	0.2	1	3	3	19.67	3.4	1059	73	2.28	SM	S	G	0.042	0.399	0.085	0.002	0.007	0.006	AWT__
A	L	0.15	0.2	1	3	3	19.67	3.4	1059	73	2.28	SM	S	G	0.045	0.407	0.089	0.002	0.007	0.007	____V
A	L	0.15	0.2	1	3	3	19.67	3.4	1059	73	2.28	SM	S	G	0.048	0.417	0.094	0.002	0.007	0.007	AW_S_
A	L	0.15	0.2	1	3	3	19.67	3.4	1059	73	2.28	SM	S	G	0.049	0.427	0.096	0.003	0.008	0.007	AWT__

A	L	0.15	0.2	1	3	3	19.67	3.4	1059	73	2.28	SM	S	G	0.054	0.448	0.104	0.003	0.008	0.007	____V
A	L	0.15	0.2	1	3	3	19.67	3.4	1059	73	2.28	SM	S	G	0.057	0.458	0.111	0.003	0.007	0.008	____V
A	L	0.15	0.2	1	3	3	19.67	3.4	1059	73	2.28	SM	S	G	0.059	0.469	0.115	0.003	0.008	0.008	AW_S_
A	L	0.15	0.2	1	3	3	19.67	3.4	1059	73	2.28	SM	S	A	0.062	0.473	0.122	0.003	0.009	0.008	AWT__
A	L	0.15	0.2	1	3	3	19.67	3.4	1059	73	2.28	SM	S	A	0.063	0.484	0.126	0.003	0.009	0.008	____V
A	L	0.15	0.2	1	3	3	19.67	3.4	1059	73	2.28	SM	S	A	0.067	0.501	0.132	0.004	0.010	0.009	AW_S_
B	L	0.15	0.1	0.44	3	3	19.67	3.4	1066	67	2.76	SM	S	G	0.019	0.609	0.031	0.005	0.003	0.004	AWT__
B	L	0.15	0.1	0.44	3	3	19.67	3.4	1066	67	2.76	SM	S	G	0.021	0.639	0.032	0.006	0.003	0.004	____V
B	L	0.15	0.1	0.44	3	3	19.67	3.4	1066	67	2.76	SM	S	G	0.024	0.674	0.036	0.006	0.004	0.004	AWT__
B	L	0.15	0.1	0.44	3	3	19.67	3.4	1066	67	2.76	SM	S	G	0.026	0.700	0.038	0.006	0.004	0.004	AW_S_
B	L	0.15	0.1	0.44	3	3	19.67	3.4	1066	67	2.76	SM	S	G	0.029	0.721	0.040	0.006	0.004	0.004	AWT__
B	L	0.15	0.1	0.44	3	3	19.67	3.4	1066	67	2.76	SM	S	G	0.031	0.746	0.042	0.007	0.005	0.004	AWT__
B	L	0.15	0.1	0.44	3	3	19.67	3.4	1066	67	2.76	SML	S	G	0.033	0.772	0.046	0.007	0.005	0.004	____V
B	L	0.15	0.1	0.44	3	3	19.67	3.4	1066	67	2.76	SML	S	G	0.035	0.793	0.048	0.008	0.005	0.004	AWT__
B	L	0.15	0.1	0.44	3	3	19.67	3.4	1066	67	2.76	SML	S	A	0.039	0.826	0.052	0.008	0.004	0.004	AWT__
B	L	0.15	0.1	0.44	3	3	19.67	3.4	1066	67	2.76	SML	S	A	0.040	0.839	0.054	0.009	0.006	0.005	____V
B	L	0.15	0.1	0.44	3	3	19.67	3.4	1066	67	2.76	SML	S	A	0.043	0.861	0.056	0.009	0.005	0.005	AW_S_
B	L	0.15	0.1	0.44	3	3	19.67	3.4	1066	67	2.76	SML	S	A	0.045	0.881	0.059	0.009	0.005	0.005	AW_S_
B	L	0.15	0.1	0.44	3	3	19.67	3.4	1066	67	2.76	SML	S	A	0.047	0.900	0.060	0.010	0.005	0.005	AWT__
B	L	0.15	0.1	0.44	3	3	19.67	3.4	1066	67	2.76	SML	S	P	0.052	0.935	0.064	0.012	0.006	0.006	AWT__
B	L	0.15	0.1	0.44	3	3	19.67	3.4	1066	67	2.76	SML	S	P	0.054	0.950	0.067	0.012	0.006	0.006	AWT__
B	L	0.15	0.1	0.44	3	3	19.67	3.4	1066	67	2.76	SML	S	P	0.056	0.974	0.071	0.012	0.007	0.006	AW_S_
B	L	0.15	0.1	0.44	3	3	19.67	3.4	1066	67	2.76	SML	S	P	0.059	0.986	0.073	0.012	0.006	0.006	AWT__
B	L	0.15	0.1	0.44	3	3	19.67	3.4	1066	67	2.76	SML	S	P	0.065	1.019	0.075	0.013	0.006	0.006	AWT__
B	L	0.15	0.1	0.44	3	3	19.67	3.4	1066	67	2.76	SML	S	P	0.063	1.031	0.077	0.013	0.005	0.006	AW_S_
B	L	0.15	0.1	0.44	3	3	19.67	3.4	1066	67	2.76	SML	S	P	0.066	1.039	0.078	0.014	0.006	0.006	AWT__
A	L	0.15	0.1	0.44	3	3	19.67	3.4	1066	67	2.76	S	S	G	0.019	0.504	0.039	0.003	0.004	0.004	AWT__
A	L	0.15	0.1	0.44	3	3	19.67	3.4	1066	67	2.76	S	S	G	0.021	0.531	0.043	0.004	0.004	0.004	AWT__
A	L	0.15	0.1	0.44	3	3	19.67	3.4	1066	67	2.76	S	S	G	0.024	0.555	0.046	0.004	0.004	0.004	____V

A	L	0.15	0.1	0.44	3	3	19.67	3.4	1066	67	2.76	S	S	G	0.026	0.582	0.051	0.004	0.004	0.004	AWT__
A	L	0.15	0.1	0.44	3	3	19.67	3.4	1066	67	2.76	S	S	G	0.029	0.611	0.055	0.005	0.005	0.004	____V
A	L	0.15	0.1	0.44	3	3	19.67	3.4	1066	67	2.76	S	S	A	0.031	0.624	0.058	0.005	0.004	0.004	AWT__
A	L	0.15	0.1	0.44	3	3	19.67	3.4	1066	67	2.76	S	S	A	0.033	0.637	0.063	0.006	0.004	0.004	AW_S_
A	L	0.15	0.1	0.44	3	3	19.67	3.4	1066	67	2.76	S	S	A	0.036	0.672	0.066	0.006	0.005	0.005	AWT__
A	L	0.15	0.1	0.44	3	3	19.67	3.4	1066	67	2.76	S	S	A	0.038	0.688	0.070	0.006	0.005	0.005	AWT__
A	L	0.15	0.1	0.44	3	3	19.67	3.4	1066	67	2.76	S	S	A	0.040	0.680	0.074	0.006	0.005	0.005	AWT__
A	L	0.15	0.1	0.44	3	3	19.67	3.4	1066	67	2.76	S	S	A	0.043	0.728	0.077	0.006	0.006	0.005	AWT__
A	L	0.15	0.1	0.44	3	3	19.67	3.4	1066	67	2.76	SM	S	A	0.045	0.735	0.080	0.008	0.005	0.005	AW_S_
A	L	0.15	0.1	0.44	3	3	19.67	3.4	1066	67	2.76	SM	S	P	0.050	0.777	0.090	0.008	0.005	0.006	____V
A	L	0.15	0.1	0.44	3	3	19.67	3.4	1066	67	2.76	SM	S	P	0.052	0.791	0.092	0.008	0.006	0.006	AWT__
A	L	0.15	0.1	0.44	3	3	19.67	3.4	1066	67	2.76	SM	S	P	0.054	0.812	0.097	0.009	0.005	0.006	AW_S_
A	L	0.15	0.1	0.44	3	3	19.67	3.4	1066	67	2.76	SM	S	P	0.057	0.828	0.100	0.009	0.006	0.006	AWT__
A	L	0.15	0.1	0.44	3	3	19.67	3.4	1066	67	2.76	SM	S	P	0.059	0.839	0.104	0.009	0.006	0.006	____V
A	L	0.15	0.1	0.44	3	3	19.67	3.4	1066	67	2.76	SM	S	P	0.062	0.861	0.110	0.010	0.007	0.007	AWT__
A	L	0.15	0.1	0.44	3	3	19.67	3.4	1066	67	2.76	SM	S	P	0.064	0.877	0.111	0.010	0.007	0.007	AWT__
A	L	0.15	0.1	0.44	3	3	19.67	3.4	1066	67	2.76	SM	S	P	0.066	0.894	0.116	0.010	0.007	0.007	AWT__
C	L	0.15	0.1	0.44	3	3	19.67	3.4	1066	67	2.76	S	S	G	0.019	0.639	0.028	0.005	0.003	0.003	AWT__
C	L	0.15	0.1	0.44	3	3	19.67	3.4	1066	67	2.76	SML	S	A	0.022	0.677	0.032	0.006	0.003	0.003	AW_S_
C	L	0.15	0.1	0.44	3	3	19.67	3.4	1066	67	2.76	SML	S	A	0.024	0.711	0.033	0.006	0.003	0.003	AWT__
C	L	0.15	0.1	0.44	3	3	19.67	3.4	1066	67	2.76	SML	S	A	0.026	0.735	0.036	0.006	0.004	0.003	AWT__
C	L	0.15	0.1	0.44	3	3	19.67	3.4	1066	67	2.76	SML	S	A	0.029	0.769	0.039	0.007	0.003	0.003	AWT__
C	L	0.15	0.1	0.44	3	3	19.67	3.4	1066	67	2.76	SML	S	A	0.031	0.795	0.041	0.007	0.003	0.003	AWT__
C	L	0.15	0.1	0.44	3	3	19.67	3.4	1066	67	2.76	SML	S	A	0.033	0.821	0.043	0.007	0.003	0.003	AWT__
C	L	0.15	0.1	0.44	3	3	19.67	3.4	1066	67	2.76	SML	S	A	0.036	0.844	0.046	0.007	0.004	0.004	AWT__
C	L	0.15	0.1	0.44	3	3	19.67	3.4	1066	67	2.76	SML	S	A	0.038	0.870	0.049	0.008	0.003	0.004	AWT__
C	L	0.15	0.1	0.44	3	3	19.67	3.4	1066	67	2.76	SML	S	A	0.040	0.890	0.051	0.008	0.005	0.004	AW_S_
C	L	0.15	0.1	0.44	3	3	19.67	3.4	1066	67	2.76	SML	S	P	0.043	0.916	0.054	0.009	0.004	0.004	AW_S_
C	L	0.15	0.1	0.44	3	3	19.67	3.4	1066	67	2.76	SML	S	P	0.047	0.960	0.058	0.010	0.005	0.004	AWT__

C	L	0.15	0.1	0.44	3	3	19.67	3.4	1066	67	2.76	SML	S	P	0.050	0.979	0.061	0.010	0.005	0.005	AWT__
C	L	0.15	0.1	0.44	3	3	19.67	3.4	1066	67	2.76	SML	S	P	0.052	1.001	0.063	0.010	0.004	0.005	AWT__
C	L	0.15	0.1	0.44	3	3	19.67	3.4	1066	67	2.76	SML	S	P	0.054	1.022	0.066	0.010	0.005	0.005	AWT__
C	L	0.15	0.1	0.44	3	3	19.67	3.4	1066	67	2.76	SML	S	P	0.057	1.042	0.068	0.010	0.005	0.005	AW_S_
C	L	0.15	0.1	0.44	3	3	19.67	3.4	1066	67	2.76	SML	S	P	0.059	1.059	0.071	0.010	0.005	0.005	____V
C	L	0.15	0.1	0.44	3	3	19.67	3.4	1066	67	2.76	SML	S	P	0.061	1.077	0.071	0.010	0.005	0.005	____V
C	L	0.15	0.1	0.44	3	3	19.67	3.4	1066	67	2.76	SML	S	P	0.064	1.112	0.075	0.011	0.006	0.006	AW_S_
C	L	0.15	0.1	0.44	3	3	19.67	3.4	1066	67	2.76	SML	S	P	0.066	1.146	0.078	0.012	0.006	0.006	AW_S_
B	L	0.15	0.2	1	3	3	19.67	3.4	1066	67	2.76	SM	S	G	0.019	0.406	0.024	0.002	0.003	0.003	____V
B	L	0.15	0.2	1	3	3	19.67	3.4	1066	67	2.76	SM	S	G	0.021	0.428	0.026	0.002	0.003	0.003	AW_S_
B	L	0.15	0.2	1	3	3	19.67	3.4	1066	67	2.76	SM	S	G	0.024	0.454	0.029	0.002	0.003	0.004	AW_S_
B	L	0.15	0.2	1	3	3	19.67	3.4	1066	67	2.76	SM	S	G	0.026	0.469	0.031	0.003	0.003	0.004	AW_S_
B	L	0.15	0.2	1	3	3	19.67	3.4	1066	67	2.76	SM	S	G	0.029	0.494	0.034	0.003	0.004	0.004	AW_S_
B	L	0.15	0.2	1	3	3	19.67	3.4	1066	67	2.76	SM	S	G	0.031	0.509	0.036	0.003	0.004	0.004	AWT__
B	L	0.15	0.2	1	3	3	19.67	3.4	1066	67	2.76	SM	S	G	0.033	0.529	0.038	0.003	0.004	0.004	AWT__
B	L	0.15	0.2	1	3	3	19.67	3.4	1066	67	2.76	SM	S	G	0.035	0.547	0.040	0.004	0.005	0.004	AWT__
B	L	0.15	0.2	1	3	3	19.67	3.4	1066	67	2.76	SM	S	G	0.038	0.563	0.043	0.004	0.005	0.004	AW_S_
B	L	0.15	0.2	1	3	3	19.67	3.4	1066	67	2.76	SM	S	G	0.040	0.572	0.045	0.004	0.005	0.005	AWT__
B	L	0.15	0.2	1	3	3	19.67	3.4	1066	67	2.76	SM	S	G	0.045	0.603	0.050	0.004	0.005	0.005	AW_S_
B	L	0.15	0.2	1	3	3	19.67	3.4	1066	67	2.76	SM	S	G	0.047	0.625	0.052	0.004	0.005	0.005	AWT__
B	L	0.15	0.2	1	3	3	19.67	3.4	1066	67	2.76	SM	S	G	0.050	0.639	0.055	0.004	0.005	0.005	AWT__
B	L	0.15	0.2	1	3	3	19.67	3.4	1066	67	2.76	SM	S	A	0.052	0.656	0.057	0.005	0.005	0.006	AW_S_
B	L	0.15	0.2	1	3	3	19.67	3.4	1066	67	2.76	SM	S	A	0.054	0.665	0.060	0.005	0.006	0.006	AW_S_
B	L	0.15	0.2	1	3	3	19.67	3.4	1066	67	2.76	SM	S	A	0.056	0.681	0.062	0.006	0.005	0.006	AWT__
B	L	0.15	0.2	1	3	3	19.67	3.4	1066	67	2.76	SM	S	A	0.059	0.704	0.065	0.006	0.007	0.006	AWT__
B	L	0.15	0.2	1	3	3	19.67	3.4	1066	67	2.76	SM	S	A	0.062	0.711	0.067	0.007	0.007	0.006	AWT__
B	L	0.15	0.2	1	3	3	19.67	3.4	1066	67	2.76	SM	S	A	0.063	0.727	0.069	0.008	0.007	0.006	AWT__
B	L	0.15	0.2	1	3	3	19.67	3.4	1066	67	2.76	SM	S	A	0.066	0.745	0.073	0.008	0.006	0.007	____V
A	L	0.15	0.2	1	3	3	19.67	3.4	1066	67	2.76	S	S	G	0.019	0.271	0.042	0.001	0.004	0.004	____V

A	L	0.15	0.2	1	3	3	19.67	3.4	1066	67	2.76	S	S	G	0.021	0.286	0.046	0.001	0.004	0.004	AWT__
A	L	0.15	0.2	1	3	3	19.67	3.4	1066	67	2.76	S	S	G	0.024	0.304	0.051	0.001	0.004	0.004	AWT__
A	L	0.15	0.2	1	3	3	19.67	3.4	1066	67	2.76	S	S	G	0.026	0.313	0.055	0.002	0.005	0.004	AWT__
A	L	0.15	0.2	1	3	3	19.67	3.4	1066	67	2.76	S	S	G	0.028	0.327	0.060	0.002	0.004	0.005	____V
A	L	0.15	0.2	1	3	3	19.67	3.4	1066	67	2.76	S	S	G	0.031	0.341	0.064	0.002	0.005	0.005	AWT__
A	L	0.15	0.2	1	3	3	19.67	3.4	1066	67	2.76	S	S	G	0.032	0.351	0.066	0.002	0.005	0.005	____V
A	L	0.15	0.2	1	3	3	19.67	3.4	1066	67	2.76	S	S	G	0.035	0.364	0.071	0.002	0.005	0.005	AWT__
A	L	0.15	0.2	1	3	3	19.67	3.4	1066	67	2.76	S	S	G	0.038	0.377	0.076	0.002	0.006	0.005	AWT__
A	L	0.15	0.2	1	3	3	19.67	3.4	1066	67	2.76	S	S	G	0.043	0.396	0.085	0.002	0.006	0.006	AW_S_
A	L	0.15	0.2	1	3	3	19.67	3.4	1066	67	2.76	S	S	G	0.045	0.406	0.088	0.002	0.006	0.006	AW_S_
A	L	0.15	0.2	1	3	3	19.67	3.4	1066	67	2.76	S	S	G	0.047	0.415	0.093	0.003	0.007	0.006	AWT__
A	L	0.15	0.2	1	3	3	19.67	3.4	1066	67	2.76	S	S	G	0.050	0.428	0.097	0.003	0.007	0.006	____V
A	L	0.15	0.2	1	3	3	19.67	3.4	1066	67	2.76	S	S	G	0.052	0.437	0.101	0.003	0.007	0.006	AWT__
A	L	0.15	0.2	1	3	3	19.67	3.4	1066	67	2.76	S	S	G	0.054	0.451	0.106	0.003	0.007	0.006	AW_S_
A	L	0.15	0.2	1	3	3	19.67	3.4	1066	67	2.76	S	S	G	0.057	0.458	0.113	0.003	0.006	0.006	____V
A	L	0.15	0.2	1	3	3	19.67	3.4	1066	67	2.76	S	S	G	0.059	0.467	0.116	0.003	0.008	0.007	AWT__
A	L	0.15	0.2	1	3	3	19.67	3.4	1066	67	2.76	S	S	G	0.062	0.476	0.121	0.003	0.006	0.007	AWT__
A	L	0.15	0.2	1	3	3	19.67	3.4	1066	67	2.76	S	S	G	0.064	0.489	0.126	0.003	0.006	0.007	AWT__
A	L	0.15	0.2	1	3	3	19.67	3.4	1066	67	2.76	S	S	G	0.066	0.499	0.129	0.004	0.007	0.007	AWT__
C	L	0.15	0.2	1	3	3	19.67	3.4	1066	67	2.76	SM	S	G	0.019	0.472	0.019	0.003	0.003	0.003	AWT__
C	L	0.15	0.2	1	3	3	19.67	3.4	1066	67	2.76	SM	S	G	0.021	0.500	0.020	0.003	0.003	0.003	AW_S_
C	L	0.15	0.2	1	3	3	19.67	3.4	1066	67	2.76	SM	S	G	0.024	0.526	0.022	0.003	0.004	0.003	AWT__
C	L	0.15	0.2	1	3	3	19.67	3.4	1066	67	2.76	SM	S	G	0.026	0.549	0.024	0.003	0.004	0.003	____V
C	L	0.15	0.2	1	3	3	19.67	3.4	1066	67	2.76	SM	S	G	0.029	0.573	0.026	0.004	0.004	0.004	AWT__
C	L	0.15	0.2	1	3	3	19.67	3.4	1066	67	2.76	SML	S	G	0.031	0.590	0.028	0.004	0.004	0.004	AWT__
C	L	0.15	0.2	1	3	3	19.67	3.4	1066	67	2.76	SML	S	G	0.033	0.615	0.030	0.004	0.004	0.004	AW_S_
C	L	0.15	0.2	1	3	3	19.67	3.4	1066	67	2.76	SML	S	G	0.035	0.629	0.032	0.005	0.004	0.004	AWT__
C	L	0.15	0.2	1	3	3	19.67	3.4	1066	67	2.76	SML	S	G	0.040	0.664	0.035	0.005	0.004	0.004	AWT__
C	L	0.15	0.2	1	3	3	19.67	3.4	1066	67	2.76	SML	S	G	0.043	0.683	0.037	0.006	0.005	0.004	____V

C	L	0.15	0.2	1	3	3	19.67	3.4	1066	67	2.76	SML	S	A	0.045	0.703	0.038	0.006	0.004	0.004	AWT__
C	L	0.15	0.2	1	3	3	19.67	3.4	1066	67	2.76	SML	S	A	0.047	0.722	0.040	0.006	0.005	0.004	AWT__
C	L	0.15	0.2	1	3	3	19.67	3.4	1066	67	2.76	SML	S	A	0.050	0.733	0.042	0.007	0.004	0.005	AWT__
C	L	0.15	0.2	1	3	3	19.67	3.4	1066	67	2.76	SML	S	A	0.052	0.754	0.045	0.007	0.005	0.005	AWT__
C	L	0.15	0.2	1	3	3	19.67	3.4	1066	67	2.76	SML	S	A	0.055	0.773	0.046	0.008	0.005	0.005	AWT__
C	L	0.15	0.2	1	3	3	19.67	3.4	1066	67	2.76	SML	S	A	0.057	0.782	0.047	0.008	0.005	0.005	AW_S_
C	L	0.15	0.2	1	3	3	19.67	3.4	1066	67	2.76	SML	S	A	0.059	0.800	0.051	0.009	0.006	0.006	AWT__
C	L	0.15	0.2	1	3	3	19.67	3.4	1066	67	2.76	SML	S	P	0.062	0.821	0.052	0.009	0.007	0.006	AW_S_
C	L	0.15	0.2	1	3	3	19.67	3.4	1066	67	2.76	SML	S	P	0.064	0.838	0.055	0.010	0.007	0.006	AWT__
C	L	0.15	0.2	1	3	3	19.67	3.4	1066	67	2.76	SML	S	P	0.067	0.859	0.058	0.010	0.007	0.006	____V

BFP : Bubble flow pattern

BS : Bubble size

APPENDIX A2 – STATISTICAL DATA FOR THE NEURAL NETWORK MODEL

EXPERIMENTAL MASS TRANSFER CO	R	Net-R	Avg. Abs.	Max. Abs.	RMS	Accuracy (20%)	Conf. Interval (95%)	Records
All	0.9816955	-0.8679794	0.000519731	0.005111712	0.000773383	0.9984448	0.001506742	643
Primary	0.9823776	-0.8661328	0.000510136	0.005111712	0.000759726	0.9981718	0.00148073	547
Secondary	0.9823776	-0.8661328	0.000510136	0.005111712	0.000759726	0.9981718	0.00148073	547
Train	0.9856786	-0.8664505	0.000478228	0.003784452	0.000687657	1	0.001341823	382
Test	0.9745769	-0.8655504	0.000584007	0.005111712	0.000904808	0.9939394	0.001774519	165
Valid	0.9784074	-0.8794579	0.000574403	0.003758281	0.000847006	1	0.001671857	96

APPENDIX A3 – APPLIED WEIGHTS (ω_{xi}) MODEL 8

Name	Hidden 1	Hidden 2	Hidden 3	Hidden 4	Hidden 5	Hidden 6	Hidden 7	Output 1
Transfer Function	tanh	tanh	tanh	tanh	tanh	tanh	tanh	sigmoid
Bias	-0.111980014	0.153272867	0.183594659	-0.436350018	0.210298643	-0.133943573	0.220185146	0.0338442
I F001 <SPARGER TYPE>								
T01 islit a	-0.170509443	0.208258495	0.466999501	-0.656854153	0.089045666	-0.393221229	0.475265503	0.0013114
T02 islit b	-0.108280711	0.91597569	-0.02846757	0.547579348	0.007043133	0.294219553	-0.195261836	-0.004192
T03 islit c	0.077151999	-0.940108061	-0.237495735	-0.328292668	0.109985091	-0.044664845	-0.053710971	0.0683363
I F002 <SPARGER PORE SIZE>								
T01 islit s	0.006569407	-0.122867733	-0.103008673	-0.006613987	-0.031553306	-0.12952365	0.186926723	-0.000132
I F003 <D_R >								
T01 Log	-0.293749124	0.069159016	-0.187590957	0.013855896	-0.083997391	-0.139246807	-0.421312004	0.2983149
T02 tanh	0.12952213	-0.135591626	0.259250343	-0.007721928	0.087566897	0.137403697	0.410556734	-0.187489
T03 Linear	0.13219282	-0.089558162	0.200462937	-0.012249987	0.0886003	0.136536539	0.410104811	-0.25907
I F004 <D_D >								
T01 Linear	0.154144362	0.018425424	0.236489907	-0.046519902	0.079794362	0.082030758	0.284179717	-0.183773
T02 Inv	0.016668679	-0.196824521	0.153313294	-0.08485876	0.064132445	0.017740674	0.127138481	-0.169118
T03 tanh	0.030144153	-0.063063949	0.124977745	-0.085468017	0.057000723	0.014533187	0.137246013	-0.174221
I F005 <A_D/A_R >								
T01 tanh	-0.057658754	-0.206633165	-0.055281203	-0.138024747	0.036811195	-0.071771488	-0.08562497	0.0208211
T02 Inv	0.001142837	-0.054019503	0.038623005	-0.133849561	0.036925215	-0.070149079	-0.087281518	0.1558749
T03 Linear	0.048894107	-0.190252796	-0.03218697	-0.130501658	0.036627624	-0.067353584	-0.083321594	0.0246702
I F006 <H_R >								
T01 Inv	0.031054098	0.028103797	-0.092095651	0.029757842	-0.04118406	-0.122592263	0.199992076	0.0647474
T02 tanh	-0.090289652	-0.046970312	0.060994834	0.028405014	-0.039405435	-0.118642747	0.192801848	-0.115206
T03 Linear	0.048695661	0.049079031	0.116295643	0.011146163	0.021495368	-0.000763399	0.300948948	-0.127398
I F007 <H_D>								
T01 tanh	-0.056304492	-0.063794687	-0.059448943	0.02967241	-0.032320369	-0.112251088	0.19221364	0.0138513
T02 Inv	0.042779353	-0.009813664	0.065975368	0.029869728	-0.032669712	-0.121338241	0.19326064	-0.097404

T03 Linear	0.024515769	-0.005465985	0.038252492	0.0096032	0.034897413	0.017155968	0.316187412	-0.285324
I F008 <H_R/D_R >								
T01 Inv	0.02706261	0.034488469	-0.087212682	0.026125224	-0.049803946	-0.142166182	0.164652407	-0.031815
T02 tanh	-0.112728067	0.059124261	-0.0594307	0.024189355	-0.046056449	-0.143831387	0.1659787	0.0252886
T03 Linear	-0.189759031	-0.045805044	-0.155996606	0.028472023	-0.091183655	-0.198314562	-0.021312244	0.1852165
I F009 <h_L >								
T01 tanh	-0.067260198	-0.026150119	-0.027921272	0.022799747	-0.03699198	-0.114037052	0.195661992	-0.051866
T02 Inv	-0.029904287	-0.002524356	0.024196601	0.02983566	-0.039670035	-0.113543086	0.202519059	-0.085734
T03 Linear	0.157206252	-0.121779434	0.012387388	0.010038412	0.017921217	-0.005802619	0.295734733	-0.023705
I F010 <ρ>								
T01 Linear	0.084746994	-0.118578747	-0.161854655	0.231976643	0.060516082	0.121261343	-0.192310154	0.7225164
T02 Log	-0.066247836	0.028105648	0.294418156	-0.302937746	0.036704931	0.032605998	-0.069206268	-0.051389
T03 Rt2	-0.082156837	-0.036337227	0.304384708	-0.169045031	0.022378482	0.073124334	-0.131561056	-0.047899
I F011 <σ>								
T01 Linear	-0.178569943	0.480002791	-0.027771564	0.716088057	-0.158740088	0.195906743	-0.154582843	-0.428882
T02 Rt4	0.069394134	-0.614134192	-0.014727286	-0.276124895	0.02253974	-0.213242203	0.22223717	-0.2323
T03 ln x/(1-x)	0.014959714	0.704976439	-0.005754725	0.305606276	-0.047029145	0.183689862	-0.162991881	0.0644094
I F012 <μ>								
T01 Linear	0.045361102	0.11763157	-0.213729009	-0.231591657	0.032627288	-0.180489972	0.291353047	0.2274771
T02 Log	-0.04771208	-0.171269089	0.153589576	0.264998198	-0.016128318	0.217694998	-0.36305359	0.1019153
T03 Rt2	-0.106936499	-0.201853365	0.202791378	0.270020157	-0.019666875	0.217131272	-0.36854285	0.0738809
I F013 <BS_R >								
T01 islit s	-0.158762425	0.291452855	0.554340661	-0.713659346	-0.044686139	-0.336591721	0.766457319	-0.046235
T02 islit sm	0.176038951	-0.114084318	-0.238988742	-0.278934121	-0.111366384	0.393429518	-0.624256134	-0.167645
T03 islit sml	0.060938343	0.095075727	0.007241387	0.489805162	-0.303573281	-0.027596418	0.106261343	-0.005045
I F014 <BS_D >								
T01 islit none	-0.281273812	0.323729783	-0.513199627	0.454049796	-0.217433512	0.0573413	-0.13564986	-0.217472
I F015 <BFP>								
T01 islit a	-0.13002947	-0.078094818	0.548852742	-0.474744767	0.134440839	0.077684499	0.037128944	0.0319153

T02 islit g	-0.12215887	0.098135255	0.432118684	0.330939412	-0.035732411	0.32719785	-0.320665985	0.0410629
T03 islit p	0.208024472	0.134631932	-0.565554023	-0.038977906	0.099270225	-0.089507841	0.288004309	-0.033848
T04 islit vp	0.00297616	0.179408208	-0.050600287	-0.249656737	0.024730971	-0.45300594	0.216598183	-0.132171
I F016 $<U_{SGR}>$								
T01 Linear	0.521862984	0.175687671	0.011970483	-0.405168921	-0.578752756	-0.110014297	-0.584019005	-0.357569
T02 Pwr2	-0.140833735	-0.041624259	0.0388784	0.552181661	0.075565919	-0.121317171	0.970517457	0.4667985
T03 tanh	-0.331580549	-0.016476614	-0.435704172	0.087389722	0.076045908	0.723531783	-0.182891101	-0.054465
T04 fzlft	-0.736116827	-0.248400882	-0.026676252	0.004074865	0.096190706	-0.103491478	-0.015157583	0.427342
T05 fzrgt	-0.21266304	-0.059755381	-0.089458317	-0.003759662	0.007533425	0.007648063	-0.022030842	-0.014435
I F017 $<U_{SLD}>$								
T01 Linear	0.164477885	-0.145058155	0.073645085	-0.220398903	-0.025208915	-0.145345435	-0.62189579	-0.024042
T02 Pwr2	0.094872661	0.199886993	0.19631803	0.291724414	-0.202140376	-0.104619868	0.439697653	-0.043691
T03 tanh	0.134792328	-0.117021412	0.064663529	0.407636166	0.03473793	0.181327432	-0.021273818	0.4397053
T04 fzrgt	0.139781103	-0.081900172	0.081603356	-7.48364E-05	-0.148086876	0.23524788	0.1526362	-0.05434
I F018 $<\varepsilon_R>$								
T01 Linear	-0.485511035	0.171290338	-0.261256754	0.123168342	-0.638005376	0.664762914	-0.085252561	0.0583704
T02 tanh	0.204428807	0.300182462	0.19464314	0.354728192	0.149308875	0.120810427	-0.65405798	-0.35741
T03 Pwr2	-0.017451689	-0.369741678	-0.026340881	-0.480677664	-0.528902173	-0.250252157	0.551740766	0.268449
T04 fzrgt	0.278172463	0.029481024	0.155042216	-0.073794223	0.319511592	0.06397932	0.04351544	-0.147033
I F019 $<\varepsilon_D>$								
T01 Linear	0.295618296	0.133248523	-0.019745413	-0.094098434	0.475803673	0.108962983	0.024261767	-0.10892
T02 Exp	0.186444744	0.116384447	0.291185409	0.878928721	-0.495382369	0.312427223	0.288717568	0.3222646
T03 tanh	0.206143498	-0.084358402	0.033323389	-0.862684906	-0.10302601	0.222462758	0.453333765	-0.208345
O F020 $<k_L a_L$ (EXP) >								
T01 Exp								
Hidden 1	0	0	0	-0.746796191	-0.475520819	-0.291686267	-0.129913449	-0.841794
Hidden 2	0	0	0	-2.227149487	0.295278311	-0.312154889	-0.191253215	-0.199611
Hidden 3	0	0	0	-1.067192793	-0.087000184	-0.00927315	-0.541173339	-0.517588
Hidden 4	0	0	0	0	0	-0.563332319	0.548359454	0.4087848

Hidden 5	0	0	0	0	0	-0.4824588	-0.029086504	0.9385625
Hidden 6	0	0	0	0	0	0	0	-0.758726
Hidden 7	0	0	0	0	0	0	0	-0.653948

Transform function key:

islit - enumerated string transform (multiple transforms are sorted alphabetically)

Log - natural logarithm function

tanh – hyperbolic tangent function

Linear – identity function

Pwr2 – square function

Rt2 – square root function

Inv – inverse function

Ln x/(1-x) – log (x/(1-x))

fzrgt – fuzzy right

fzlft – fuzzy left

APPENDIX B1 – VALIDATION DATA (SPARGER TYPE A FOR FAKHARI et al. (2014))

SPARGER TYPE	SPARGER PORE SIZE	D_R	D_D	A_D/A_R	H_R	H_D	H_R/D_R	h_L	ρ	σ	μ	BS_R	BS_D	BFP	U_{SGR}	U_{SLD}	ε_R	ε_D	k_La_L (EXP)	k_La_L (PRED)
B	S	0.15	0.1	0.44	4.2	4.03	28.13	4.7	997.05	72	1.08	SML	S	G	0.026	1.054	0.050	0.013	0.005	0.008
B	S	0.15	0.1	0.44	4.2	4.03	28.13	4.7	997.05	72	1.08	SML	S	G	0.031	1.115	0.051	0.017	0.006	0.008
B	S	0.15	0.1	0.44	4.2	4.03	28.13	4.7	997.05	72	1.08	SML	S	G	0.035	1.151	0.053	0.017	0.007	0.008
B	S	0.15	0.1	0.44	4.2	4.03	28.13	4.7	997.05	72	1.08	SML	S	G	0.041	1.202	0.058	0.020	0.007	0.009
B	S	0.15	0.1	0.44	4.2	4.03	28.13	4.7	997.05	72	1.08	SML	S	G	0.046	1.258	0.062	0.021	0.008	0.010
B	S	0.15	0.1	0.44	4.2	4.03	28.13	4.7	997.05	72	1.08	SML	S	G	0.050	1.298	0.066	0.022	0.008	0.011
B	S	0.15	0.1	0.44	4.2	4.03	28.13	4.7	997.05	72	1.08	SML	S	G	0.056	1.330	0.070	0.024	0.009	0.012
B	S	0.15	0.1	0.44	4.2	4.03	28.13	4.7	997.05	72	1.08	SML	S	G	0.061	1.370	0.074	0.025	0.010	0.013
B	S	0.15	0.1	0.44	4.2	4.03	28.13	4.7	997.05	72	1.08	SML	S	P	0.066	1.430	0.080	0.028	0.012	0.013
B	S	0.15	0.1	0.44	4.2	4.03	28.13	4.7	997.05	72	1.08	SML	S	P	0.071	1.461	0.089	0.030	0.013	0.014
C	S	0.1	0.1	0.906	1.1	1.1	10.5	1.37	846.00	34	13.05	S	S	G	0.008	0.168	0.021	0.011	0.003	0.004
C	S	0.1	0.1	0.906	1.1	1.1	10.5	1.37	846.00	34	13.05	S	S	G	0.015	0.167	0.029	0.022	0.006	0.004
C	S	0.1	0.1	0.906	1.1	1.1	10.5	1.37	846.00	34	13.05	S	S	G	0.024	0.249	0.047	0.034	0.007	0.007
C	S	0.1	0.1	0.906	1.1	1.1	10.5	1.37	846.00	34	13.05	S	S	P	0.032	0.250	0.063	0.045	0.009	0.007
C	S	0.1	0.1	0.906	1.1	1.1	10.5	1.37	846.00	34	13.05	S	S	P	0.040	0.250	0.074	0.055	0.011	0.008
A	S	0.1	0.07	0.49	1.7	1	17	1.22	998.20	72.8	0.902	SML	S	G	0.002	0.094	0.004	0.000	0.001	0.004
A	S	0.1	0.07	0.49	1.7	1	17	1.22	998.20	72.8	0.902	SML	S	G	0.004	0.110	0.007	0.014	0.002	0.006
A	S	0.1	0.07	0.49	1.7	1	17	1.22	998.20	72.8	0.902	SML	S	G	0.006	0.122	0.010	0.068	0.003	0.005
A	S	0.1	0.07	0.49	1.7	1	17	1.22	998.20	72.8	0.902	SML	S	G	0.008	0.133	0.016	0.067	0.004	0.005
A	S	0.1	0.07	0.49	1.7	1	17	1.22	998.20	72.8	0.902	SML	S	G	0.010	0.129	0.015	0.103	0.004	0.005
A	S	0.23	0.23	1	7.5	9.6	33.33	5.84	997.05	72	1.08	S	S	G	0.017	0.724	0.015	0.004	0.021	0.008
A	S	0.23	0.23	1	7.5	9.6	33.33	5.84	997.05	72	1.08	S	S	G	0.026	0.772	0.018	0.005	0.026	0.011
A	S	0.23	0.23	1	7.5	9.6	33.33	5.84	997.05	72	1.08	S	S	G	0.035	0.823	0.024	0.006	0.031	0.013
A	S	0.23	0.23	1	7.5	9.6	33.33	5.84	997.05	72	1.08	S	S	G	0.043	0.860	0.023	0.007	0.034	0.016
A	S	0.23	0.23	1	7.5	9.6	33.33	5.84	997.05	72	1.08	SML	S	G	0.051	0.905	0.027	0.009	0.039	0.021
A	S	0.23	0.23	1	7.5	9.6	33.33	5.84	997.05	72	1.08	SML	S	G	0.060	0.944	0.028	0.008	0.044	0.023

A	S	0.23	0.23	1	7.5	9.6	33.33	5.84	997.05	72	1.08	SML	S	G	0.068	0.978	0.030	0.010	0.050	0.025
A	S	0.23	0.23	1	7.5	9.6	33.33	5.84	997.05	72	1.08	SML	S	G	0.078	1.030	0.034	0.011	0.056	0.026
A	S	0.23	0.23	1	7.5	9.6	33.33	5.84	997.05	72	1.08	SML	S	A	0.088	1.090	0.037	0.012	0.062	0.026
A	S	0.23	0.23	1	7.5	9.6	33.33	5.84	997.05	72	1.08	SML	S	A	0.103	1.120	0.040	0.013	0.071	0.026
A	S	0.23	0.23	1	7.5	9.6	33.33	5.84	997.05	72	1.08	SML	S	A	0.11	1.15	0.042	0.01	0.075	0.026
A	S	0.23	0.23	1	7.5	9.6	33.33	5.84	997.05	72	1.08	SML	S	A	0.127	1.190	0.046	0.014	0.079	0.026
A	S	0.23	0.23	1	7.5	9.6	33.33	5.84	997.05	72	1.08	SML	S	A	0.140	1.230	0.050	0.015	0.084	0.026
A	S	0.23	0.23	1	7.5	9.6	33.33	5.84	997.05	72	1.08	SML	S	P	0.153	1.250	0.059	0.017	0.090	0.027
A	S	0.23	0.23	1	7.5	9.6	33.33	5.84	997.05	72	1.08	SML	S	P	0.164	1.270	0.065	0.020	0.097	0.027
A	L	0.15	0.1	0.44	3	2.95	20.67	3.4	997.05	72	1.08	SML	S	A	0.043	0.738	0.078	0.007	0.014	0.009
C	L	0.15	0.1	0.44	3	2.95	20.67	3.4	997.05	72	1.08	SML	S	A	0.040	0.890	0.049	0.008	0.008	0.007
B	L	0.15	0.1	0.44	3	2.95	20.67	3.4	997.05	72	1.08	SML	S	P	0.049	0.891	0.058	0.011	0.009	0.010
A	L	0.15	0.15	1	3	2.95	20.67	3.4	997.05	72	1.08	SML	S	A	0.045	0.419	0.083	0.002	0.012	0.010
B	L	0.15	0.15	1	3	2.95	20.67	3.4	997.05	72	1.08	SML	S	G	0.040	0.574	0.043	0.003	0.011	0.008
C	L	0.15	0.15	1	3	2.95	20.67	3.4	997.05	72	1.08	S	S	G	0.035	0.636	0.030	0.004	0.006	0.006
A	S	0.23	0.23	1	5.4	5.4	24	5.84	997.05	72	1.08	S	S	G	0.036	0.568	0.068	0.002	0.017	0.017
B	S	0.15	0.15	1	4.2	4.03	28.13	4.7	997.05	72	1.08	SML	S	P	0.081	0.771	0.071	0.023	0.016	0.015
B	S	0.15	0.1	0.44	4.2	4.03	28.13	4.7	997.05	72	1.08	SML	S	G	0.043	1.273	0.051	0.022	0.010	0.009
A	L	0.15	0.1	0.44	3	2.95	20.67	3.4	1033	64.5	1.68	SM	S	A	0.045	0.744	0.082	0.007	0.007	0.007
C	L	0.15	0.1	0.44	3	2.95	20.67	3.4	1033	64.5	1.68	SM	S	A	0.042	0.932	0.052	0.010	0.006	0.006
B	L	0.15	0.1	0.44	3	2.95	20.67	3.4	1033	64.5	1.68	SM	NONE	A	0.040	0.850	0.052	0.009	0.006	0.005
B	L	0.15	0.15	1	3	2.95	20.67	3.4	1033	64.5	1.68	S	S	A	0.038	0.568	0.044	0.004	0.006	0.006
A	L	0.15	0.15	1	3	2.95	20.67	3.4	1033	64.5	1.68	SML	S	G	0.033	0.361	0.067	0.002	0.005	0.005
C	L	0.15	0.15	1	3	2.95	20.67	3.4	1033	64.5	1.68	S	S	A	0.031	0.590	0.029	0.004	0.005	0.005
B	L	0.15	0.1	0.44	3	2.95	20.67	3.4	1047	73.1	2.136	SM	S	A	0.029	0.732	0.041	0.008	0.005	0.005
A	L	0.15	0.1	0.44	3	2.95	20.67	3.4	1047	73.1	2.136	SM	S	G	0.026	0.591	0.053	0.004	0.005	0.005
C	L	0.15	0.1	0.44	3	2.95	20.67	3.4	1047	73.1	2.136	SM	S	A	0.023	0.699	0.035	0.007	0.004	0.004
B	L	0.15	0.15	1	3	2.95	20.67	3.4	1047	73.1	2.136	S	S	G	0.021	0.431	0.027	0.002	0.004	0.004
A	L	0.15	0.15	1	3	2.95	20.67	3.4	1047	73.1	2.136	S	S	P	0.066	0.498	0.133	0.004	0.009	0.009

C	L	0.15	0.15	1	3	2.95	20.67	3.4	1047	73.1	2.136	SML	S	P	0.065	0.855	0.057	0.009	0.008	0.007
B	L	0.15	0.1	0.44	3	2.95	20.67	3.4	1059	72.8	2.28	SML	S	P	0.064	1.053	0.081	0.015	0.006	0.007
A	L	0.15	0.1	0.44	3	2.95	20.67	3.4	1059	72.8	2.28	SML	S	P	0.061	0.868	0.113	0.010	0.008	0.007
C	L	0.15	0.1	0.44	3	2.95	20.67	3.4	1059	72.8	2.28	SML	S	P	0.059	1.057	0.072	0.013	0.007	0.006
C	L	0.15	0.15	1	3	2.95	20.67	3.4	1059	72.8	2.28	SML	S	P	0.057	0.785	0.049	0.007	0.006	0.005
B	L	0.15	0.15	1	3	2.95	20.67	3.4	1059	72.8	2.28	SM	S	P	0.054	0.672	0.060	0.006	0.007	0.006
A	L	0.15	0.15	1	3	2.95	20.67	3.4	1059	72.8	2.28	SM	S	G	0.052	0.438	0.101	0.003	0.007	0.007
B	L	0.15	0.1	0.44	3	2.95	20.67	3.4	1066	67.2	2.76	SML	S	P	0.050	0.923	0.061	0.010	0.006	0.005
A	L	0.15	0.1	0.44	3	2.95	20.67	3.4	1066	67.2	2.76	SM	S	P	0.047	0.764	0.085	0.008	0.005	0.006
C	L	0.15	0.1	0.44	3	2.95	20.67	3.4	1066	67.2	2.76	SML	S	P	0.045	0.935	0.056	0.010	0.004	0.004
B	L	0.15	0.15	1	3	2.95	20.67	3.4	1066	67.2	2.76	SM	S	G	0.042	0.595	0.048	0.004	0.005	0.005
A	L	0.15	0.15	1	3	2.95	20.67	3.4	1066	67.2	2.76	S	S	G	0.040	0.388	0.080	0.002	0.005	0.005
C	L	0.15	0.15	1	3	2.95	20.67	3.4	1066	67.2	2.76	SML	S	G	0.038	0.639	0.033	0.005	0.005	0.004
B	S	0.06	0.06	1	0.9	0.87	14.45	1.81	997.1	72	1.08	S	NONE	G	0.02	1.71	0.033	0	0.004	0.003
B	S	0.06	0.06	1	0.9	0.87	14.45	1.81	997.1	72	1.08	S	NONE	G	0.03	1.82	0.044	0	0.005	0.004
B	S	0.06	0.06	1	0.9	0.87	14.45	1.81	997.1	72	1.08	S	NONE	G	0.04	1.93	0.065	0	0.006	0.006

APPENDIX B2 – VALIDATION DATA (SPARGER TYPE B FOR FAKHARI et al. (2014))

SPARGER TYPE	SPARGER PORE SIZE	D_R	D_D	A_D/A_R	H_R	H_D	H_R/D_R	h_L	ρ	σ	μ	BS_R	BS_D	BFP	U_{SGR}	U_{SLD}	ε_R	ε_D	k_La_L (EXP)	k_La_L (PRED)
B	S	0.15	0.1	0.44	4.22	4.03	28.13	4.7	997.05	72	1.08	SML	S	G	0.026	1.054	0.050	0.013	0.005	0.008
B	S	0.15	0.1	0.44	4.22	4.03	28.13	4.7	997.05	72	1.08	SML	S	G	0.031	1.115	0.051	0.017	0.006	0.008
B	S	0.15	0.1	0.44	4.22	4.03	28.13	4.7	997.05	72	1.08	SML	S	G	0.035	1.151	0.053	0.017	0.007	0.008
B	S	0.15	0.1	0.44	4.22	4.03	28.13	4.7	997.05	72	1.08	SML	S	G	0.041	1.202	0.058	0.020	0.007	0.009
B	S	0.15	0.1	0.44	4.22	4.03	28.13	4.7	997.05	72	1.08	SML	S	G	0.046	1.258	0.062	0.021	0.008	0.010
B	S	0.15	0.1	0.44	4.22	4.03	28.13	4.7	997.05	72	1.08	SML	S	G	0.050	1.298	0.066	0.022	0.008	0.011
B	S	0.15	0.1	0.44	4.22	4.03	28.13	4.7	997.05	72	1.08	SML	S	G	0.056	1.330	0.070	0.024	0.009	0.012
B	S	0.15	0.1	0.44	4.22	4.03	28.13	4.7	997.05	72	1.08	SML	S	G	0.061	1.370	0.074	0.025	0.010	0.013
B	S	0.15	0.1	0.44	4.22	4.03	28.13	4.7	997.05	72	1.08	SML	S	P	0.066	1.430	0.080	0.028	0.012	0.013
B	S	0.15	0.1	0.44	4.22	4.03	28.13	4.7	997.05	72	1.08	SML	S	P	0.071	1.461	0.089	0.030	0.013	0.014
C	S	0.1	0.1	0.906	1.1	1.1	10.5	1.37	846.00	34	13.05	S	S	G	0.008	0.168	0.021	0.011	0.003	0.004
C	S	0.1	0.1	0.906	1.1	1.1	10.5	1.37	846.00	34	13.05	S	S	G	0.015	0.167	0.029	0.022	0.006	0.004
C	S	0.1	0.1	0.906	1.1	1.1	10.5	1.37	846.00	34	13.05	S	S	G	0.024	0.249	0.047	0.034	0.007	0.007
C	S	0.1	0.1	0.906	1.1	1.1	10.5	1.37	846.00	34	13.05	S	S	P	0.032	0.250	0.063	0.045	0.009	0.007
C	S	0.1	0.1	0.906	1.1	1.1	10.5	1.37	846.00	34	13.05	S	S	P	0.040	0.250	0.074	0.055	0.011	0.008
B	S	0.1	0.07	0.49	1.7	0.995	17	1.22	998.20	72.8	0.902	SML	S	G	0.002	0.094	0.004	0.000	0.001	0.004
B	S	0.1	0.07	0.49	1.7	0.995	17	1.22	998.20	72.8	0.902	SML	S	G	0.004	0.110	0.007	0.014	0.002	0.006
B	S	0.1	0.07	0.49	1.7	0.995	17	1.22	998.20	72.8	0.902	SML	S	G	0.006	0.122	0.010	0.068	0.003	0.006
B	S	0.1	0.07	0.49	1.7	0.995	17	1.22	998.20	72.8	0.902	SML	S	G	0.008	0.133	0.016	0.067	0.004	0.006
B	S	0.1	0.07	0.49	1.7	0.995	17	1.22	998.20	72.8	0.902	SML	S	G	0.010	0.129	0.015	0.103	0.004	0.006
A	S	0.23	0.23	1	7.5	9.6	33.33	5.84	997.05	72	1.08	S	S	G	0.017	0.724	0.015	0.004	0.021	0.008
A	S	0.23	0.23	1	7.5	9.6	33.33	5.84	997.05	72	1.08	S	S	G	0.026	0.772	0.018	0.005	0.026	0.011
A	S	0.23	0.23	1	7.5	9.6	33.33	5.84	997.05	72	1.08	S	S	G	0.035	0.823	0.024	0.006	0.031	0.013
A	S	0.23	0.23	1	7.5	9.6	33.33	5.84	997.05	72	1.08	S	S	G	0.043	0.860	0.023	0.007	0.034	0.016
A	S	0.23	0.23	1	7.5	9.6	33.33	5.84	997.05	72	1.08	SML	S	G	0.051	0.905	0.027	0.009	0.039	0.021
A	S	0.23	0.23	1	7.5	9.6	33.33	5.84	997.05	72	1.08	SML	S	G	0.060	0.944	0.028	0.008	0.044	0.023

A	S	0.23	0.23	1	7.5	9.6	33.33	5.84	997.05	72	1.08	SML	S	G	0.068	0.978	0.030	0.010	0.050	0.025
A	S	0.23	0.23	1	7.5	9.6	33.33	5.84	997.05	72	1.08	SML	S	G	0.078	1.030	0.034	0.011	0.056	0.026
A	S	0.23	0.23	1	7.5	9.6	33.33	5.84	997.05	72	1.08	SML	S	A	0.088	1.090	0.037	0.012	0.062	0.026
A	S	0.23	0.23	1	7.5	9.6	33.33	5.84	997.05	72	1.08	SML	S	A	0.103	1.120	0.040	0.013	0.071	0.026
A	S	0.23	0.23	1	7.5	9.6	33.33	5.84	997.05	72	1.08	SML	S	A	0.114	1.15	0.042	0.013	0.075	0.026
A	S	0.23	0.23	1	7.5	9.6	33.33	5.84	997.05	72	1.08	SML	S	A	0.127	1.190	0.046	0.014	0.079	0.026
A	S	0.23	0.23	1	7.5	9.6	33.33	5.84	997.05	72	1.08	SML	S	A	0.140	1.230	0.050	0.015	0.084	0.026
A	S	0.23	0.23	1	7.5	9.6	33.33	5.84	997.05	72	1.08	SML	S	P	0.153	1.250	0.059	0.017	0.090	0.027
A	S	0.23	0.23	1	7.5	9.6	33.33	5.84	997.05	72	1.08	SML	S	P	0.164	1.270	0.065	0.020	0.097	0.027
A	L	0.15	0.1	0.44	2.95	2.95	20.67	3.4	997.05	72	1.08	SML	S	A	0.043	0.738	0.078	0.007	0.014	0.009
C	L	0.15	0.1	0.44	2.95	2.95	20.67	3.4	997.05	72	1.08	SML	S	A	0.040	0.890	0.049	0.008	0.008	0.007
B	L	0.15	0.1	0.44	2.95	2.95	20.67	3.4	997.05	72	1.08	SML	S	P	0.049	0.891	0.058	0.011	0.009	0.010
A	L	0.15	0.15	1	2.95	2.95	20.67	3.4	997.05	72	1.08	SML	S	A	0.045	0.419	0.083	0.002	0.012	0.010
B	L	0.15	0.15	1	2.95	2.95	20.67	3.4	997.05	72	1.08	SML	S	G	0.040	0.574	0.043	0.003	0.011	0.008
C	L	0.15	0.15	1	2.95	2.95	20.67	3.4	997.05	72	1.08	S	S	G	0.035	0.636	0.030	0.004	0.006	0.006
A	S	0.23	0.23	1	5.4	5.4	24	5.84	997.05	72	1.08	S	S	G	0.036	0.568	0.068	0.002	0.017	0.017
B	S	0.15	0.15	1	4.22	4.03	28.13	4.7	997.05	72	1.08	SML	S	P	0.081	0.771	0.071	0.023	0.016	0.015
B	S	0.15	0.1	0.44	4.22	4.03	28.13	4.7	997.05	72	1.08	SML	S	G	0.043	1.273	0.051	0.022	0.010	0.009
A	L	0.15	0.1	0.44	2.95	2.95	20.67	3.4	1033	64.5	1.68	SM	S	A	0.045	0.744	0.082	0.007	0.007	0.007
C	L	0.15	0.1	0.44	2.95	2.95	20.67	3.4	1033	64.5	1.68	SM	S	A	0.042	0.932	0.052	0.010	0.006	0.006
B	L	0.15	0.1	0.44	2.95	2.95	20.67	3.4	1033	64.5	1.68	SM	NONE	A	0.040	0.850	0.052	0.009	0.006	0.005
B	L	0.15	0.15	1	2.95	2.95	20.67	3.4	1033	64.5	1.68	S	S	A	0.038	0.568	0.044	0.004	0.006	0.006
A	L	0.15	0.15	1	2.95	2.95	20.67	3.4	1033	64.5	1.68	SML	S	G	0.033	0.361	0.067	0.002	0.005	0.005
C	L	0.15	0.15	1	2.95	2.95	20.67	3.4	1033	64.5	1.68	S	S	A	0.031	0.590	0.029	0.004	0.005	0.005
B	L	0.15	0.1	0.44	2.95	2.95	20.67	3.4	1047	73.1	2.136	SM	S	A	0.029	0.732	0.041	0.008	0.005	0.005
A	L	0.15	0.1	0.44	2.95	2.95	20.67	3.4	1047	73.1	2.136	SM	S	G	0.026	0.591	0.053	0.004	0.005	0.005
C	L	0.15	0.1	0.44	2.95	2.95	20.67	3.4	1047	73.1	2.136	SM	S	A	0.023	0.699	0.035	0.007	0.004	0.004
B	L	0.15	0.15	1	2.95	2.95	20.67	3.4	1047	73.1	2.136	S	S	G	0.021	0.431	0.027	0.002	0.004	0.004
A	L	0.15	0.15	1	2.95	2.95	20.67	3.4	1047	73.1	2.136	S	S	P	0.066	0.498	0.133	0.004	0.009	0.009

C	L	0.15	0.15	1	2.95	2.95	20.67	3.4	1047	73.1	2.136	SML	S	P	0.065	0.855	0.057	0.009	0.008	0.007
B	L	0.15	0.1	0.44	2.95	2.95	20.67	3.4	1059	72.8	2.28	SML	S	P	0.064	1.053	0.081	0.015	0.006	0.007
A	L	0.15	0.1	0.44	2.95	2.95	20.67	3.4	1059	72.8	2.28	SML	S	P	0.061	0.868	0.113	0.010	0.008	0.007
C	L	0.15	0.1	0.44	2.95	2.95	20.67	3.4	1059	72.8	2.28	SML	S	P	0.059	1.057	0.072	0.013	0.007	0.006
C	L	0.15	0.15	1	2.95	2.95	20.67	3.4	1059	72.8	2.28	SML	S	P	0.057	0.785	0.049	0.007	0.006	0.005
B	L	0.15	0.15	1	2.95	2.95	20.67	3.4	1059	72.8	2.28	SM	S	P	0.054	0.672	0.060	0.006	0.007	0.006
A	L	0.15	0.15	1	2.95	2.95	20.67	3.4	1059	72.8	2.28	SM	S	G	0.052	0.438	0.101	0.003	0.007	0.007
B	L	0.15	0.1	0.44	2.95	2.95	20.67	3.4	1066	67.2	2.76	SML	S	P	0.050	0.923	0.061	0.010	0.006	0.005
A	L	0.15	0.1	0.44	2.95	2.95	20.67	3.4	1066	67.2	2.76	SM	S	P	0.047	0.764	0.085	0.008	0.005	0.006
C	L	0.15	0.1	0.44	2.95	2.95	20.67	3.4	1066	67.2	2.76	SML	S	P	0.045	0.935	0.056	0.010	0.004	0.004
B	L	0.15	0.15	1	2.95	2.95	20.67	3.4	1066	67.2	2.76	SM	S	G	0.042	0.595	0.048	0.004	0.005	0.005
A	L	0.15	0.15	1	2.95	2.95	20.67	3.4	1066	67.2	2.76	S	S	G	0.040	0.388	0.080	0.002	0.005	0.005
C	L	0.15	0.15	1	2.95	2.95	20.67	3.4	1066	67.2	2.76	SML	S	G	0.038	0.639	0.033	0.005	0.005	0.004
B	S	0.06	0.06	1	0.87	0.867	14.45	1.81	997.1	72	1.08	S	NONE	G	0.0178	1.71	0.033	0	0.0041	0.003
B	S	0.06	0.06	1	0.87	0.867	14.45	1.81	997.1	72	1.08	S	NONE	G	0.0295	1.82	0.044	0	0.0049	0.004
B	S	0.06	0.06	1	0.87	0.867	14.45	1.81	997.1	72	1.08	S	NONE	G	0.0414	1.93	0.065	0	0.0059	0.006

APPENDIX B3 – VALIDATION DATA (SPARGER TYPE C FOR FAHKARI et al. (2014))

SPARGER TYPE	SPARGER PORE SIZE	D_R	D_D	A_D/A_R	H_R	H_D	H_R/D_R	h_L	ρ	σ	μ	BS_R	BS_D	BFP	U_{SGR}	U_{SLD}	ε_R	ε_D	k_La_L (EXP)	k_La_L (PRED)
B	S	0.15	0.1	0.44	4.22	4.03	28.13	4.7	997.05	72	1.08	SML	S	G	0.026	1.054	0.050	0.013	0.005	0.008
B	S	0.15	0.1	0.44	4.22	4.03	28.13	4.7	997.05	72	1.08	SML	S	G	0.031	1.115	0.051	0.017	0.006	0.008
B	S	0.15	0.1	0.44	4.22	4.03	28.13	4.7	997.05	72	1.08	SML	S	G	0.035	1.151	0.053	0.017	0.007	0.008
B	S	0.15	0.1	0.44	4.22	4.03	28.13	4.7	997.05	72	1.08	SML	S	G	0.041	1.202	0.058	0.020	0.007	0.009
B	S	0.15	0.1	0.44	4.22	4.03	28.13	4.7	997.05	72	1.08	SML	S	G	0.046	1.258	0.062	0.021	0.008	0.010
B	S	0.15	0.1	0.44	4.22	4.03	28.13	4.7	997.05	72	1.08	SML	S	G	0.050	1.298	0.066	0.022	0.008	0.011
B	S	0.15	0.1	0.44	4.22	4.03	28.13	4.7	997.05	72	1.08	SML	S	G	0.056	1.330	0.070	0.024	0.009	0.012
B	S	0.15	0.1	0.44	4.22	4.03	28.13	4.7	997.05	72	1.08	SML	S	G	0.061	1.370	0.074	0.025	0.010	0.013
B	S	0.15	0.1	0.44	4.22	4.03	28.13	4.7	997.05	72	1.08	SML	S	P	0.066	1.430	0.080	0.028	0.012	0.013
B	S	0.15	0.1	0.44	4.22	4.03	28.13	4.7	997.05	72	1.08	SML	S	P	0.071	1.461	0.089	0.030	0.013	0.014
C	S	0.1	0.1	0.906	1.1	1.1	10.5	1.37	846.00	34	13.05	S	S	G	0.008	0.168	0.021	0.011	0.003	0.004
C	S	0.1	0.1	0.906	1.1	1.1	10.5	1.37	846.00	34	13.05	S	S	G	0.015	0.167	0.029	0.022	0.006	0.004
C	S	0.1	0.1	0.906	1.1	1.1	10.5	1.37	846.00	34	13.05	S	S	G	0.024	0.249	0.047	0.034	0.007	0.007
C	S	0.1	0.1	0.906	1.1	1.1	10.5	1.37	846.00	34	13.05	S	S	P	0.032	0.250	0.063	0.045	0.009	0.007
C	S	0.1	0.1	0.906	1.1	1.1	10.5	1.37	846.00	34	13.05	S	S	P	0.040	0.250	0.074	0.055	0.011	0.008
C	S	0.1	0.07	0.49	1.7	1	17	1.22	998.20	72.8	0.902	SML	S	G	0.002	0.094	0.004	0.000	0.001	0.004
C	S	0.1	0.07	0.49	1.7	1	17	1.22	998.20	72.8	0.902	SML	S	G	0.004	0.110	0.007	0.014	0.002	0.005
C	S	0.1	0.07	0.49	1.7	1	17	1.22	998.20	72.8	0.902	SML	S	G	0.006	0.122	0.010	0.068	0.003	0.005
C	S	0.1	0.07	0.49	1.7	1	17	1.22	998.20	72.8	0.902	SML	S	G	0.008	0.133	0.016	0.067	0.004	0.005
C	S	0.1	0.07	0.49	1.7	1	17	1.22	998.20	72.8	0.902	SML	S	G	0.010	0.129	0.015	0.103	0.004	0.005
A	S	0.23	0.23	1	7.5	9.6	33.33	5.84	997.05	72	1.08	S	S	G	0.017	0.724	0.015	0.004	0.021	0.008
A	S	0.23	0.23	1	7.5	9.6	33.33	5.84	997.05	72	1.08	S	S	G	0.026	0.772	0.018	0.005	0.026	0.011
A	S	0.23	0.23	1	7.5	9.6	33.33	5.84	997.05	72	1.08	S	S	G	0.035	0.823	0.024	0.006	0.031	0.013
A	S	0.23	0.23	1	7.5	9.6	33.33	5.84	997.05	72	1.08	S	S	G	0.043	0.860	0.023	0.007	0.034	0.016
A	S	0.23	0.23	1	7.5	9.6	33.33	5.84	997.05	72	1.08	SML	S	G	0.051	0.905	0.027	0.009	0.039	0.021
A	S	0.23	0.23	1	7.5	9.6	33.33	5.84	997.05	72	1.08	SML	S	G	0.060	0.944	0.028	0.008	0.044	0.023

A	S	0.23	0.23	1	7.5	9.6	33.33	5.84	997.05	72	1.08	SML	S	G	0.068	0.978	0.030	0.010	0.050	0.025
A	S	0.23	0.23	1	7.5	9.6	33.33	5.84	997.05	72	1.08	SML	S	G	0.078	1.030	0.034	0.011	0.056	0.026
A	S	0.23	0.23	1	7.5	9.6	33.33	5.84	997.05	72	1.08	SML	S	A	0.088	1.090	0.037	0.012	0.062	0.026
A	S	0.23	0.23	1	7.5	9.6	33.33	5.84	997.05	72	1.08	SML	S	A	0.103	1.120	0.040	0.013	0.071	0.026
A	S	0.23	0.23	1	7.5	9.6	33.33	5.84	997.05	72	1.08	SML	S	A	0.114	1.15	0.042	0.0129	0.075	0.026
A	S	0.23	0.23	1	7.5	9.6	33.33	5.84	997.05	72	1.08	SML	S	A	0.127	1.190	0.046	0.014	0.079	0.026
A	S	0.23	0.23	1	7.5	9.6	33.33	5.84	997.05	72	1.08	SML	S	A	0.140	1.230	0.050	0.015	0.084	0.026
A	S	0.23	0.23	1	7.5	9.6	33.33	5.84	997.05	72	1.08	SML	S	P	0.153	1.250	0.059	0.017	0.090	0.027
A	S	0.23	0.23	1	7.5	9.6	33.33	5.84	997.05	72	1.08	SML	S	P	0.164	1.270	0.065	0.020	0.097	0.027
A	L	0.15	0.1	0.44	2.95	2.95	20.67	3.4	997.05	72	1.08	SML	S	A	0.043	0.738	0.078	0.007	0.014	0.009
C	L	0.15	0.1	0.44	2.95	2.95	20.67	3.4	997.05	72	1.08	SML	S	A	0.040	0.890	0.049	0.008	0.008	0.007
B	L	0.15	0.1	0.44	2.95	2.95	20.67	3.4	997.05	72	1.08	SML	S	P	0.049	0.891	0.058	0.011	0.009	0.010
A	L	0.15	0.15	1	2.95	2.95	20.67	3.4	997.05	72	1.08	SML	S	A	0.045	0.419	0.083	0.002	0.012	0.010
B	L	0.15	0.15	1	2.95	2.95	20.67	3.4	997.05	72	1.08	SML	S	G	0.040	0.574	0.043	0.003	0.011	0.008
C	L	0.15	0.15	1	2.95	2.95	20.67	3.4	997.05	72	1.08	S	S	G	0.035	0.636	0.030	0.004	0.006	0.006
A	S	0.23	0.23	1	5.4	5.4	24	5.84	997.05	72	1.08	S	S	G	0.036	0.568	0.068	0.002	0.017	0.017
B	S	0.15	0.15	1	4.22	4.03	28.13	4.7	997.05	72	1.08	SML	S	P	0.081	0.771	0.071	0.023	0.016	0.015
B	S	0.15	0.1	0.44	4.22	4.03	28.13	4.7	997.05	72	1.08	SML	S	G	0.043	1.273	0.051	0.022	0.010	0.009
A	L	0.15	0.1	0.44	2.95	2.95	20.67	3.4	1033	64.5	1.68	SM	S	A	0.045	0.744	0.082	0.007	0.007	0.007
C	L	0.15	0.1	0.44	2.95	2.95	20.67	3.4	1033	64.5	1.68	SM	S	A	0.042	0.932	0.052	0.010	0.006	0.006
B	L	0.15	0.1	0.44	2.95	2.95	20.67	3.4	1033	64.5	1.68	SM	NONE	A	0.040	0.850	0.052	0.009	0.006	0.005
B	L	0.15	0.15	1	2.95	2.95	20.67	3.4	1033	64.5	1.68	S	S	A	0.038	0.568	0.044	0.004	0.006	0.006
A	L	0.15	0.15	1	2.95	2.95	20.67	3.4	1033	64.5	1.68	SML	S	G	0.033	0.361	0.067	0.002	0.005	0.005
C	L	0.15	0.15	1	2.95	2.95	20.67	3.4	1033	64.5	1.68	S	S	A	0.031	0.590	0.029	0.004	0.005	0.005
B	L	0.15	0.1	0.44	2.95	2.95	20.67	3.4	1047	73.1	2.136	SM	S	A	0.029	0.732	0.041	0.008	0.005	0.005
A	L	0.15	0.1	0.44	2.95	2.95	20.67	3.4	1047	73.1	2.136	SM	S	G	0.026	0.591	0.053	0.004	0.005	0.005
C	L	0.15	0.1	0.44	2.95	2.95	20.67	3.4	1047	73.1	2.136	SM	S	A	0.023	0.699	0.035	0.007	0.004	0.004
B	L	0.15	0.15	1	2.95	2.95	20.67	3.4	1047	73.1	2.136	S	S	G	0.021	0.431	0.027	0.002	0.004	0.004
A	L	0.15	0.15	1	2.95	2.95	20.67	3.4	1047	73.1	2.136	S	S	P	0.066	0.498	0.133	0.004	0.009	0.009

C	L	0.15	0.15	1	2.95	2.95	20.67	3.4	1047	73.1	2.136	SML	S	P	0.065	0.855	0.057	0.009	0.008	0.007
B	L	0.15	0.1	0.44	2.95	2.95	20.67	3.4	1059	72.8	2.28	SML	S	P	0.064	1.053	0.081	0.015	0.006	0.007
A	L	0.15	0.1	0.44	2.95	2.95	20.67	3.4	1059	72.8	2.28	SML	S	P	0.061	0.868	0.113	0.010	0.008	0.007
C	L	0.15	0.1	0.44	2.95	2.95	20.67	3.4	1059	72.8	2.28	SML	S	P	0.059	1.057	0.072	0.013	0.007	0.006
C	L	0.15	0.15	1	2.95	2.95	20.67	3.4	1059	72.8	2.28	SML	S	P	0.057	0.785	0.049	0.007	0.006	0.005
B	L	0.15	0.15	1	2.95	2.95	20.67	3.4	1059	72.8	2.28	SM	S	P	0.054	0.672	0.060	0.006	0.007	0.006
A	L	0.15	0.15	1	2.95	2.95	20.67	3.4	1059	72.8	2.28	SM	S	G	0.052	0.438	0.101	0.003	0.007	0.007
B	L	0.15	0.1	0.44	2.95	2.95	20.67	3.4	1066	67.2	2.76	SML	S	P	0.050	0.923	0.061	0.010	0.006	0.005
A	L	0.15	0.1	0.44	2.95	2.95	20.67	3.4	1066	67.2	2.76	SM	S	P	0.047	0.764	0.085	0.008	0.005	0.006
C	L	0.15	0.1	0.44	2.95	2.95	20.67	3.4	1066	67.2	2.76	SML	S	P	0.045	0.935	0.056	0.010	0.004	0.004
B	L	0.15	0.15	1	2.95	2.95	20.67	3.4	1066	67.2	2.76	SM	S	G	0.042	0.595	0.048	0.004	0.005	0.005
A	L	0.15	0.15	1	2.95	2.95	20.67	3.4	1066	67.2	2.76	S	S	G	0.040	0.388	0.080	0.002	0.005	0.005
C	L	0.15	0.15	1	2.95	2.95	20.67	3.4	1066	67.2	2.76	SML	S	G	0.038	0.639	0.033	0.005	0.005	0.004
B	S	0.06	0.06	1	0.87	0.87	14.45	1.81	997.1	72	1.08	S	NONE	G	0.018	1.71	0.033	0	0.004	0.003
B	S	0.06	0.06	1	0.87	0.87	14.45	1.81	997.1	72	1.08	S	NONE	G	0.03	1.82	0.044	0	0.005	0.004
B	S	0.06	0.06	1	0.87	0.87	14.45	1.81	997.1	72	1.08	S	NONE	G	0.041	1.93	0.065	0	0.006	0.006